AD_________________

Award Number: WX81XWH-06-2-0025

TITLE: Carcinogenicity of Embedded Tungsten Alloys in Mice

PRINCIPAL INVESTIGATOR: John F. Kalinich, Ph.D.

CONTRACTING ORGANIZATION: Henry M. Jackson Foundation for the Advancement of Military Medicine
Rockville, MD 20852

REPORT DATE: March 2011

TYPE OF REPORT: Final

PREPARED FOR: U.S. Army Medical Research and Materiel Command
Fort Detrick, Maryland 21702-5012

REPORT DOCUMENTATION PAGE

Form Approved
OMB No. 0704-0188

1. REPORT DATE *(DD-MM-YYYY)*	2. REPORT TYPE	3. DATES COVERED *(From - To)*
08-03-2011	Final	10Feb06 - 09Feb11

4. TITLE AND SUBTITLE
Carcinogenicity of Embedded Tungsten Alloys in Mice

5a. CONTRACT NUMBER

5b. GRANT NUMBER
W81XWH-06-2-0025

5c. PROGRAM ELEMENT NUMBER

6. AUTHOR(S)
John F. Kalinich, Ph.D.

Email: kalinich@afrri.usuhs.mil

5d. PROJECT NUMBER

5e. TASK NUMBER

5f. WORK UNIT NUMBER

7. PERFORMING ORGANIZATION NAME(S) AND ADDRESS(ES)
Henry M. Jackson Foundation for the Advancement of Military Medicine
Rockville, MD 20852

8. PERFORMING ORGANIZATION REPORT NUMBER

9. SPONSORING / MONITORING AGENCY NAME(S) AND ADDRESS(ES)
U.S. Army Medical Research
and Materiel Command
Fort Detrick, MD 21702-5012

10. SPONSOR/MONITOR'S ACRONYM(S)

11. SPONSOR/MONITOR'S REPORT NUMBER(S)

12. DISTRIBUTION / AVAILABILITY STATEMENT
Approved for Public release; Distribution Unlimited

13. SUPPLEMENTARY NOTES
Contains color figures.

14. ABSTRACT
A variety of unique metal mixtures have entered the military arsenals of many countries in recent years. One such material is the tungsten alloys, which have been proposed as replacements for depleted uranium (DU) in armor-penetrating munitions. As a result, opportunities for exposure are increasingly likely. This leads to questions, similar to those originally surrounding DU, as to the health effects of exposure to the tungsten alloys, especially for embedded fragment exposures. The Armed Forces Radiobiology Research Institute (AFRRI) recently performed research that showed one of the militarily promising tungsten alloys to be a potent carcinogen when implanted in rats. The need to confirm the carcinogenicity of such alloys in another rodent species is an important second step required in biological as well as regulatory terms to better assess the cancer risk in humans. Results of this work will help in formulating policies for military surgeons who must treat personnel wounded by fragments of the alloys. Indications of unacceptable risks of exposure will also help determine the advisability of deploying (or developing) similar munitions. The results of this study showed, that as in the F344 rat model, tungsten/nickel/cobalt alloy induced tumors, identified as rhabdomyosarcomas, at the implantation site. Tests with another militarily relevant alloy, tungsten/nickel/iron, showed no tumor development when implanted intramuscularly.

15. SUBJECT TERMS
Tungsten alloy; carcinogenicity; munitions; mice

16. SECURITY CLASSIFICATION OF:			17. LIMITATION OF ABSTRACT	18. NUMBER OF PAGES	19a. NAME OF RESPONSIBLE PERSON
					USAMRMC
a. REPORT	b. ABSTRACT	c. THIS PAGE	UU	160	19b. TELEPHONE NUMBER *(include area code)*
U	U	U			

Standard Form 298 (Rev. 8-98)
Prescribed by ANSI Std. Z39.18

Table of Contents

INTRODUCTION

A variety of unique metal mixtures have entered the military arsenals of many countries in recent years. One such material is the tungsten alloys, which have been proposed as replacements for depleted uranium (DU) in armor-penetrating munitions. As a result, opportunities for exposure are increasingly likely. This leads to questions, similar to those originally surrounding DU, as to the health effects of exposure to the tungsten alloys, especially for embedded fragment exposures. The Armed Forces Radiobiology Research Institute (AFRRI) recently performed research that showed one of the militarily promising tungsten alloys to be a potent carcinogen when implanted in rats. The need to confirm the carcinogenicity of such alloys in another rodent species is an important second step required in biological as well as regulatory terms to better assess the cancer risk in humans. Results of this work will help in formulating policies for military surgeons who must treat personnel wounded by fragments of the alloys. Indications of unacceptable risks of exposure will also help determine the advisability of deploying (or developing) similar munitions. The National Toxicology Program (NTP) Two-Year Study Protocol carried out in two rodent species is the recommended approach in the U.S. for identifying human carcinogens. This investigation aimed to confirm the previous AFRRI data in rats by carrying out a two-year protocol in mice based upon NTP guidelines. The study used the B6C3F1 hybrid mouse, a strain commonly used in carcinogenicity and toxicity assessment studies, implanted with pellets of tungsten alloys, the individual component metals of the alloys, tantalum (negative control), or nickel (positive control). The protocol included serial collection of tissues 1, 3, 6, and 12 months post-implantation aimed at identifying early changes relevant to the development of carcinogenic endpoints.

BODY

AFRRI research recently showed that mixtures of tungsten, nickel, and cobalt are tumorigenic and genotoxic in HOS cells (1) and that embedded pellets of the alloy tungsten-nickel-cobalt cause cancer in rats (2). However, studies with cultured cells and rats are not in themselves sufficient to allow designation of a substance as carcinogenic in humans. In general, the National Toxicology Program (NTP) and the Environmental Protection Agency (EPA), two agencies involved in cancer risk determination, agree that convincing evidence that the agent is probably carcinogenic in humans is obtained if the agent demonstrates carcinogenic potential in two rodent species, using the NTP two-year carcinogenicity protocol. This study proposes to obtain that data.

The original Principal Investigator (PI) of this Project, Dr. David McClain, abruptly retired in April 2007. Application was made to the Peer-Reviewed Medical Research Program (PRMRP) at that time requesting a change in PI and consideration of a revised Statement of Work to more adequately address the research goals within the allotted budget. This request was approved on July 17, 2007 and Dr. John Kalinich assumed the role of Project PI. The approved Statement of Work is below,

We hypothesize that the alloys tungsten/nickel/cobalt and tungsten/nickel/iron are carcinogenic in the mouse as indicated by the NTP two-year carcinogenicity protocol. Our test of this hypothesis incorporates the following Aims.

Aim 1: Determine whether the alloys tungsten-nickel-cobalt and tungsten-nickel-iron cause cancer in mice. Include in the protocol mice embedded with pellets of the individual metals composing the alloys and the various metal combinations (blended with biologically inert tantalum at the same percentages present in the alloys).

Pellets of the alloys or the various component metals will be implanted in the quadriceps muscles of mice, and mice will be maintained and monitored for 24 months

post-implantation. The response in alloy-implanted mice will be compared to mice implanted with pellets of 100% nickel, a known carcinogen (positive controls) and mice implanted with tantalum, an inert metal used in prosthetic devices (negative control). At the end of the study or whenever sacrifice of participating mice is required, necropsies will be performed to obtain evidence of tumor development. Data of tumor sites and incidence will be compiled. Tumors will be histologically examined and classified.

Aim 2: Sacrifice mice at various times after alloy implantation to detect early signs of tumor development.

Subgroups of animals treated identically to the mice described in Aim 1 will be euthanized 1, 3, 6, and 12 months after metal implantation to identify any early signs of histopathology associated with exposure to the implanted metals.

Aim 3: Measure tissue levels of the various metals that compose the alloys to correlate metal levels with tumor development.

Levels of W, Ni, Fe, Co, and Ta will be measured in organs from the animals used in Aims 1 and 2. Data will be used to relate tissue metal levels to any cancer incidence observed in those particular tissues. These data will allow a correlation of tissue metal content with tumor development.

Methods and Experimental Design

The B6C3F1 male mouse was used for these experiments. The hybrid B6C3F1 mouse is commonly used in a wide variety of research applications, particularly toxicology, and is the strain recommended by the National Toxicology Project for two-year carcinogenicity investigations. B6C3F1 male mice (4 weeks of age, Harlan, Dublin, VA) were maintained in an Association for Assessment and Accreditation of Laboratory Animal Care International (AAALAC)-accredited facility in accordance with the Guide for the Care and Use of Laboratory Animals (3). All procedures were approved by the

Armed Forces Radiobiology Research Institute (AFRRI) Animal Care and Use Committee. Upon arrival, animals were screened for common rodent pathogens. Mice were group-housed in plastic microisolator cages with hardwood chips for bedding. Rodent chow and acidified water were provided *ad libitum*. Animals were on a 12-hr light/dark cycle with no twilight. A study employing 1200 mice provided a sufficient number to perform the described two-year carcinogenicity assessment protocol using fifteen treatment groups, serial sacrifices to test for early changes in exposed animals, and sufficient additional animals to serve as colony sentinels and backups.

The project focused on two tungsten alloys of special interest to the military: 91.1% tungsten/6% nickel/2.9% cobalt and 91% tungsten/7% nickel/2% iron. All of the tests included fifteen treatment groups consisting of various controls, tungsten alloy metal tests, and a toxicity reference metal (lead). Alloy pellets were custom-fabricated by Aerojet Ordnance Tennessee (Jonesborough, TN) using sintered metal powder technology similar to that used for military munitions. Pellets designed to test individual metals in the alloys contained the same percentage content by weight as the full alloy, with the balance made up with the biologically inert metal tantalum (Table 1, Appendices). Tantalum, lead, and nickel pellets (negative control, toxicity reference metal and positive control, respectively) were cut from wires of pure metal (Alfa Aesar, Ward Hill, MA) and formed to a dimension identical to the alloy pellets. The individual test groups are described as follows:

1. Sham-implantation controls
2. Tantalum pellet-implanted (implantation controls)
3. Nickel (100%) pellet-implanted (positive controls)
4. Lead (100%) pellet-implanted (reference metal)
5. Tungsten/nickel/cobalt pellet-implanted
6. Tungsten/nickel/iron pellet-implanted
7. Tungsten/tantalum pellet-implanted
8. Nickel/tantalum pellet-implanted
9. Cobalt/tantalum pellet-implanted
10. Iron/tantalum pellet-implanted

11. Tungsten/nickel/tantalum pellet-implanted
12. Tungsten/cobalt/tantalum pellet-implanted
13. Tungsten/iron/tantalum pellet-implanted
14. Cobalt/nickel/tantalum pellet-implanted
15. Iron/nickel/tantalum pellet-implanted

Exposures were accomplished by implantation of the metals as pellets in the form of cylinders 1 mm in diameter and 2 mm long. Before implantation surgery, all pellets were cleaned and chemically sterilized (4,5). For pellet implantation, anesthesia was induced by continuous administration of isoflurane using an open circuit system with a scavenger/recapture system. All surgery was done using aseptic techniques. After the surgical sites were clipped and cleansed with betadine, an incision was made through the skin. Pellets were implanted in the quadriceps muscle; spread approximately 1.5 mm apart on the lateral side of each leg. Two pellets were implanted in each quadriceps. The incision was closed with surgical adhesive. Mice were closely monitored after surgery until they were ambulatory. An analgesic (buprenorphine hydrochloride, Reckitt and Colman, Hull, UK) was administered preoperatively and then as needed postoperatively. At various times postimplantation or when moribund, mice were euthanized by isoflurane overdose.

Two-Year Carcinogenicity Study (Aim 1)

These experiments tested the carcinogenic potential of two doses of pellets implanted in mice for 24 months. Twenty male mice were used in each treatment group. The doses used and manner in which the animals are exposed were based on successful mouse and rat pellet implantation models designed at AFRRI and used for over a decade. Mice were weighed on a weekly basis and observed for any changes indicative of developing pathology. At the end of the 24-month period or at any time mice appeared moribund, they were sacrificed. At the time of sacrifice, blood was drawn for a complete hematological assessment, and the mice underwent a full necropsy,

preserving selected tissues and organs and preparing slides for histopathological examination as required.

Results

The survival curves of the 24-month high-dose (4 pellet) and low-dose (2 pellet) implantation groups are shown in Figures 1 and 2 (Appendices). For clarity, the dose groups are shown in three separate panels: Panel A shows the surgical sham, tantalum, nickel, lead, tungsten/nickel/cobalt, and tungsten/nickel/iron groups. Panel B shows the single metal permutation groups (tungsten/tantalum, nickel/tantalum, cobalt/tantalum, iron/tantalum) compared to sham and tantalum control groups. The third panel group consists of the two metal permutations (tungsten/nickel/tantalum, tungsten/cobalt/tantalum, tungsten/iron/tantalum, nickel/iron/tantalum, nickel/cobalt/tantalum) as well as the sham and tantalum control groups. Because of the extended time these animals are studied, age-related health issues become a problem. As have others (6,7), we have seen a significant increase in the number of hepatic neoplasias across all groups. To better reflect the health impact of the implanted fragments while avoiding those effects due to age, we have also presented the survival data mean time to euthanasia and as the time (in weeks) it takes to reach 50% survival (SF50) for the various implantation groups (Tables 2 and 3, Appendices). For the high-dose groups, five treatments resulted in decreased survival: nickel, tungsten/nickel/cobalt, tungsten/tantalum, iron/tantalum, and tungsten/nickel/tantalum. Nickel pellet implantation resulted in a mean survival of 62 weeks while implantation with tungsten/nickel/cobalt pellets resulted in a mean survival time of 75 weeks (Table 2, Appendices). Both these results are significantly lower than control group survival. For the three other groups showing decreased survival (tungsten/tantalum; iron/tantalum; tungsten/nickel/tantalum), survival was significantly lower than control, but not as low as that see with the other 2 groups. There were three low-dose experimental groups that demonstrated decreased survival after pellet implantation: nickel, nickel/tantalum, and cobalt/tantalum. Although the results with nickel were not surprising, the decreased survival seen with the nickel/tantalum and cobalt/tantalum

was unexpected, especially since there was no significant survival difference seen in the corresponding high-dose groups. In fact, when survival between the low-dose and high-dose implantation groups is compared, survival in the high-dose groups was significantly increased over low-dose in the nickel/tantalum, cobalt/tantalum, and nickel/cobalt/tantalum implantation groups (Table 3, Appendices). The reason for this is unknown, but could represent separate metal-induced damage pathways depending upon metal concentration.

Body weight gain has been shown to be an excellent indicator of overall health in rodents, as well as a sign of systemic toxicity as a result of experimental treatments. Figures 3 and 4 (Appendices) show body weight gain for both the low- and high-dose 24-month groups. With several exceptions, most of the test pellets did not affect weight gain. Nickel-implanted groups, both low- and high-dose, exhibited decreased body weight gain compared to controls. In addition, mice implanted with tungsten/nickel/cobalt, cobalt/tantalum, nickel/tantalum, or iron/tantalum also gained weight at a slower rate than controls, but only in the high-dose groups. The body weight results for nickel and tungsten/nickel/cobalt are similar to those reported for the previously published study for metal-implanted F344 rats (2).

At necropsy, weights of several organs including spleen, kidney, liver, and testes were obtained and normalized to body weight. Tissue-to-body weight ratio often gives an indication of tissue-specific toxicities. Tissue-to-body weight ratios for the 24-month high-dose groups are shown in Tables 12 - 15 (Appendices). Only minor changes were observed as a result of any of the treatments. Surprisingly, organ-to-body weight ratios for the tungsten/nickel/cobalt-implanted B6C3F1 mouse were far different than those reported for the alloy-implanted F344 rat (2). In the rat study, large increases in spleen weight were observed in the high-dose tungsten/nickel/cobalt -implanted animals; however, no such changes were observed for the tungsten/nickel/cobalt -implanted mice.

Hematology assessments for the low- and high-dose 24-month groups are shown in Tables 20 and 21 (Appendices). The high-dose nickel-implanted mice showed a significant decrease in the number of white blood cells and total granulocyte numbers

(neutrophils, eosinophils, and basophils) compared to control. Platelet numbers were also significantly decreased in the high-dose tungsten/nickel/cobalt-implanted mice. Again, the hematological perturbations seen in the tungsten/nickel/cobalt -implanted F344 rats (elevated RBC, hemoglobin, hematocrit) (2) were not observed in the tungsten/nickel/cobalt-implanted B6C3F1 mice. The reason for this is unclear at this time. There were no significant hematological differences seen in any of the low-dose implantation groups.

Upon necropsy, tumors were found at the pellet implantation sites in both the nickel- and tungsten/nickel/cobalt-implanted groups. Tumor incidence was 100% for the nickel-implanted group and 95% for the tungsten/nickel/cobalt-implanted group (Table 22, Appendices). No indications of pellet-induced neoplasias were seen in any of the other experimental groups. An increased incidence of liver tumors was observed across all experimental groups, a finding noted by others (6,7).

Histopathological examination of the metal-associated muscle tumors indicates that they are malignant spindle cell sarcomas most likely rhabdomyosarcomas. Photomicrographs of hematoxylin-and-eosin-stained muscle sections are shown in Figure 46 (Appendices). The tumor type found in the B6C3F1 mouse model is similar to the classification of the tumors found in metal-implanted F344 rats (2). However, unlike in the rat model, the muscle tumors did not metastasize in the mouse model, nor did they exhibit the aggressive growth characteristics of the rat tumors.

Serial Sacrifice Study (Aim 2)

The serial sacrifice study ran in parallel with the two-year carcinogenicity study and also included the fifteen treatments groups. Ten male mice were employed in each treatment group. One, 3, 6, and 12 months after pellet implantation, mice were sacrificed, and gross pathologies performed. Selected tissues were collected and preserved and hematological tests performed. Histopathological surveys of selected animals were performed.

<u>Results</u>

There were no significant differences in survival between the various implantation groups at 1-, 3-, 6-, or 12-months. As with the 24-month implantation groups, at necropsy, the weights of several organs including spleen, kidney, liver, and testes were obtained and normalized to body weight. These data are found in Tables 4 - 11 in the Appendices. No signs of overt organ toxicity were noted.

Hematological assessment results from the 1-, 3-, 6-, or 12-month implantation groups can be found in Tables 16 - 19 (Appendices). In the 1-month experimental groups, the percentage of lymphocytes found in the peripheral blood is universally lower in all treatment groups compared to control, while both the percentage and total number of granulocytes are elevated. In the 3-month groups, both the percentage and total number of monocytes in the peripheral blood are significantly elevated compared to the control group. By 6-months, the percentage and total number of monocytes in the peripheral blood remains elevated and the percentage of lymphocytes decreases. In addition, red blood cell numbers, hemoglobin levels and hematocrit rise in many of the experimental groups. Lymphocyte percentage and absolute numbers decrease in the 12-month implantation groups while the percentage of monocytes and granulocytes rise. Decreases in platelet number were also observed in many of the 12-month groups.

No significant pathology findings were discovered at necropsy with the exception of metal implantation sites in the nickel- and tungsten/nickel/cobalt-implanted mice (Table 22, Appendices). In the nickel-implanted groups 60% of the mice exhibited a malignant sarcoma at the pellet implantation site, while in the tungsten/nickel/cobalt-implanted group, 40% of the mice showed sarcoma development.

Metal Levels in Tissue (Aim 3)

Metal levels in tissues obtained from mice in the two-year carcinogenicity (Aim 1) and serial euthanasia (Aim 2) studies were analyzed for metal content using inductively coupled-plasma mass spectrometry (ICP-MS). In addition, serum and urine samples were also assessed for metal content. Urine samples did not require any preparation, except dilution, prior to analysis. Serum samples, after the addition of rhodium as a recovery

standard, were wet-ashed with 3 ml of 70% nitric acid (Optima Ultrapure Grade, Fisher Scientific) and 200 µl of 30% hydrogen peroxide (Semiconductor grade, Sigma Chemical Co., St. Louis, MO) by heating to just below boiling (to avoid sample splashing) until completely evaporated. After wet-ashing, samples were dry-ashed at 600°C for 8-12 h in a muffle furnace (Fisher Isotemp Muffle Furnace, Fisher Scientific, Pittsburgh, PA) and then wet-ashed again with nitric acid and hydrogen peroxide. After the second wet-ashing, the white residue was dissolved in 2% nitric acid and analyzed. Tissue samples, prior to wet-ashing as described above, were heated in the muffle furnace for 24 h at 100°C, 24 h at 350°C, and finally 48 h at 600°C.

The metal content of the samples was determined using an inductively coupled-plasma mass spectrometer (PQ ExCell ICPMS System, ThermoElemental, Franklin, MA) equipped with a Cetac ASX500 Autosampler. High-pressure liquid argon, 99.997%, was used for the plasma gas. Instrument operating parameters are given in Table 23 of the Appendices. The instrument was calibrated with external standards of the appropriate metal standard in 2% HNO_3. The sample probe was washed with a constant flow of 2% nitric acid between measurements. Quantitative analysis was obtained by reference to the slope of the calibration curve (counts per second / ng per liter) as well as an internal standard. Tissue data were normalized to tissue weight. Serum data were normalized to the volume of serum analyzed and urine data were normalized to creatinine levels. Creatinine content was determined utilizing a modified Jaffe reaction (8,9) with a commercially available colorimetric kit (Oxford Biomedical Research, Oxford, MI).

<u>Progress/Results</u>

Metal analysis results for all experimental groups are found in Figures 5 - 45 (Appendices). The high endogenous levels of iron in the biological samples have rendered these measurements of little use in determining Fe release from the implanted pellets; however, the other metals associated with these mixtures provide an accurate indication of pellet solubility. Very little of the metals (tungsten, nickel, cobalt, tantalum) that solubilize from the implanted pellets localize to the brain. The same holds true for femur, with the exception of tungsten, which deposits in a time-dependent manner up to 12 months for the

tungsten/nickel/cobalt-implanted mice and in an inverse manner for the tungsten/nickel/iron-implanted mice. Tungsten deposition in bone was not unexpected based on the report of Leggett describing tissue distribution patterns (10). Elevated levels of pellet-associated metals were found in kidney tissue as early as 1-month post-implantation, with lesser amounts found in liver, spleen, and testes. However, the highest metal levels were found in the urine collected at necropsy. Both the tungsten/nickel/cobalt and tungsten/nickel/iron alloys degrade *in vivo* with the metals excreted in the urine. Similar results were seen in tungsten/nickel/cobalt -implanted F344 rats (11). The importance of this finding is that it indicates that urinary metal levels appear to be excellent indicators of the identity of embedded metal fragments. If these data hold, urinary metal analysis could be an important first step in identifying the composition of embedded fragments without the need for invasive and potentially destructive surgical retrieval.

KEY RESEARCH ACCOMPLISHMENTS

- All experimental aims as detailed in the Statement of Work have been accomplished.
- Mice in the 24-month low- and high-dose nickel and tungsten/nickel/cobalt cohorts developed tumors at the pellet implantation sites.
- No pellet-associated tumors were found in any other experimental group, including the tungsten/nickel/iron alloy group.
- Time to tumor development in the B6C3F1 mouse was far slower than in the F344 rat.
- Tumors were identified as rhabdomyosarcomas.
- Tumors were not aggressive growing and did not metastasize to other organ systems.
- Metal analysis using inductively coupled-plasma mass spectrometry showed that both the tungsten/nickel/cobalt and tungsten/nickel/iron pellets degraded *in vivo* with the associated metals excreted in the urine. The tungsten/nickel/iron alloy appeared to degrade at a much slower rate than the tungsten/nickel/cobalt. Nonetheless, urinary metal analysis appears to be an excellent method by which to

preliminarily identify the composition of embedded fragments without the need for invasive surgical retrieval.

REPORTABLE OUTCOMES

Oral Presentations

Kalinich, JF (23 March 07) Health Effects of Embedded Tungsten Alloy and Depleted Uranium. AFRRI Seminar. Bethesda, MD.

Kalinich, JF (29 May 07) Health Effects of Embedded Tungsten Alloy. Briefing to Deputy Undersecretary of Defense for Acquisition, Technology, and Logistics and Deputy Assistant Secretary of Defense for Force Health Protection and Readiness. Arlington, VA.

Kalinich, JF (24 July 07) Tissue Distribution Patterns of Tungsten Alloy Component Metals from Embedded Fragments. Presentation at the Force Health Protection Embedded Fragment Working Group Meeting. Falls Church, VA.

Kalinich, JF (06 November 07) Health Effects of Embedded Tungsten Alloy. Presentation at the Baltimore Veterans Administration Medical Center / Toxic Embedded Fragment Center. Baltimore, MD.

Kalinich, JF (09 January 08) Health Effects of Embedded Tungsten Alloy. Presentation at the Baltimore Veterans Administration Medical Center / Toxic Embedded Fragment Center's Expert Panel Meeting. Baltimore, MD.

Kalinich, JF (14 March 08) Health Effects of Embedded Fragments. AFRRI Seminar. Bethesda, MD.

Kalinich, JF (12 August 08) Carcinogenicity of Embedded Tungsten Alloys. Force Health Protection Conference. Albuquerque, NM.

Kalinich, JF (30 April 09) Carcinogenicity of Embedded Tungsten Alloys. Toxicology and Risk Assessment Conference. Cincinnati, OH.

Kalinich, JF (02 June 09) Health Effects of Embedded Fragments. Briefing to Dr. W.W. Cheatham, Director of Clinical Research, U.S. Navy Bureau of Medicine. Bethesda, MD.

Kalinich, JF (05 November 09) Carcinogenicity of Embedded Tungsten Alloys:

Update of AFRRI Research. Briefing to CAPT Alan Cowan, United Kingdom Ministry of Defense Liaison Officer to the U.S. Department of Defense Force Health Protection Office. Bethesda, MD.

Kalinich, JF (5 March 10) Health Effects of Embedded Fragments. AFRRI Seminar. Bethesda, MD.

Kalinich, JF (25 May 10) Health Effects of Embedded Fragments. Briefing to the Walter Reed Army Medical Center Perioperative Nursing Staff. Washington, DC.

Kalinich, JF (10 August 10) Carcinogenicity of Embedded Tungsten Alloys. Force Health Protection Conference. Phoenix, AZ.

Kalinich, JF (8 December 10) Health Effects of Embedded Tungsten Alloys. Society for Risk Assessment and Analysis. Salt Lake City, UT.

Book Chapter

Kalinich, JF "Heavy Metal-Induced Carcinogenicity: Depleted Uranium and Heavy-Metal Tungsten Alloy" in Cellular Effects of Heavy Metals (G. Banfalvi, editor), Springer Science Media (in press, 2011, see Appendices).

CONCLUSION

A variety of tungsten alloys have been proposed as replacements for depleted uranium in armor-penetrating munitions. One of these formulations, tungsten/nickel/cobalt, was shown to induce highly aggressive rhabdomyosarcomas when embedded into the leg muscles of F344 rats (2). The need to confirm the carcinogenicity of such alloys in another rodent species is an important second step required in biological as well as regulatory terms to better assess the cancer risk in humans. Results of this work will help in formulating policies for military surgeons who must treat personnel wounded by fragments of the alloys. Indications of unacceptable risks of exposure will also help determine the advisability of deploying (or developing) similar munitions.

The results from this study showed that tungsten/nickel/cobalt pellets, implanted into the quadriceps muscle of male B6C3F1 mice, induced tumor formation at the implantation site. Mice with nickel-implanted pellets also developed tumors. No other

experimental groups including the militarily relevant alloy, tungsten/nickel/iron, exhibited tumor formation. The implantation site tumors were identified as rhabdomyosarcomas. Unlike those in the F344 rat model, these tumors were not rapidly growing and did not metastasize to other organ systems. Although tumor development was much slower than that observed in the F344 rat (2), it was not unexpected considering the long latency period for implanted-metal carcinogenesis in the B6C3F1 mouse reported by others (12,13). In addition, the hematological and splenic changes induced by tungsten/nickel/cobalt in the F344 rat were not observed in the B6C3F1 mouse.

Metal analysis demonstrated that the implanted pellets degrade *in vivo* and the solubilized metals can localize to a variety of tissues, including liver, spleen, testes, and kidney. However, most of the solubilized metals are excreted in the urine suggesting that, in many cases, the components of an embedded fragment may be able to be preliminarily identified by urinary metal measurements.

The results of this research and our previous studies on embedded metal fragments demonstrates the need for basic toxicity studies on components of new munitions systems prior to extensive development and deployment of those systems.

REFERENCES

1. Miller AC, Mog S, McKinney L, Luo L, Allen J, Xu J, Page N: Neoplastic transformation of human osteoblast cells to the tumorigenic phenotype by heavy metal-tungsten alloy particles: induction of genotoxic effects. Carcinogenesis 22: 115-125 (2001).
2. Kalinich JF, Emond CA, Dalton TK, Mog SR, Coleman GD, Kordell JE, Miller AC, McClain DE: Embedded weapons-grade tungsten alloy shrapnel rapidly induces metastatic high-grade rhabdomyosarcomas in F344 rats. Environmental Health Perspectives 113: 729-734 (2005).
3. Institute of Laboratory Animal Resources. Guide for the Care and Use of Laboratory Animals. 8^{th} edition. Washington, DC: National Academy Press, (2011).

4. Castro CA, Benson KA, Bogo V, Daxon EG, Hogan JB, Jacocks HM, Landauer MR, McBride SA, Shehata CW: Establishment of an animal model to evaluate the biological effects of intramuscularly embedded depleted uranium fragments. AFRRI Technical Report TR96-3, (1996).
5. Pellmar TC, Fuciarelli AF, Ejnik JW, Hamilton M, Hogan J, Strocko S, Emond C, Mottaz HM, Landauer MR: Distribution of uranium in rats implanted with depleted uranium pellets. Toxicological Sciences 49: 29-39 (1999).
6. Tamano S, Hagiwara A, Shibata M-A, Kurata Y, Fukushima S, Ito N: Spontaneous tumors in aging (C57BL/6N X C3H/HeN)F1 (B6C3F1) Mice. Toxicologic Pathology 16: 321-326 (1988).
7. Eiben R: Frequency and time trends of spontaneous tumors found in B6C3F1 mice oncogenicity studies over 10 years. Experimental and Toxicologic Pathology 53: 399-408 (2001).
8. Slot C: Plasma creatinine determination. A new and specific Jaffe reaction method. Scandinavian Journal of Clinical Laboratory Investagation 17: 381-7 (1965).
9. Heinegard D, Tiderstrom G: Determination of serum creatinine by a direct colorimetric method. Clinica Chimica Acta 43: 305-10 (1973).
10. Leggett RW: A model of the distribution and retention of tungsten in the human body. Science of the Total Environment 206: 147-165 (1997).
11. Kalinich JF, Vergara VB, Emond CA: Urinary metal levels as indicators of embedded tungsten alloy fragments. Military Medicine 173: 754-758 (2008).
12. Rodriguez RE, Misra M, Diwan BA, Riggs CW, Kasprzak KS: Relative susceptibilities of C57BL/6, (C57BL/6 x C3H/He) F1, and C3H/He mice to acute toxicity and carcinogenicity of nickel subsulfide. Toxicology 107: 131-140 (1996).
13. Hahn H, Nitzki F, Schorban T, Hemmerlein B, Threadgill D, Rosemann M: Genetic mapping of a *Ptch1*-associated rhabdomyosarcoma susceptibility locus on mouse chromosome 2. Genomics 84: 853-858 (2004).

APPENDICES

Table 1: Pellet Compositions.

Pellet / Metal (%)	W	Ni	Co	Fe	Ta	Pb
Tantalum (Ta)					100	
Nickel (Ni)		100				
Lead (Pb)						100
Tungsten / Nickel / Cobalt (WNiCo)	91.1	6.0	2.9			
Tungsten / Nickel / Iron (WNiFe)	91.0	7.0		2.0		
Tungsten / Tantalum (WTa)	91.1				8.9	
Nickel / Tantalum (NiTa)		6.0			94.0	
Cobalt / Tantalum (CoTa)			2.9		97.1	
Iron / Tantalum (FeTa)				2.0	98.0	
Tungsten / Nickel / Tantalum (WNiTa)	91.1	6.0			2.9	
Tungsten / Cobalt / Tantalum (WCoTa)	91.1		2.9		6.0	
Tungsten / Iron / Tantalum (WFeTa)	91.0			2.0	7.0	
Nickel / Iron / Tantalum (NiFeTa)		6.0		2.0	92.0	
Nickel / Cobalt / Tantalum (NiCoTa)		6.0	2.9		91.1	

Figure 1: Survival Curves of 24-Month High-Dose (4-Pellet) Implantation Groups

A.

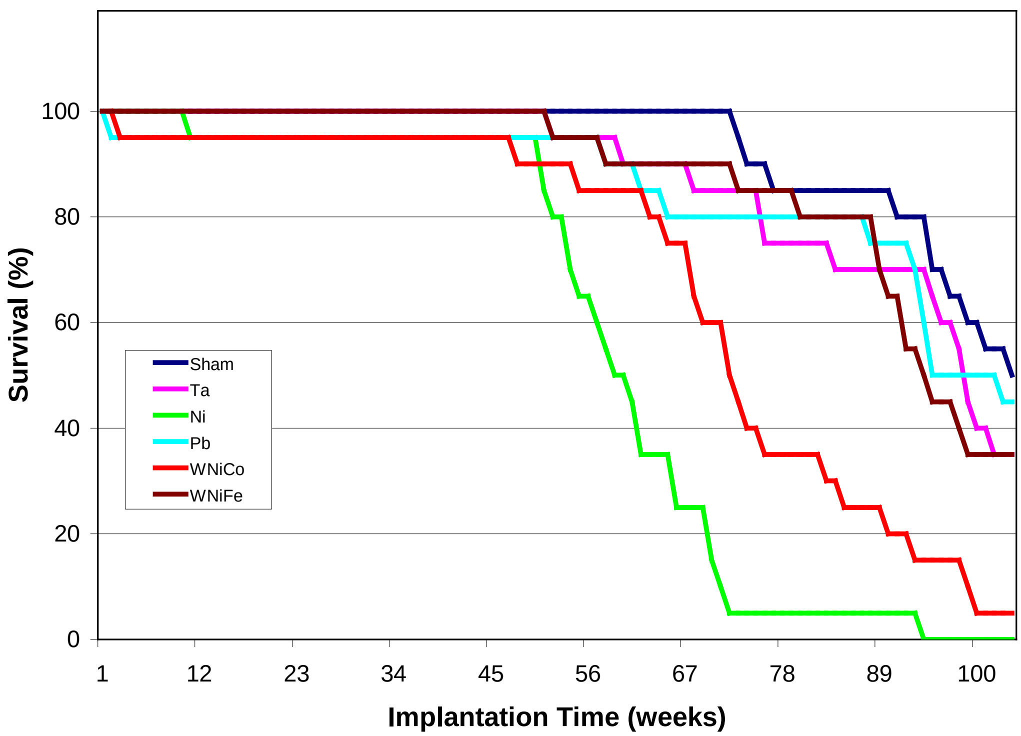

Figure 1 (continued): Survival Curves of 24-Month High-Dose (4-Pellet) Implantation Groups

B.

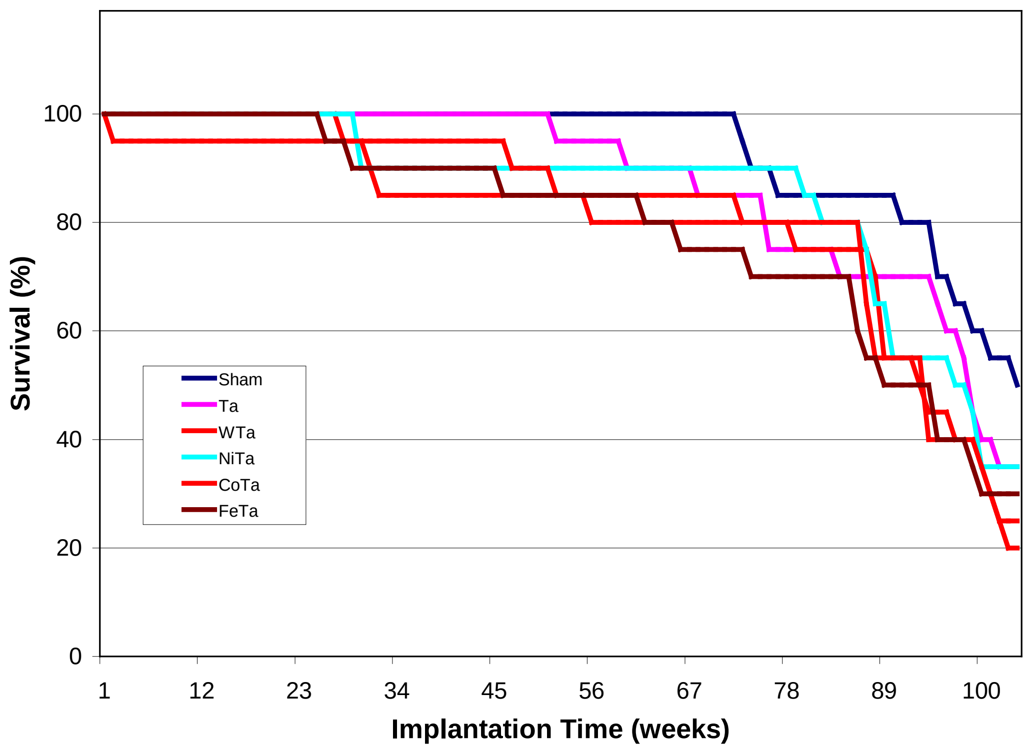

Figure 1 (continued): Survival Curves of 24-Month High-Dose (4-Pellet) Implantation Groups

C.

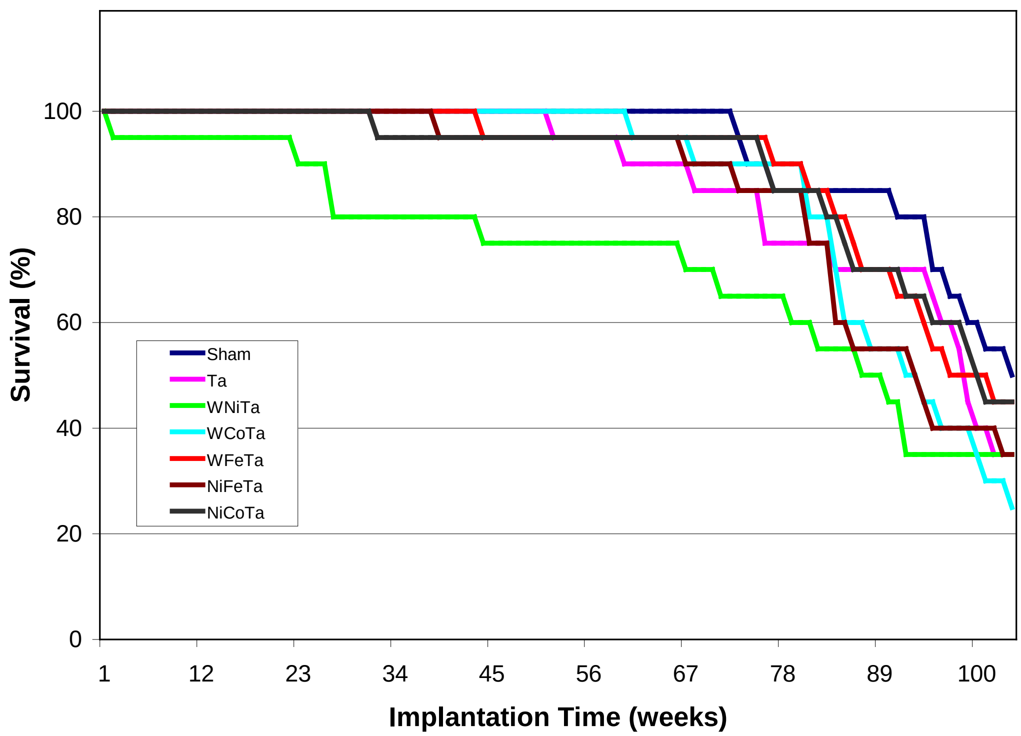

Figure 2: Survival Curves of 24-Month Low-Dose (2-Pellet) Implantation Groups

A.

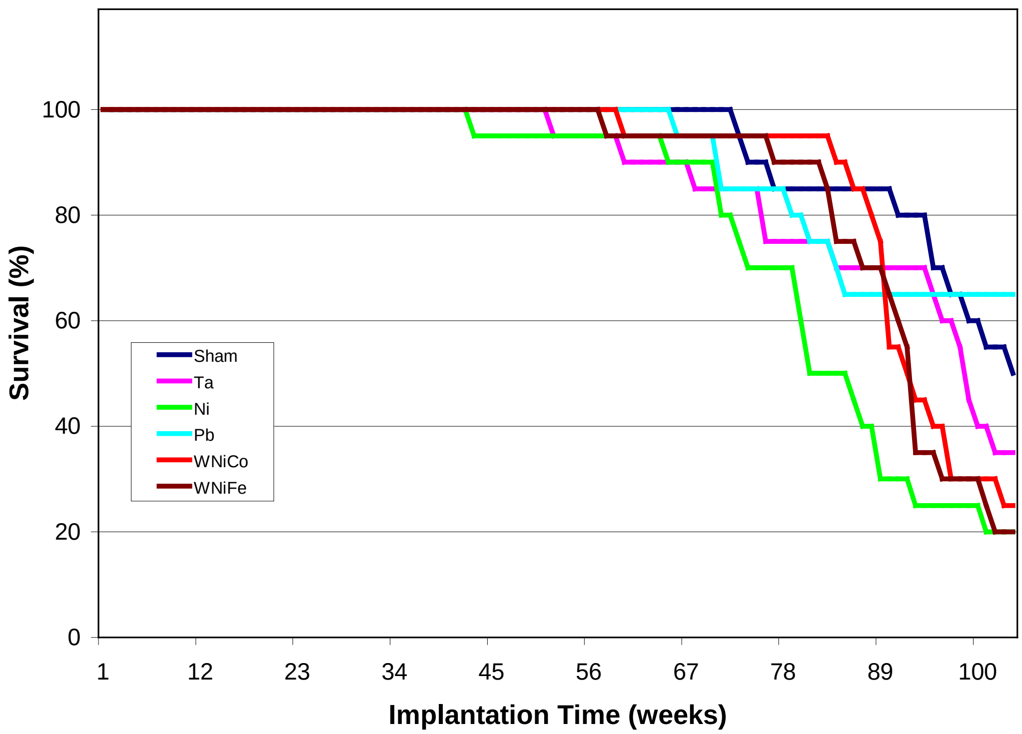

Figure 2 (continued): Survival Curves of 24-Month Low-Dose (2-Pellet) Implantation Groups

B.

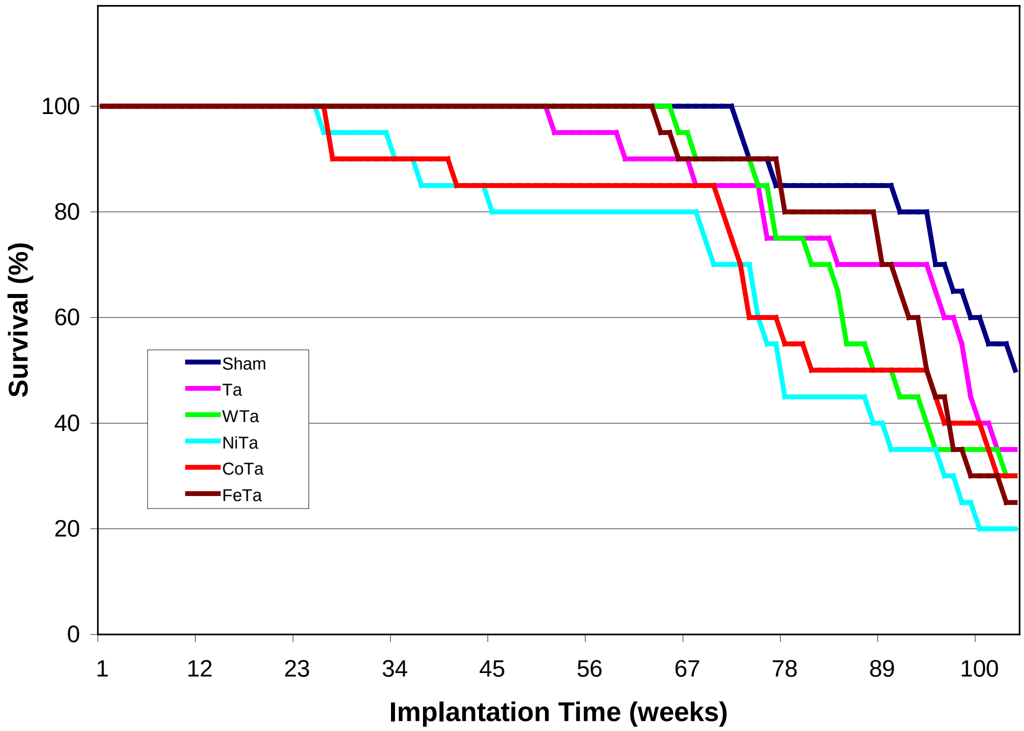

Figure 2 (continued): Survival Curves of 24-Month Low-Dose (2-Pellet) Implantation Groups

C.

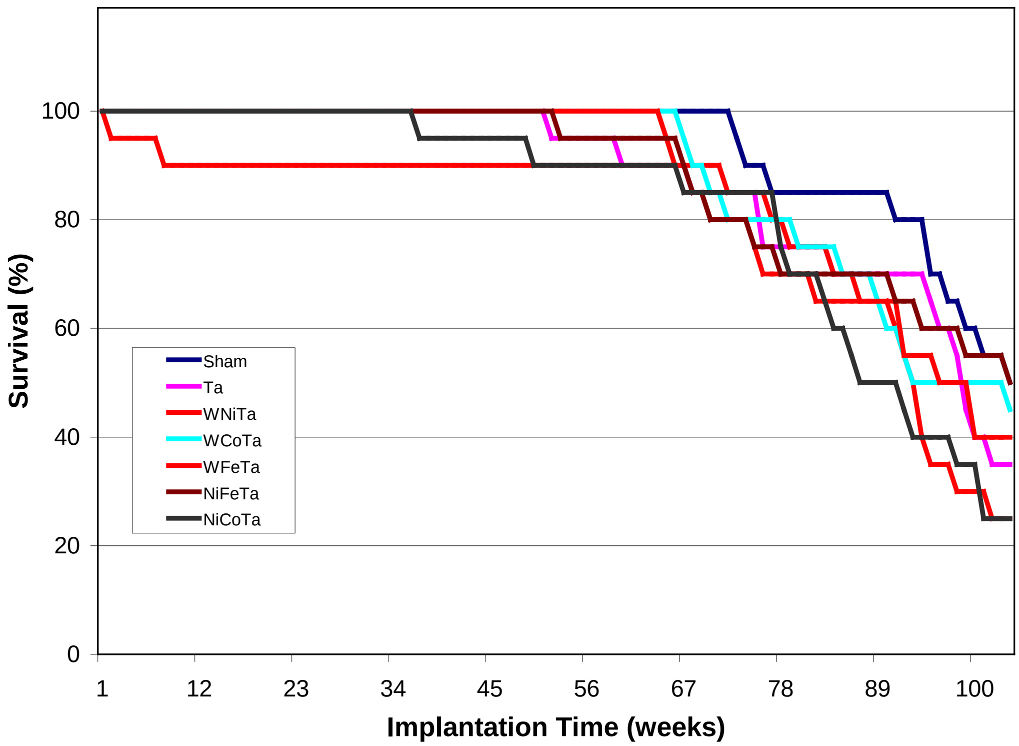

Table 2: Age (in weeks) at Euthanasia for Low- and High-Dose 24-Month Implantation Groups.

	Low-Dose	High-Dose
Sham	96.8 ± 2.4	96.8 ± 2.4
Ta	91.5 ± 2.5	91.5 ± 2.5
Ni	83.2 ± 3.6 *	62.1 ± 2.4 *
Pb	94.1 ± 3.2	93.4 ± 3.6
WNiCo	92.3 ± 2.5	75.5 ± 3.5 *
WNiFe	90.8 ± 2.7	90.9 ± 3.5
WTa	88.8 ± 3.1	83.6 ± 5.9 *
NiTa	78.5 ± 5.4 *	88.7 ± 4.9
CoTa	77.2 ± 6.3 *	89.8 ± 3.7
FeTa	91.2 ± 3.1	82.5 ± 5.7 *
WNiTa	89.0 ± 4.2	78.8 ± 6.7 *
WCoTa	91.8 ± 3.2	91.7 ± 2.6
WFeTa	90.1 ± 3.5	93.0 ± 3.4
NiFeTa	91.5 ± 3.8	88.8 ± 3.7
NiCoTa	87.5 ± 3.8	95.5 ± 2.4

Data represent the mean of 20 independent observations. Error represents standard error of the mean. An * indicates a statistically significant difference from control (sham) at $P < 0.05$ as determined by one-way ANOVA followed by Dunnett's test for group mean comparisons.

Table 3: Weeks to Fifty Percent Survival (SF50) for Low- and High-Dose 24-Month Implantation Groups.

	Low-Dose	High-Dose
Sham	104	104
Ta	98	98
Ni	81	59
Pb	104	95
WNiCo	92	72
WNiFe	92	94
WTa	88	93
NiTa	77	97
CoTa	81	93
FeTa	94	89
WNiTa	93	87
WCoTa	93	92
WFeTa	96	97
NiFeTa	104	93
NiCoTa	87	100

Data represent the time (in weeks) after implantation at which 50% of the mice were surviving. Maximum time would be 104 weeks (24 months).

Figure 3: Effect of Pellet Implantation on Body Weight Gain in High-Dose (4 Pellet) Groups

A.

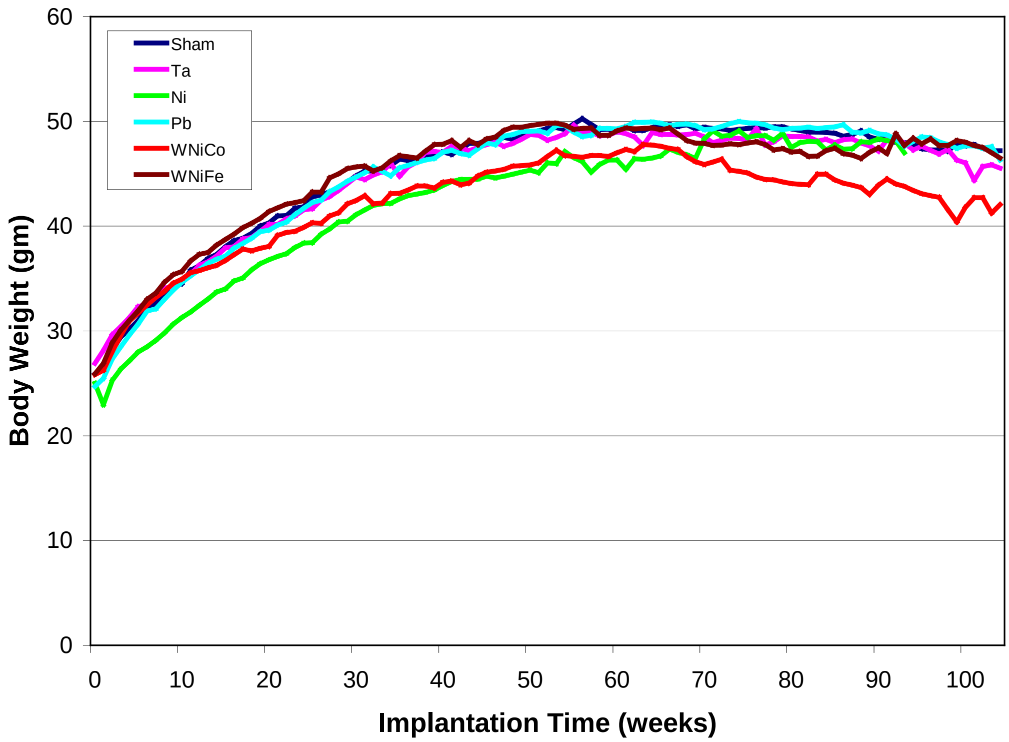

Figure 3 (continued): Effect of Pellet Implantation on Body Weight Gain in High-Dose (4 Pellet) Groups

B.

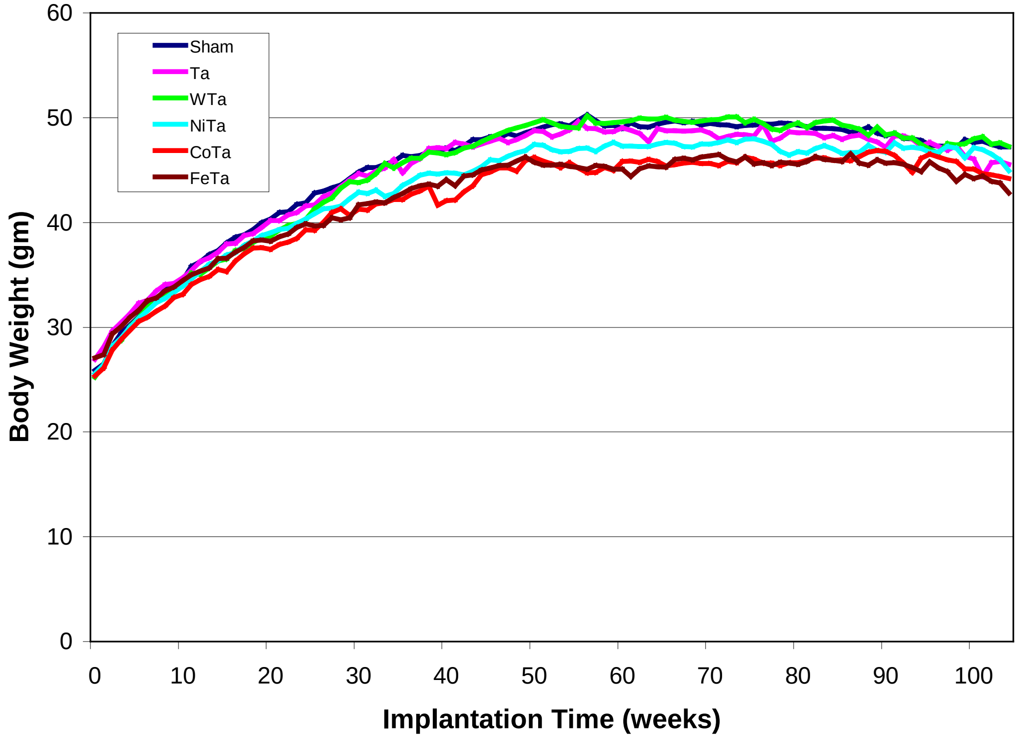

Figure 3 (continued): Effect of Pellet Implantation on Body Weight Gain in High-Dose (4 Pellet) Groups

C.

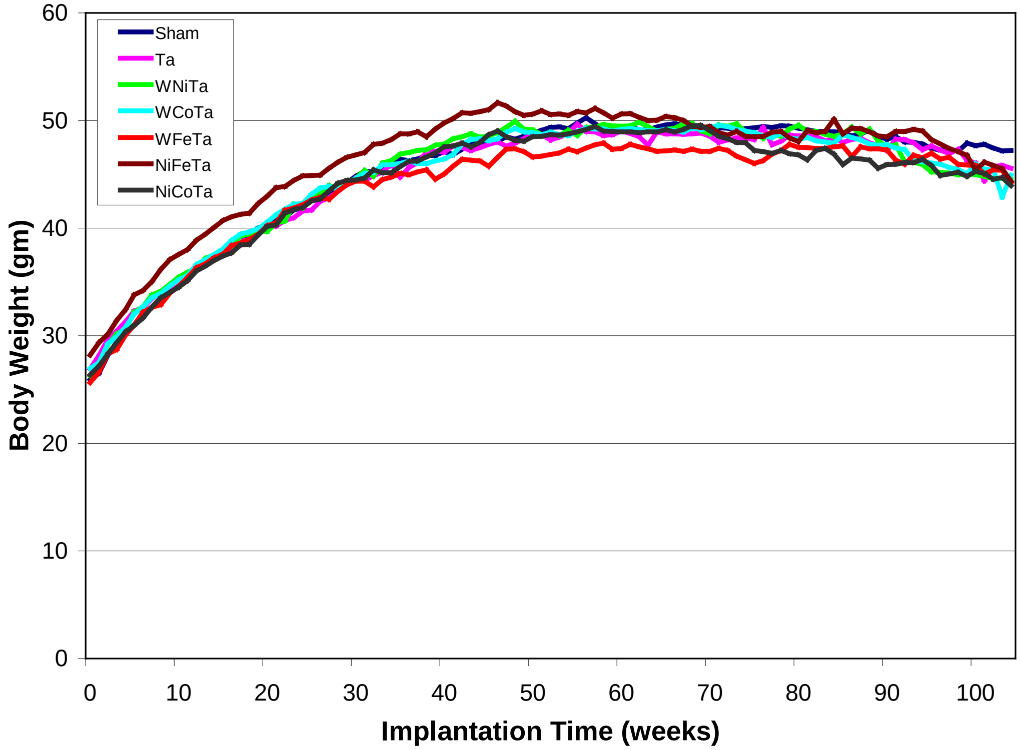

Figure 4: Effect of Pellet Implantation on Body Weight Gain in Low-Dose (2 Pellet) Groups

A.

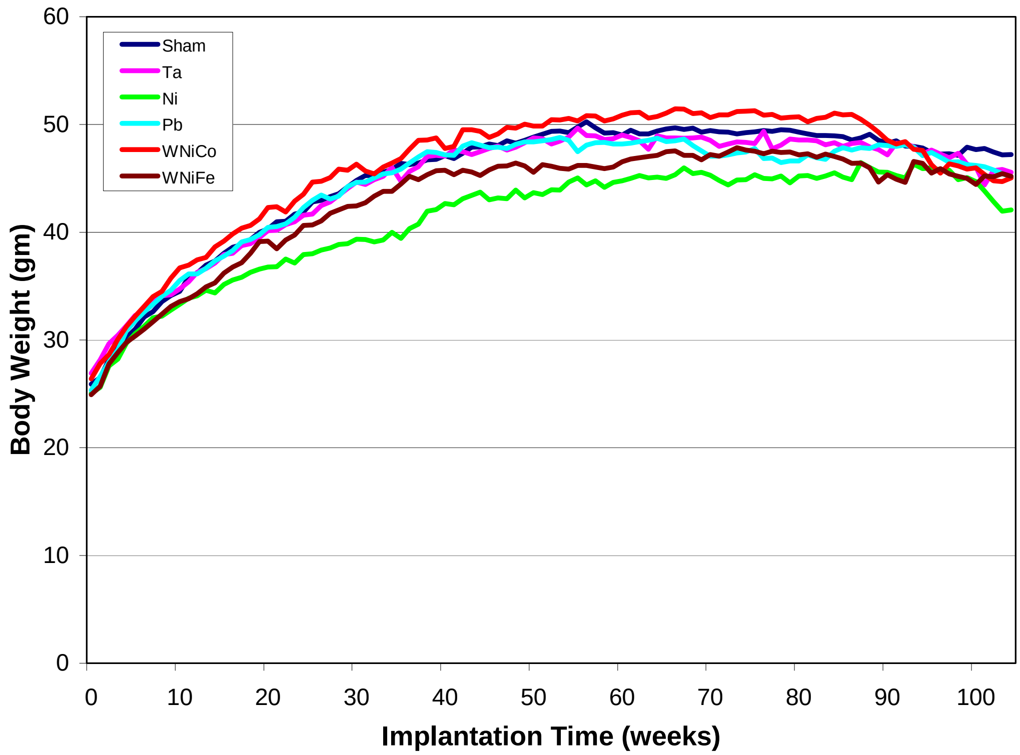

Figure 4 (continued): Effect of Pellet Implantation on Body Weight Gain in Low-Dose (2 Pellet) Groups

B.

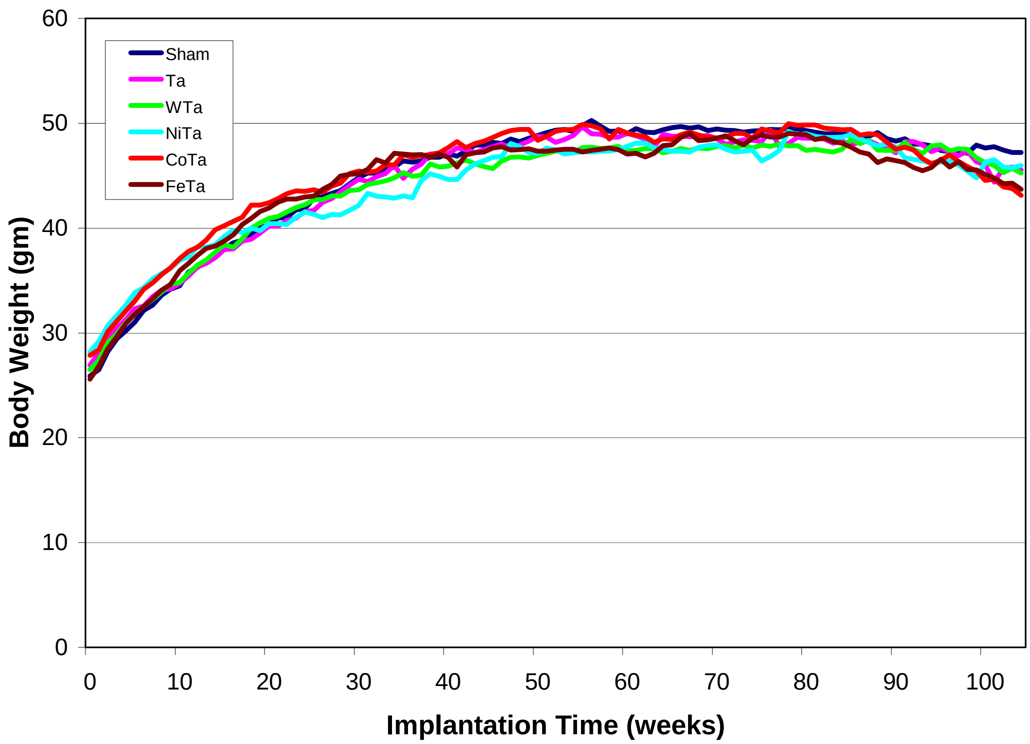

Figure 4 (continued): Effect of Pellet Implantation on Body Weight Gain in Low-Dose (2 Pellet) Groups

C.

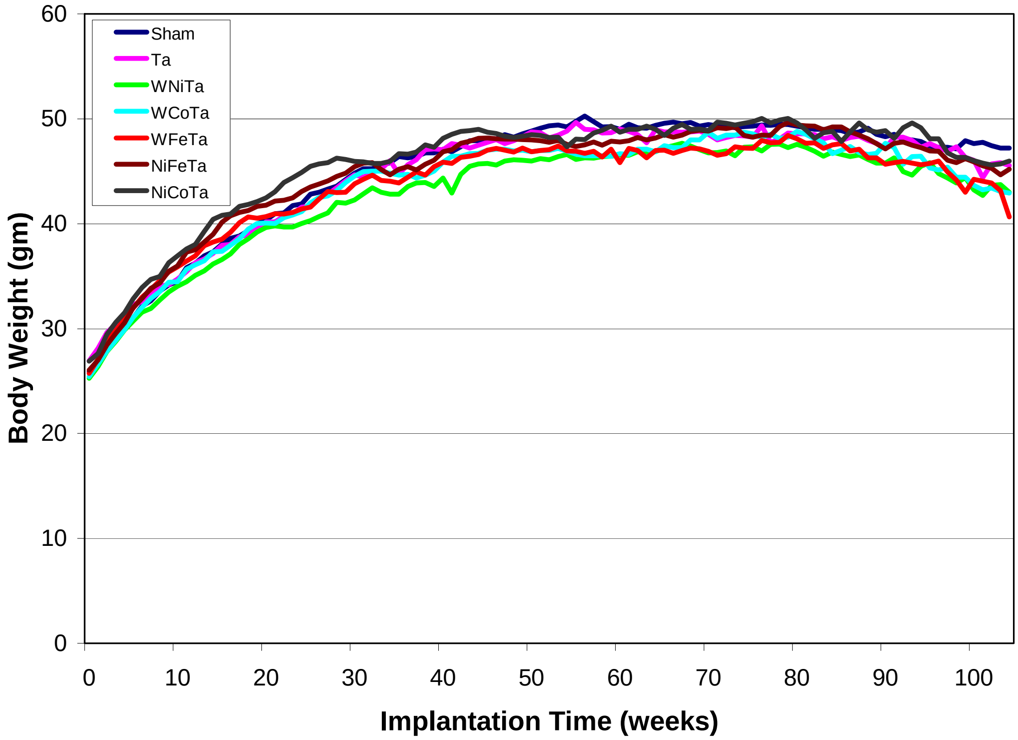

Table 4: Organ Weights from Mice in 1-month High-dose Implantation Groups

Group \ Organ	Spleen (gm)	Kidney (gm)	Liver (gm)	Testes (gm)
Sham	0.077 ± 0.003	0.437 ± 0.010	1.359 ± 0.032	0.203 ± 0.007
Ta	0.091 ± 0.007	0.446 ± 0.009	1.580 ± 0.046 *	0.206 ± 0.004
Ni	0.133 ± 0.006 *	0.424 ± 0.011	1.482 ± 0.067	0.204 ± 0.004
Pb	0.095 ± 0.008	0.451 ± 0.014	1.525 ± 0.061*	0.210 ± 0.007
WNiCo	0.119 ± 0.019	0.418 ± 0.012	1.445 ± 0.055	0.191 ± 0.005
WNiFe	0.100 ± 0.010	0.440 ± 0.010	1.442 ± 0.059	0.197 ± 0.010
WTa	0.084 ± 0.005	0.443 ± 0.009	1.430 ± 0.025	0.211 ± 0.005
NiTa	0.108 ± 0.009 *	0.477 ± 0.012 *	1.569 ± 0.054 *	0.199 ± 0.017
CoTa	0.130 ± 0.019 *	0.477 ± 0.015	1.543 ± 0.063 *	0.211 ± 0.004
FeTa	0.119 ± 0.016	0.463 ± 0.010	1.561 ± 0.048 *	0.206 ± 0.005
WNiTa	0.098 ± 0.008	0.442 ± 0.019	1.542 ± 0.079	0.199 ± 0.006
WCoTa	0.112 ± 0.016	0.464 ± 0.023	1.543 ± 0.058 *	0.211 ± 0.008
WFeTa	0.090 ± 0.007	0.488 ± 0.009 *	1.524 ± 0.048 *	0.212 ± 0.006
NiFeTa	0.103 ± 0.009 *	0.469 ± 0.014	1.515 ± 0.049 *	0.200 ± 0.007
NiCoTa	0.085 ± 0.005	0.454 ± 0.018	1.470 ± 0.050	0.198 ± 0.012

Data are the mean of 10 independent observations. Error represents standard error of the mean. An * indicates a result that is statistically different than control (sham) at $P < 0.05$ using one-way ANOVA followed by Dunnett's test for group mean comparisons.

Table 5: Organ Body Weight Ratios from Mice in 1-month High-dose Implantation Groups

Group \ Organ/BW	Spleen / BW (mg/gm)	Kidney / BW (mg/gm)	Liver / BW (mg/gm)	Testes / BW (mg/gm)
Sham	2.632 ± 0.103	14.961 ± 0.203	46.540 ± 0.646	6.970 ± 0.237
Ta	2.924 ± 0.193	14.388 ± 0.230	51.053 ±1.364*	6.662 ± 0.145
Ni	4.573 ± 0.211 *	14.548 ± 0.181	50.615 ± 1.183	7.009 ± 0.163
Pb	3.039 ± 0.199	14.544 ± 0.219	49.151 ±1.210*	6.810 ± 0.263
WNiCo	3.961 ± 0.560	14.225 ±0.119*	49.105 ± 0.793	6.551 ±0.205
WNiFe	3.217 ± 0.295	14.328 ±0.135*	46.886 ± 1.391	6.425 ± 0.350
WTa	2.822 ± 0.187	14.784 ± 0.232	47.719 ± 0.555	7.023 ± 0.139
NiTa	3.328 ± 0.229 *	14.891 ± 0.156	48.891 ±0.872*	6.272 ± 0.570
CoTa	4.132 ± 0.560 *	15.302 ± 0.218	49.393 ±1.248*	6.793 ± 0.225
FeTa	3.816 ± 0.514	14.834 ± 0.215	49.999 ±1.072*	6.622 ± 0.218
WNiTa	3.146 ± 0.210	14.295 ± 0.215	49.701 ± 0.699	6.497 ± 0.265
WCoTa	3.515 ± 0.458	14.729 ± 0.400	49.271 ±1.367*	6.753 ± 0.248
WFeTa	2.807 ± 0.184	15.320 ± 0.297	47.662 ±0.863*	6.651 ± 0.218
NiFeTa	3.270 ± 0.278	14.881 ± 0.262	48.056 ±0.889*	6.358 ± 0.209
NiCoTa	2.654 ± 0.094	14.298 ± 0.226	46.314 ± 0.378	6.306 ± 0.391

Data are the mean of 10 independent observations. Error represents standard error of the mean. An * indicates a result that is statistically different than control (sham) at $P < 0.05$ using one-way ANOVA followed by Dunnett's test for group mean comparisons.

Table 6: Organ Weights from Mice in 3-month High-dose Implantation Groups

Group \ Organ	Spleen (gm)	Kidney (gm)	Liver (gm)	Testes (gm)
Sham	0.103 ± 0.009	0.456 ± 0.008	1.538 ± 0.039	0.221 ± 0.003
Ta	0.095 ± 0.007	0.491 ± 0.010*	1.746 ± 0.039*	0.221 ± 0.003
Ni	0.097 ± 0.006	0.491 ± 0.013	1.550 ± 0.052	0.219 ± 0.003
Pb	0.105 ± 0.010	0.451 ± 0.011	1.489 ± 0.061	0.216 ± 0.004
WNiCo	0.090 ± 0.015	0.472 ± 0.006	1.451 ± 0.025	0.202 ± 0.018
WNiFe	0.100 ± 0.010	0.480 ± 0.011	1.629 ± 0.051	0.222 ± 0.006
WTa	0.095 ± 0.005	0.500 ± 0.014*	1.786 ± 0.059*	0.222 ± 0.005
NiTa	0.119 ± 0.010	0.557 ± 0.017*	1.954 ± 0.071*	0.232 ± 0.002*
CoTa	0.116 ± 0.010	0.489 ± 0.015	1.773 ± 0.069*	0.218 ± 0.010
FeTa	0.094 ± 0.011	0.472 ± 0.011	1.575 ± 0.039	0.224 ± 0.007
WNiTa	0.097 ± 0.005	0.470 ± 0.010	1.610 ± 0.163	0.216 ± 0.004
WCoTa	0.130 ± 0.011	0.519 ± 0.009*	1.728 ± 0.046*	0.217 ± 0.004
WFeTa	0.134 ± 0.013	0.517 ± 0.016*	1.747 ± 0.057*	0.206 ± 0.005
NiFeTa	0.104 ± 0.011	0.502 ± 0.014*	1.755 ± 0.070*	0.220 ± 0.005
NiCoTa	0.086 ± 0.004	0.459 ± 0.010	1.627 ± 0.047	0.217 ± 0.006

Data are the mean of 10 independent observations. Error represents standard error of the mean. An * indicates a result that is statistically different than control (sham) at $P < 0.05$ using one-way ANOVA followed by Dunnett's test for group mean comparisons.

Table 7: Organ Body Weight Ratios from Mice in 3-month High-dose Implantation Groups

Organ/BW Group	Spleen / BW (mg/gm)	Kidney / BW (mg/gm)	Liver / BW (mg/gm)	Testes / BW (mg/gm)
Sham	3.016 ± 0.231	13.436 ± 0.341	45.162 ± 0.691	6.520 ± 0.146
Ta	2.552 ± 0.186	13.247 ± 0.243	47.140 ± 1.041	5.957 ± 0.082*
Ni	3.026 ± 0.147	15.400 ±0.207*	48.451 ±0.346*	6.910 ± 0.199
Pb	3.104 ± 0.296	13.311 ± 0.258	43.803 ± 1.261	6.386 ± 0.182
WNiCo	2.656 ± 0.485	13.721 ± 0.350	42.131 ± 1.003	5.884 ± 0.538
WNiFe	2.831 ± 0.314	13.546 ± 0.330	45.966 ± 1.355	6.286 ± 0.222
WTa	2.495 ± 0.137	13.084 ± 0.281	46.735 ± 1.036	5.818 ± 0.145*
NiTa	3.007 ± 0.242	14.092 ± 0.315	49.435 ±1.518*	5.884 ± 0.097*
CoTa	3.214 ± 0.228	13.649 ± 0.306	49.413 ±1.034*	6.129 ± 0.332
FeTa	2.748 ± 0.316	13.782 ± 0.187	45.995 ± 0.848	6.552 ± 0.243
WNiTa	2.638 ± 0.153	12.819 ± 0.169	43.468 ± 4.242	5.891 ± 0.093*
WCoTa	3.571 ± 0.316	14.255 ± 0.187	47.435 ± 0.985	5.969 ± 0.109*
WFeTa	3.672 ± 0.386	14.145 ± 0.361	47.830 ± 1.353	5.643 ± 0.137*
NiFeTa	2.769 ± 0.250	13.483 ± 0.265	47.029 ± 1.223	5.913 ± 0.172*
NiCoTa	2.431± 0.102	12.986 ± 0.305	45.945 ± 0.750	6.166 ± 0.236

Data are the mean of 10 independent observations. Error represents standard error of the mean. An * indicates a result that is statistically different than control (sham) at $P < 0.05$ using one-way ANOVA followed by Dunnett's test for group mean comparisons.

Table 8: Organ Weights from Mice in 6-month High-dose Implantation Groups

Organ / Group	Spleen (gm)	Kidney (gm)	Liver (gm)	Testes (gm)
Sham	0.103 ± 0.010	0.525 ± 0.025	1.744 ± 0.091	0.231 ± 0.009
Ta	0.116 ± 0.011	0.699 ± 0.180	1.799 ± 0.075	0.220 ± 0.008
Ni	0.126 ± 0.027	0.528 ± 0.011	1.966 ± 0.166	0.229 ± 0.003
Pb	0.103 ± 0.008	0.530 ± 0.011	1.784 ± 0.063	0.221 ± 0.004
WNiCo	0.073 ± 0.001	0.492 ± 0.012	1.702 ± 0.048	0.219 ± 0.006
WNiFe	0.096 ± 0.004	0.508 ± 0.008	1.764 ± 0.042	0.214 ± 0.007
WTa	0.103 ± 0.005	0.561 ± 0.018	1.862 ± 0.027	0.227 ± 0.006
NiTa	0.096 ± 0.008	0.547 ± 0.017	1.902 ± 0.078	0.222 ± 0.006
CoTa	0.123 ± 0.013	0.548 ± 0.015	1.910 ± 0.058	0.224 ± 0.005
FeTa	0.107 ± 0.007	0.556 ± 0.021	1.945 ± 0.052	0.227 ± 0.007
WNiTa	0.108 ± 0.010	0.547 ± 0.011	1.866 ± 0.063	0.219 ± 0.003
WCoTa	0.082 ± 0.003	0.519 ± 0.013	1.668 ± 0.055	0.221 ± 0.005
WFeTa	0.086 ± 0.005	0.545 ± 0.013	1.684 ± 0.029	0.229 ± 0.004
NiFeTa	0.107 ± 0.008	0.535 ± 0.012	1.898 ± 0.043	0.216 ± 0.003
NiCoTa	0.108 ± 0.007	0.563 ± 0.023	2.071 ± 0.074	0.220 ± 0.006

Data are the mean of 10 independent observations. Error represents standard error of the mean. An * indicates a result that is statistically different than control (sham) at $P < 0.05$ using one-way ANOVA followed by Dunnett's test for group mean comparisons.

Table 9: Organ Body Weight Ratios from Mice in 6-month High-dose Implantation Groups

Group \ Organ/BW	Spleen / BW (mg/gm)	Kidney / BW (mg/gm)	Liver / BW (mg/gm)	Testes / BW (mg/gm)
Sham	2.445 ± 0.195	12.619 ± 0.312	41.839 ± 1.221	5.565 ± 0.150
Ta	2.851 ± 0.278	16.371 ± 3.332	43.962 ± 0.753	5.395 ± 0.150
Ni	3.256 ± 0.785	13.400 ± 0.272	50.285 ± 5.032	5.821 ± 0.117
Pb	2.683 ± 0.197	13.942 ±0.241*	46.865 ±1.429*	5.822 ± 0.111
WNiCo	1.842 ± 0.051	12.324 ± 0.134	42.603 ± 0.393	5.480 ± 0.096
WNiFe	2.357 ± 0.118	12.407 ± 0.209	43.057 ± 0.737	5.230 ± 0.195
WTa	2.578 ± 0.138	13.976 ±0.407*	46.377 ±0.693*	5.670 ± 0.174
NiTa	2.475 ± 0.201	14.184 ± 0.667	49.281 ± 2.608	5.718 ± 0.120
CoTa	3.100 ± 0.405	13.567 ± 0.257	47.231 ±0.965*	5.556 ± 0.137
FeTa	2.507 ± 0.173	13.021 ± 0.392	45.619 ± 1.044	5.328 ± 0.206
WNiTa	2.724 ± 0.244	13.754 ±0.289*	46.901 ±1.448*	5.506 ± 0.138
WCoTa	2.022 ± 0.063	12.860 ± 0.392	41.195 ± 1.042	5.479 ± 0.129
WFeTa	2.220 ± 0.148	13.968 ±0*.294	43.181 ± 0.955	5.869 ± 0.103
NiFeTa	2.642 ± 0.205	13.222 ± 0.304	46.853 ±0.824*	5.355 ± 0.139
NiCoTa	2.503 ± 0.168	12.968 ± 0.225	47.906 ±1.316*	5.097 ± 0.079

Data are the mean of 10 independent observations. Error represents standard error of the mean. An * indicates a result that is statistically different than control (sham) at P < 0.05 using one-way ANOVA followed by Dunnett's test for group mean comparisons.

Table 10: Organ Weights from Mice in 12-month High-dose Implantation Groups

Group \ Organ	Spleen (gm)	Kidney (gm)	Liver (gm)	Testes (gm)
Sham	0.118 ± 0.006	0.623 ± 0.015	2.090 ± 0.071	0.229 ± 0.004
Ta	0.135 ± 0.011	0.660 ± 0.022	2.135 ± 0.047	0.227 ± 0.007
Ni	0.140 ± 0.017	0.667 ± 0.020	1.922 ± 0.099	0.230 ± 0.009
Pb	0.120 ± 0.006	0.612 ± 0.025	2.131 ± 0.091	0.224 ± 0.010
WNiCo	0.129 ± 0.021	0.551 ± 0.022*	1.814 ± 0.057*	0.214 ± 0.007
WNiFe	0.108 ± 0.005	0.668 ± 0.031	2.554 ± 0.245	0.221 ± 0.007
WTa	0.102 ± 0.008	0.640 ± 0.045	2.069 ± 0.139	0.211 ± 0.011
NiTa	0.146 ± 0.046	0.569 ± 0.026	1.869 ± 0.071	0.219 ± 0.005
CoTa	0.100 ± 0.005	0.584 ± 0.021	1.856 ± 0.063*	0.214 ± 0.008
FeTa	0.113 ± 0.010	0.620 ± 0.014	2.110 ± 0.075	0.224 ± 0.003
WNiTa	0.109 ± 0.004	0.621 ± 0.032	2.132 ± 0.054	0.223 ± 0.009
WCoTa	0.098 ± 0.004*	0.593 ± 0.020	1.993 ± 0.101	0.223 ± 0.008
WFeTa	0.097 ± 0.005*	0.574 ± 0.013*	2.131 ± 0.114	0.220 ± 0.004
NiFeTa	0.110 ± 0.006	0.628 ± 0.039	2.211 ± 0.105	0.215 ± 0.004*
NiCoTa	0.110 ± 0.006	0.635 ± 0.019	2.111 ± 0.059	0.207 ± 0.015

Data are the mean of 10 independent observations. Error represents standard error of the mean. An * indicates a result that is statistically different than control (sham) at $P < 0.05$ using one-way ANOVA followed by Dunnett's test for group mean comparisons.

Table 11: Organ Body Weight Ratios from Mice in 12-month High-dose Implantation Groups

Group \ Organ/BW	Spleen / BW (mg/gm)	Kidney / BW (mg/gm)	Liver / BW (mg/gm)	Testes / BW (mg/gm)
Sham	2.518 ± 0.119	13.281 ± 0.295	44.537 ± 1.352	4.876 ± 0.086
Ta	2.768 ± 0.245	13.515 ± 0.349	43.796 ± 0.858	4.665 ± 0.165
Ni	3.065 ± 0.421	14.379 ± 0.345	41.275 ± 1.549	4.978 ± 0.225
Pb	2.426 ± 0.109	12.356 ±0.194*	43.094 ± 1.258	4.540 ± 0.167
WNiCo	2.878 ± 0.491	12.215 ± 0.364	40.230 ±0.826*	4.755 ± 0.145
WNiFe	2.225 ± 0.114	13.710 ± 0.430	52.866 ± 5.406	4.539 ± 0.116
WTa	2.222 ± 0.249	13.422 ± 0.561	43.624 ± 1.339	4.477 ± 0.128*
NiTa	3.817 ± 1.448	13.694 ± 0.291	45.078 ± 0.787	5.329 ± 0.152*
CoTa	2.330 ± 0.145	13.586 ± 0.455	43.123 ± 1.160	4.994 ± 0.184
FeTa	2.426 ± 0.202	13.357 ± 0.233	45.368 ± 0.955	4.844 ± 0.107
WNiTa	2.398 ± 0.154	13.364 ± 0.407	46.314 ± 1.351	4.827 ± 0.142
WCoTa	2.235 ± 0.103	13.535 ± 0.432	45.154 ± 1.113	5.067 ± 0.111
WFeTa	2.127 ± 0.052*	12.710 ± 0.237	46.882 ± 1.367	4.883 ± 0.161
NiFeTa	2.336 ± 0.110	13.334 ± 0.600	46.873 ± 0.904	4.612 ± 0.178
NiCoTa	2.293 ± 0.084	13.267 ± 0.281	44.093 ± 0.630	4.374 ± 0.330

Data are the mean of 10 independent observations. Error represents standard error of the mean. An * indicates a result that is statistically different than control (sham) at $P < 0.05$ using one-way ANOVA followed by Dunnett's test for group mean comparisons.

Table 12: Organ Weights from Mice in 24-month High-dose Implantation Groups

Group \ Organ	Spleen (gm)	Kidney (gm)	Liver (gm)	Testes (gm)
Sham	0.278 ± 0.080	0.584 ± 0.020	2.397 ± 0.181	0.203 ± 0.005
Ta	0.403 ± 0.104	0.680 ± 0.035	2.652 ± 0.162	0.200 ± 0.005
Ni	0.174 ± 0.020	0.634 ± 0.016	2.044 ± 0.138	0.224 ± 0.004*
Pb	0.315 ± 0.102	0.621 ± 0.022	2.430 ± 0.184	0.207 ± 0.003
WNiCo	0.485 ± 0.192	0.558 ± 0.013	2.008 ± 0.090	0.211 ± 0.006
WNiFe	0.268 ± 0.071	0.589 ± 0.017	2.965 ± 0.489	0.203 ± 0.004
WTa	0.409 ± 0.241	0.612 ± 0.027	2.556 ± 0.337	0.210 ± 0.004
NiTa	0.228 ± 0.054	0.591 ± 0.016	2.706 ± 0.314	0.203 ± 0.004
CoTa	0.314 ± 0.067	0.588 ± 0.014	2.445 ± 0.266	0.198 ± 0.006
FeTa	0.202 ± 0.032	0.572 ± 0.024	2.231 ± 0.222	0.198 ± 0.006
WNiTa	0.173 ± 0.024	0.608 ± 0.024	2.175 ± 0.187	0.211 ± 0.006
WCoTa	0.473 ± 0.200	0.603 ± 0.019	2.671 ± 0.302	0.208 ± 0.004
WFeTa	0.647 ± 0.333*	0.586 ± 0.018	2.677 ± 0.307	0.198 ± 0.007
NiFeTa	0.481 ± 0.162	0.586 ± 0.025	2.668 ± 0.345	0.215 ± 0.004
NiCoTa	0.298 ± 0.081	0.593 ± 0.016	2.322 ± 0.166	0.211 ± 0.003

Data are the mean of 20 independent observations. Error represents standard error of the mean. An * indicates a result that is statistically different than control (sham) at P < 0.05 using one-way ANOVA followed by Dunnett's test for group mean comparisons.

Table 13: Organ Body Weight Ratios from Mice in 24-month High-dose Implantation Groups

Group \ Organ/BW	Spleen / BW (mg/gm)	Kidney / BW (mg/gm)	Liver / BW (mg/gm)	Testes / BW (mg/gm)
Sham	6.251 ± 1.889	12.767 ± 0.406	52.922 ± 4.512	4.433 ± 0.096
Ta	9.090 ± 2.272	15.438 ±0.798*	60.911 ± 4.111	4.587 ± 0.135
Ni	39.776 ±5.578*	14.169 ±0.300*	45.297 ± 2.588	5.058 ± 0.177*
Pb	7.161 ± 2.360	13.825 ± 0.515	54.659 ± 4.741	4.618 ± 0.084
WNiCo	11.101 ± 4.351	12.548 ± 0.353	45.018 ± 1.888	4.721 ± 0.086
WNiFe	6.238 ± 1.623	13.643 ± 0.311	70.103±12.668	4.708 ± 0.064*
WTa	9.566 ± 5.623	14.065 ± 0.292	59.870 ± 8.502	4.906 ± 0.147*
NiTa	5.255 ± 1.202	13.664 ± 0.359	63.896 ± 8.369	4.723 ± 0.133
CoTa	7.384 ± 1.522	13.938 ±0.270*	57.686 ± 5.869	4.701 ± 0.156
FeTa	5.013 ± 0.844	13.879 ± 0.475	54.064 ± 5.374	4.842 ± 0.171
WNiTa	3.763 ± 0.510	13.321 ± 0.481	47.351 ± 3.725	4.668 ± 0.176
WCoTa	10.918 ± 4.675	13.719 ± 0.350	60.205 ± 6.426	4.784 ± 0.164
WFeTa	12.848 ± 6.155	13.385 ± 0.294	61.522 ± 7.143	4.516 ± 0.110
NiFeTa	11.102 ± 3.693	13.329 ± 0.381	60.607 ± 7.651	4.935 ± 0.117*
NiCoTa	6.950 ± 2.029	13.720 ± 0.272	53.246 ± 3.588	4.938 ± 0.161*

Data are the mean of 20 independent observations. Error represents standard error of the mean. An * indicates a result that is statistically different than control (sham) at P < 0.05 using one-way ANOVA followed by Dunnett’s test for group mean comparisons.

Table 14: Organ Weights from Mice in 24-month Low-dose Implantation Groups

Group \ Organ	Spleen (gm)	Kidney (gm)	Liver (gm)	Testes (gm)
Sham	0.278 ± 0.080	0.584 ± 0.020	2.397 ± 0.181	0.203 ± 0.005
Ta	0.403 ± 0.104	0.680 ± 0.035	2.652 ± 0.162	0.200 ± 0.005
Ni	0.288 ± 0.076	0.607 ± 0.019	2.108 ± 0.105	0.206 ± 0.006
Pb	0.218 ± 0.045	0.569 ± 0.019	2.050 ± 0.140	0.210 ± 0.003
WNiCo	0.275 ± 0.054	0.613 ± 0.020	2.417 ± 0.190	0.221 ± 0.004*
WNiFe	0.381 ± 0.111	0.537 ± 0.031	2.859 ± 0.454	0.193 ± 0.005
WTa	0.270 ± 0.083	0.572 ± 0.034	2.836 ± 0.321	0.204 ± 0.007
NiTa	0.154 ± 0.014	0.615 ± 0.023	2.611 ± 0.374	0.217 ± 0.005
CoTa	0.580 ± 0.269	0.616 ± 0.016	2.865 ± 0.324	0.200 ± 0.006
FeTa	0.353 ± 0.097	0.566 ± 0.022	2.707 ± 0.361	0.208 ± 0.003
WNiTa	0.264± 0.092	0.545 ± 0.018	2.348 ± 0.255	0.207 ± 0.003
WCoTa	0.207 ± 0.026	0.605 ± 0.015	2.398 ± 0.171	0.197 ± 0.006
WFeTa	0.165 ± 0.016	0.563 ± 0.019	2.591 ± 0.346	0.198 ± 0.005
NiFeTa	0.397 ± 0.181	0.573 ± 0.019	2.738 ± 0.308	0.205 ± 0.004
NiCoTa	0.174 ± 0.029	0.616 ± 0.019	2.321 ± 0.233	0.216 ± 0.003

Data are the mean of 20 independent observations. Error represents standard error of the mean. An * indicates a result that is statistically different than control (sham) at $P < 0.05$ using one-way ANOVA followed by Dunnett's test for group mean comparisons.

Table 15: Organ Body Weight Ratios from Mice in 24-month Low-dose Implantation Groups

Group \ Organ/BW	Spleen / BW (mg/gm)	Kidney / BW (mg/gm)	Liver / BW (mg/gm)	Testes / BW (mg/gm)
Sham	6.251 ± 1.889	12.767 ± 0.406	52.922 ± 4.512	4.433 ± 0.096
Ta	9.090 ± 2.272	15.438 ±0.798*	60.911 ± 4.111	4.587 ± 0.135
Ni	6.832 ± 1.702	14.195 ±0.320*	49.124 ± 1.937	4.839 ± 0.157
Pb	4.902 ± 0.979	12.863 ± 0.232	45.894 ± 2.265	4.786 ± 0.107*
WNiCo	5.852 ± 1.187	13.026 ± 0.355	50.818 ± 3.213	4.715 ± 0.087
WNiFe	8.819 ± 2.487	12.711 ± 0.700	67.857±10.725	4.622 ± 0.142
WTa	6.113 ± 1.865	12.867 ± 0.673	65.165 ± 8.030	4.644 ± 0.164
NiTa	3.504 ± 0.336	13.797 ± 0.247	59.967 ± 9.611	4.918 ± 0.117*
CoTa	13.726 ± 6.003	14.675 ±0.407*	68.257 ± 7.596	4.783 ± 0.172
FeTa	7.870 ± 1.964	13.190 ± 0.402	63.617 ± 8.723	4.894 ± 0.113*
WNiTa	6.566 ± 2.448	13.191 ± 0.484	56.804 ± 6.658	5.030 ± 0.190*
WCoTa	4.893 ± 0.625	14.388 ±0.276*	57.332 ± 4.526	4.691 ± 0.132
WFeTa	4.013 ± 0.359	13.945 ± 0.325	63.457 ± 8.747	4.917 ± 0.127*
NiFeTa	9.066 ± 4.141	13.198 ± 0.402	63.365 ± 7.386	4.729 ± 0.120
NiCoTa	4.127 ± 0.758	14.395 ±0.309*	54.417 ± 5.484	5.085 ± 0.133*

Data are the mean of 20 independent observations. Error represents standard error of the mean. An * indicates a result that is statistically different than control (sham) at P < 0.05 using one-way ANOVA followed by Dunnett’s test for group mean comparisons.

TABLE 16: Hematological parameters of 1-month implantation groups

Group	WBC ($10^3/\mu l$)	RBC ($10^6/\mu l$)	HGB (g/dL)	HCT (%)	PLT ($10^3/\mu l$)
Sham	4.60 ± 0.35	9.42 ± 0.12	14.50 ± 0.16	45.48 ± 0.47	892.4 ± 5.9
Ta	4.97 ± 0.96	8.54 ± 0.17	14.07 ± 0.27	41.51 ± 0.88 *	726.3 ± 51.1
Ni	3.93 ± 0.30	8.42 ± 0.13 *	13.55 ±0.17 *	39.73 ±0.59 *	1005.2 ±54.9
Pb	4.86 ± 0.53	8.98 ± 0.08 *	14.13 ± 0.17	44.01 ± 0.41	797.0 ± 77.9
WNiCo	4.65 ± 0.42	8.25 ± 0.30 *	13.00 ±0.44 *	40.38 ±1.36 *	832.7 ± 91.7
WNiFe	4.23 ± 0.36	8.91 ± 0.16	13.96 ± 0.20	43.43 ± 0.80	903.7 ± 72.6
WTa	3.86 ± 0.52	9.28 ± 0.09	14.38 ± 0.20	41.15 ± 4.01	785.9 ± 85.5
NiTa	6.13 ± 0.40 *	9.05 ± 0.13	14.13 ± 0.19	44.31 ± 0.62	963.2 ± 44.5
CoTa	5.28 ± 0.65	8.53 ±0.55	12.97 ± 0.91	41.33 ± 2.64	936.1 ± 69.8
FeTa	6.28 ± 0.73	9.13 ± 0.22	14.34 ± 0.26	44.31 ± 0.79	980.7 ± 35.9
WNiTa	5.89 ± 0.90	9.31 ± 0.24	14.23 ± 0.36	44.13 ± 1.11	901.0 ± 69.0
WCoTa	5.46 ± 0.51	9.03 ± 0.15	14.24 ± 0.23	43.77 ± 0.62	981.8 ± 42.1
WFeTa	5.93 ± 0.48	9.25 ±0.11	14.66 ± 0.20	45.15 ± 0.55	967.0 ± 34.4
NiFeTa	5.04 ± 0.26	9.13 ± 0.11	14.66 ±0.19	44.35 ± 0.52	953.0 ±29.5
NiCoTa	5.37 ± 0.39	9.52 ± 0.16	15.09 ± 0.2	46.11 ± 0.77	868.8 ± 24.1

Data represent the mean and standard error of the mean of 10 independent observations. An * indicates a result that is statistically different than control (sham) at $P < 0.05$ using a one-way ANOVA followed by Dunnett's test for group mean comparisons. WBC - white blood cells; RBC - red blood cells; HGB - hemoglobin; HCT - hematocrit; PLT - platelets.

TABLE 16 (continued): Hematological parameters of 1-month implantation groups

Group	Lymphocytes %	Monocytes %	Granulocytes %	Lymphocytes $10^3/\mu l$	Monocytes $10^3/\mu l$	Granulocytes $10^3/\mu l$
Sham	60.66 ± 0.59	11.94±0.22	27.40 ± 0.55	2.76 ± 0.22	0.50 ±0.05	1.34 ± 0.09
Ta	51.41±3.07 *	10.78±0.47	37.81±3.41*	2.34±0.28	0.46±0.06	2.17±0.66
Ni	51.63±1.53*	12.66±0.29	35.71±1.77*	1.99±0.18*	0.46±0.04	1.48±0.12
Pb	44.66±3.10*	10.35±0.74	44.99±3.80*	2.14±0.30	0.44±0.07	2.29±0.25*
WNiCo	48.69±3.11*	10.99±0.53	40.33±3.52*	2.15±0.20	0.43±0.04	2.08±0.29
WNiFe	50.07±2.60*	11.23±0.45	38.70±2.98*	2.04±0.15	0.41±0.04	3.34±1.49
WTa	51.45±1.57*	11.38±0.40	37.17±1.86*	1.90±0.21*	0.39±0.05	1.57±0.28
NiTa	44.48±2.30*	11.12±0.34	44,40±2.52*	2.67±0.21	0.62±0.05	2.84±0.23*
CoTa	44.14±3.70*	10.43±0.62	45.42±4.24*	2.18±0.25	0.48±0.06	2.62±0.48
FeTa	44.59±3.77*	9.97±0.58*	45.44±4.31*	2.53±0.17	0.56±0.05	3.19±0.68*
WNiTa	43.91±4.43*	9.74±0.70*	46.23±5.11*	2.24±0.25	0.47±0.06	3.18±0.76
WCoTa	47.34±2.43*	10.49±0.43*	42.17±2.79*	2.48±0.23	0.52±0.05	2.46±0.30*
WFeTa	48.87±2.89*	10.56±0.51	40.57±3.33*	2.74±0.15	0.57±0.03	2.62±0.39*
NiFeTa	49.44±2.32*	10.54±0.43*	40.02±2.72*	2.42±0.15	0.48±0.03	2.14±0.20*
NiCoTa	49.28±1.87*	10.19±0.34*	40.53±2.03*	2.57±0.22	0.49±0.03	2.31±0.19*

Data represent the mean and standard error of the mean of 10 independent observations. An * indicates a result that is statistically different than control (sham) at $P < 0.05$ using a one-way ANOVA followed by Dunnett’s test for group mean comparisons.

TABLE 17: Hematological parameters of 3-month implantation groups

Group	WBC (10^3/µl)	RBC (10^6/µl)	HGB (g/dL)	HCT (%)	PLT (10^3/µl)
Sham	4.09 ± 0.51	8.60 ± 0.19	13.16 ± 0.25	40.55 ± 0.89	1070.1 ±75.4
Ta	4.29 ± 0.50	9.26 ± 0.13 *	14.13 ±0.14 *	44.90 ±0.65*	864.3±26.0 *
Ni	3.68 ± 0.50	8.70 ± 0.14	13.39 ± 0.23	42.07 ± 0.67	865.3±45.0
Pb	4.63 ± 0.61	9.18 ± 0.16	13.60 ± 0.18	43.68 ±0.70*	899.3 ± 20.9
WNiCo	3.93 ± 0.91	8.55 ± 0.23	13.20 ± 0.37	41.49 ± 1.16	857.2 ± 80.0
WNiFe	3.42 ± 0.29	8.55 ± 0.21	13.29 ± 0.31	41.95 ± 0.90	786.7 ± 70.3*
WTa	3.79 ± 0.34	8.83 ± 0.15	13.69 ± 0.23	43.18 ± 0.75	805.9 ± 67.9*
NiTa	4.66 ± 0.40	8.87 ± 0.20	13.39 ± 0.29	43.11 ± 1.06	901.9 ± 32.1
CoTa	5.03 ± 0.36	9.02 ± 0.21	14.03 ± 0.29	43.54 ± 1.02	1111.1 ±58.2
FeTa	6.48 ± 1.25	9.19 ± 0.20	14.31 ± 0.25*	44.31 ± 0.98*	912.5 ± 95.8
WNiTa	5.31 ± 0.49	9.19 ± 0.05	14.28 ± 0.10*	44.22 ± 0.29*	1006.3 ±35.5
WCoTa	5.16 ± 0.50	8.95 ± 0.09	14.17 ± 0.14*	43.07 ± 0.47*	1094.4 ±43.9
WFeTa	3.97 ± 0.40	8.99 ± 0.15	13.80 ± 0.23	42.52 ± 0.77	964.6 ± 91.8
NiFeTa	4.93 ± 0.53	8.53 ± 0.29	13.31 ± 0.40	40.79 ± 1.40	1080.3 ±40.8
NiCoTa	5.13 ± 0.31	9.02 ± 0.14	13.97 ± 0.19*	43.24 ± 0.73	1010.3 ±49.3

Data represent the mean and standard error of the mean of 10 independent observations. An * indicates a result that is statistically different than control (sham) at $P < 0.05$ using a one-way ANOVA followed by Dunnett's test for group mean comparisons. WBC - white blood cells; RBC - red blood cells; HGB - hemoglobin; HCT - hematocrit; PLT - platelets.

TABLE 17 (continued): Hematological parameters of 3-month implantation groups

Group	Lymphocytes %	Monocytes %	Granulocytes %	Lymphocytes $10^3/\mu l$	Monocytes $10^3/\mu l$	Granulocytes $10^3/\mu l$
Sham	54.99±3.65	6.53±1.07	37.74±3.20	2.13±0.31	0.22±0.04	1.71±0.28
Ta	43.80±4.57	9.79±0.63*	46.41±5.07	1.70±0.07	0.34±0.03*	2.24±0.48
Ni	51.24±1.96	12.34±0.55*	36.41±2.05	1.86±0.28	0.40±0.05*	1.42±0.19
Pb	43.92±3.12	9.99±0.75*	46.09±3.72	1.84±0.17	0.37±0.03*	2.42±0.46
WNiCo	38.86±6.87	10.64±1.55*	50.50±8.33	1.34±0.08*	0.34±0.02*	2.77±0.87
WNiFe	48.10±1.91	11.96±0.36*	39.94±2.14	1.59±0.12	0.80±0.47	1.48±0.17
WTa	47.82±3.14	11.34±0.64*	40.83±3.70	1.78±0.22	0.38±0.04*	1.63±0.19
NiTa	43.87±1.50*	11.24±0.31*	44.89±1.62	1.97±0.16	0.46±0.04*	2.23±0.24
CoTa	47.11±3.57	11.93±0.41*	40.96±3.93	2.33±0.26	0.55±0.04*	2.15±0.23
FeTa	41.96±3.98	10.05±0.84*	47.99±4.74	2.33±0.20	0.53±0.05*	3.63±1.14
WNiTa	45.55±2.59	10.38±0.51*	44.07±3.03	2.31±0.20	0.49±0.05*	2.51±0.35
WCoTa	36.76±4.04*	9.27±0.94	53.98±4.94*	1.70±0.15	0.39±0.03*	3.07±0.52
WFeTa	44.89±1.60*	11.68±0.53*	43.43±1.73	1.74±0.20	0.40±0.04*	1.83±0.20
NiFeTa	41.88±3.41*	9.88±0.68*	48.24±4.04	2.01±0.28	0.42±0.05*	2.50±0.36
NiCoTa	47.24±1.32	11.51±0.45*	41.24±1.65	2.40±0.18	0.56±0.05*	2.19±0.13

Data represent the mean and standard error of the mean of 10 independent observations. An * indicates a result that is statistically different than control (sham) at $P< 0.05$ using a one-way ANOVA followed by Dunnett's test for group mean comparisons.

TABLE 18: Hematological parameters of 6-month implantation groups

Group	WBC (10^3/µl)	RBC (10^6/µl)	HGB (g/dL)	HCT (%)	PLT (10^3/µl)
Sham	3.79 ± 0.36	8.46 ± 0.11	13.09 ± 0.16	39.75 ± 0.64	1159.2 ±71.6
Ta	4.86 ± 0.74	8.99 ± 0.11*	13.77 ± 0.23	47.33 ± 0.67*	988.4 ±57.0
Ni	4.34 ± 0.70	8.51 ± 0.39	13.04 ± 0.49	40.89 ± 1.64	966.4 ±35.9
Pb	4.31 ± 0.23	9.10 ± 0.14*	13.68 ± 0.20	43.32 ± 0.76*	853.1 ±69.7*
WNiCo	3.99 ± 0.33	9.19 ± 0.14*	13.64 ± 0.23	43.93 ± 0.71*	958.2±37.8*
WNiFe	4.32 ± 0.42	9.24 ± 0.11*	13.80 ± 0.22*	43.94 ± 0.57*	836.4±22.8*
WTa	4.71 ± 0.34	9.01 ± 0.15*	13.88 ± 0.10*	43.76 ± 0.38*	967.4±44.3
NiTa	13.82 ± 8.30	8.50 ± 0.34	12.91 ± 0.56	40.69 ± 1.50	847.0±138.6
CoTa	5.98 ± 0.98	8.99 ± 0.11*	13.62 ± 0.15	42.60 ± 0.49*	1114.8±35.1
FeTa	5.71 ± 0.58*	9.11 ± 0.13*	13.98 ± 0.19*	43.89 ± 0.56*	993.21±128.4
WNiTa	6.23 ± 0.96	8.75 ± 0.10	13.75 ± 0.17	41.98 ± 0.51*	1091.7±54.2
WCoTa	4.11 ± 0.41	9.14 ± 0.16*	14.34 ± 0.21*	43.94 ± 0.76*	990.0±41.4
WFeTa	3.88 ± 0.28	8.98 ± 0.07*	14.25 ± 0.13*	43.23 ± 0.36*	1149.0±37.2
NiFeTa	4.38 ± 0.25	8.63 ± 0.17	13.39 ± 0.53	41.30 ± 0.75	980.1±56.8
NiCoTa	4.43 ± 0.29	9.00 ± 0.11*	14.30 ± 0.11*	43.26 ± 0.46*	1021.6±59.3

Data represent the mean and standard error of the mean of 10 independent observations. An * indicates a result that is statistically different than control (sham) at $P < 0.05$ using a one-way ANOVA followed by Dunnett's test for group mean comparisons. WBC - white blood cells; RBC - red blood cells; HGB - hemoglobin; HCT - hematocrit; PLT - platelets.

TABLE 18 (continued): Hematological parameters of 6-month implantation groups

Group	Lymphocytes %	Monocytes %	Granulocytes %	Lymphocytes 10^3/µl	Monocytes 10^3/µl	Granulocytes 10^3/µl
Sham	61.13 ± 2.94	5.85±1.07	31.95±2.27	2.33±0.30	0.19±0.04	1.23±0.12
Ta	44.26±5.30*	8.58±0.71	44.17±5.90	1.92±0.29	0.34±0.04*	2.59±0.77
Ni	56.44±1.16	10.48±0.33	33.09±1.20	2.68±0.39	0.46±0.07*	1.64±0.18
Pb	49.32±2.17*	10.15±0.28*	40.53±2.20*	2.07±0.14	0.38±0.02*	1.86±0.14*
WNiCo	52.13±1.33*	12.11±0.28*	35.76±1.50	2.05±0.19	0.41±0.04*	1.53±0.13
WNiFe	50.00±2.21*	10.20±0.47*	39.80±2.27*	2.06±0.16	0.39±0.05*	1.88±0.24
WTa	50.71±2.19*	10.95±0.26*	38.34±2.38	2.36±0.24	0.49±0.05*	1.86±0.10*
NiTa	33.93±6.34*	8.49±1.31	57.58±7.62*	1.77±0.23	0.53±0.14	11.53±8.13
CoTa	41.77±3.68*	10.23±0.67*	48.00±4.22*	2.26±0.24	0.51±0.05*	3.21±0.86
FeTa	48.66±1.69*	10.96±0.46*	40.39±1.62*	2.72±0.29	0.56±0.07*	2.43±0.27*
WNiTa	40.78±5.89*	8.89±1.03	50.34±6.85	2.14±0.22	0.44±0.03*	3.65±1.01
WCoTa	46.86±2.40*	10.75±0.25*	42.39±2.44*	1.93±0.27	0.39±0.05*	1.79±0.14*
WFeTa	47.66±1.49*	10.95±0.49*	41.39±1.67*	1.80±0.14	0.37±0.02*	1.71±0.18
NiFeTa	47.09±1.57*	10.48±0.35*	42.43±1.56*	2.01±0.17	0.40±0.03*	1.97±0.08*
NiCoTa	48.84±1.50*	10.30±0.26*	40.89±1.59*	2.10±0.15	0.40±0.02*	1.93±0.15*

Data represent the mean and standard error of the mean of 10 independent observations. An * indicates a result that is statistically different than control (sham) at $P < 0.05$ using a one-way ANOVA followed by Dunnett's test for group mean comparisons.

TABLE 19: Hematological parameters of 12-month implantation groups

Group	WBC (10^3/µl)	RBC (10^6/µl)	HGB (g/dL)	HCT (%)	PLT (10^3/µl)
Sham	6.65 ± 0.36	8.50 ± 0.26	13.89 ± 0.19	42.65 ± 0.48	1256.5±60.2
Ta	6.06 ± 0.96	8.89 ± 0.20	13.80 ± 0.27	42.57 ± 0.79	1205.4 ±70.5
Ni	5.17 ± 0.55	8.50 ± 0.14	12.88 ± 0.21*	40.37 ± 0.69*	982.3 ±86.1*
Pb	6.10 ± 0.72	9.14 ± 0.20	14.58 ± 0.34	44.47 ± 1.11	1067.8±44.9*
WNiCo	5.61 ± 0.45	8.70 ± 0.22	13.33 ± 0.34	41.47 ± 1.18	927.4±85.3*
WNiFe	4.83 ± 0.42	9.28 ± 0.19*	13.75 ± 0.24	43.23 ± 0.70	1097.8±47.4
WTa	5.23 ± 0.74	8.58 ± 0.70	12.95 ± 1.06	40.65 ± 3.47	1030.6±34.0*
NiTa	5.19 ± 0.49	8.81 ± 0.10	13.20 ± 0.21	41.76 ± 0.61	990.7±28.1*
CoTa	5.27 ± 0.61	8.28 ± 0.15	12.53 ± 0.20*	39.31 ± 0.62*	910.2±20.3*
FeTa	7.86 ± 1.95	8.58 ± 0.26	12.81 ± 0.31*	40.60 ± 1.17	1007.7±36.9*
WNiTa	5.47 ± 0.39	9.24 ± 0.11*	13.83 ± 0.19	44.00 ± 0.63	1048.3±25.6*
WCoTa	5.66 ± 0.78	8.16 ± 0.77	12.50 ± 1.17	38.82 ± 3.72	929.0±37.3*
WFeTa	5.35 ± 0.45	8.85 ± 0.18	13.23 ± 0.23	41.83 ± 0.74	994.7±91.7
NiFeTa	6.42 ± 1.02	8.99 ± 0.17	14.01 ± 0.20	43.43 ± 0.64	1204.7±45.3
NiCoTa	4.40 ± 0.60	8.82 ± 0.07	13.10 ± 0.17	41.10 ± 0.41	716.0±55.1

Data represent the mean and standard error of the mean of 10 independent observations. An * indicates a result that is statistically different than control (sham) at $P < 0.05$ using a one-way ANOVA followed by Dunnett’s test for group mean comparisons. WBC - white blood cells; RBC - red blood cells; HGB - hemoglobin; HCT - hematocrit; PLT - platelets.

TABLE 19 (continued): Hematological parameters of 12-month implantation groups

Group	Lymphocytes %	Monocytes %	Granulocytes %	Lymphocytes $10^3/\mu l$	Monocytes $10^3/\mu l$	Granulocytes $10^3/\mu l$
Sham	61.59 ± 3.20	6.44 ±0.86	31.39 ± 2.62	3.45 ± 0.30	0.33±0.05	1.55±0.20
Ta	45.03 ±3.46*	8.41±0.42	46.56±3.76*	2.52±0.34	0.43±0.06	3.10±0.65
Ni	42.59±3.19*	8.67±0.47	48.74±3.58*	2.08±0.25*	0.40±0.06	2.69±0.36
Pb	51.50±1.91*	8.71±0.29*	39.79±2.01*	3.01±0.29	0.48±0.06	2.61±0.41
WNiCo	37.44±3.52*	8.51±0.61	54.05±4.11*	1.98±0.21*	0.42±0.04	2.91±0.49
WNiFe	49.39±1.45*	9.30±0.43*	40.31±1.03*	2.42±0.27*	0.40±0.04	2.01±0.14
WTa	49.52±2.13*	8.91±0.40*	41.59±2.41*	2.67±0.44	0.44±0.08	2.12±0.22
NiTa	42.32±2.37*	7.74±0.56	49.93±2.92*	2.11±0.19*	0.34±0.03	2.73±0.35
CoTa	36.01±2.77*	7.48±0.60	56.51±3.34*	1.79±0.24*	0.33±0.04	3.14±0.45*
FeTa	38.76±6.85*	7.16±1.18	54.09±7.97*	2.23±0.25*	0.39±0.03	5.20±1.92
WNiTa	47.57±1.98*	9.37±0.19*	43.06±2.08*	2.60±0.27	0.48±0.03*	2.40±0.11
WCoTa	51.22±0.84*	9.40±0.34*	39.38±0.91*	2.88±0.43	0.48±0.07	2.30±0.29
WFeTa	46.90±2.08*	9.38±0.49*	43.73±2.33*	2.48±0.28	0.45±0.05	2.43±0.20
NiFeTa	40.87±1.86*	8.48±0.38*	50.65±2.17*	2.46±0.32	0.49±0.08	3.47±0.66
NiCoTa	52.80±0.84*	8.30±0.36*	38.90±0.85*	2.30±0.30	0.30±0.06*	1.80±0.27

Data represent the mean and standard error of the mean of 10 independent observations. An * indicates a result that is statistically different than control (sham) at P< 0.05 using a one-way ANOVA followed by Dunnett's test for group mean comparisons.

TABLE 20: Hematological parameters of high-dose 24-month implantation groups

Group	WBC (10^3/µl)	RBC (10^6/µl)	HGB (g/dL)	HCT (%)	PLT (10^3/µl)
Sham	8.66 ± 1.00	8.47 ± 0.36	12.86 ± 0.52	39.18 ± 1.65	1124.1±74.6
Ta	7.16 ± 0.83	9.66 ± 0.49	13.89 ± 0.55	43.14 ± 1.87	1085.6±72.4
Ni	4.56 ± 0.37*	8.29 ± 0.20	12.39 ± 0.25	38.22 ± 0.84	960.8±63.3
Pb	6.76 ± 0.58	7.70 ± 0.43	11.69 ± 0.53	35.92 ± 1.60	1226.9±116.9
WNiCo	7.67 ± 1.40	7.55 ± 0.34	11.34± 0.44	34.27 ± 1.66	748.4±101.2*
WNiFe	7.04 ± 0.84	8.74 ± 0.66	13.03 ±0.82	41.05 ± 2.67	1182.5±81.8
WTa	6.34 ± 0.38	8.72 ± 0.59	12.98 ± 0.72	39.83 ± 2.35	1146.5±108.4
NiTa	11.61 ± 4.99	8.74 ± 0.55	12.88 ± 0.54	39.68 ± 2.00	1154.7±79.8
CoTa	8.54 ± 1.27	8.90 ± 0.45	13.12 ± 0.58	40.58 ± 1.94	1103.5±84.5
FeTa	8.31 ± 1.25	8.59 ± 0.50	12.83 ± 0.55	39.49 ± 1.98	1027.3±92.2
WNiTa	6.93 ± 0.86	8.39 ± 0.36	13.09 ± 0.40	39.65 ± 1.31	1045.1±77.4
WCoTa	6.88 ± 0.95	8.62 ± 0.58	12.64 ± 0.61	39.31 ± 2.04	1038.4±112.5
WFeTa	12.57 ± 4.53	9.40 ± 0.60	13.23 ± 0.64	40.16 ± 2.53	1023.2±94.0
NiFeTa	13.03 ± 4.64	8.24 ± 0.61	12.06 ± 0.73	37.34 ± 2.37	923.1±110.5
NiCoTa	8.87 ± 1.48	7.87 ± 0.46	12.14 ± 0.67	37.57 ± 2.14	1011.5±116.6

Data represent the mean and standard error of the mean of 10 independent observations. An * indicates a result that is statistically different than control (sham) at P< 0.05 using a one-way ANOVA followed by Dunnett's test for group mean comparisons. WBC - white blood cells; RBC - red blood cells; HGB - hemoglobin; HCT - hematocrit; PLT - platelets.

TABLE 20 (continued): Hematological parameters of high-dose 24-month implantation groups

Group	Lymphocytes %	Monocytes %	Granulocytes %	Lymphocytes $10^3/\mu l$	Monocytes $10^3/\mu l$	Granulocytes $10^3/\mu l$
Sham	35.00±4.09	7.31±0.79	57.69±4.70	2.74±0.43	0.58±0.13	5.35±0.85
Ta	32.75±3.46	7.13±0.63	60.08±3.65	2.19±0.32	0.43±0.06	4.53±0.66
Ni	42.01±2.18	8.50±0.24	49.49±2.29	1.90±0.20	0.33±0.03	2.33±0.19*
Pb	37.63±3.58	6.64±0.43	55.74±3.92	2.48±0.30	0.40±0.05	3.88±0.47
WNiCo	36.83±3.75	7.21±0.52	55.94±4.16	2.99±0.76	0.59±0.16	4.54±0.64
WNiFe	36.86±2.98	8.99±1.01	54.15±3.15	2.42±0.27	0.66±0.20	3.96±0.52
WTa	35.08±3.07	7.11±0.34	57.81±3.16	2.16±0.23	0.39±0.03	3.79±0.32
NiTa	41.47±3.08	7.73±0.35	50.80±3.11	2.96±0.47	0.54±0.12	3.70±0.57
CoTa	31.68±2.59	6.08±0.45	62.19±2.93	2.33±0.25	0.42±0.05	5.79±1.23
FeTa	38.13±3.26	7.49±0.61	54.37±3.71	3.31±0.72	0.59±0.12	4.41±0.58
WNiTa	40.22±2.06	8.21±0.49	51.57±2.30	2.64±0.29	0.51±0.07	3.78±0.58
WCoTa	34.53±3.73	11.12±4.12	52.85±4.95	2.30±0.31	0.96±0.51	4.09±0.73
WFeTa	36.19±2.37	8.00±0.67	55.81±2.66	2.91±0.30	0.65±0.11	4.52±0.31
NiFeTa	32.68±3.08	7.21±0.52	60.12±3.37	2.32±0.41	0.65±0.26	6.12±2.01
NiCoTa	34.08±3.29	6.99±0.61	56.44±4.95	3.01±0.62	0.62±0.18	5.63±0.90

Data represent the mean and standard error of the mean of 10 independent observations. An * indicates a result that is statistically different than control (sham) at $P< 0.05$ using a one-way ANOVA followed by Dunnett’s test for group mean comparisons.

TABLE 21: Hematological parameters of low-dose 24-month implantation groups

Group	WBC (10^3/µl)	RBC (10^6/µl)	HGB (g/dL)	HCT (%)	PLT (10^3/µl)
Sham	8.66 ± 1.00	8.47 ± 0.36	12.86 ± 0.52	39.18 ± 1.65	1124.1±74.6
Ta	7.16 ± 0.83	9.66 ± 0.49	13.89 ± 0.55	43.14 ± 1.87	1085.6±72.4
Ni	8.26 ± 1.63	7.87 ± 0.47	11.90 ± 0.62	36.52 ± 1.94	1107.5±71.3
Pb	9.69 ± 2.19	8.78 ± 0.20	12.98 ± 0.29	40.27 ± 1.00	1080.7±51.4
WNiCo	9.10 ± 2.78	8.22 ± 1.32	12.38 ± 0.42	37.71 ± 1.34	865.8±90.4
WNiFe	7.96 ± 0.72	8.48 ± 0.51	12.63 ± 0.59	39.17 ± 1.86	1054.5±95.5
WTa	9.44 ± 1.59	8.76 ± 0.58	12.84 ± 0.70	39.75 ± 2.28	1139.8±67.4
NiTa	7.75 ± 1.15	8.83 ± 0.52	13.13 ± 0.51	40.98 ± 1.73	1164.3±52.8
CoTa	6.13 ± 0.72	9.31 ± 0.63	13.49 ± 0.70	42.17 ± 2.47	1123.3±75.6
FeTa	7.29 ± 1.14	8.79 ± 0.65	12.69 ± 0.72	39.62 ± 2.53	1070.2±91.9
WNiTa	7.42 ± 2.00	8.43 ± 0.40	12.44 ± 0.50	38.76 ± 1.67	1001.4±103.7
WCoTa	7.76 ± 0.86	8.71 ± 0.38	12.77 ± 0.47	39.87 ± 1.52	1069.2±71.7
WFeTa	6.70 ± 0.50	9.41 ± 0.50	13.50 ± 0.51	42.23 ± 1.83	1155.0±45.2
NiFeTa	6.56 ± 0.57	7.97 ± 0.67	11.91 ± 0.86	37.07 ± 2.77	1105.0±75.4
NiCoTa	7.01 ± 0.83	8.20 ± 0.43	12.25 ± 0.50	37.75 ± 1.62	1132.9±58.8

Data represent the mean and standard error of the mean of 10 independent observations. An * indicates a result that is statistically different than control (sham) at $P < 0.05$ using a one-way ANOVA followed by Dunnett's test for group mean comparisons. WBC - white blood cells; RBC - red blood cells; HGB - hemoglobin; HCT - hematocrit; PLT - platelets.

TABLE 21 (continued): Hematological parameters of low-dose 24-month implantation groups

Group	Lymphocytes %	Monocytes %	Granulocytes %	Lymphocytes 10^3/µl	Monocytes 10^3/µl	Granulocytes 10^3/µl
Sham	35.00±4.09	7.31±4.70	57.69±4.70	2.74±0.43	0.58±0.13	5.35±0.85
Ta	32.75±3.46	7.13±0.63	60.08±3.65	2.19±0.32	0.43±0.06	4.53±0.66
Ni	33.29±3.87	6.24±0.44	60.45±4.18	2.16±0.28	0.39±0.05	5.72±1.61
Pb	40.41±2.22	8.59±1.01	50.99±2.29	3.67±0.68	1.15±0.47	5.38±1.30
WNiCo	29.05±2.85	6.32±0.50	64.62±3.17	1.86±0.19	0.40±0.06	6.84±2.63
WNiFe	32.91±2.35	7.25±0.39	59.84±2.60	2.51±0.28	0.53±0.07	4.92±0.51
WTa	34.56±2.89	7.01±0.43	58.42±3.17	2.82±0.37	0.55±0.10	6.20±1.33
NiTa	38.05±3.43	7.19±0.43	54.76±3.72	2.89±0.54	0.51±0.10	4.35±0.71
CoTa	31.31±2.64	6.91±0.40	61.77±2.98	1.79±0.29	0.36±0.06	3.98±0.52
FeTa	34.01±3.49	7.53±0.50	56.46±3.92	2.10±0.30	0.45±0.07	4.74±0.96
WNiTa	33.72±3.56	8.61±2.30	55.47±4.67	2.00±0.21	0.40±0.11	5.11±1.91
WCoTa	34.07±2.30	6.75±0.42	59.71±2.49	2.37±0.25	0.48±0.08	4.91±0.64
WFeTa	37.74±2.76	8.34±0.75	53.92±2.85	2.45±0.23	0.53±0.08	3.72±0.34
NiFeTa	40.65±2.82	7.52±0.41	51.83±2.98	2.67±0.34	0.43±0.04	3.46±0.32
NiCoTa	37.34±2.46	7.62±0.51	55.05±2.85	2.47±0.33	0.48±0.08	4.06±0.52

Data represent the mean and standard error of the mean of 10 independent observations. An * indicates a result that is statistically different than control (sham) at $P < 0.05$ using a one-way ANOVA followed by Dunnett's test for group mean comparisons.

Table 22: Tumor Incidence in Metal-Implanted B6C3F1 Mice

	12 Month	24 Month
Sham	0 / 10	0 / 20
Ta	0 / 10	0 / 20
Ni	6 / 10 *	20 / 20 *
Pb	0 / 10	0 / 20
WNiCo	4 / 10 *	19 / 20 *
WNiFe	0 / 10	0 / 20
WTa	0 / 10	0 / 20
NiTa	0 / 10	0 / 20
CoTa	0 / 10	0 / 20
FeTa	0 / 10	0 / 20
WNiTa	0 / 10	0 / 20
WCoTa	0 / 10	0 / 20
WFeTa	0 / 10	0 / 20
NiFeTa	0 / 10	0 / 20
NiCoTa	0 / 10	0 / 20

* Tumors were identified by histopathological examination as rhabdomyosarcomas.

Table 23: ICP-MS Operating Conditions and Parameters

Instrument	
Nebulizer type	Concentric
Spray chamber	Conical, with impact bead
Sampler cone	Platinum, 1 mm orifice diameter
Skimmer cone	Platinum, 0.7 mm orifice diameter
Sample uptake rate	1.0 ml/min
Sample read delay	60 sec
Plasma conditions	
RF power	1350 W
Plasma argon gas flow	13 L/min
Auxiliary argon gas flow	0.9 L/min
Nebulizer gas flow	1.3 L/min
Mass spectrometer settings	
Scanning mode	Survey run
Sweeps	15
Dwell time	600 µs
Channels/mass	20
Acquisition time	42 sec
Number of readings/replicate	1
Number of replicates	1

Figure 5: Brain Metal Levels in 1-Month Implantation Groups

A. Brain Tungsten Levels

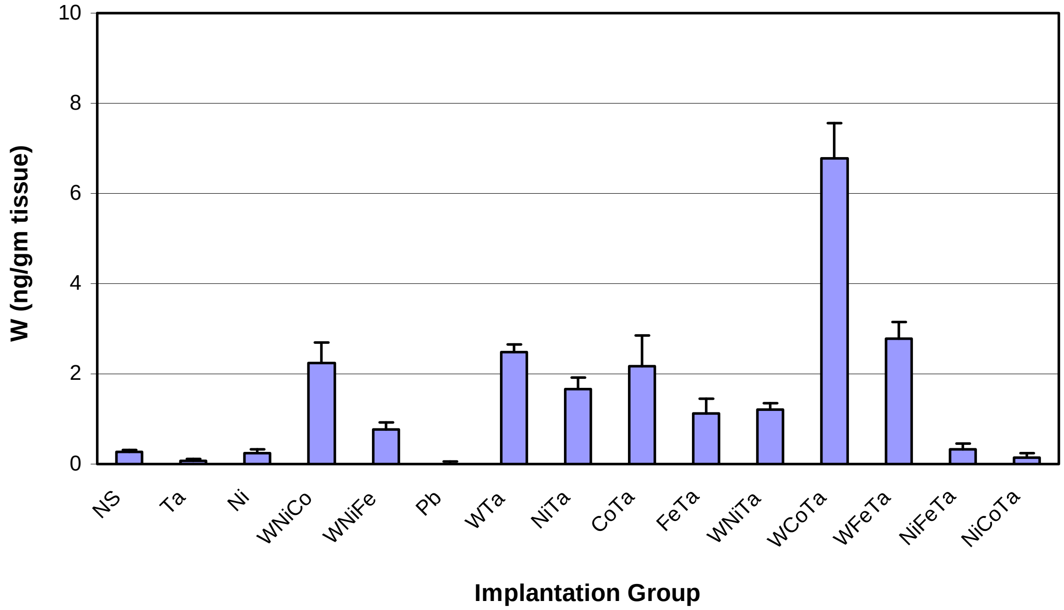

B. Brain Nickel Levels

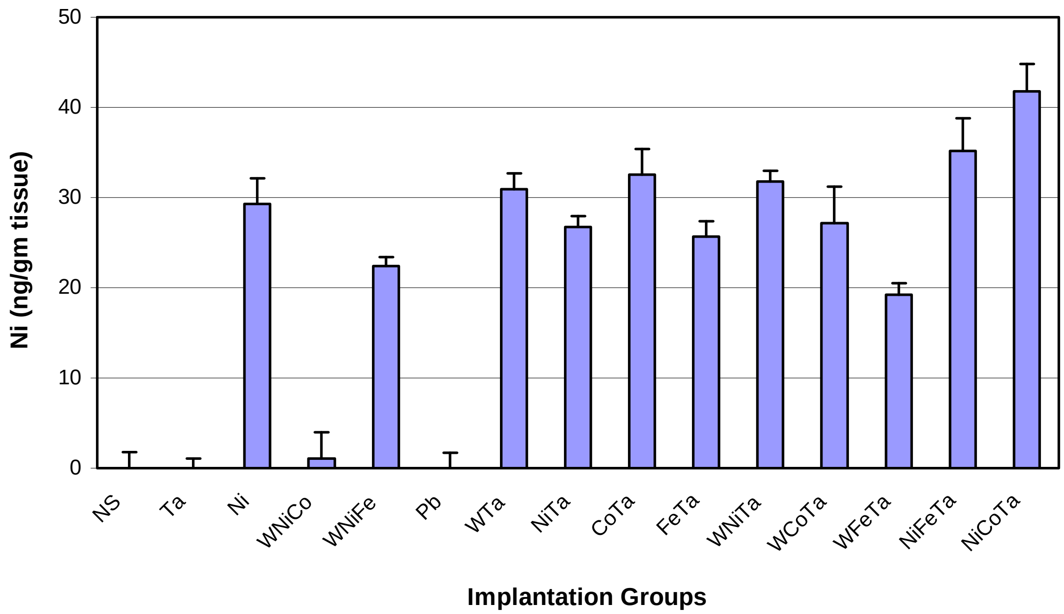

Figure 5 (continued): Brain Metal Levels in 1-Month Implantation Groups

C. Brain Cobalt Levels

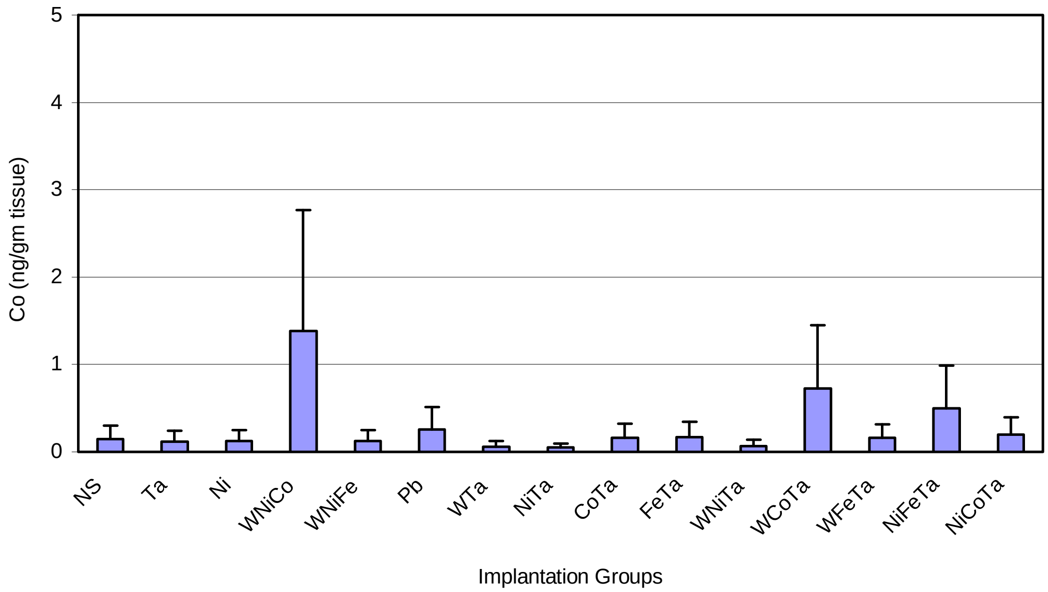

D. Brain Tantalum Levels

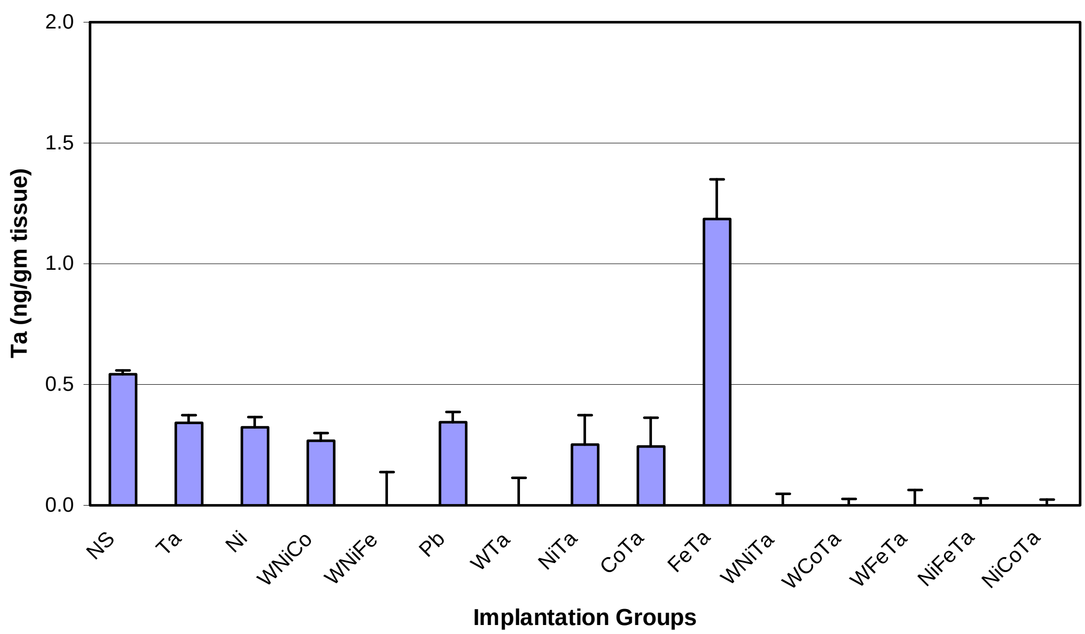

Figure 6: Femur Metals Levels in 1-Month Implantation Groups

A. Femur Tungsten Levels

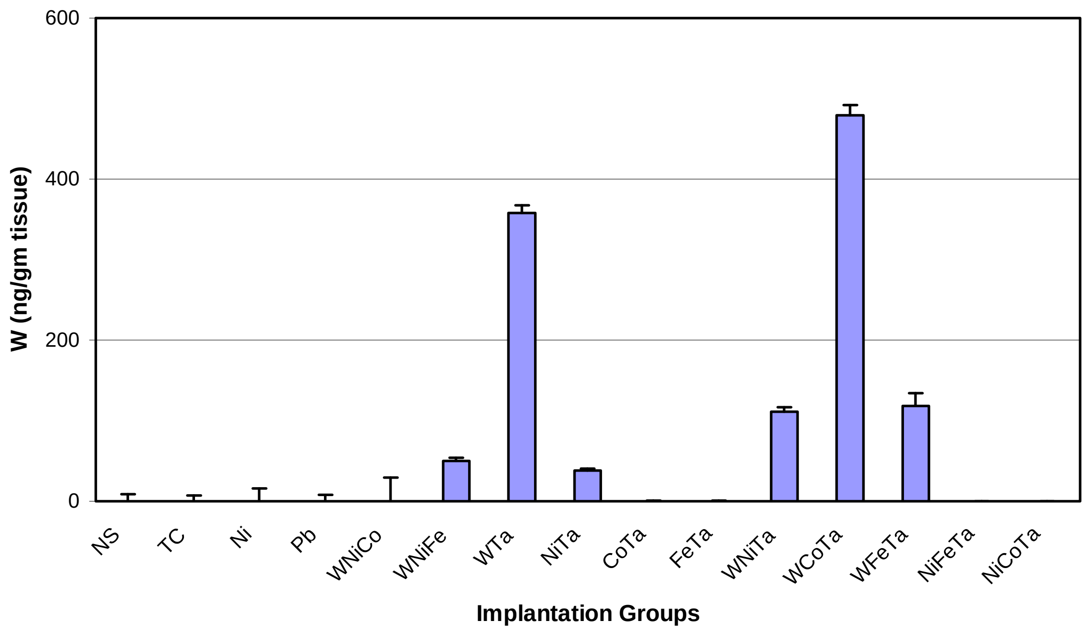

B. Femur Nickel Levels

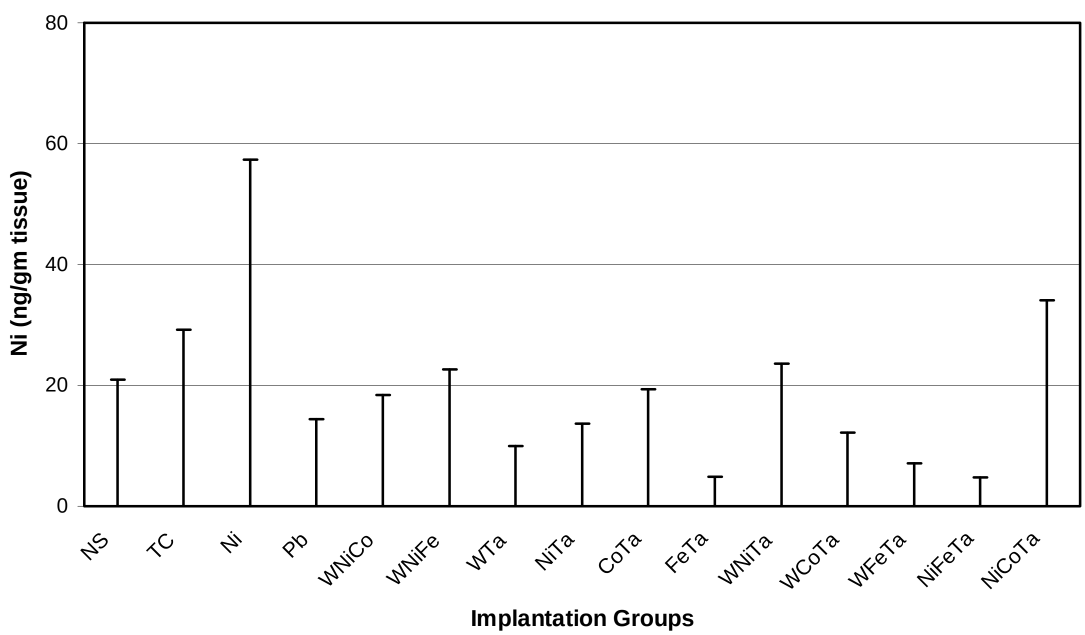

Figure 6 (continued): Femur Metals Levels in 1-Month Implantation Groups

C. Femur Cobalt Levels

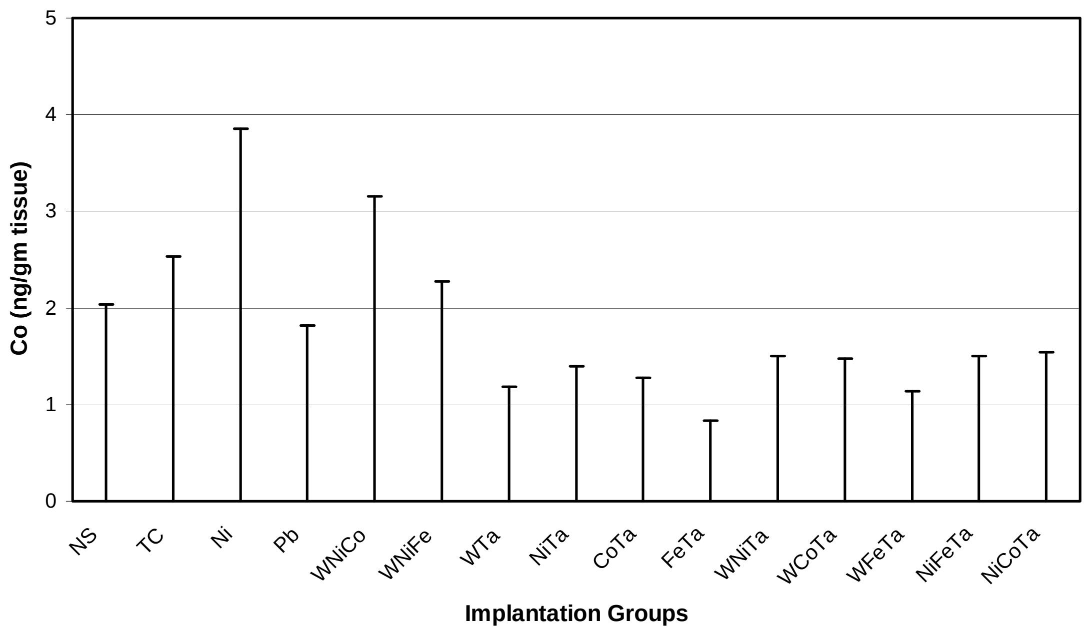

D. Femur Tantalum Levels

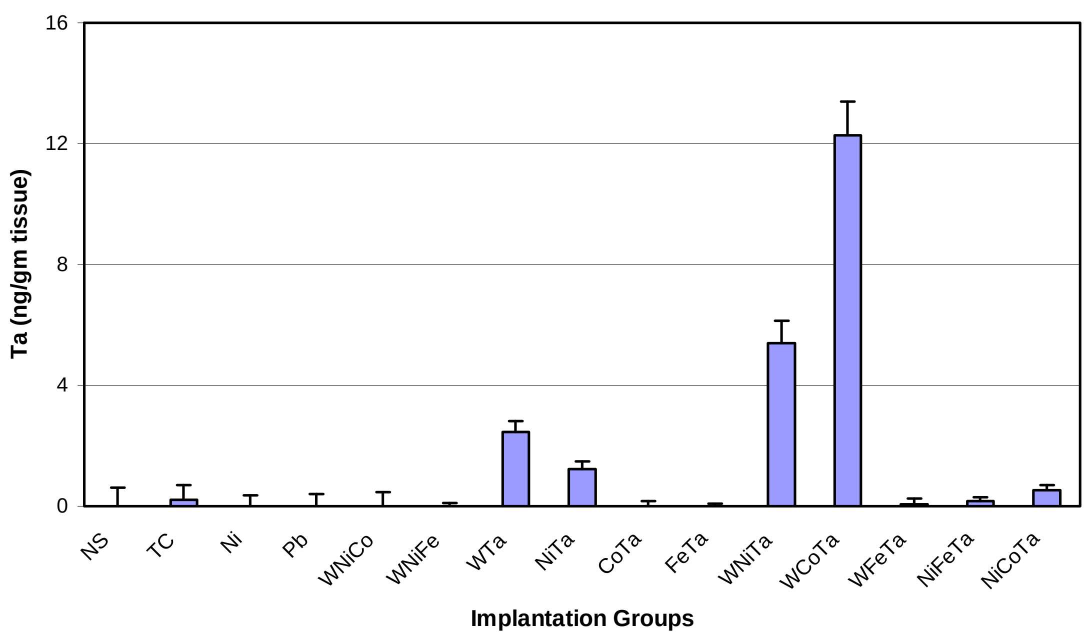

Figure 7: Kidney Metal Levels in 1-Month Implantation Groups

A. Kidney Tungsten Levels

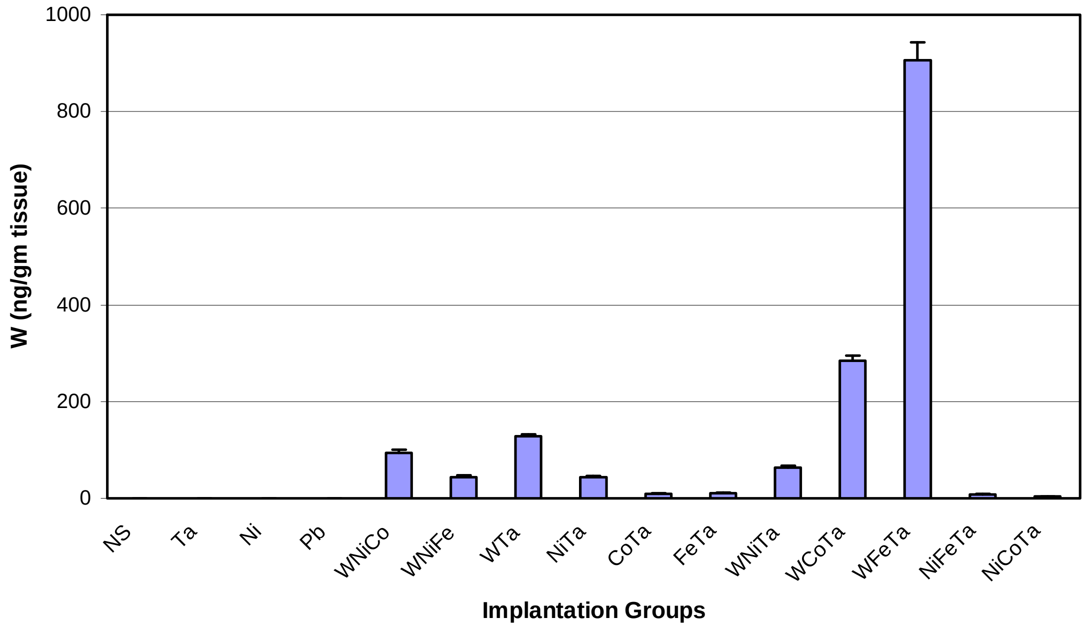

B. Kidney Nickel Levels

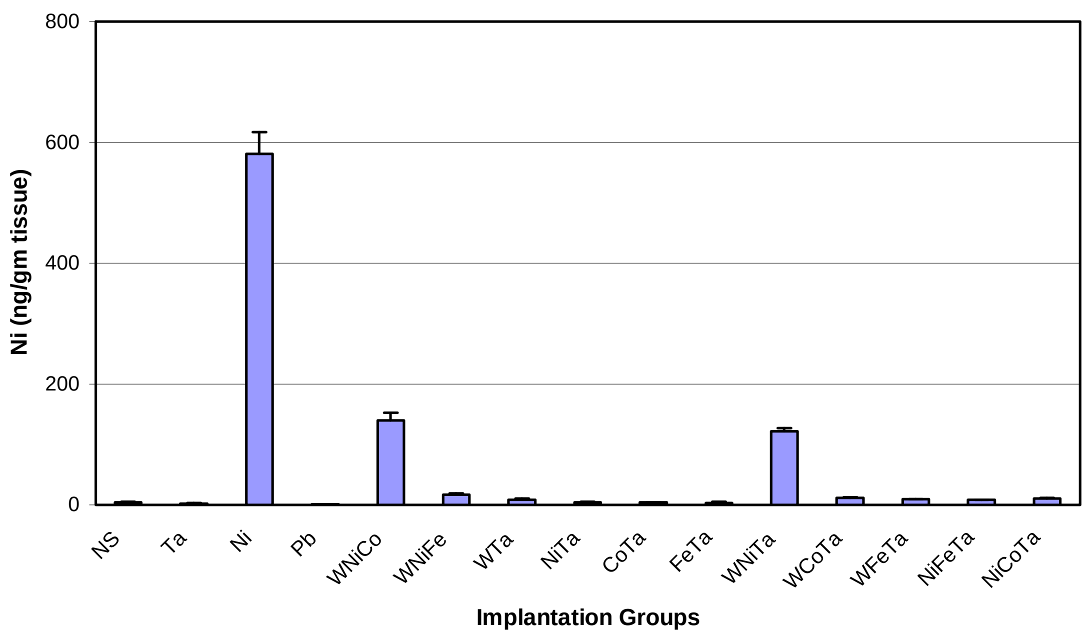

Figure 7 (continued) : Kidney Metal Levels in 1-Month Implantation Groups

C. Kidney Cobalt Levels

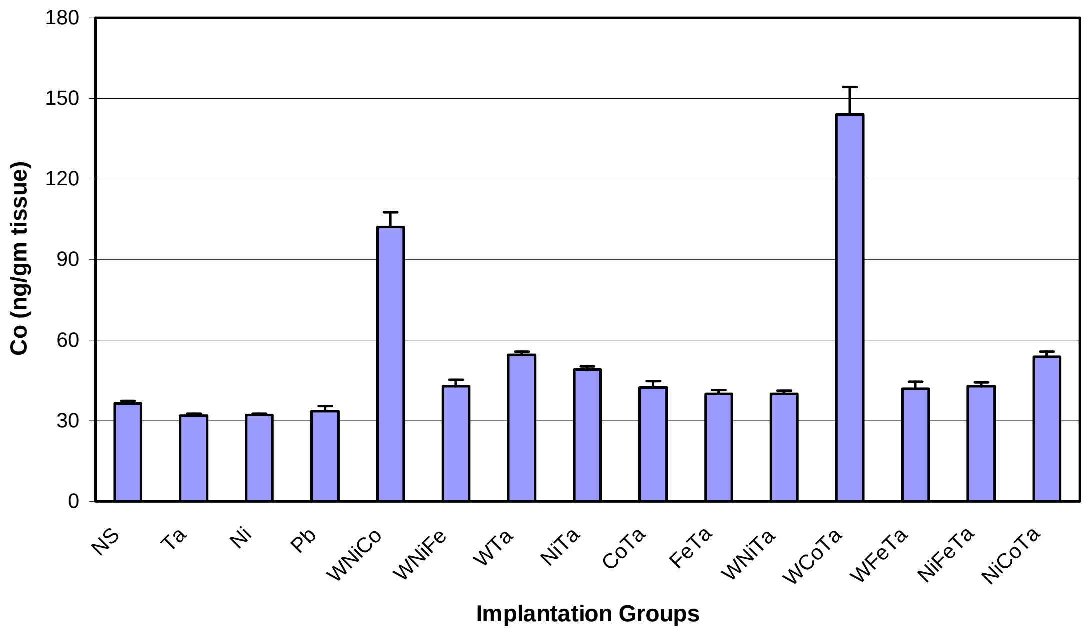

D. Kidney Tantalum Levels

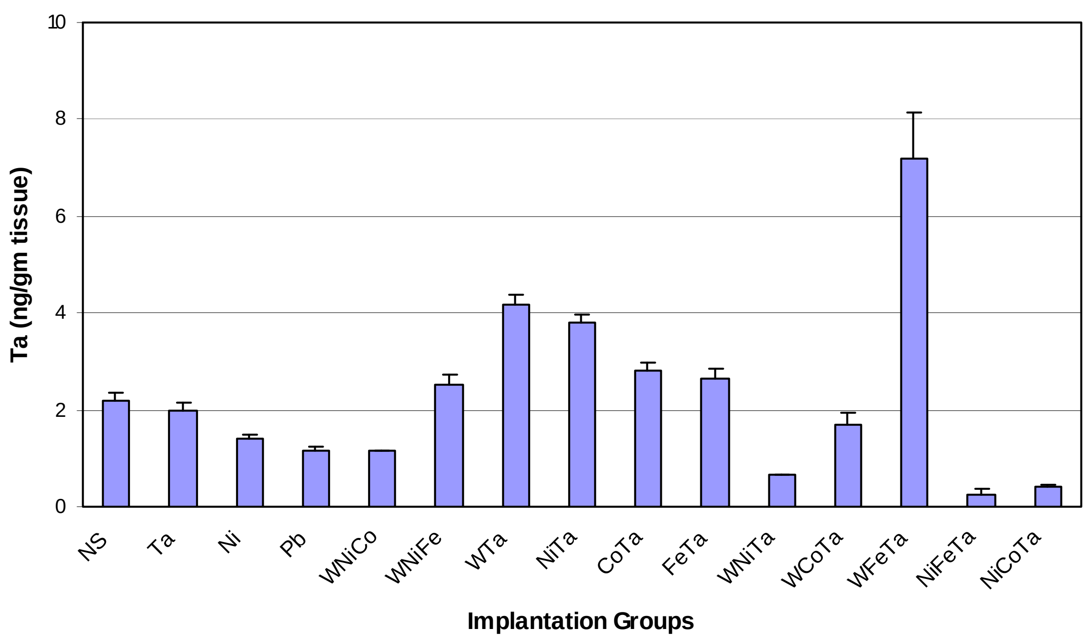

Figure 8: Liver Metal Levels in 1-Month Implantation Groups

A. Liver Tungsten Levels

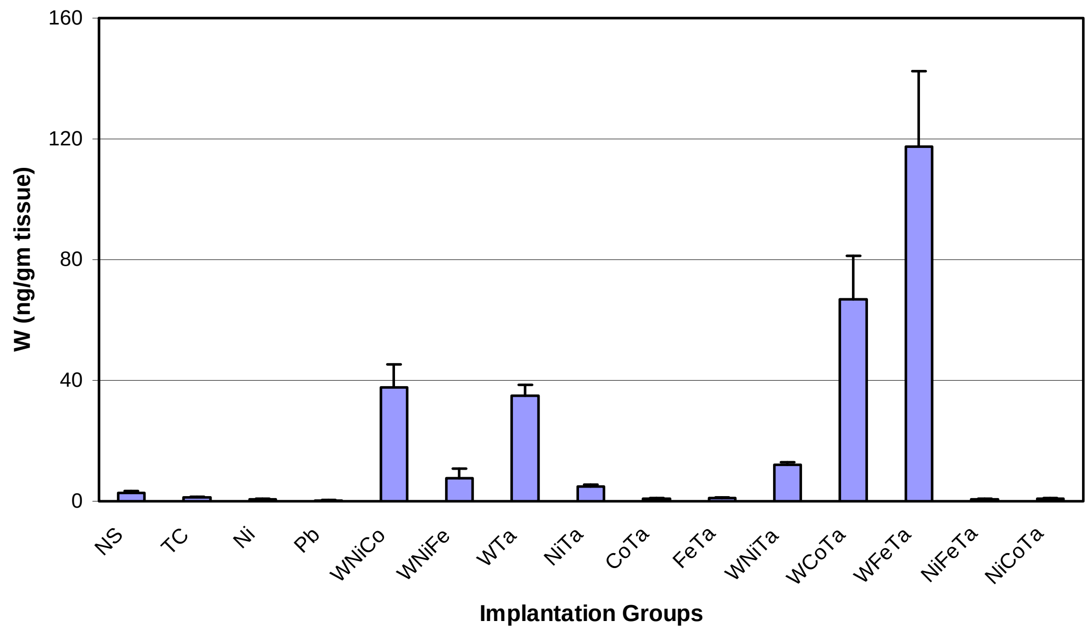

B. Liver Nickel Levels

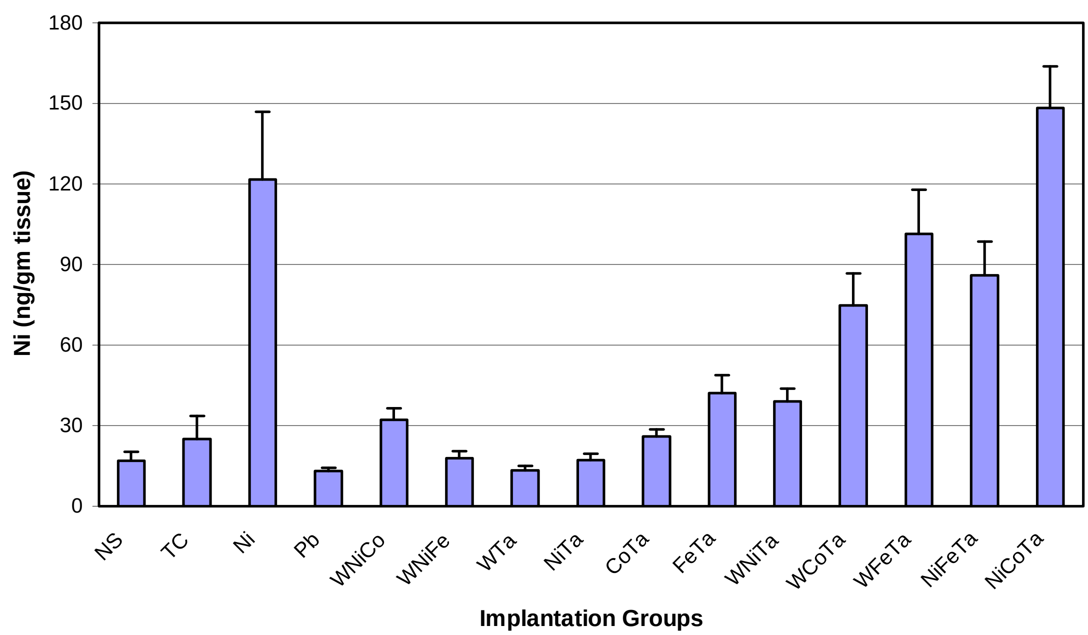

Figure 8 (continued): Liver Metal Levels in 1-Month Implantation Groups

C. Liver Cobalt Levels

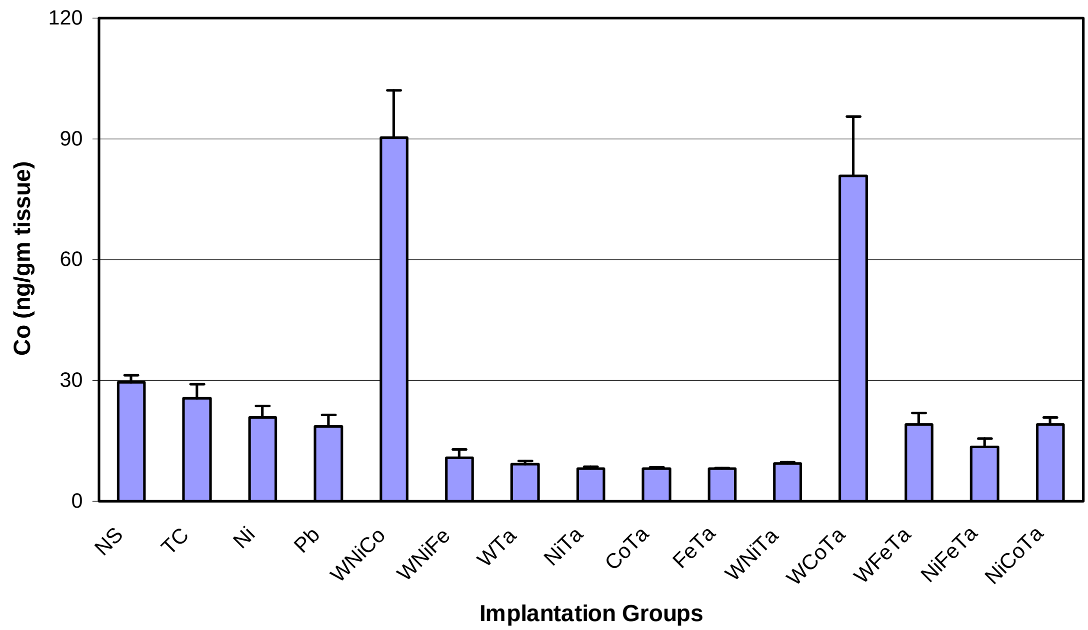

D. Liver Tantalum Levels

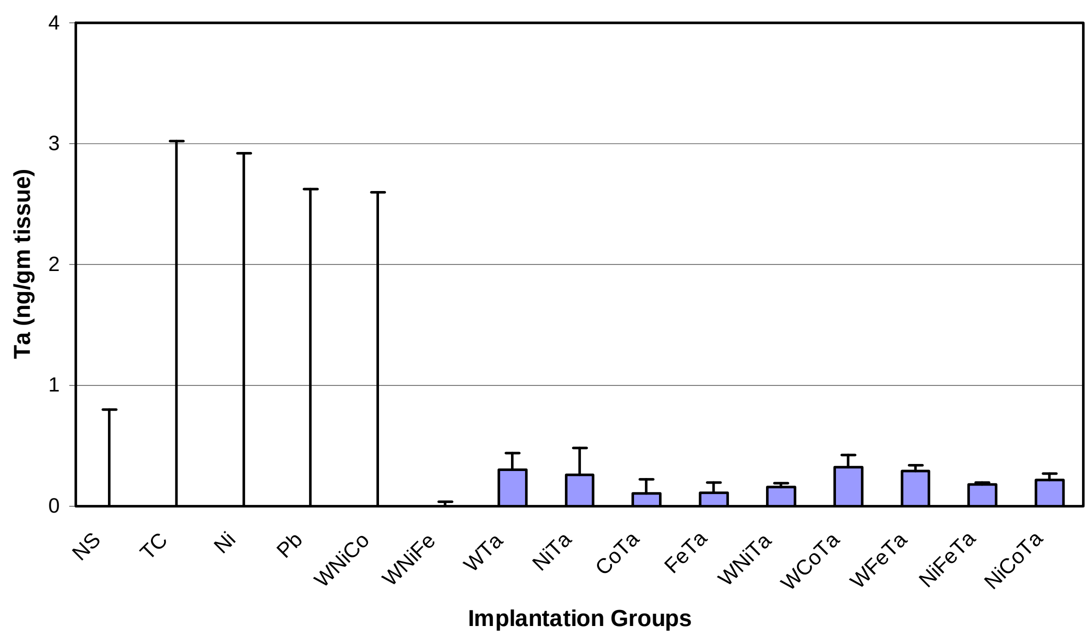

Figure 9: Serum Metals Levels in 1-Month Implantation Groups

A. Serum Tungsten Levels

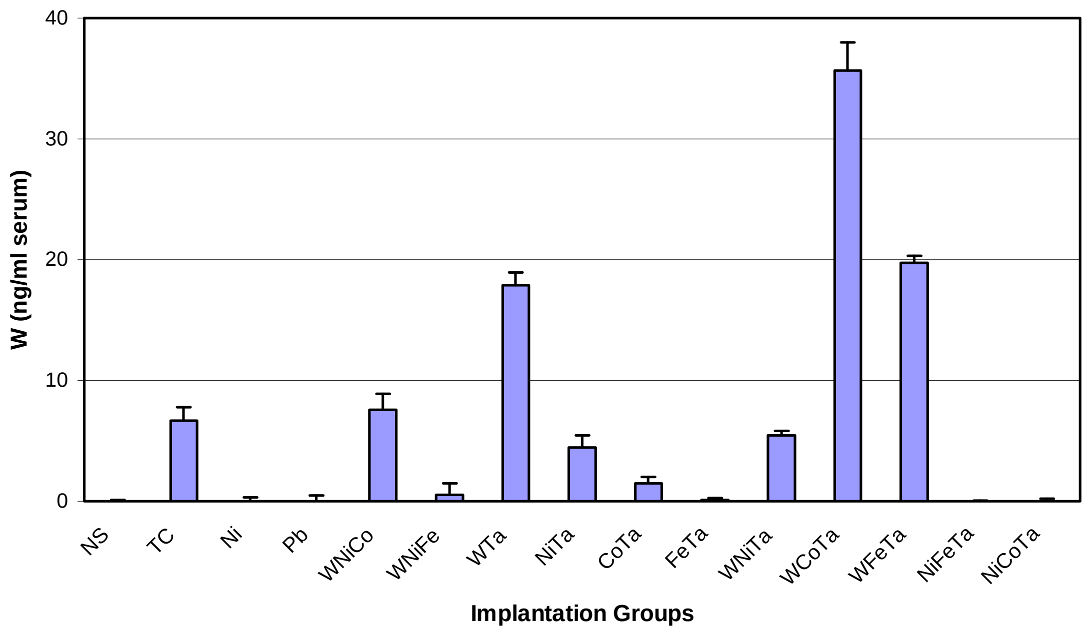

B. Serum Nickel Levels

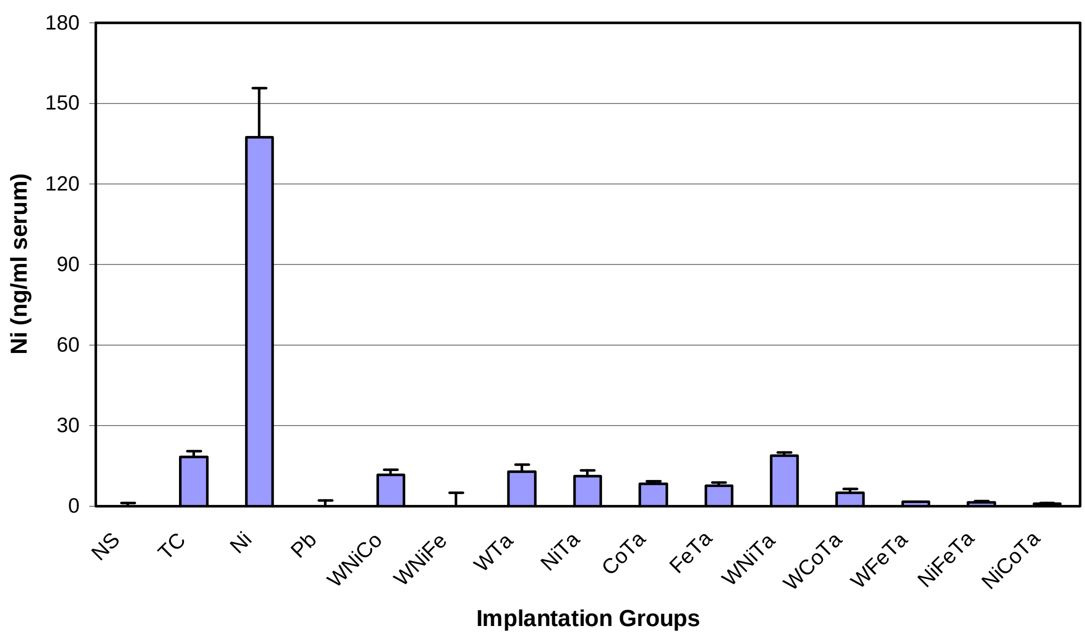

Figure 9 (continued): Serum Metals Levels in 1-Month Implantation Groups

C. Serum Cobalt Levels

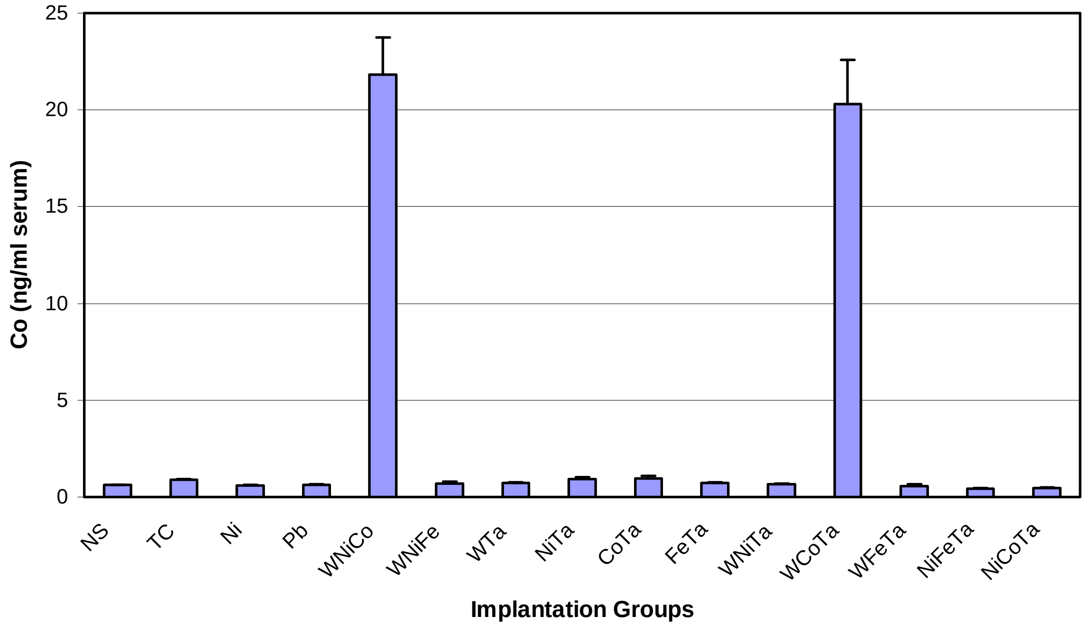

D. Serum Tantalum Levels

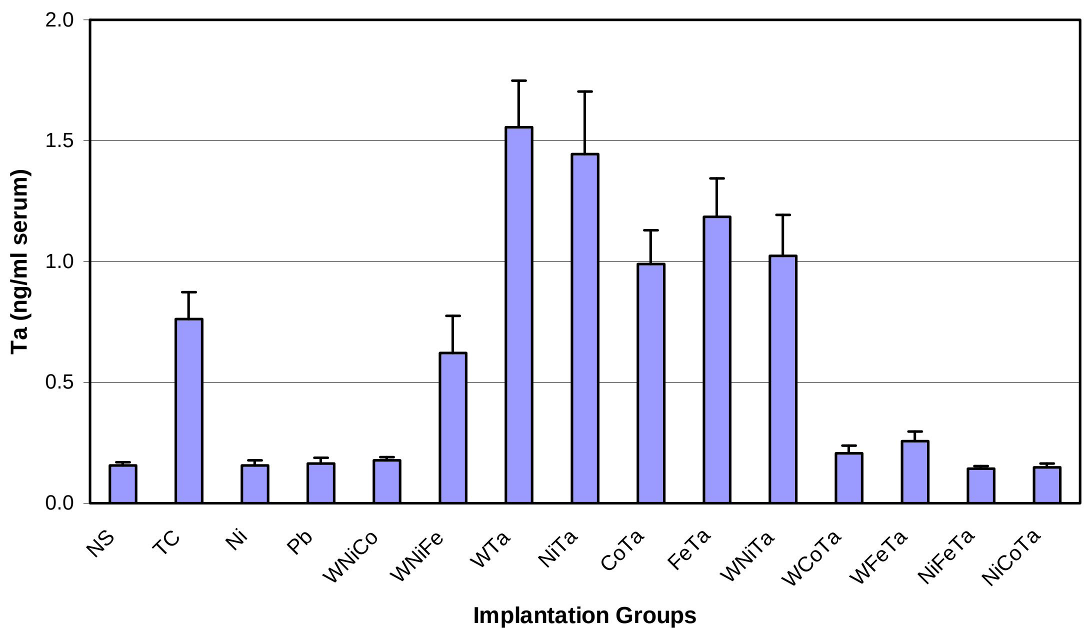

Figure 10: Spleen Metal Levels in 1-Month Implantation Groups

A. Spleen Tungsten Levels

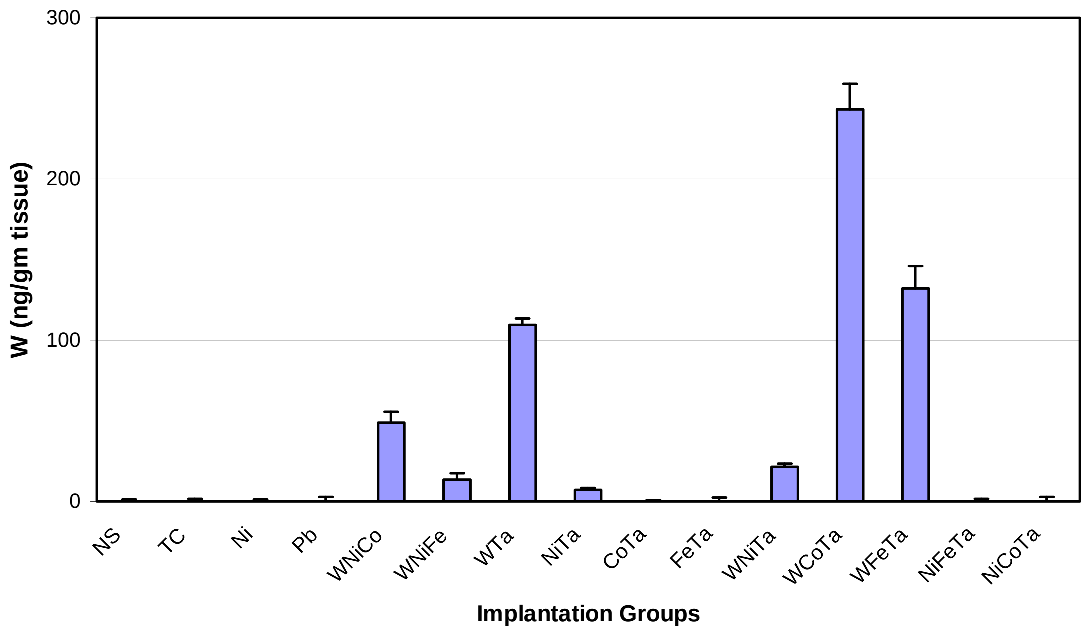

B. Spleen Nickel Levels

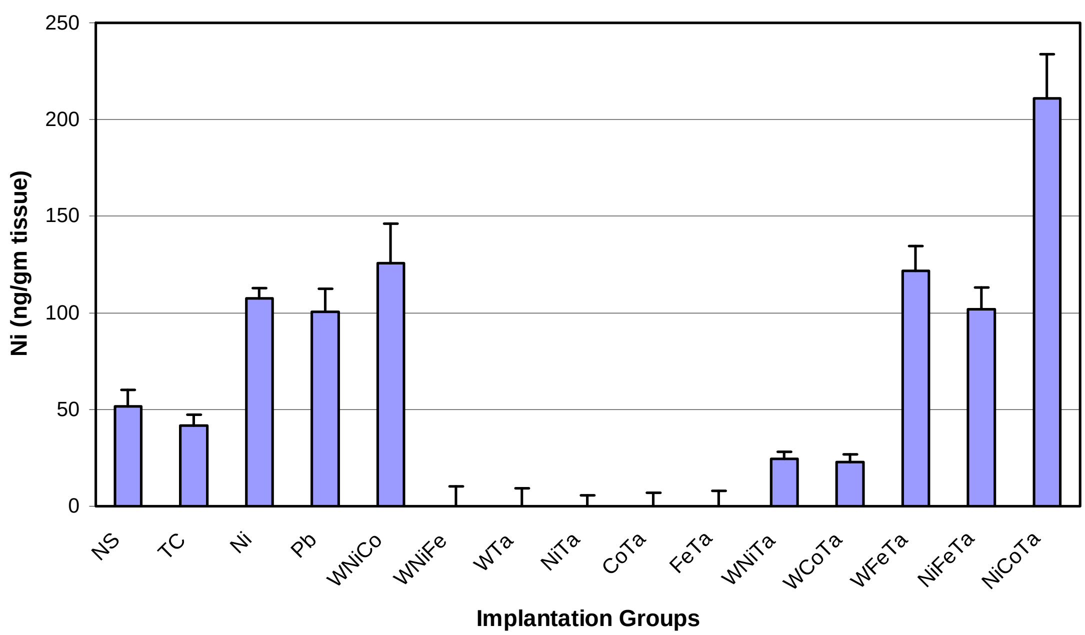

Figure 10 (continued): Spleen Metal Levels in 1-Month Implantation Groups

C. Spleen Cobalt Levels

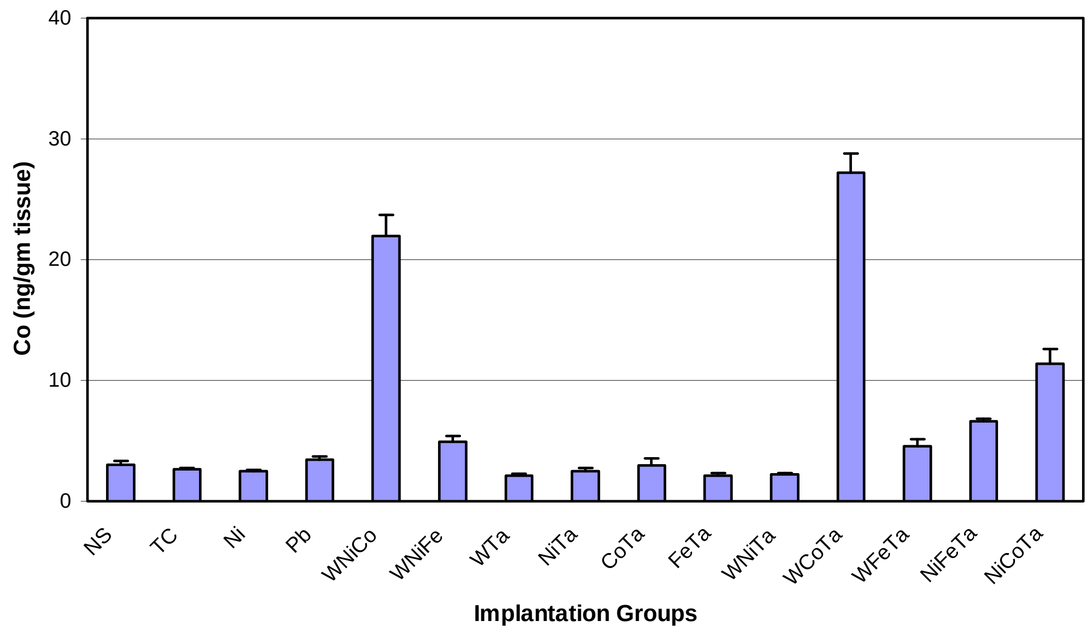

D. Spleen Tantalum Levels

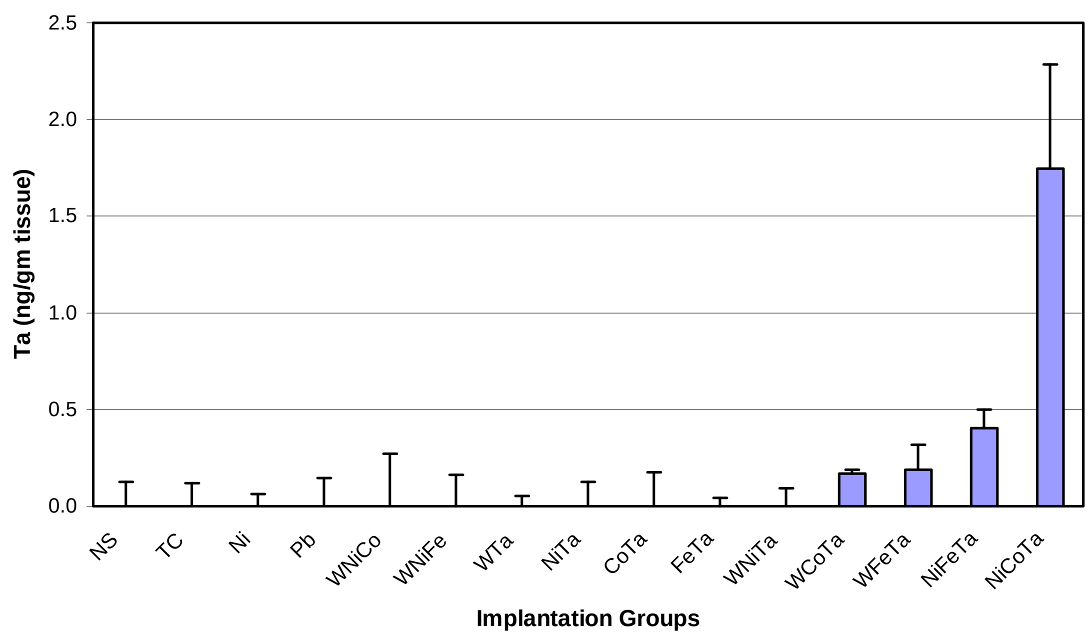

Figure 11: Testes Metal Levels in 1-Month Implantation Groups

A. Testes Tungsten Levels

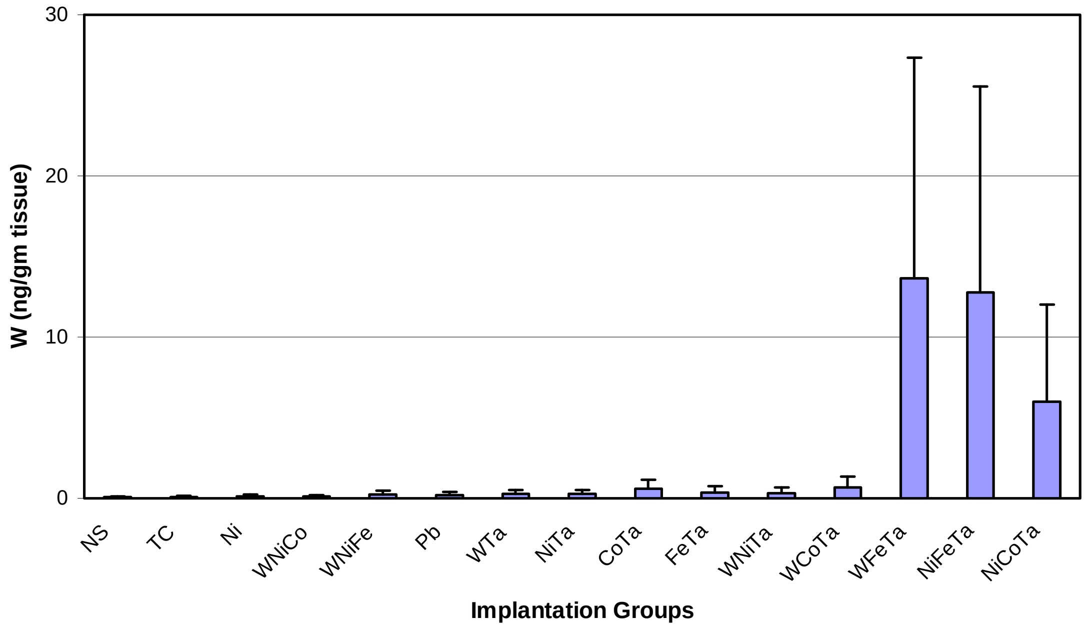

B. Testes Nickel Level

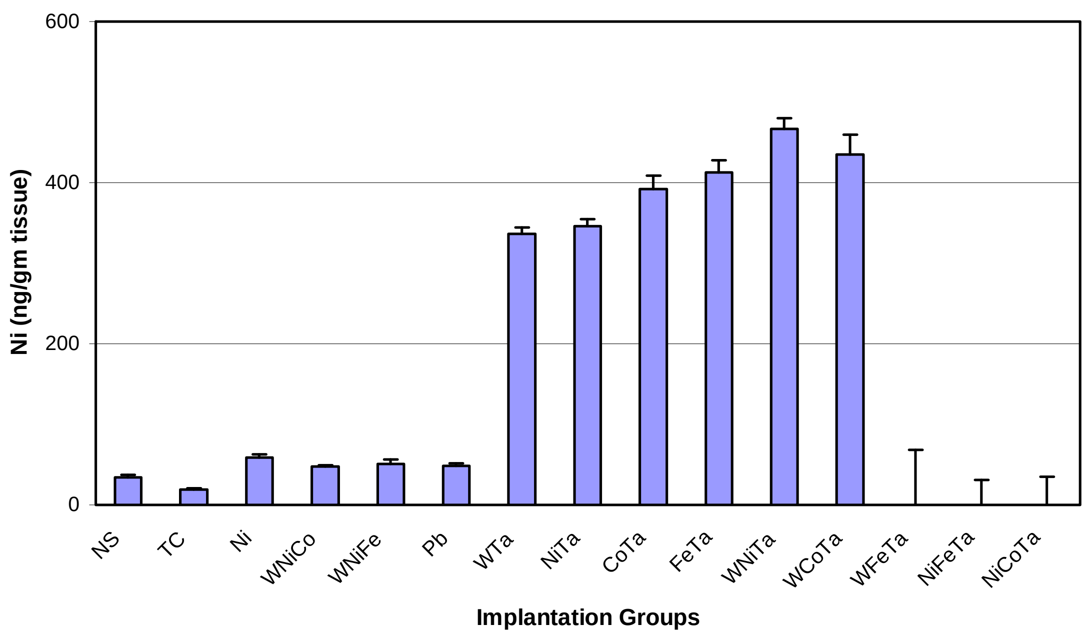

Figure 11 (continued): Testes Metal Levels in 1-Month Implantation Groups

C. Testes Cobalt Levels

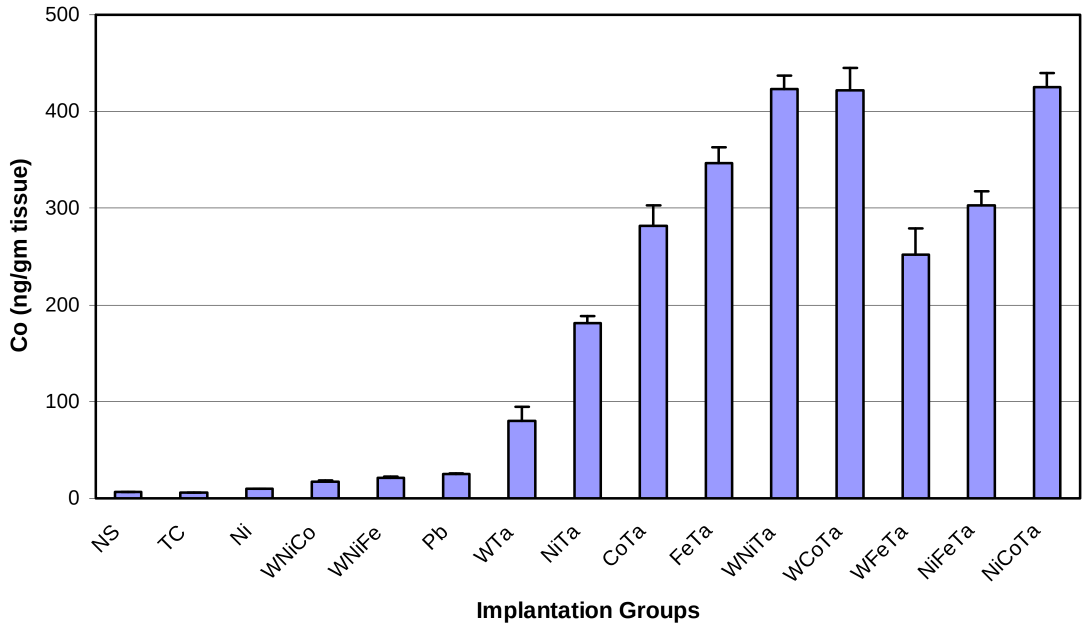

D. Testes Tantalum Levels

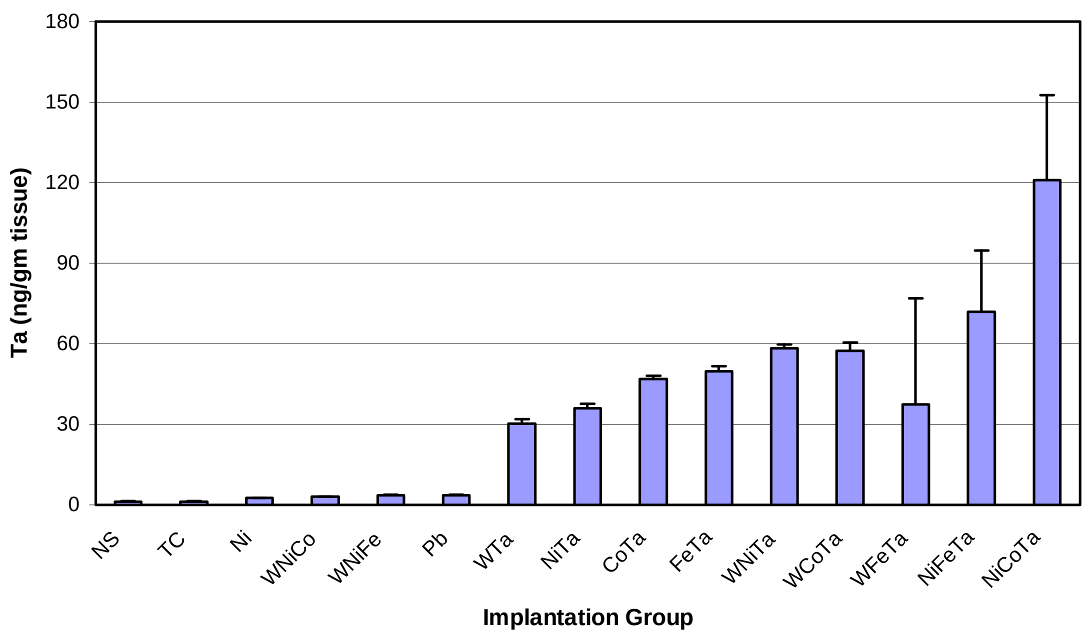

Figure 12: Urinary Metal Levels in 1-Month Implantation Groups

A. Urinary Tungsten Levels

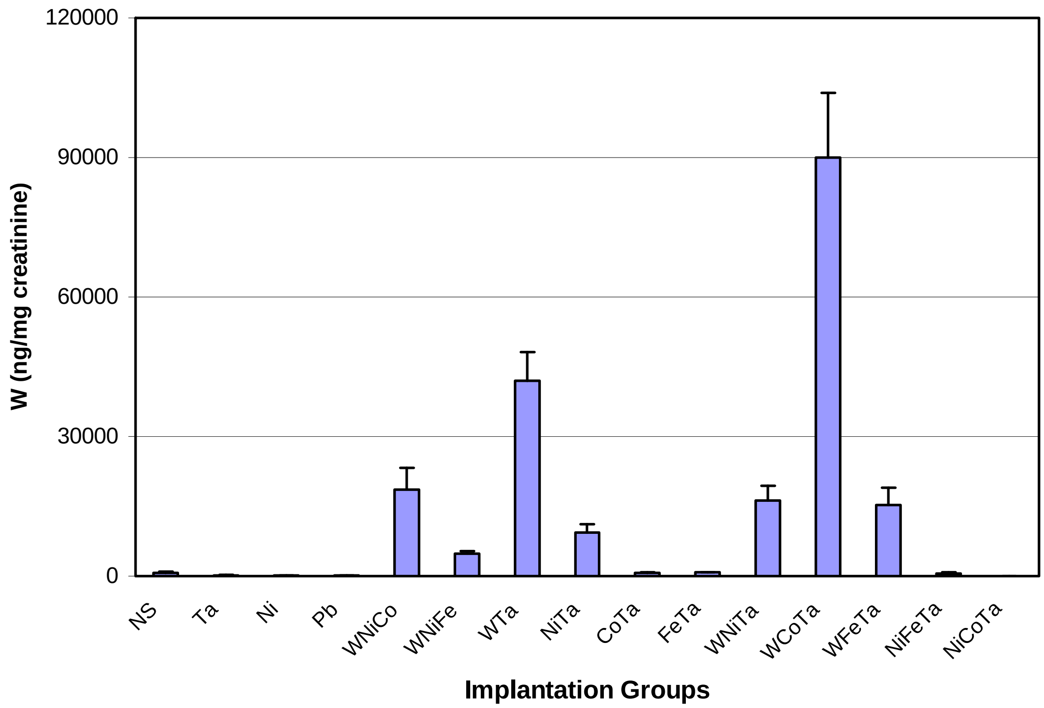

B. Urinary Nickel Levels

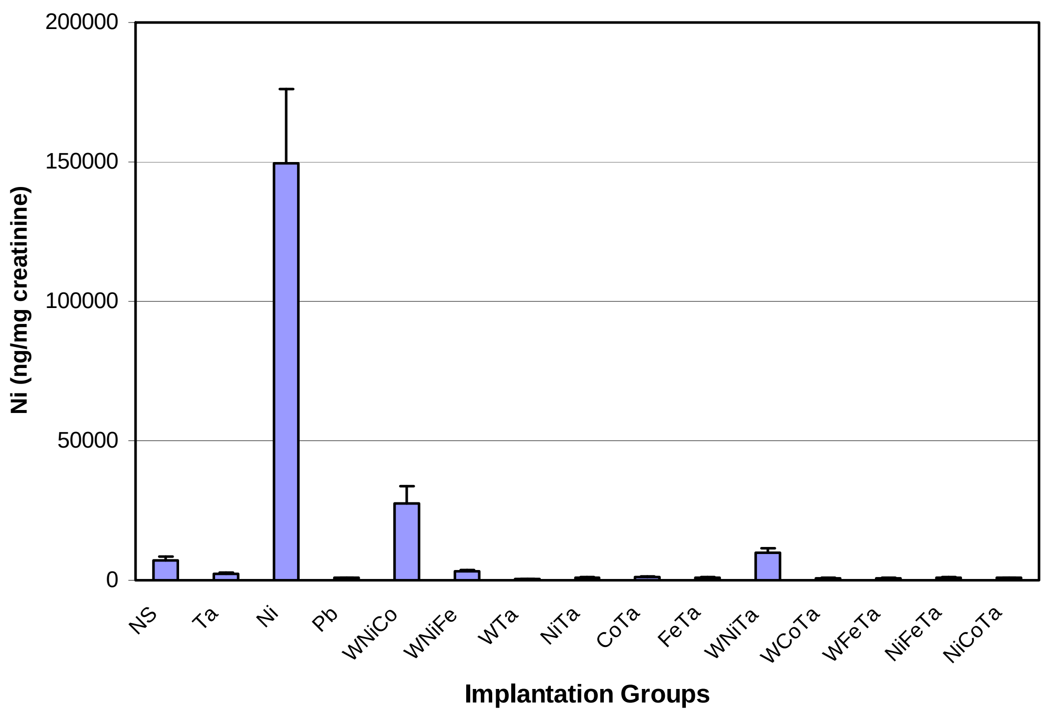

Figure 12 (continued): Urinary Metal Levels in 1-Month Implantation Groups

C. Urinary Cobalt Levels

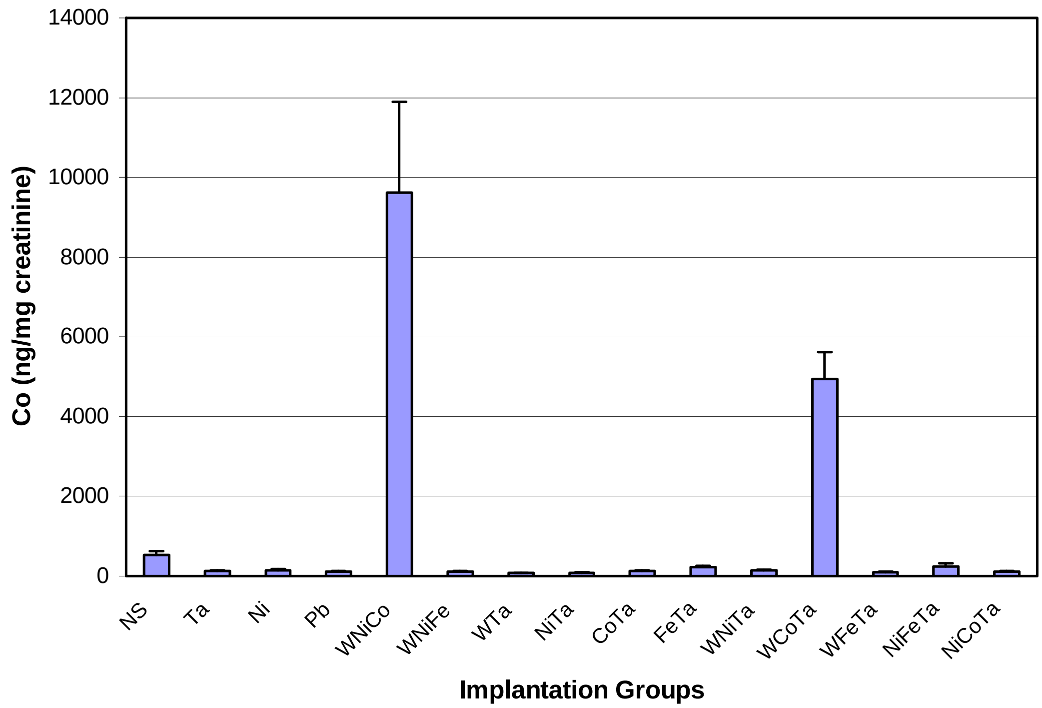

D. Urinary Tantalum Levels

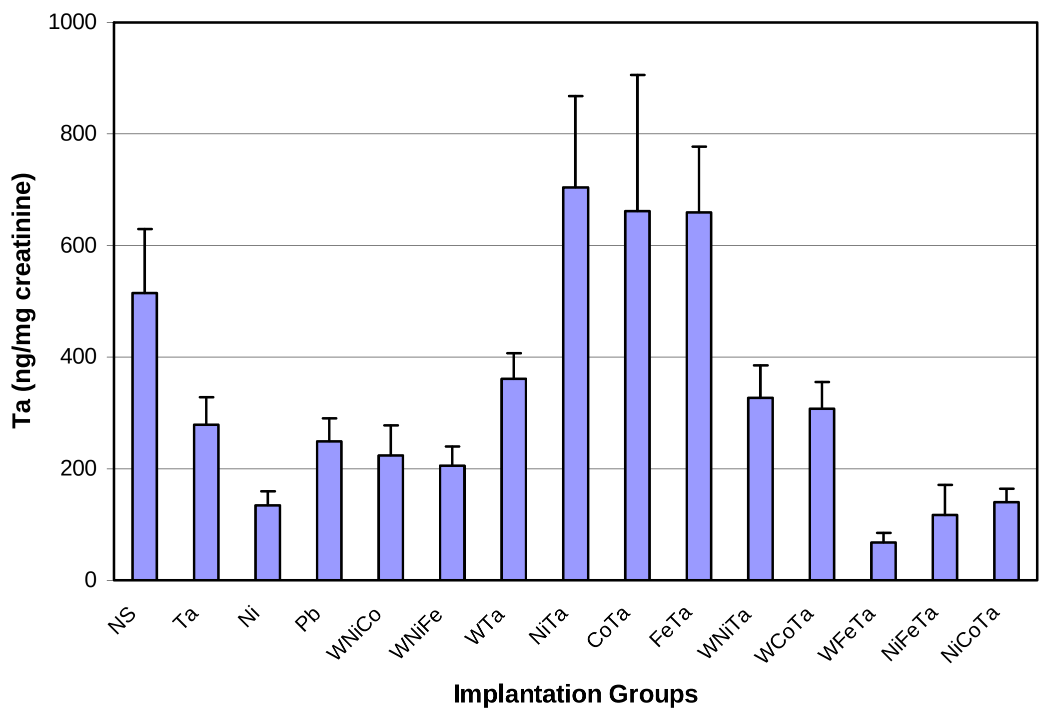

Figure 13: Brain Metal Levels in 3-Month Implantation Groups

A. Brain Tungsten Levels

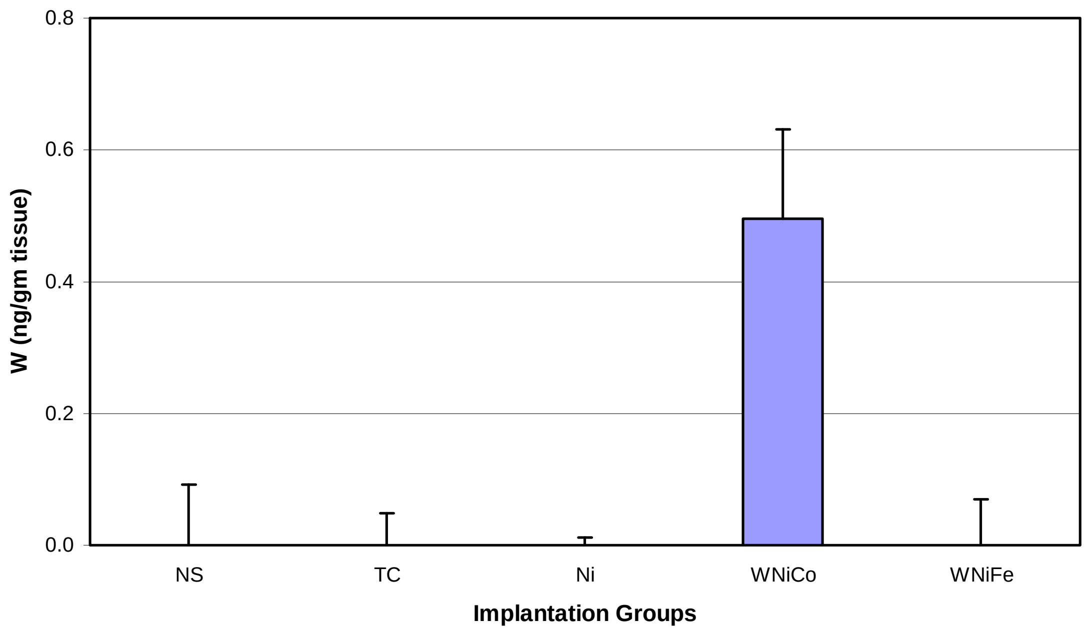

B. Brain Nickel Levels

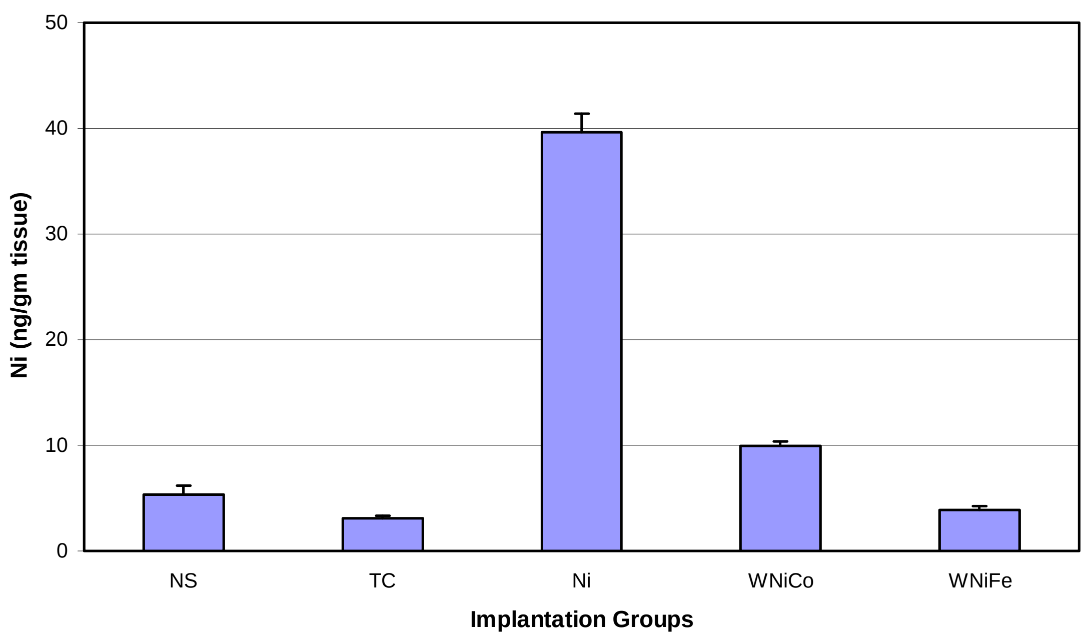

Figure 13 (continued): Brain Metal Levels in 3-Month Implantation Groups

C. Brain Cobalt Levels

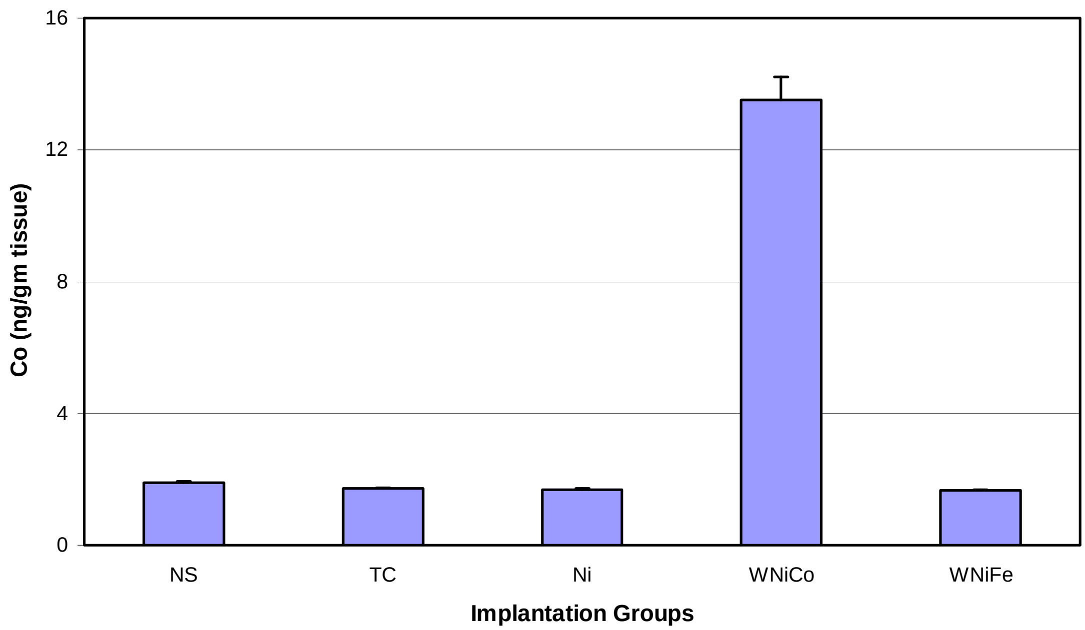

D. Brain Tantalum Levels

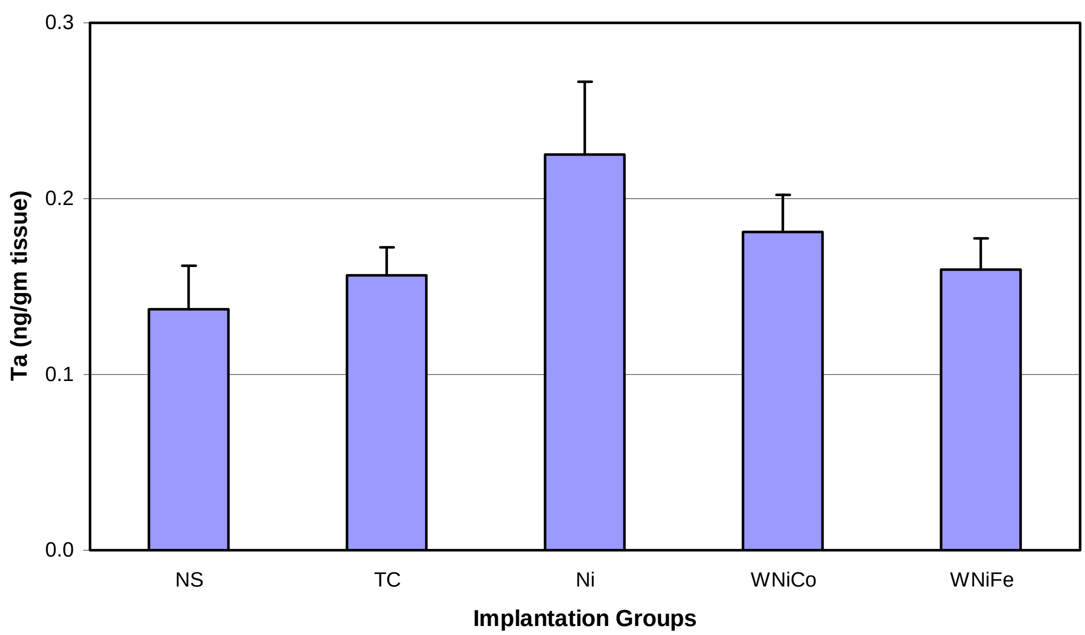

Figure 14: Femur Metal Levels in 3-Month Implantation Groups

A. Femur Tungsten Levels

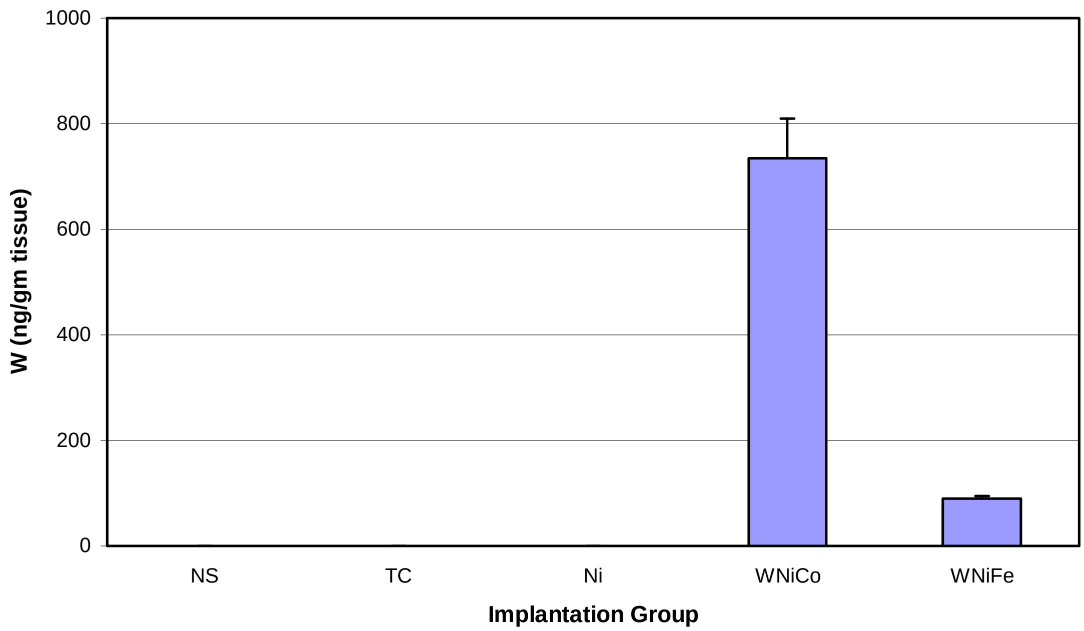

B. Femur Nickel Levels

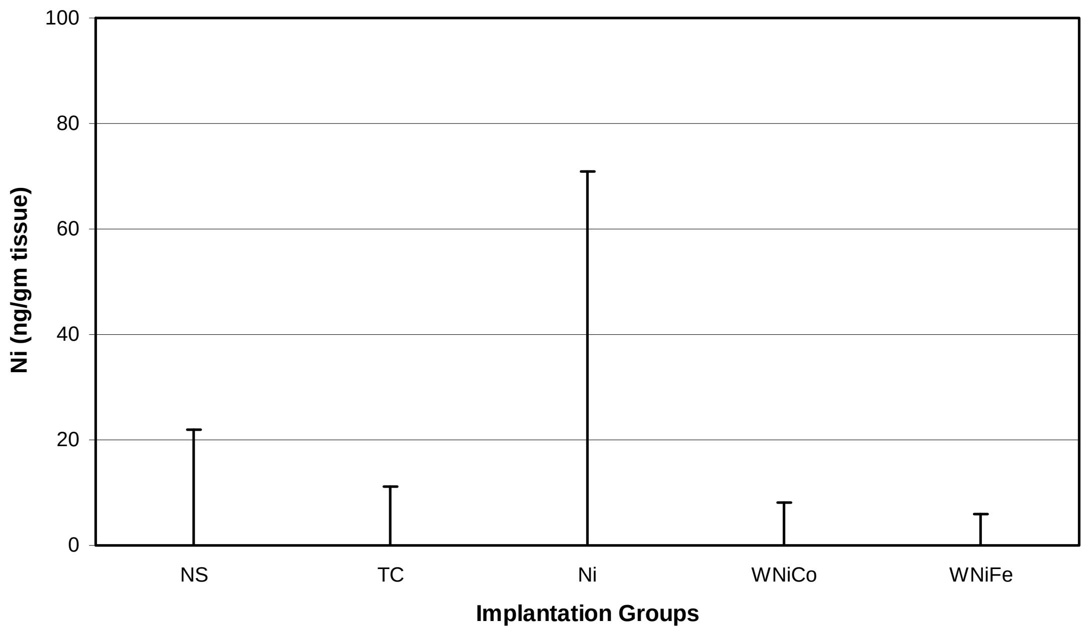

Figure 14 (continued): Femur Metal Levels in 3-Month Implantation Groups

C. Femur Cobalt Levels

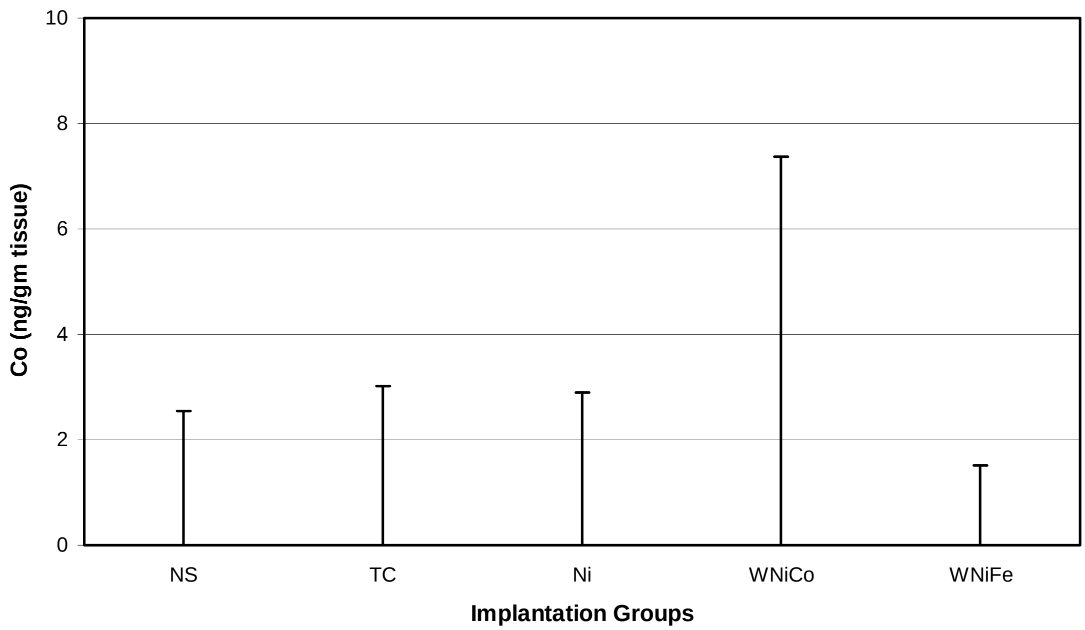

D. Femur Tantalum Levels

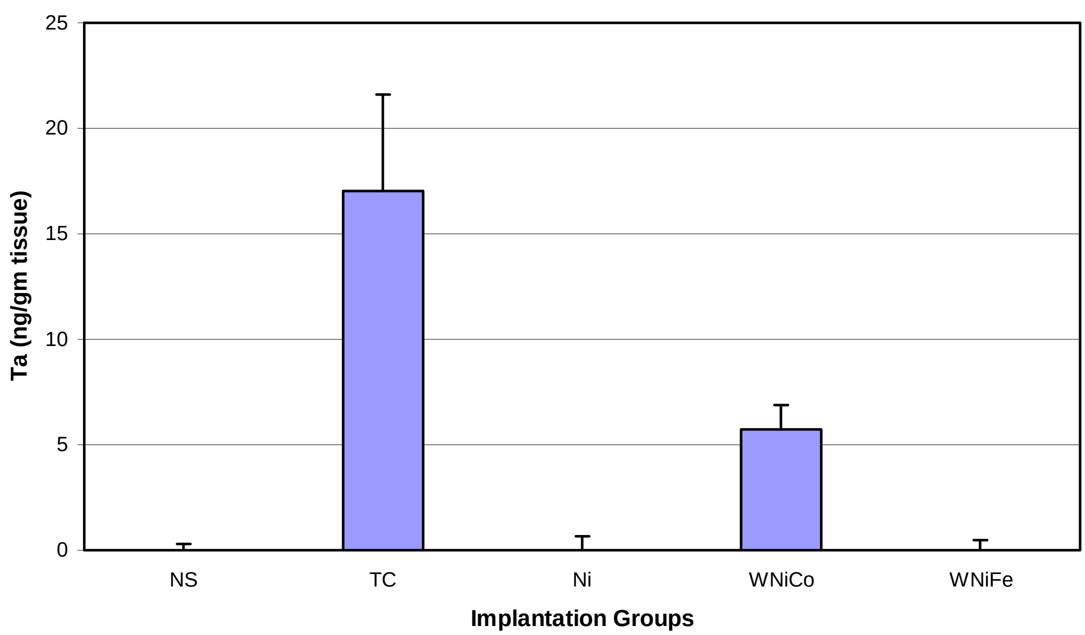

Figure 15: Kidney Metal Levels in 3-Month Implantation Groups

A. Kidney Tungsten Levels

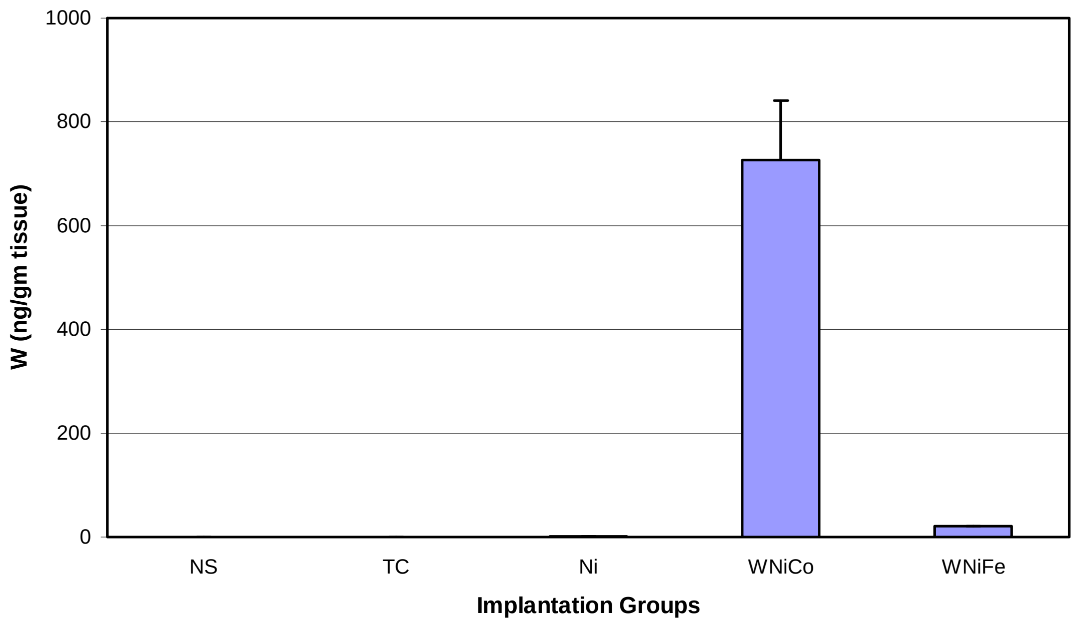

B. Kidney Nickel Levels

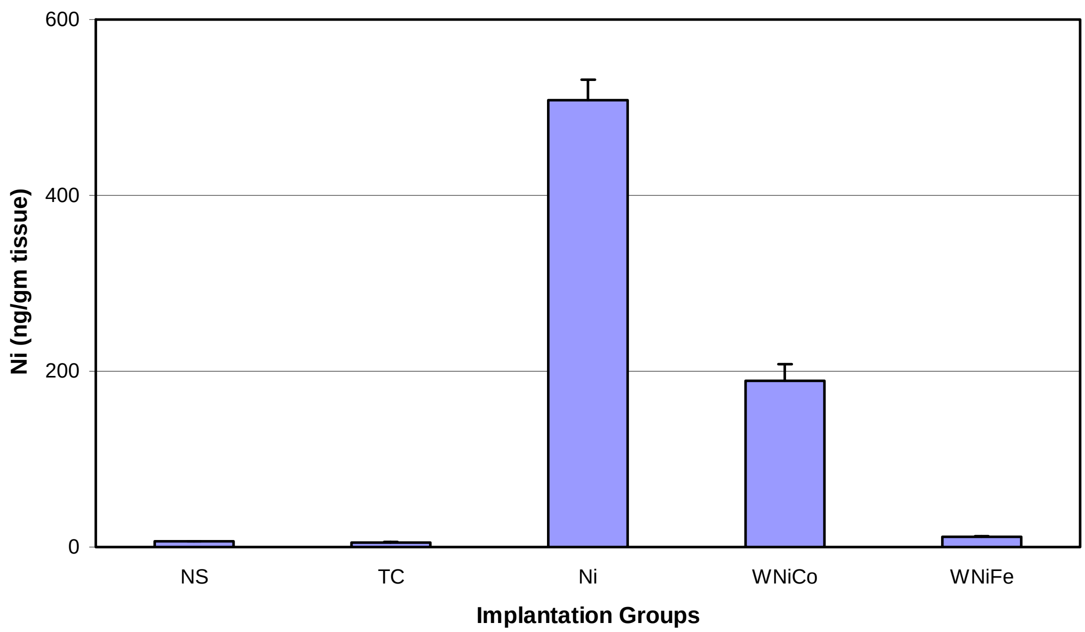

Figure 15 (continued): Kidney Metal Levels in 3-Month Implantation Groups

C. Kidney Cobalt Levels

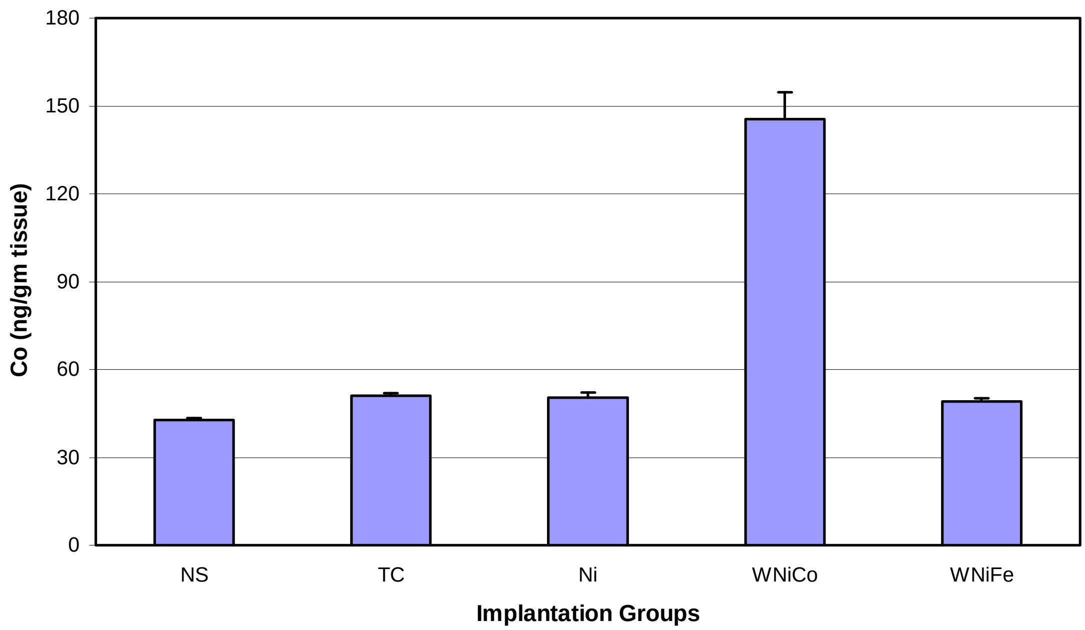

D. Kidney Tantalum Levels

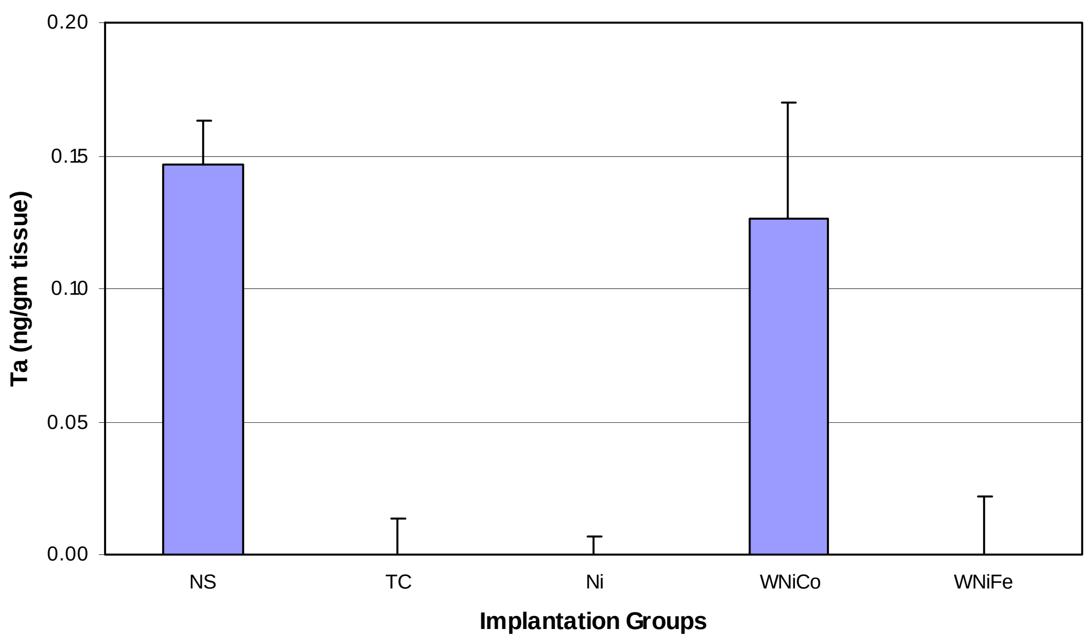

Figure 16: Liver Metal Levels in 3-Month Implantation Groups

A. Liver Tungsten Levels

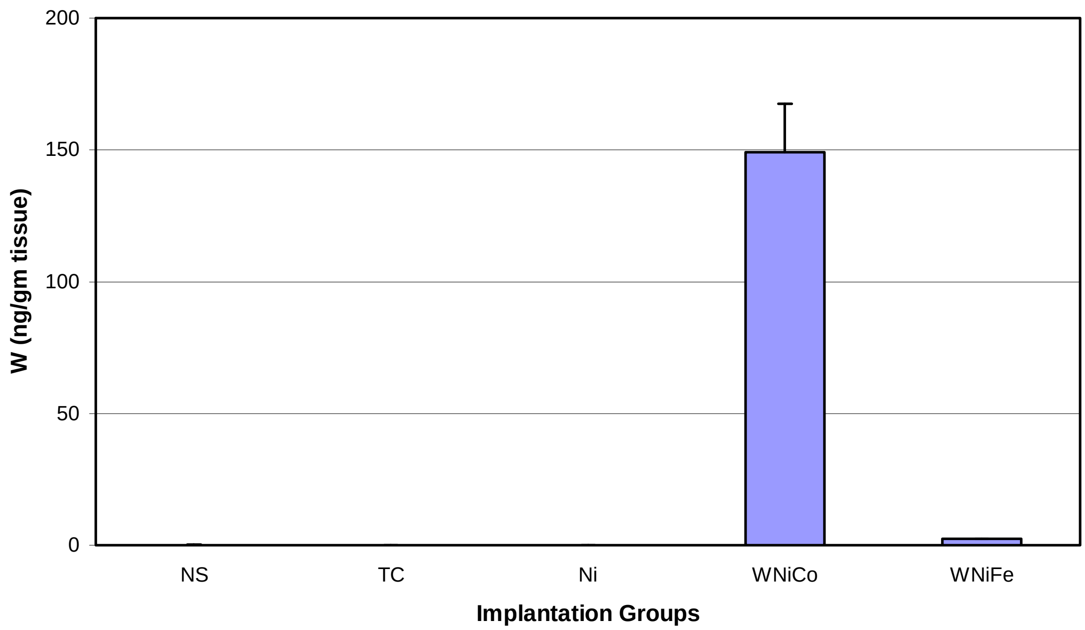

B. Liver Nickel Levels

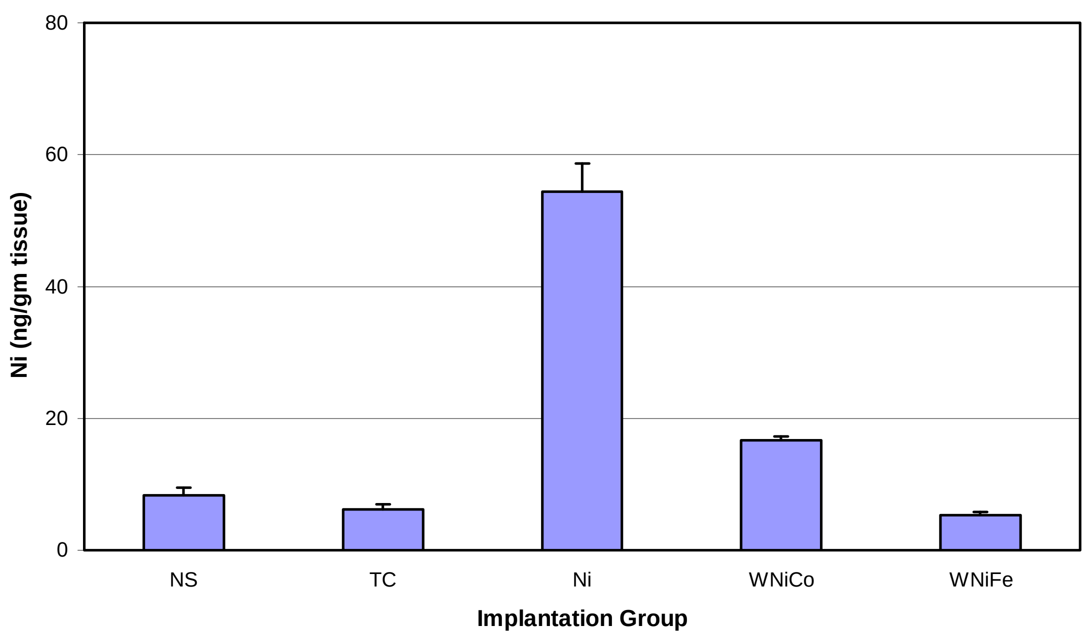

Figure 16 (continued): Liver Metal Levels in 3-Month Implantation Groups

C. Liver Cobalt Levels

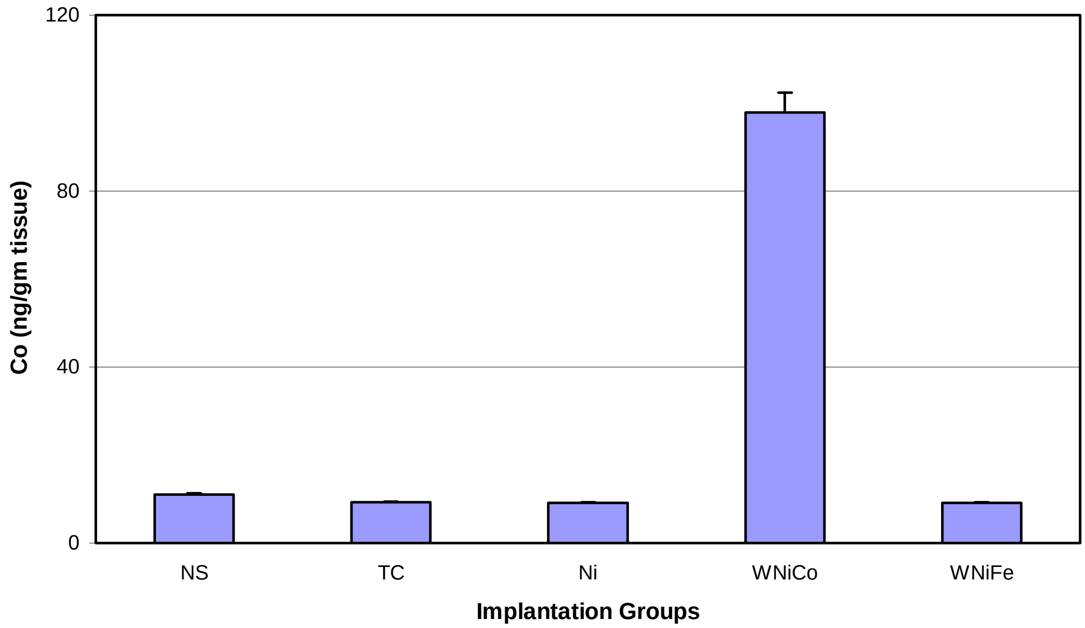

D. Liver Tantalum Levels

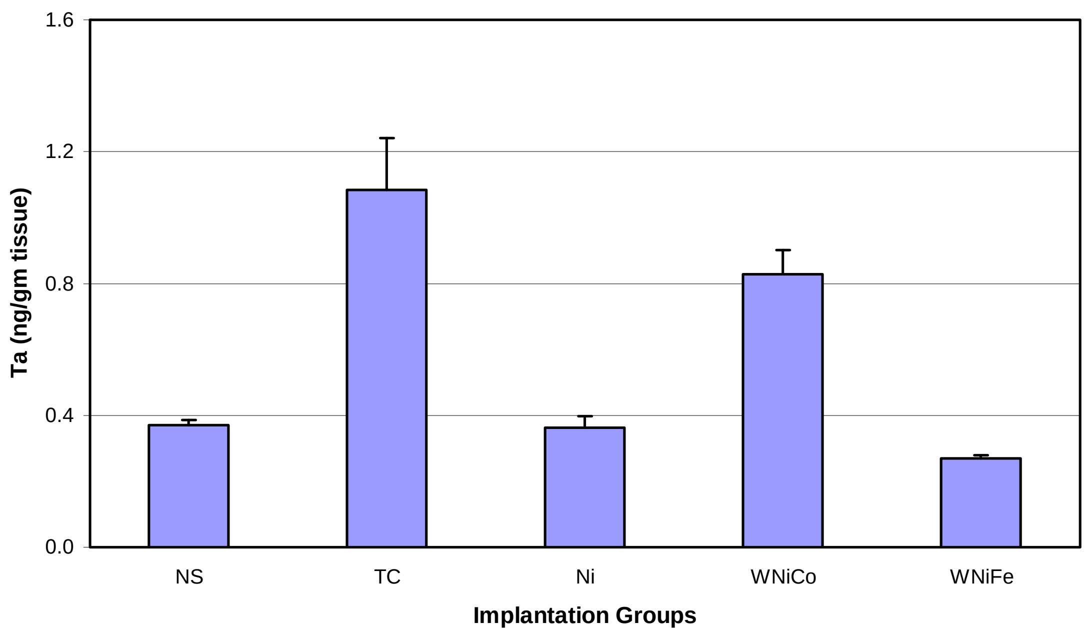

Figure 17: Serum Metals Levels in 3-Month Implantation Groups

A. Serum Tungsten Levels

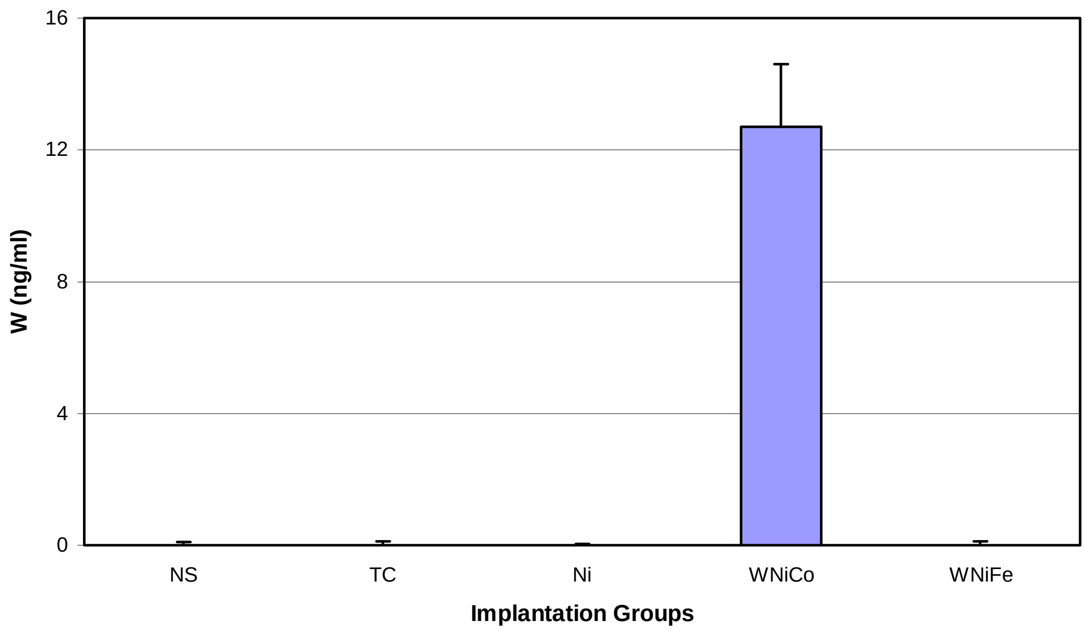

B. Serum Nickel Levels

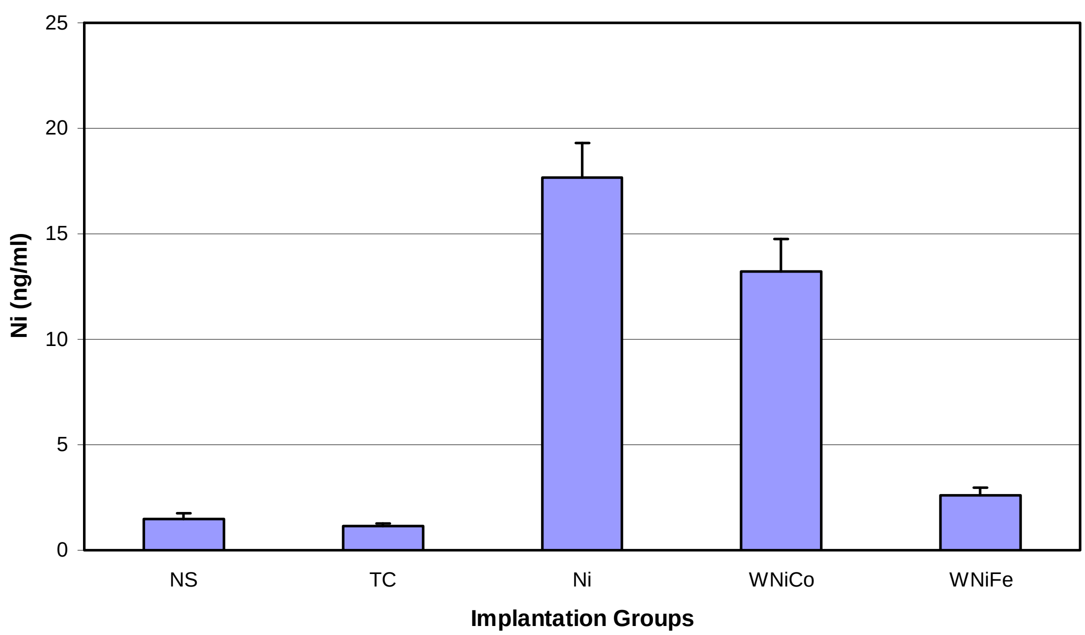

Figure 17 (continued): Serum Metals Levels in 3-Month Implantation Groups

C. Serum Cobalt Levels

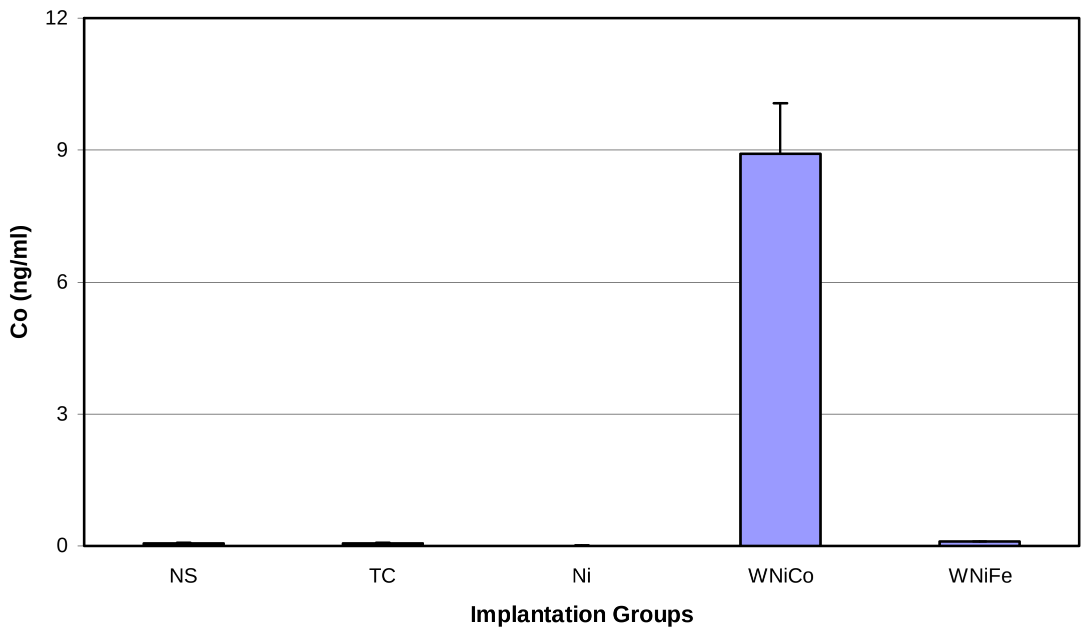

D. Serum Tantalum Levels

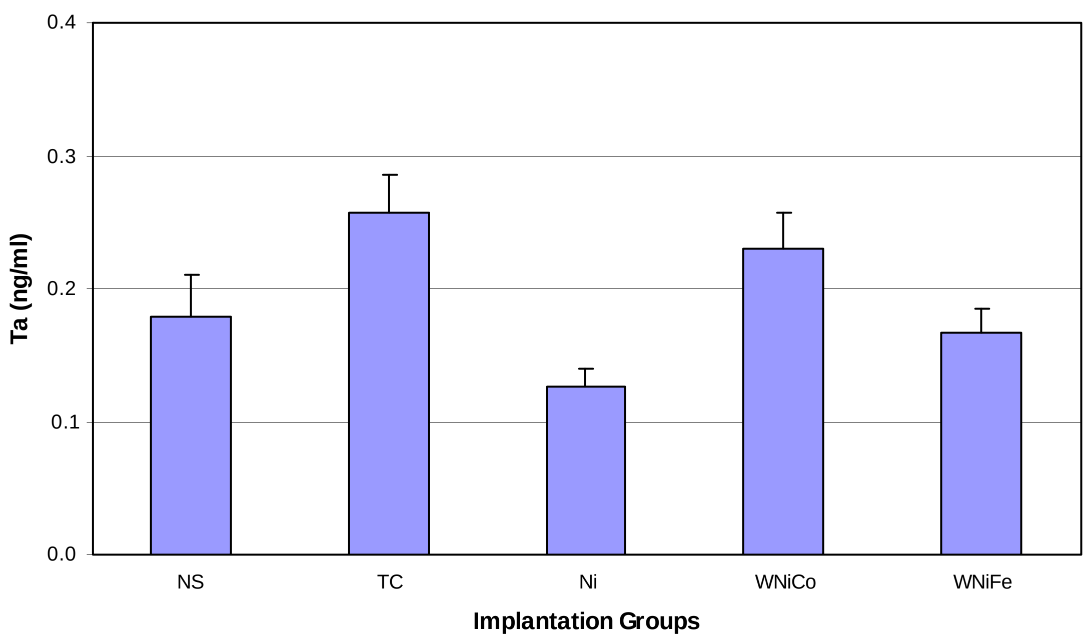

Figure 18: Spleen Metal Levels in 3-Month Implantation Groups

A. Spleen Tungsten Levels

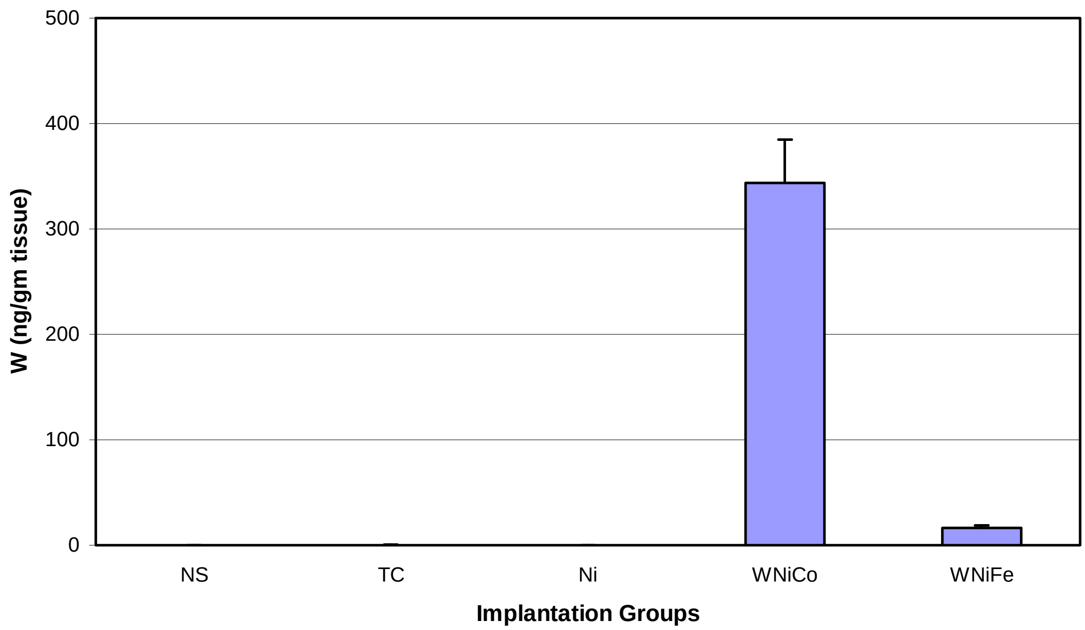

B. Spleen Nickel Levels

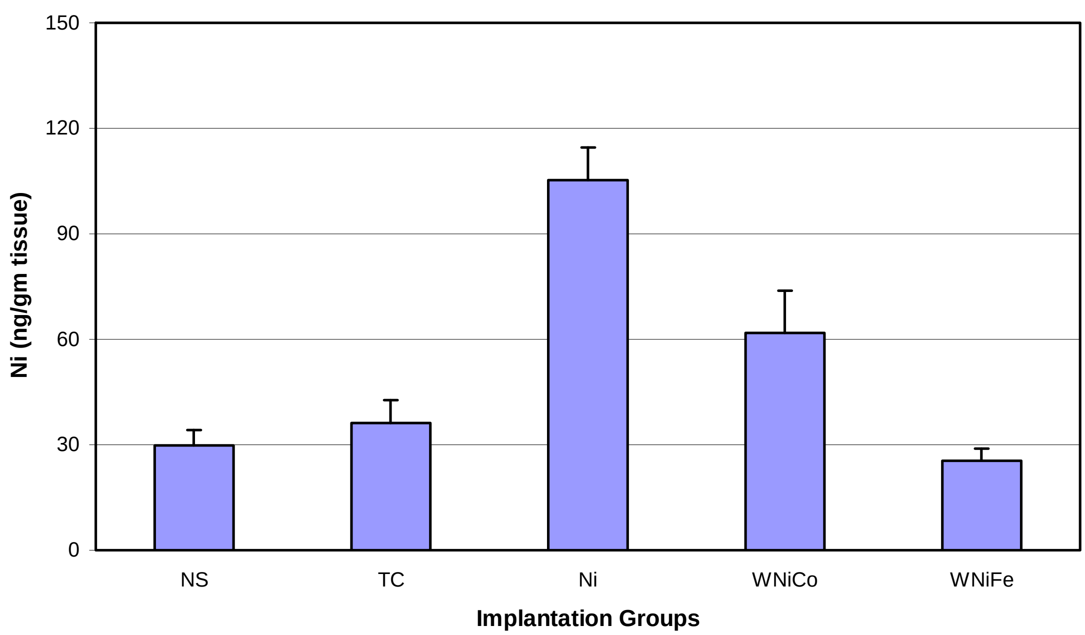

Figure 18 (continued): Spleen Metal Levels in 3-Month Implantation Groups

C. Spleen Cobalt Levels

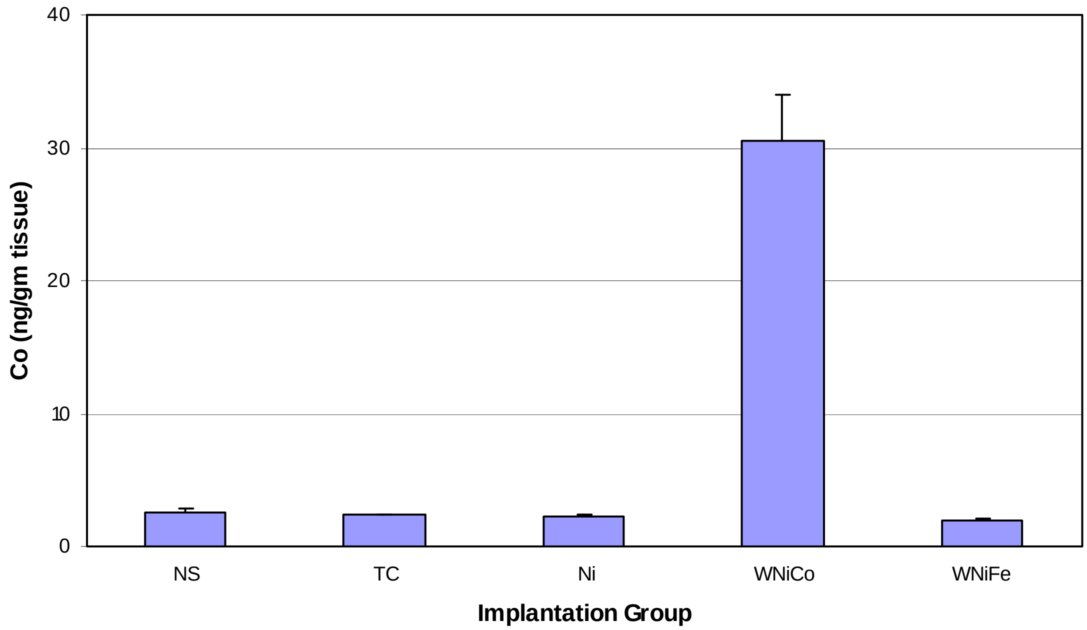

D. Spleen Tantalum Levels

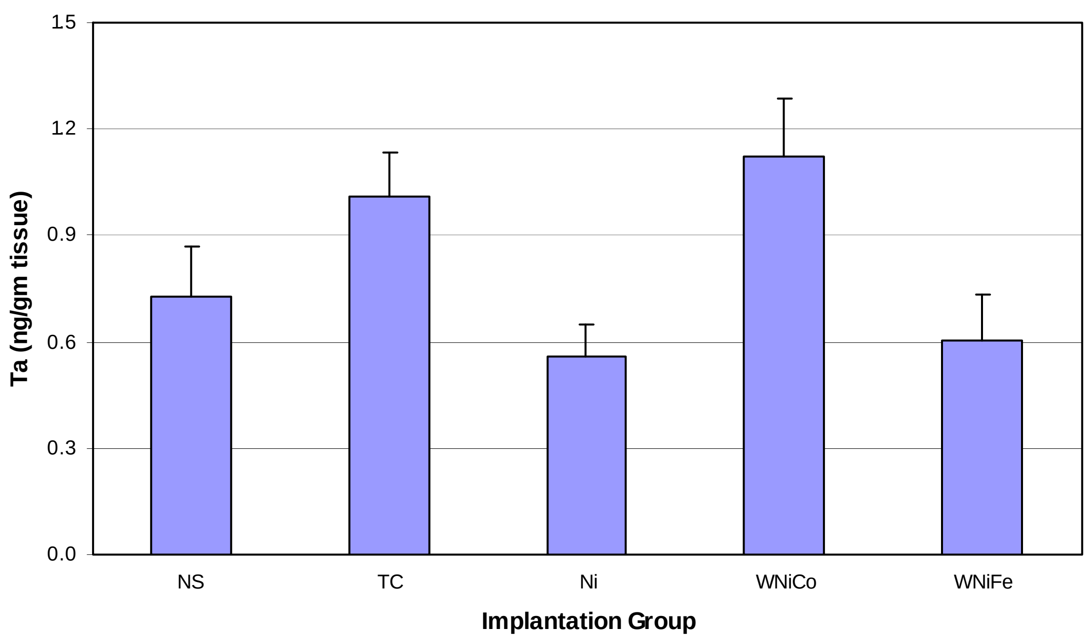

Figure 19: Testes Metal Levels in 3-Month Implantation Groups

A. Testes Tungsten Levels

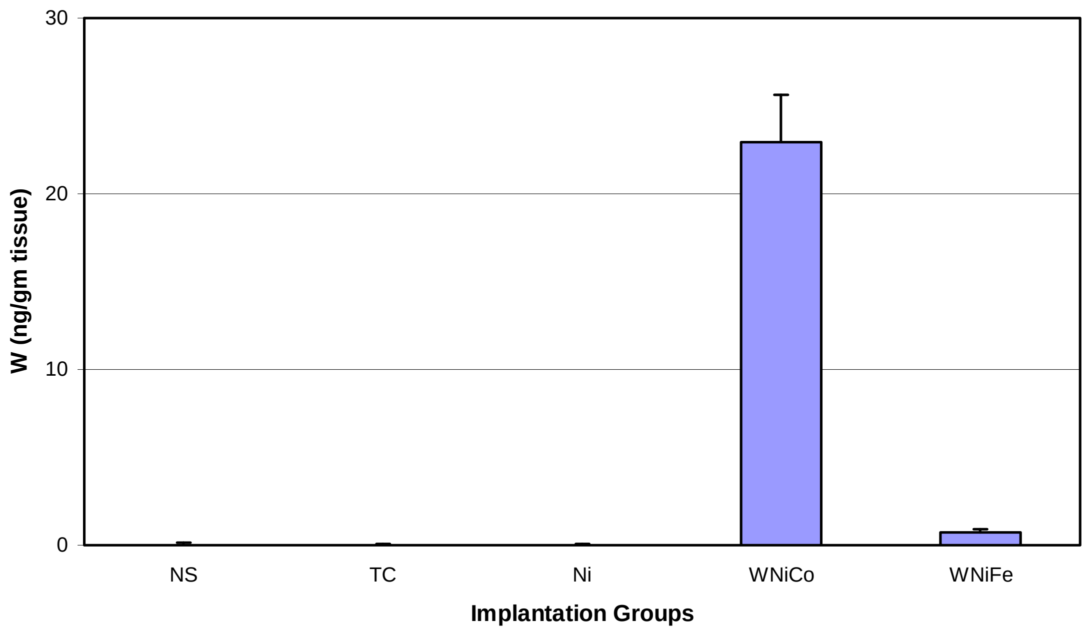

B. Testes Nickel Levels

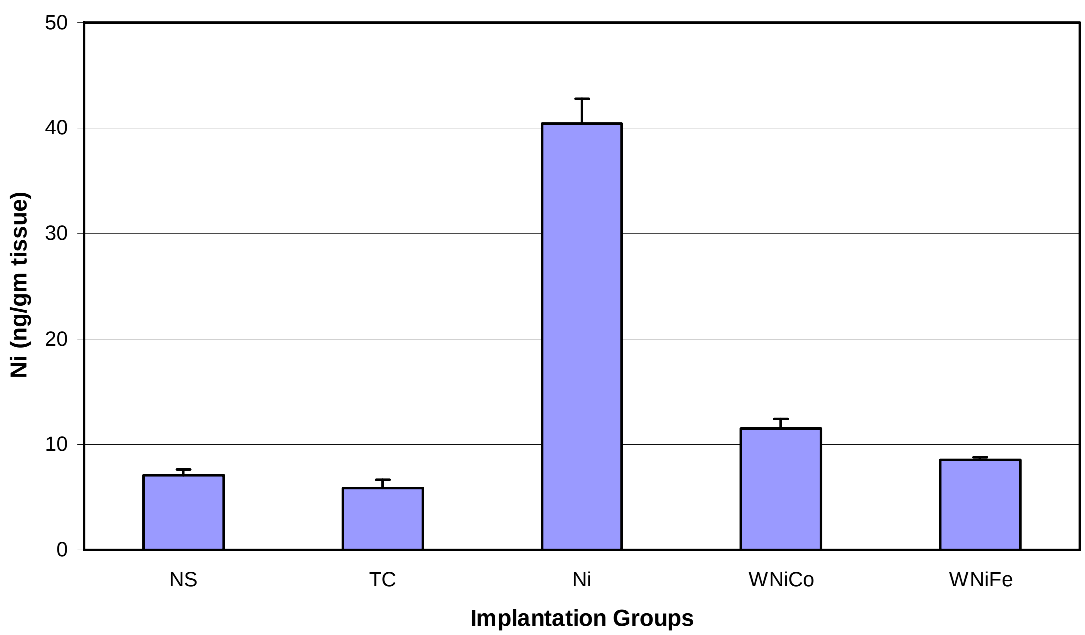

Figure 19 (continued): Testes Metal Levels in 3-Month Implantation Groups

C. Testes Cobalt Levels

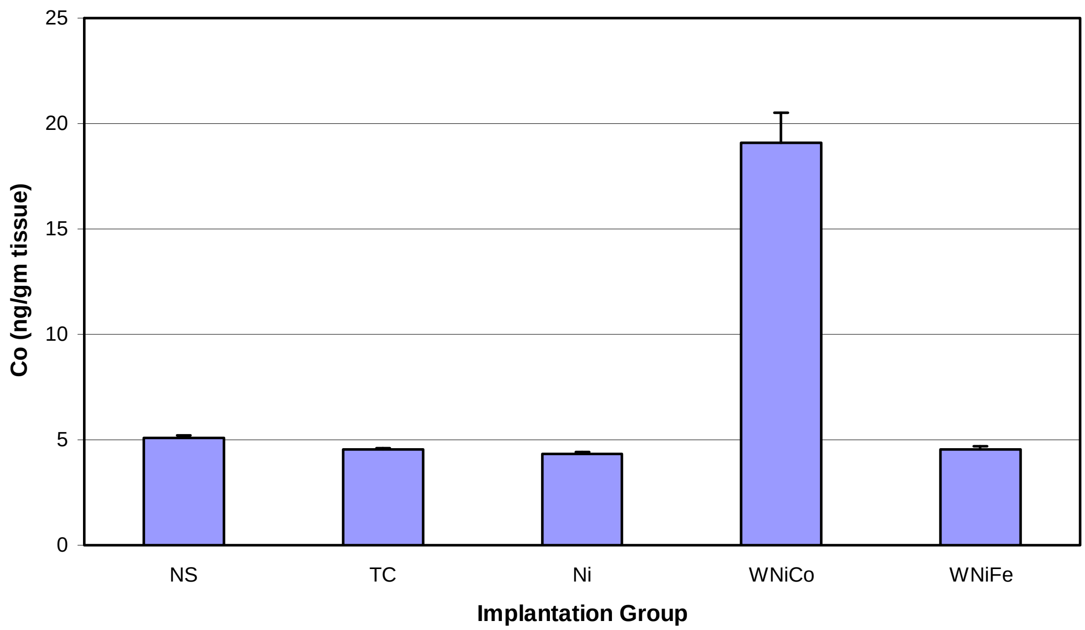

D. Testes Tantalum Levels

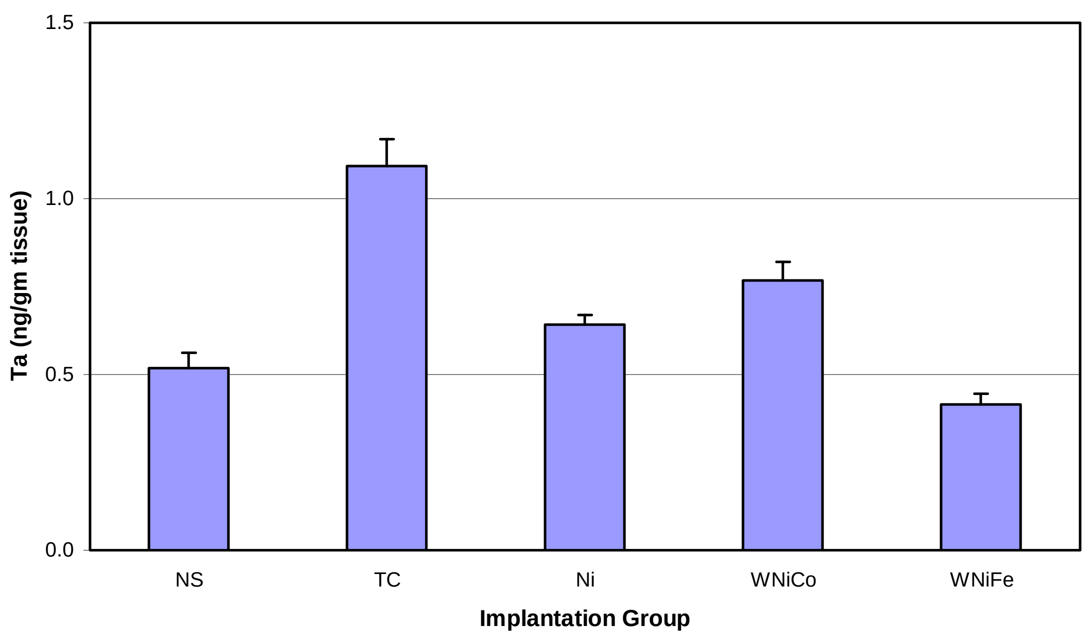

Figure 20: Urinary Metal Levels in 3-Month Implantation Groups

A. Urinary Tungsten Levels

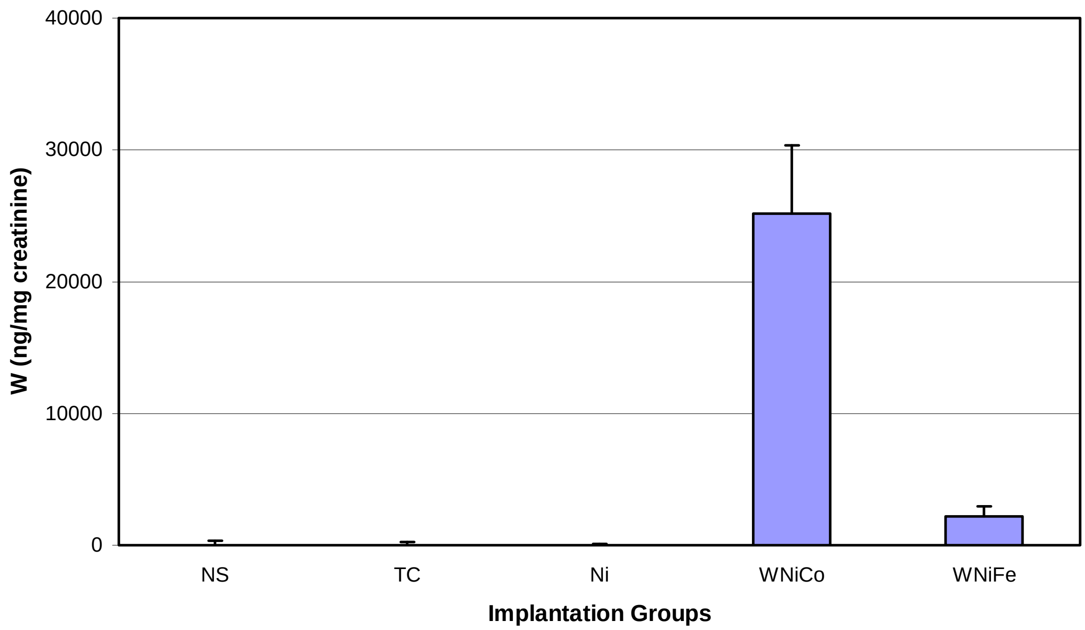

B. Urinary Nickel Levels

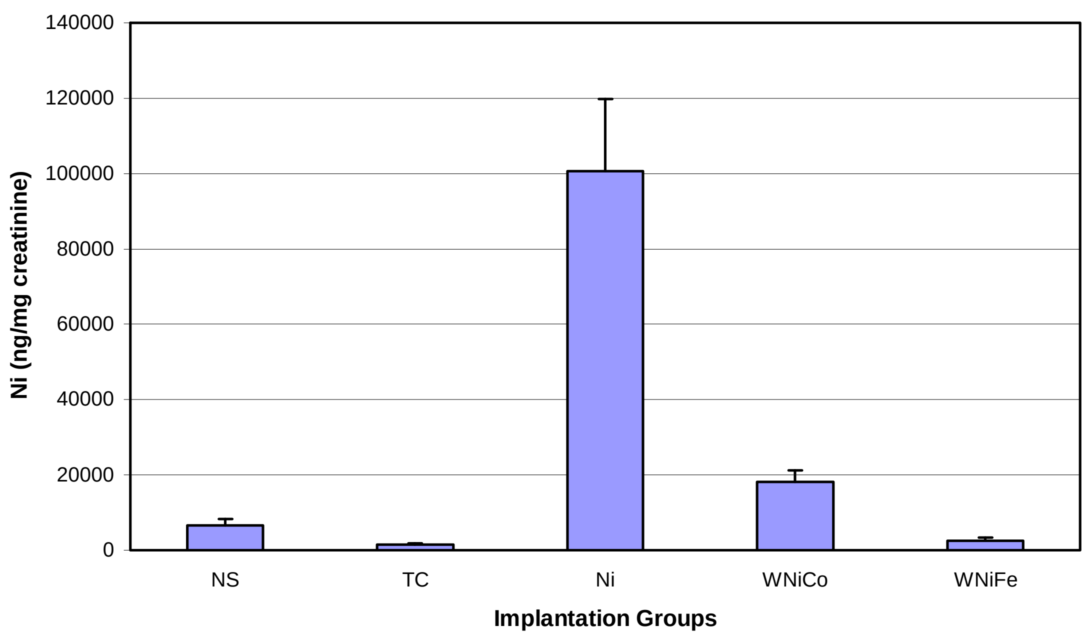

Figure 20 (continued): Urinary Metal Levels in 3-Month Implantation Groups

C. Urinary Cobalt Levels

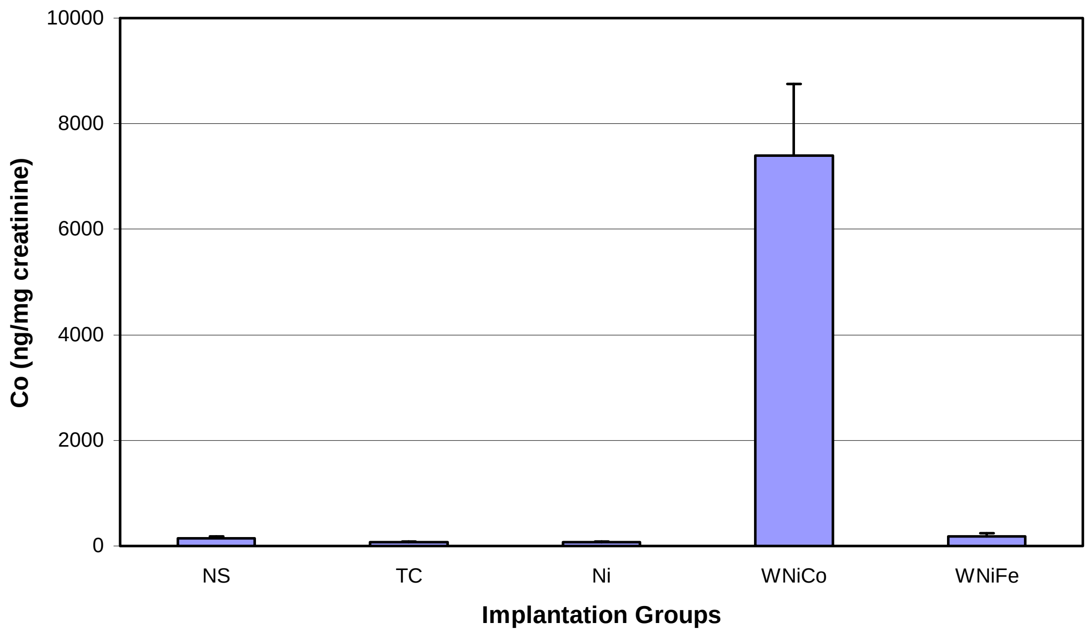

D. Urinary Tantalum Levels

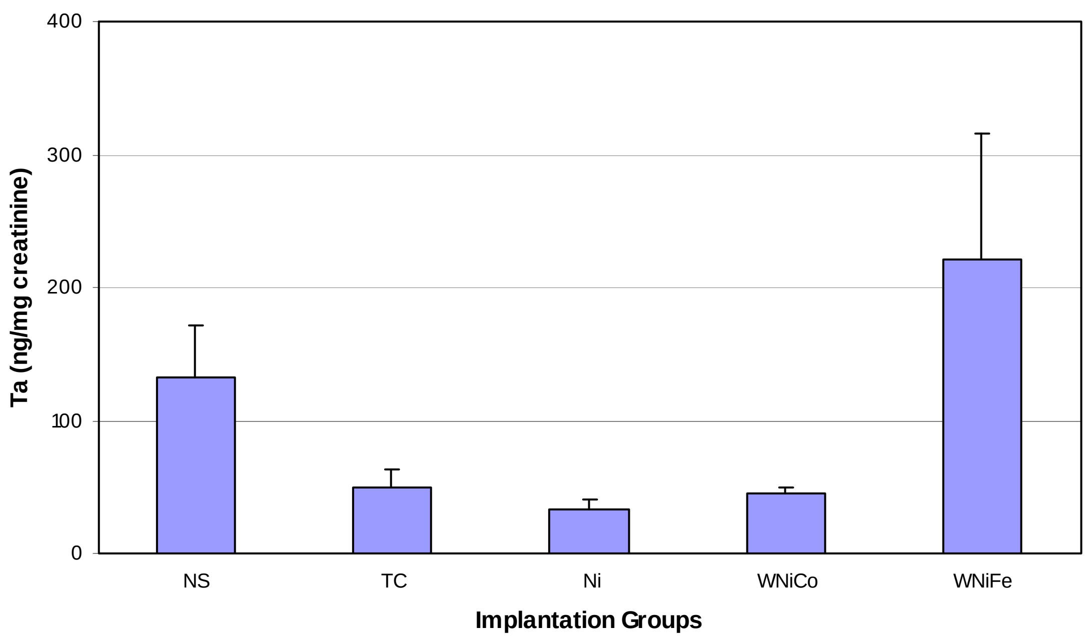

Figure 21: Brain Metal Levels in 6-Month Implantation Groups

A. Brain Tungsten Levels

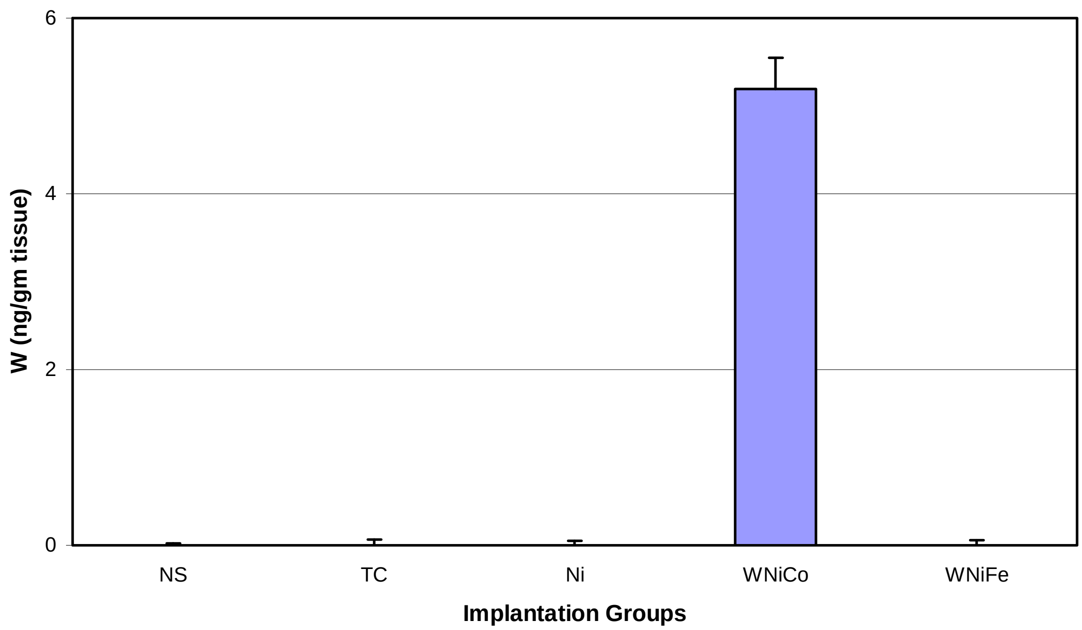

B. Brain Nickel Levels

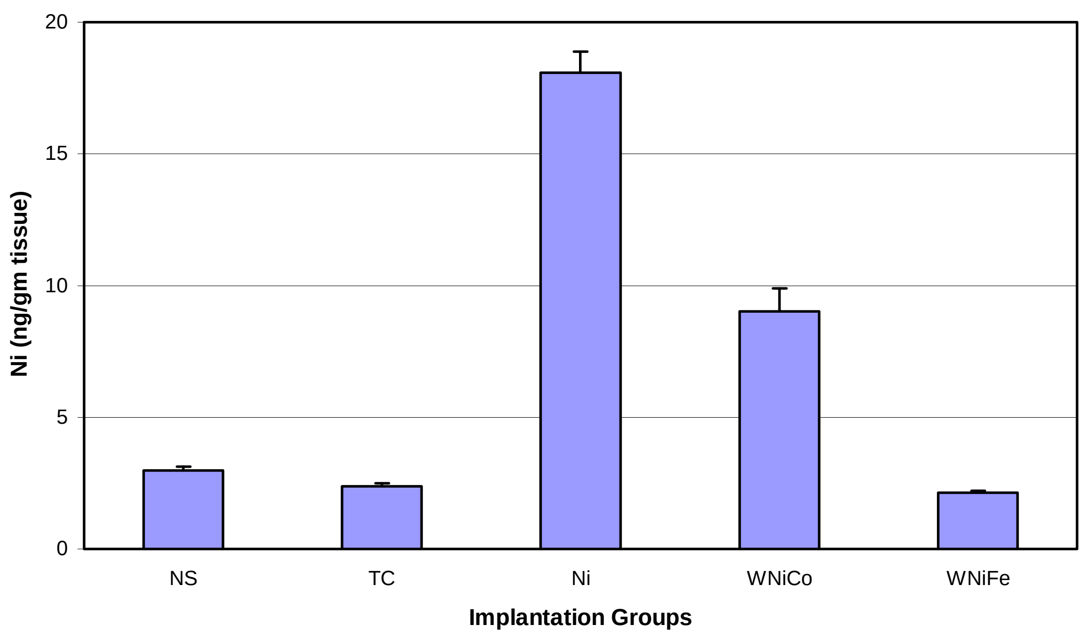

Figure 21 (continued): Brain Metal Levels in 6-Month Implantation Groups

C. Brain Cobalt Levels

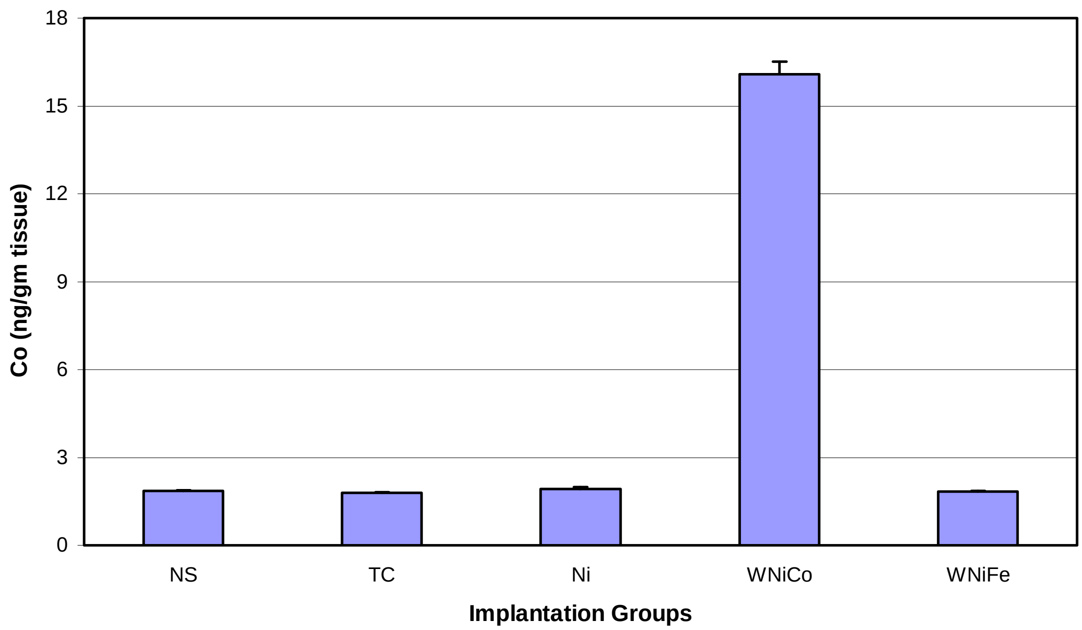

D. Brain Tantalum Levels

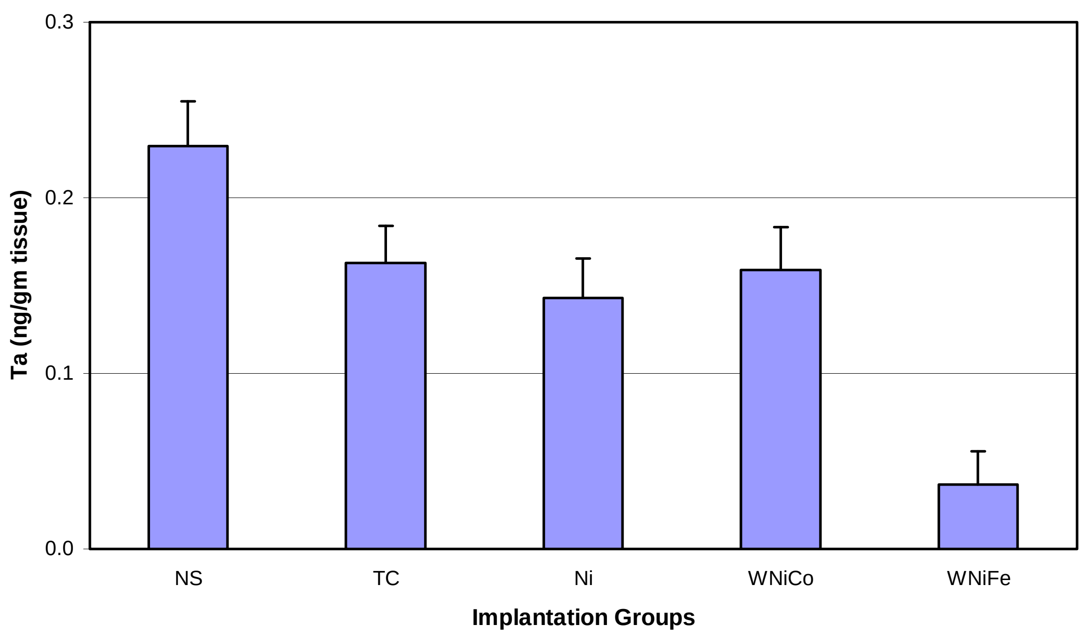

Figure 22: Femur Metal Levels in 6-Month Implantation Groups

A. Femur Tungsten Levels

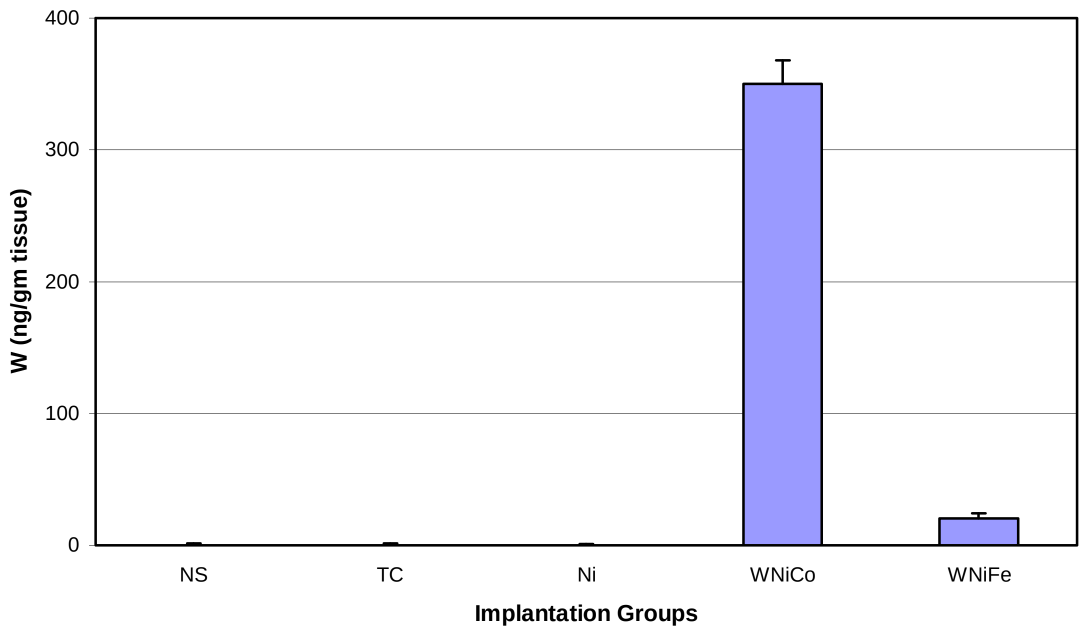

B. Femur Nickel Levels

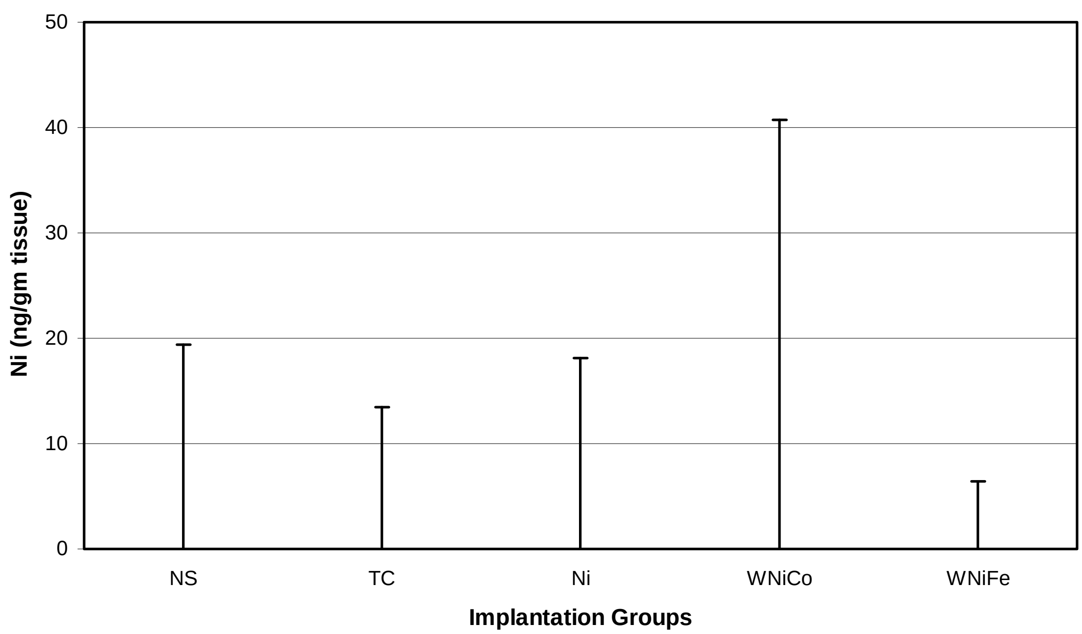

Figure 22 (continued): Femur Metal Levels in 6-Month Implantation Groups

C. Femur Cobalt Levels

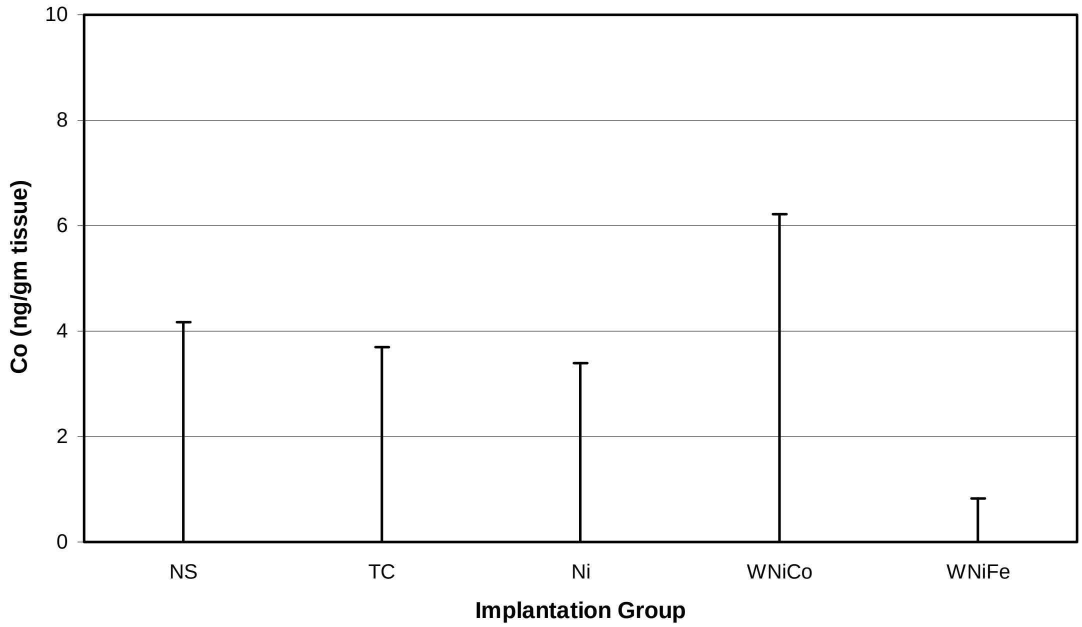

D. Femur Tantalum Levels

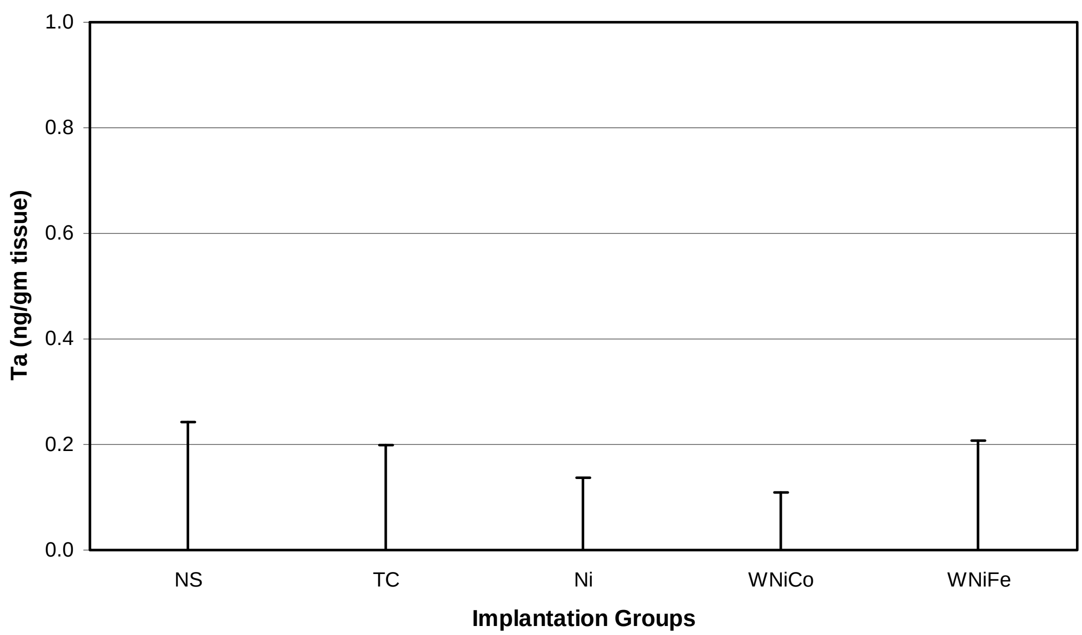

Figure 23: Kidney Metal Levels in 6-Month Implantation Groups

A. Kidney Tungsten Levels

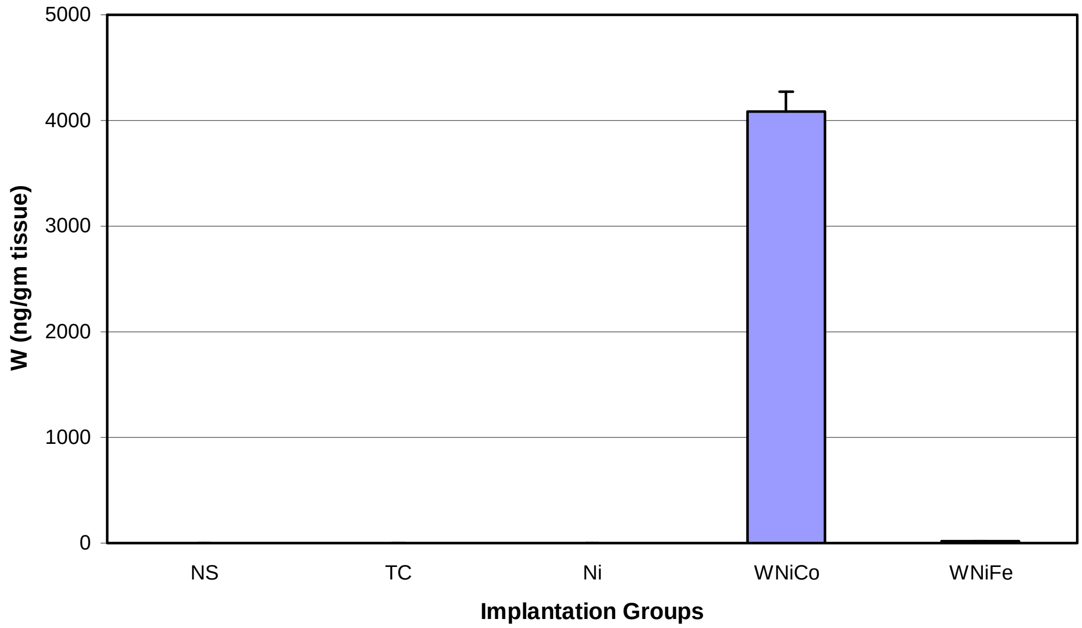

B. Kidney Nickel Levels

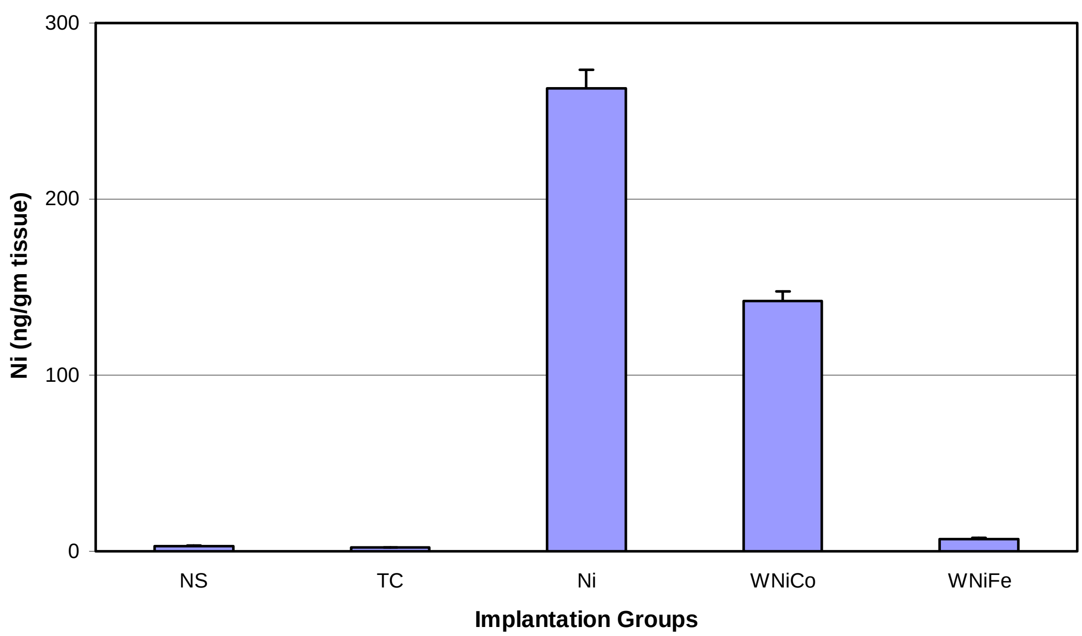

Figure 23 (continued): Kidney Metal Levels in 6-Month Implantation Groups

C. Kidney Cobalt Levels

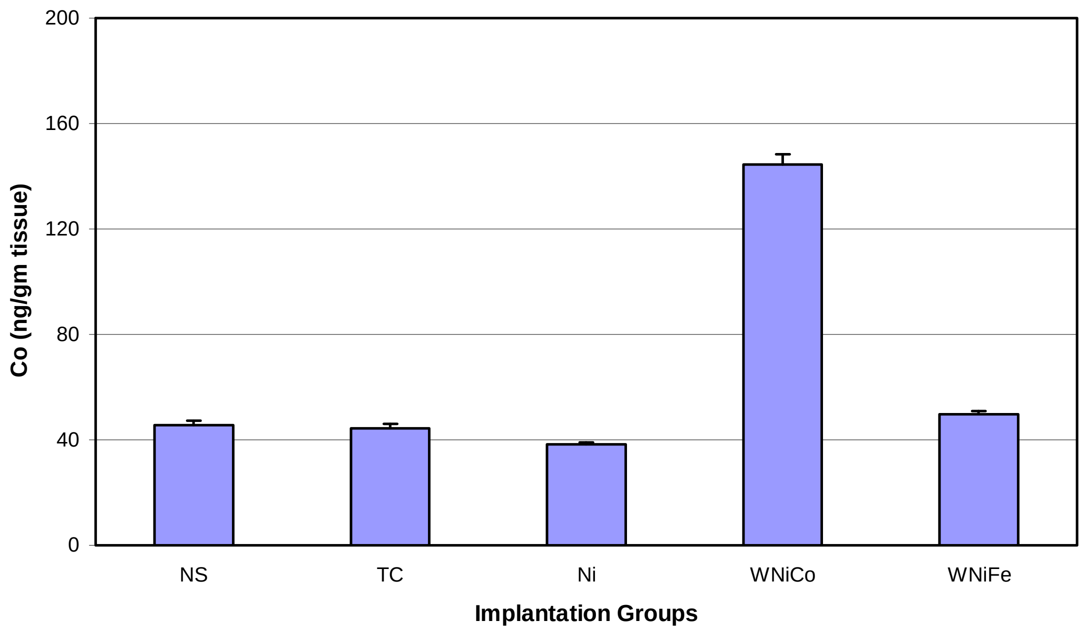

D. Kidney Tantalum Levels

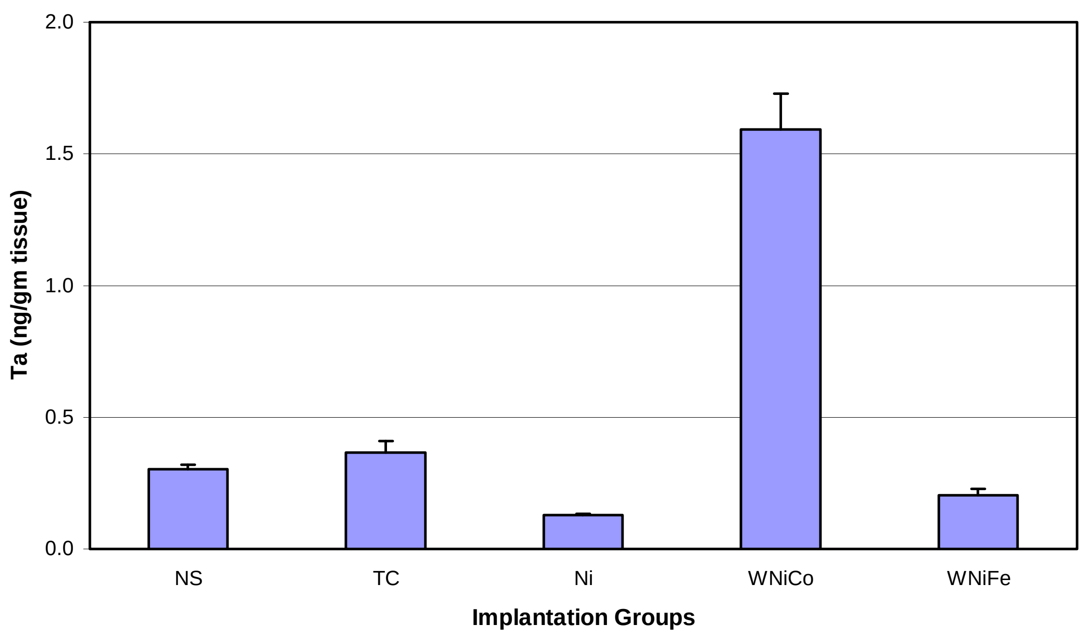

Figure 24: Liver Metal Levels in 6-Month Implantation Groups

A. Liver Tungsten Levels

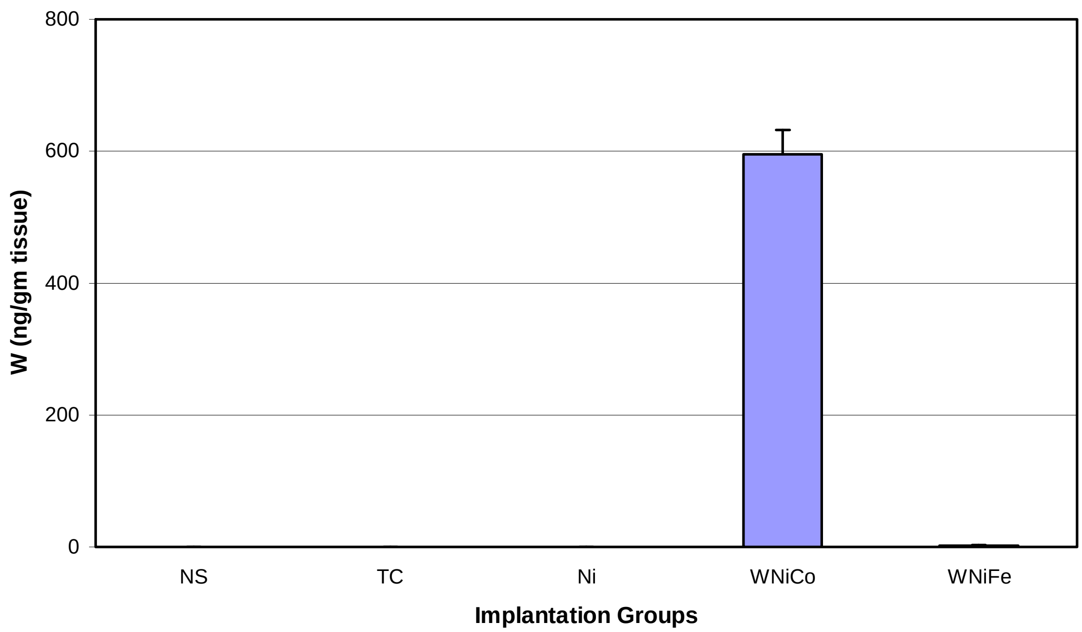

B. Liver Nickel Levels

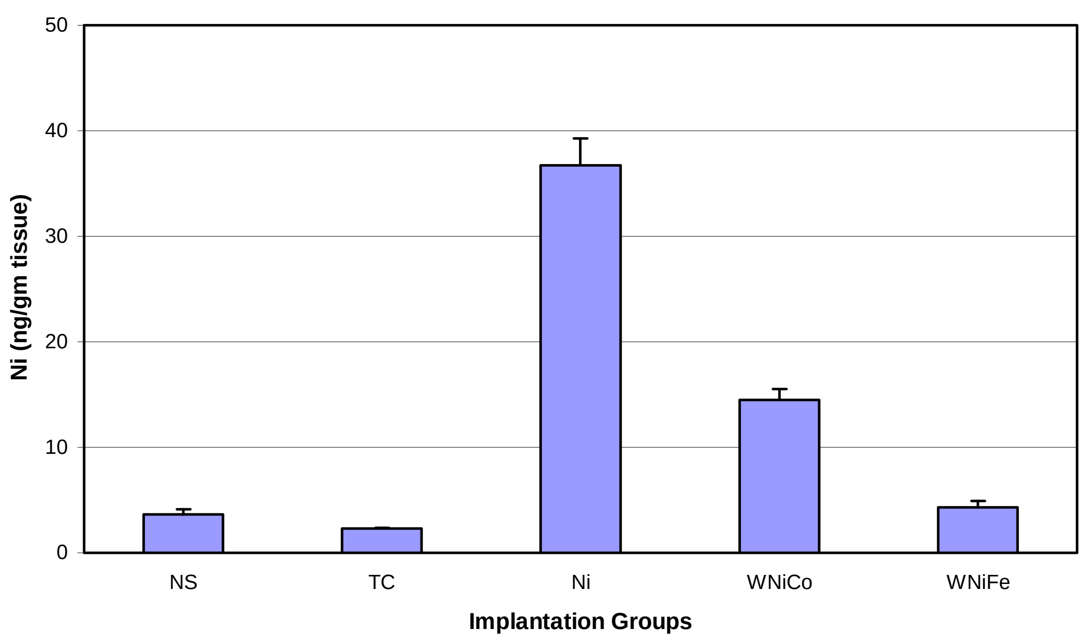

Figure 24 (continued): Liver Metal Levels in 6-Month Implantation Groups

C. Liver Cobalt Levels

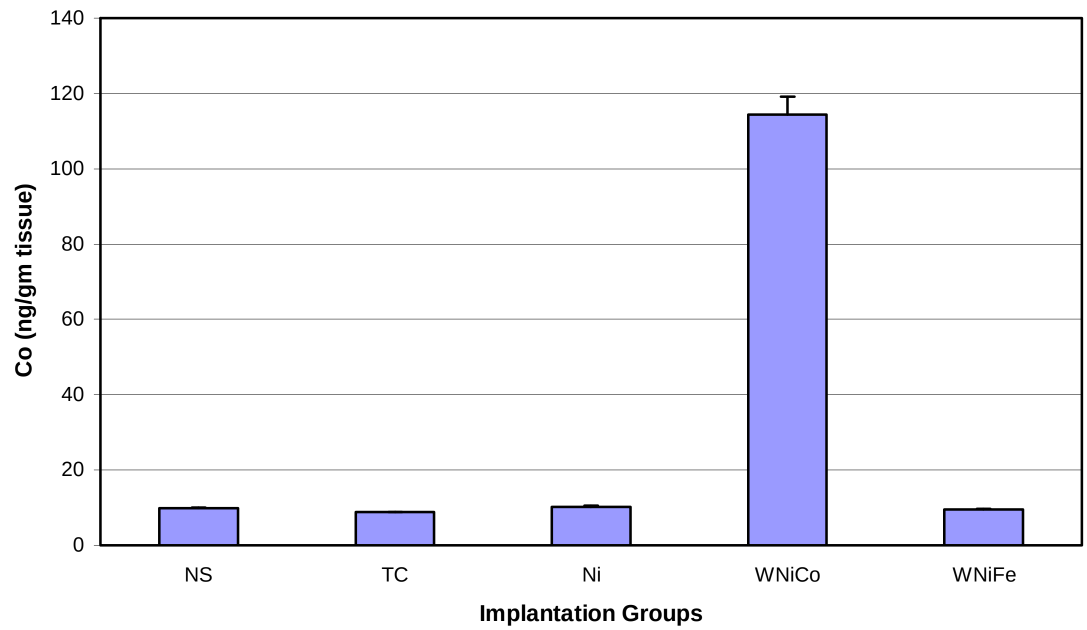

D. Liver Tantalum Levels

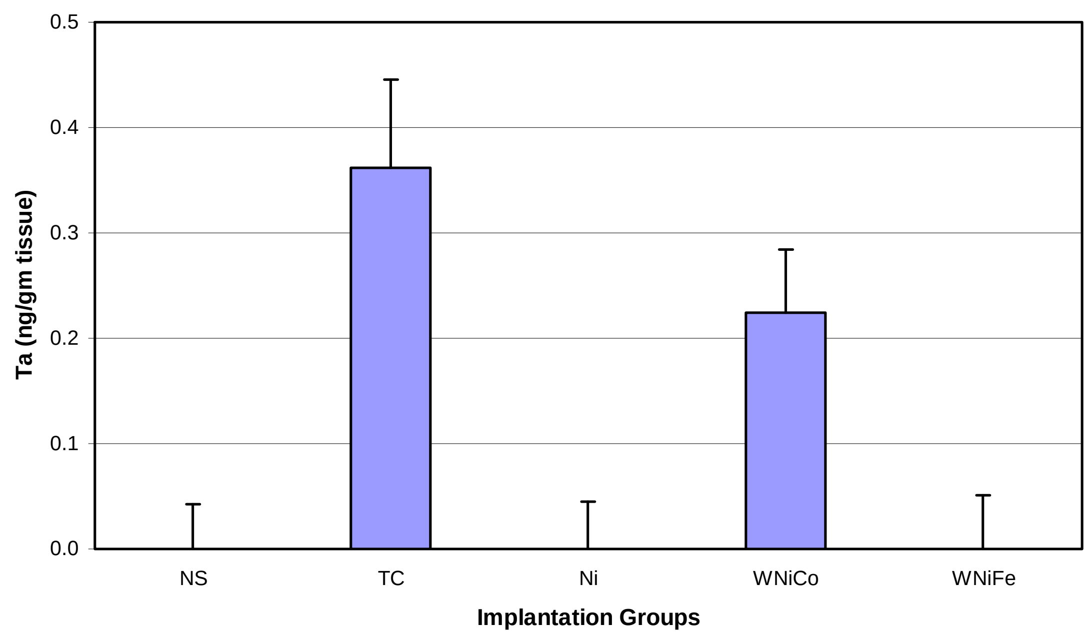

Figure 25: Serum Metals Levels in 6-Month Implantation Groups

A. Serum Tungsten Levels

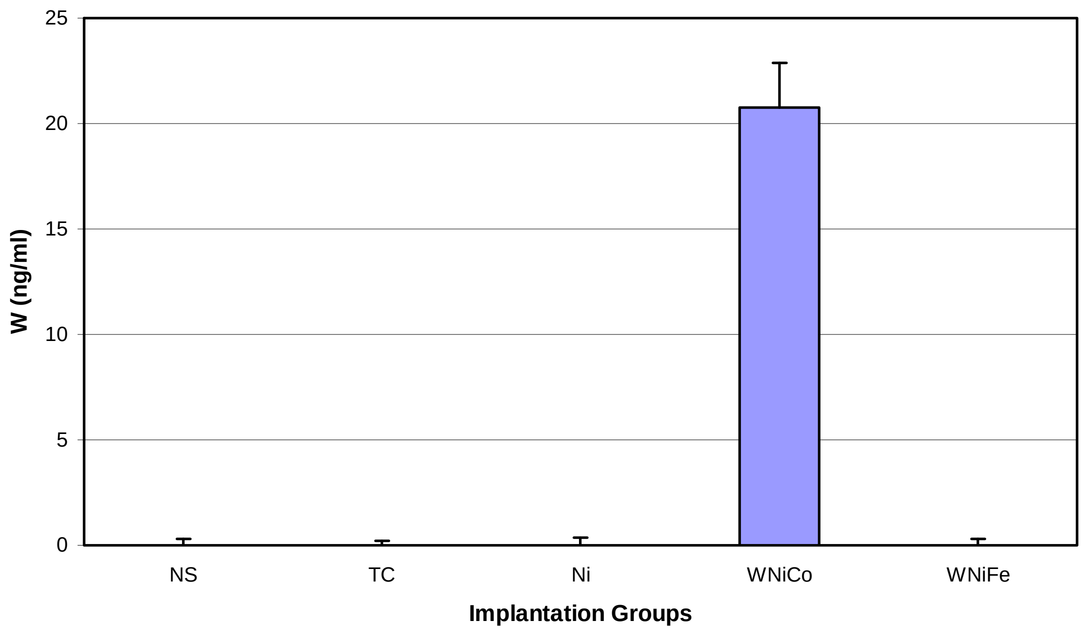

B. Serum Nickel Levels

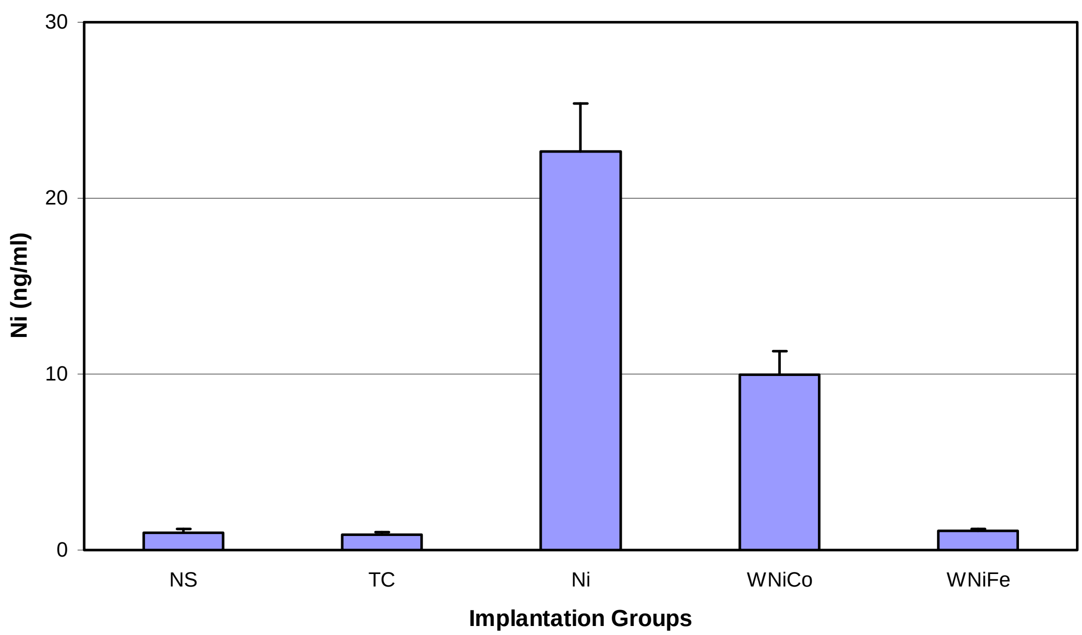

Figure 25 (continued): Serum Metals Levels in 6-Month Implantation Groups

C. Serum Cobalt Levels

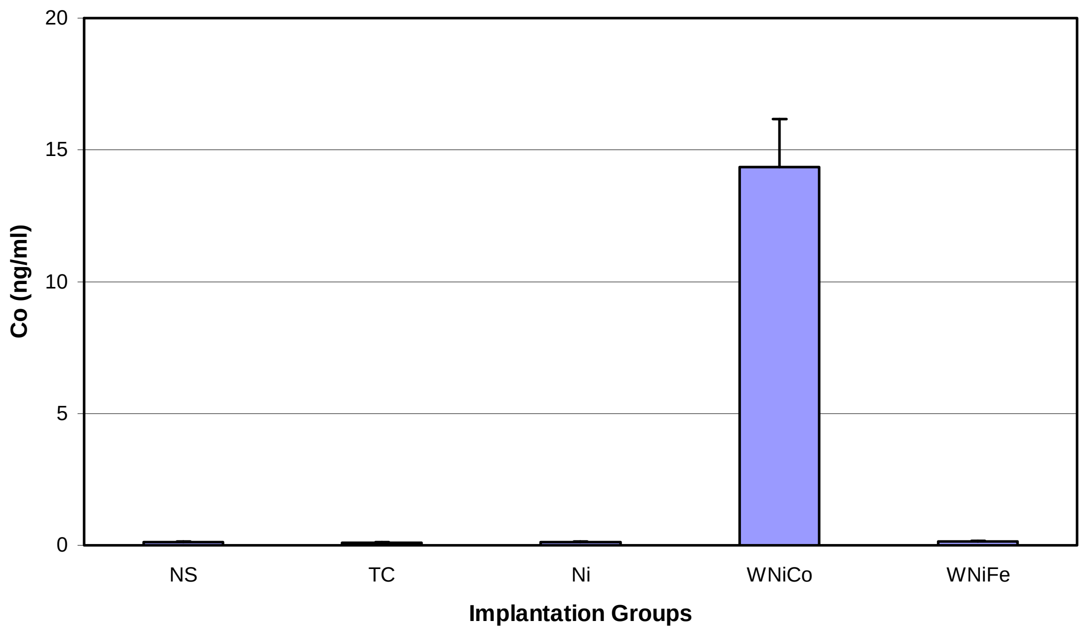

D. Serum Tantalum Levels

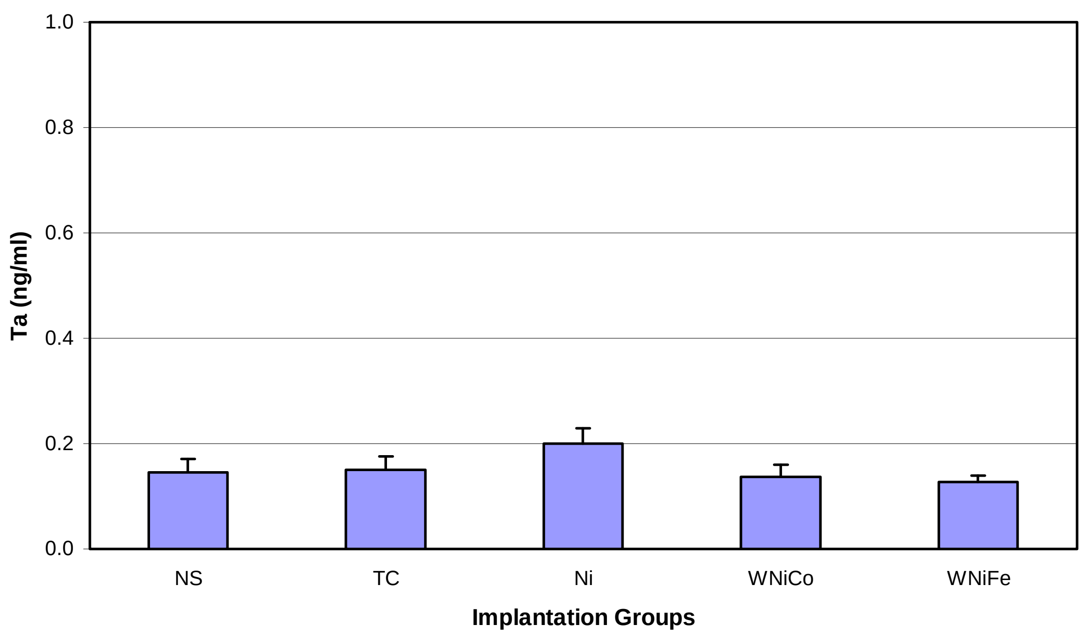

Figure 26: Spleen Metal Levels in 6-Month Implantation Groups

A. Spleen Tungsten Levels

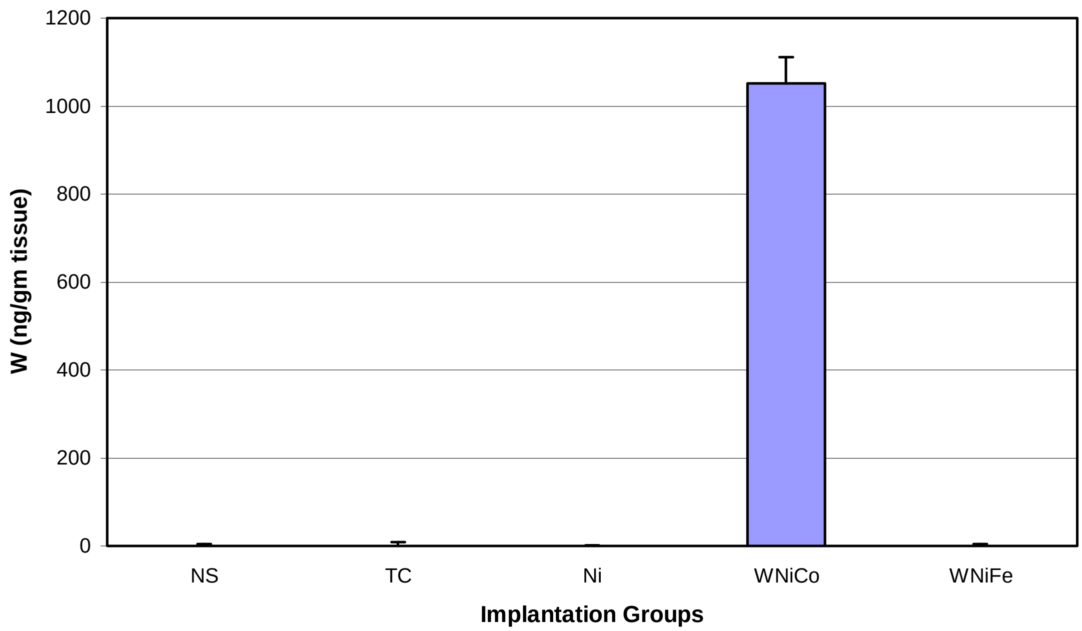

B. Spleen Nickel Levels

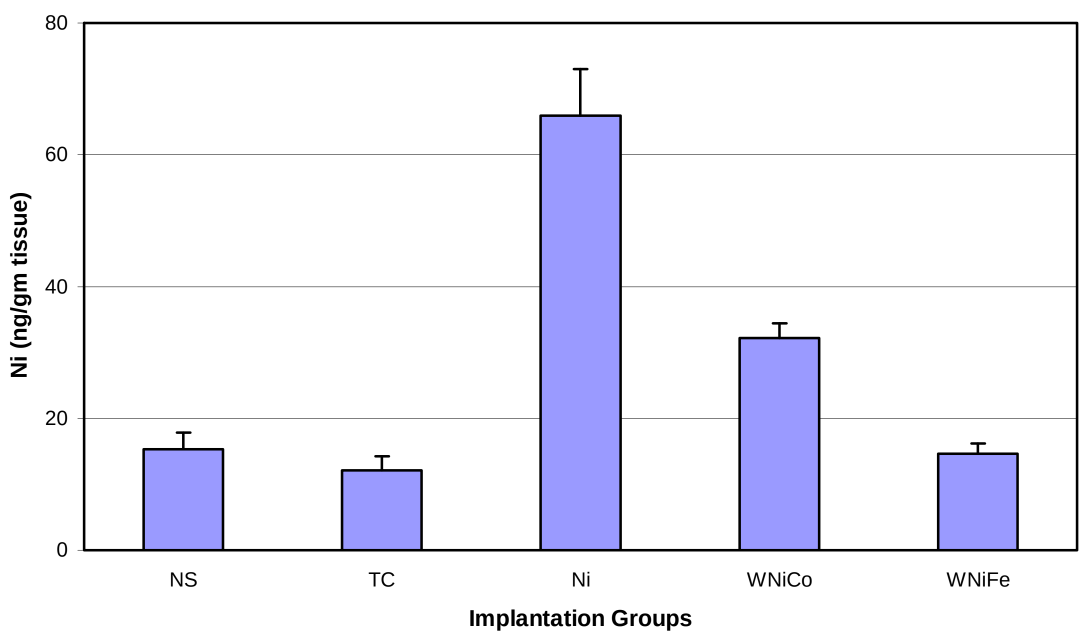

Figure 26 (continued): Spleen Metal Levels in 6-Month Implantation Groups

C. Spleen Cobalt Levels

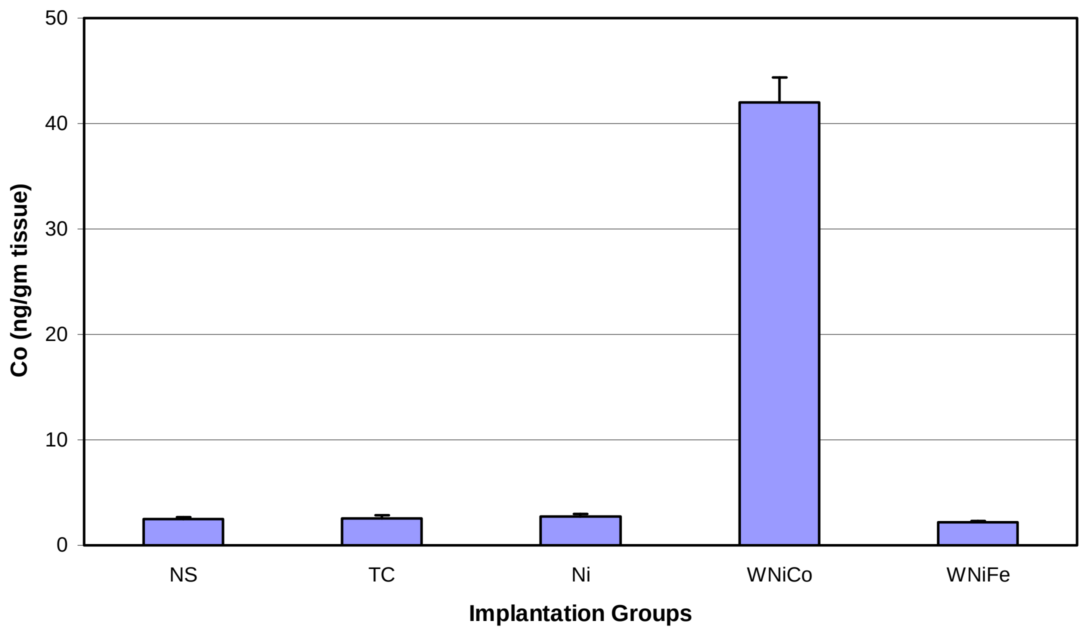

D. Spleen Tantalum Levels

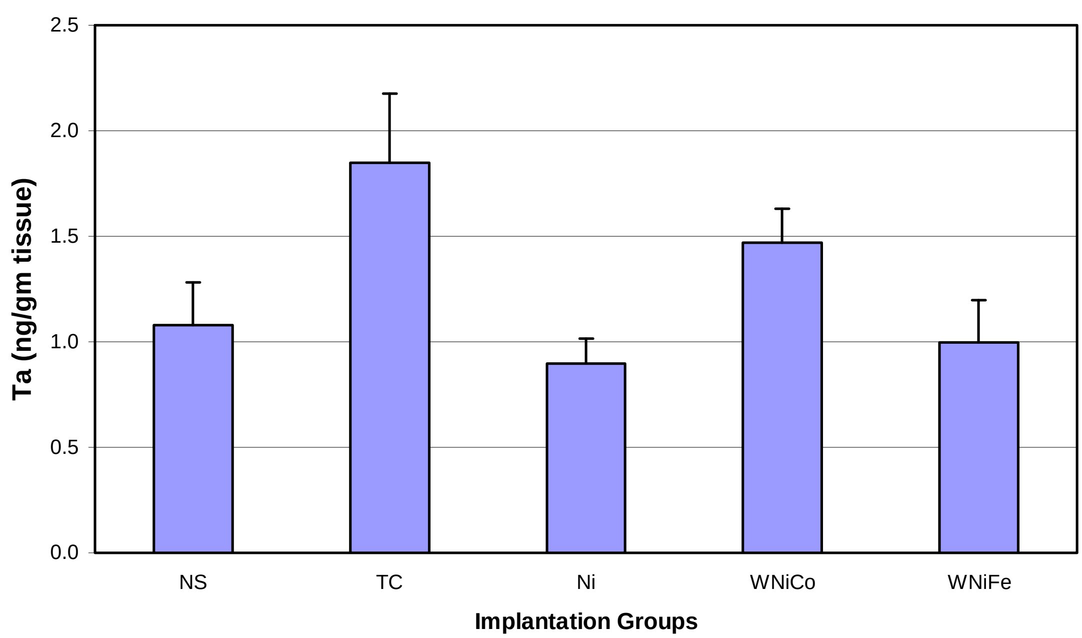

Figure 27: Testes Metal Levels in 6-Month Implantation Groups

A. Testes Tungsten Levels

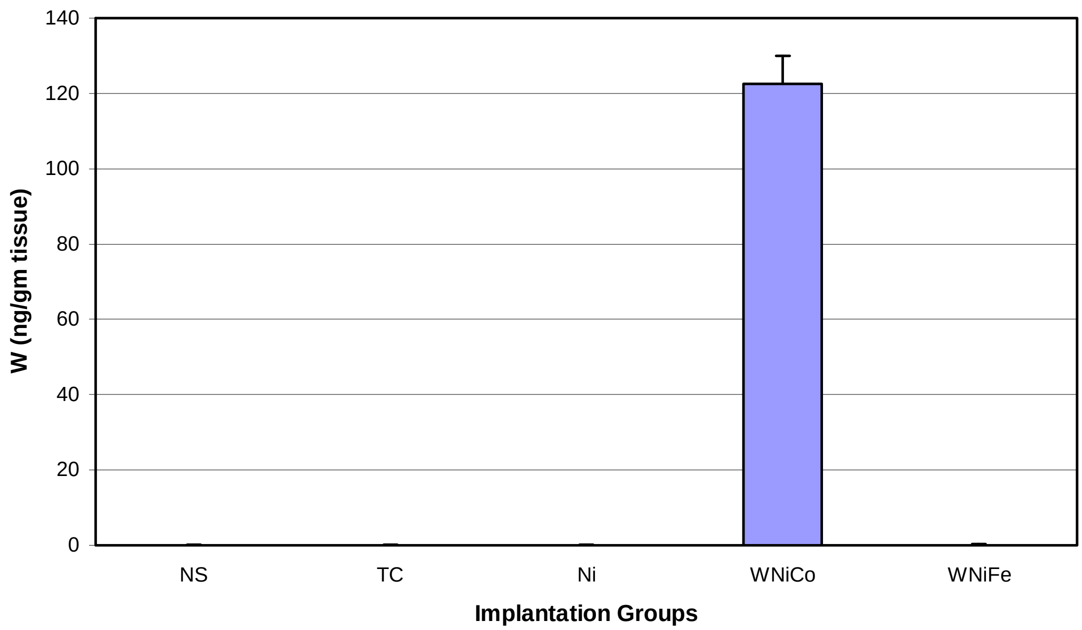

B. Testes Nickel Levels

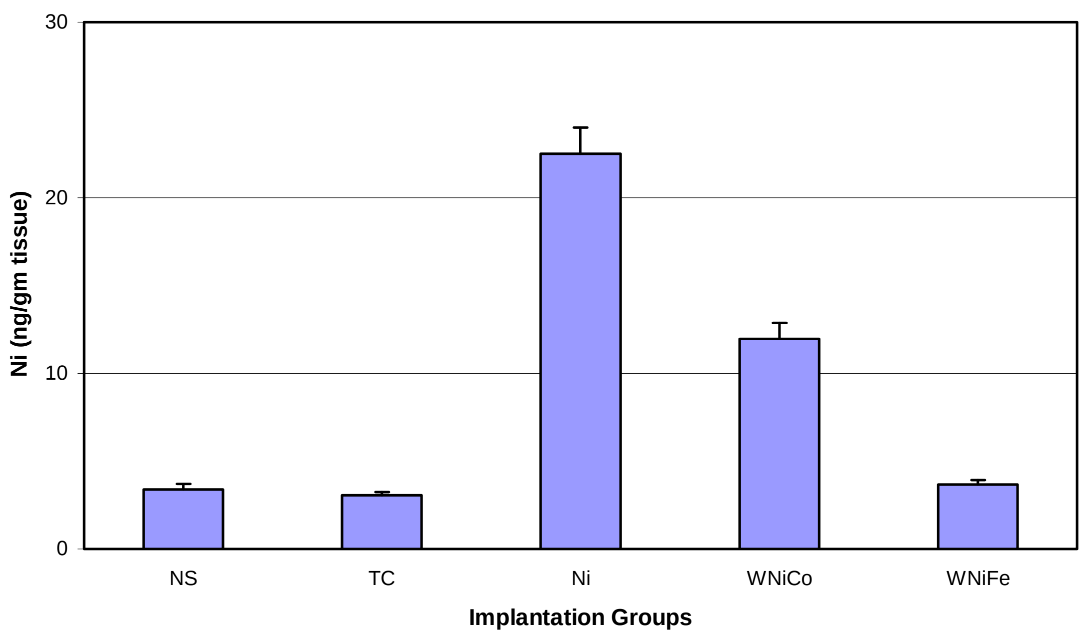

Figure 27 (continued): Testes Metal Levels in 6-Month Implantation Groups

C. Testes Cobalt Levels

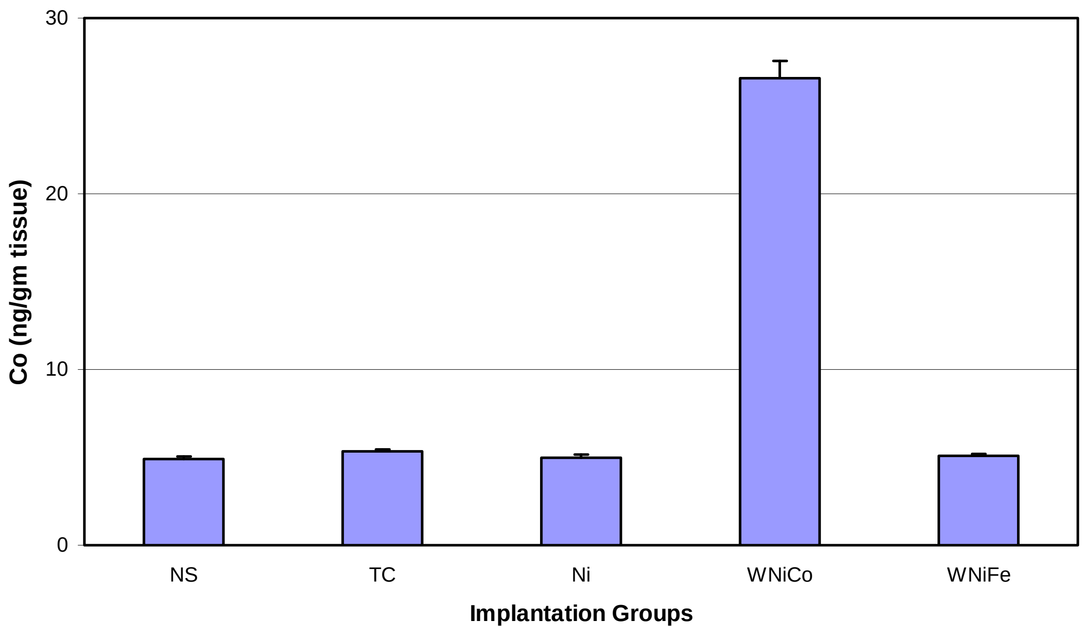

D. Testes Tantalum Levels

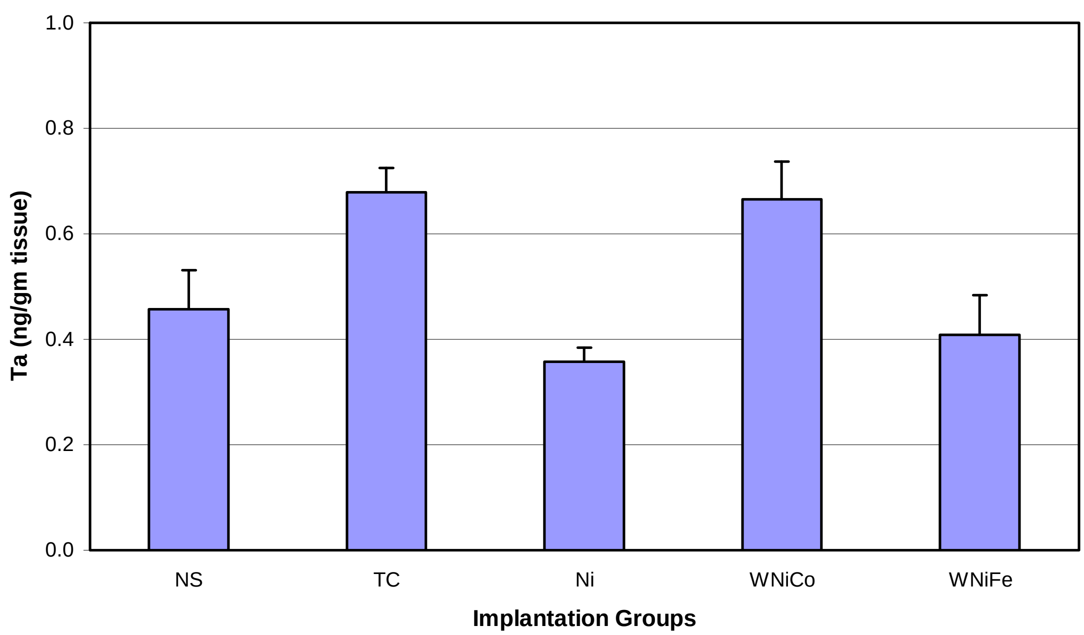

Figure 28: Urinary Metal Levels in 6-Month Implantation Groups

A. Urinary Tungsten Levels

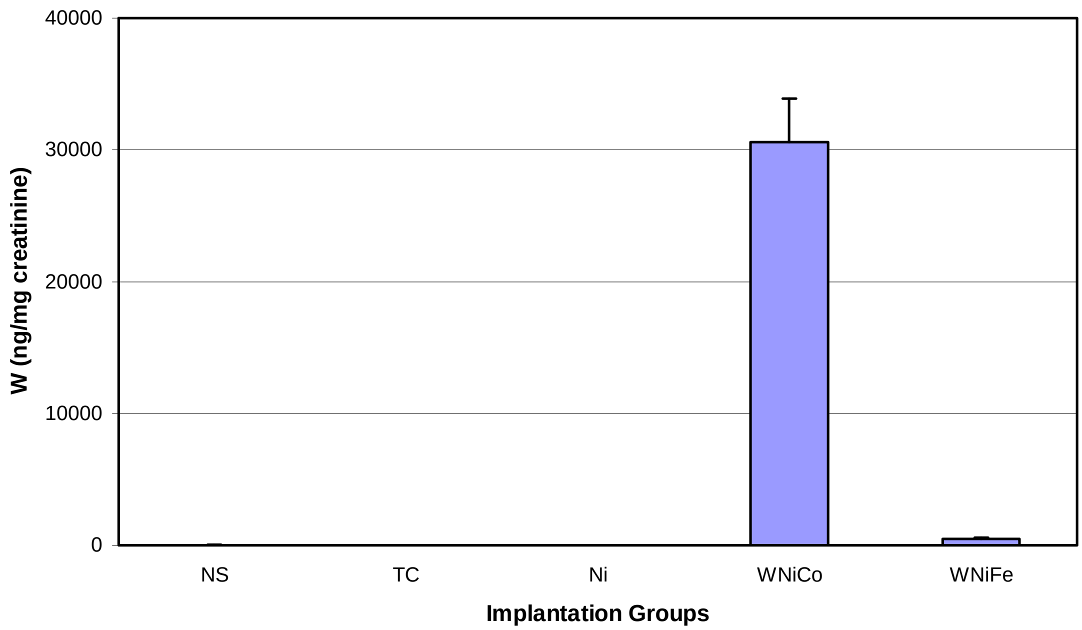

B. Urinary Nickel Levels

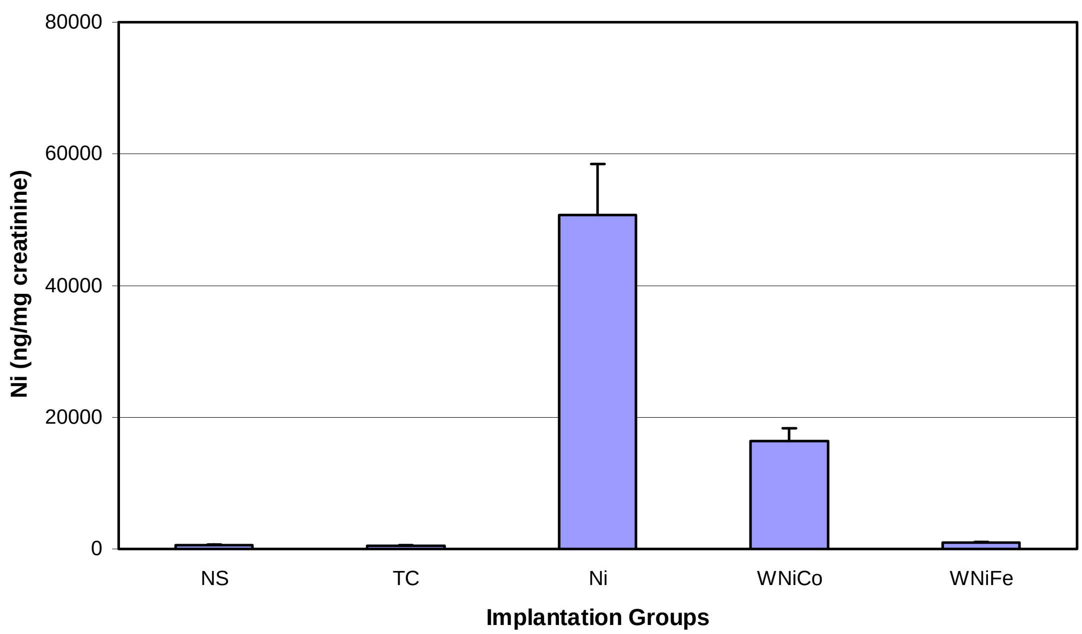

Figure 28 (continued): Urinary Metal Levels in 6-Month Implantation Groups

C. Urinary Cobalt Levels

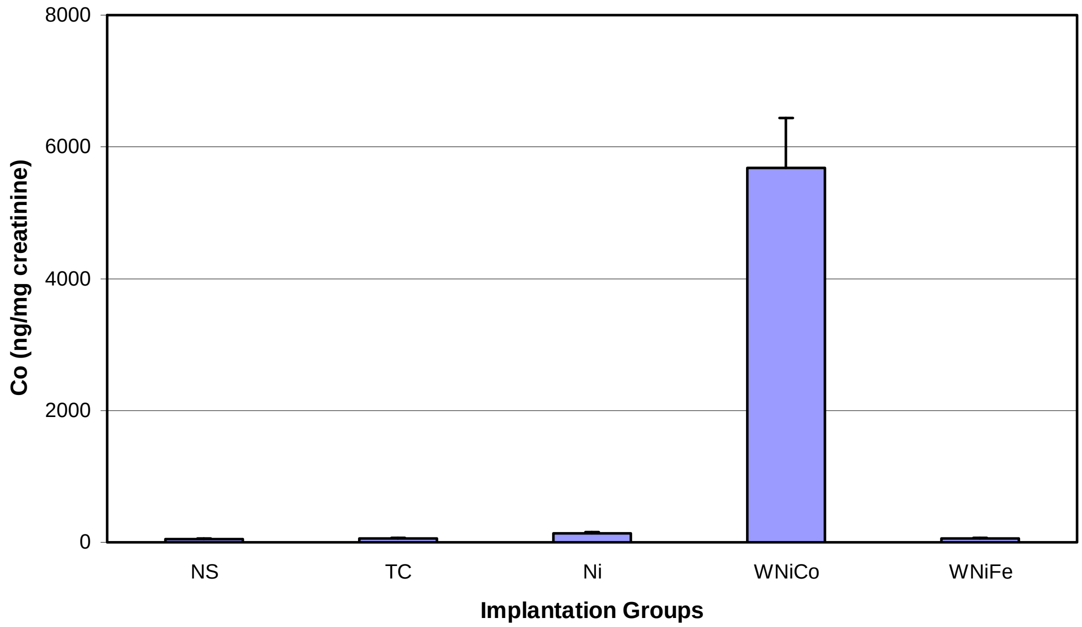

D. Urinary Tantalum Levels

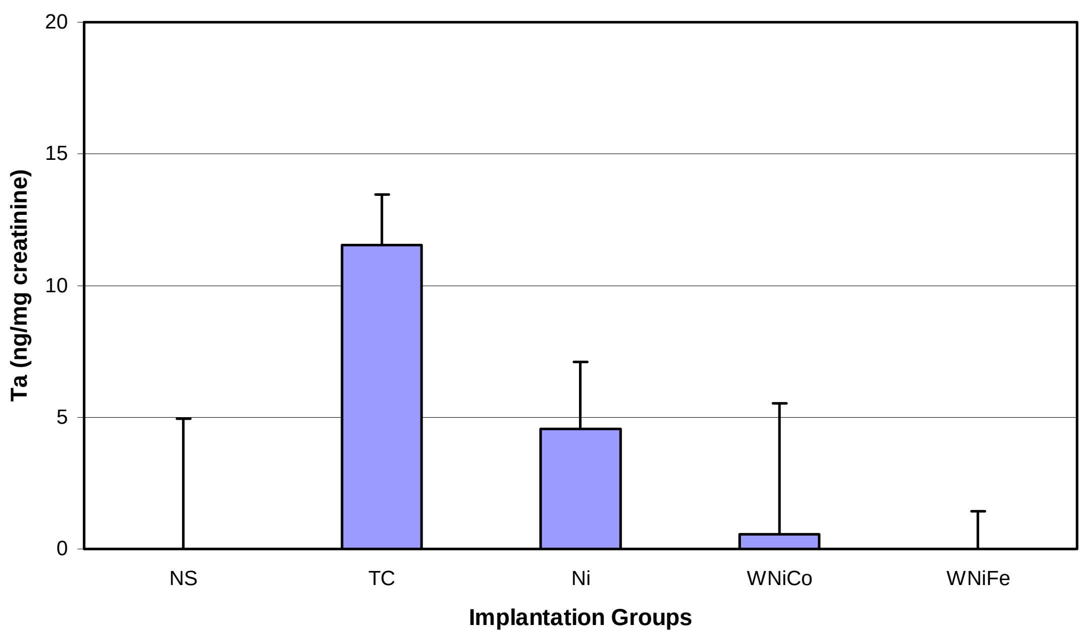

Figure 29: Brain Metal Levels in 12-Month Implantation Groups

A. Brain Tungsten Levels

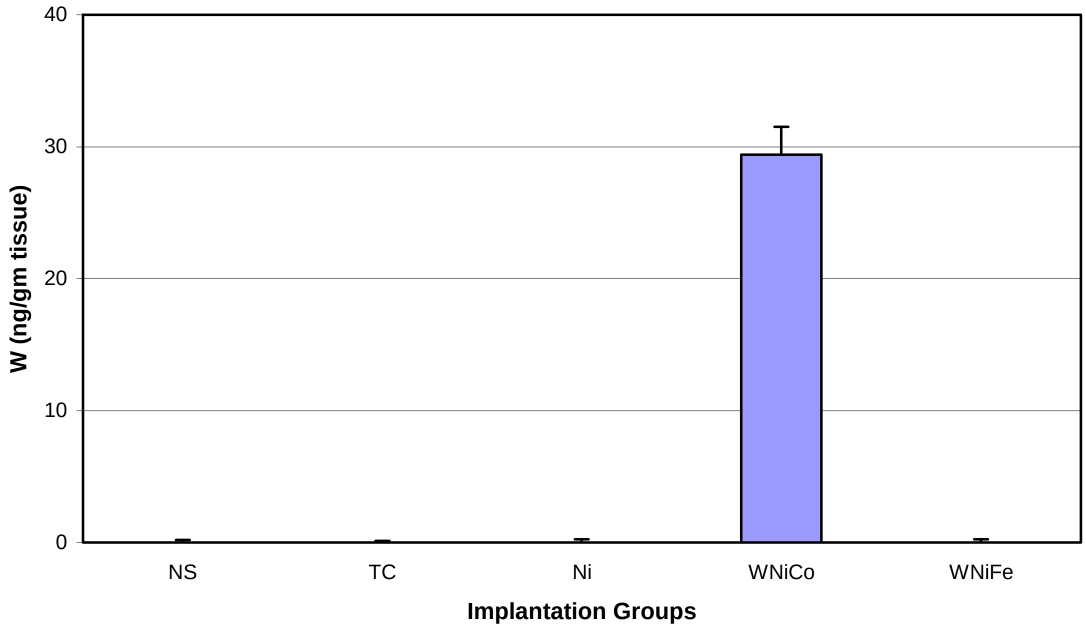

B. Brain Nickel Levels

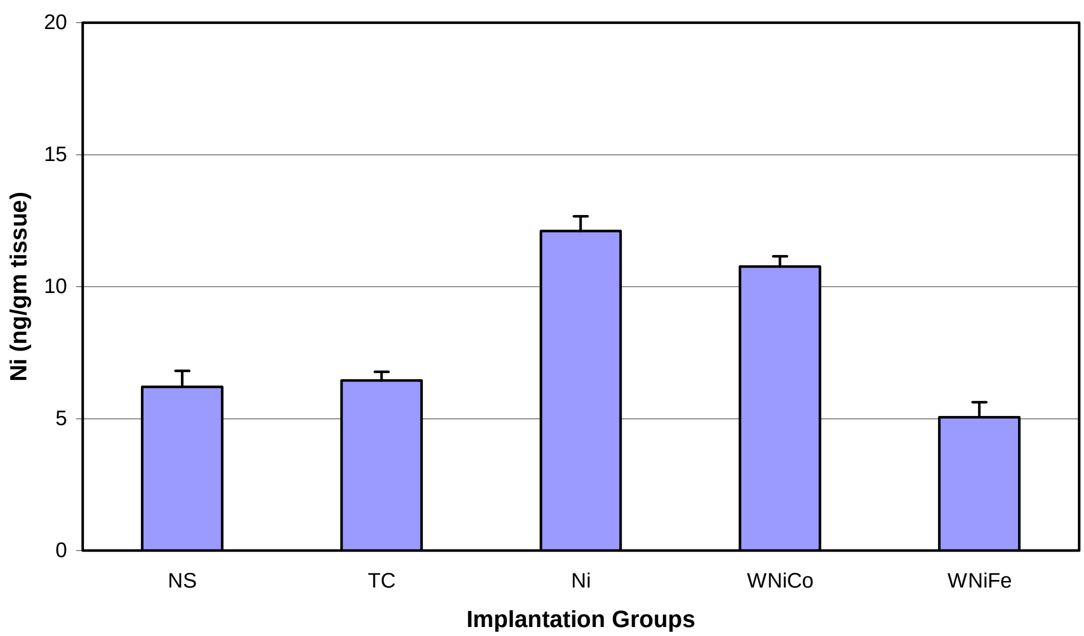

Figure 29 (continued): Brain Metal Levels in 12-Month Implantation Groups

C. Brain Cobalt Levels

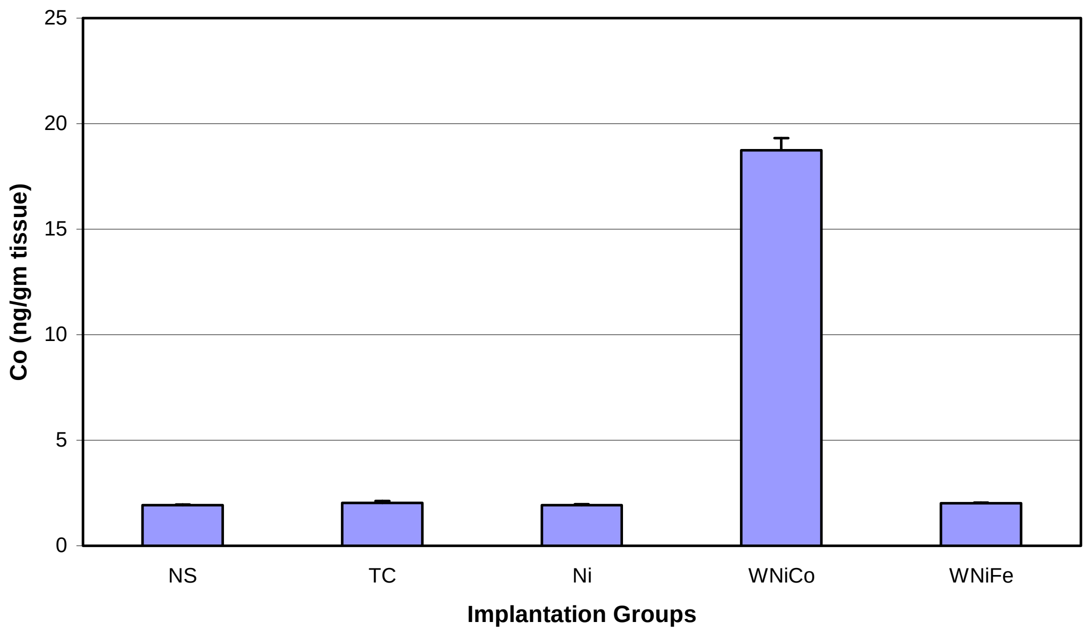

D. Brain Tantalum Levels

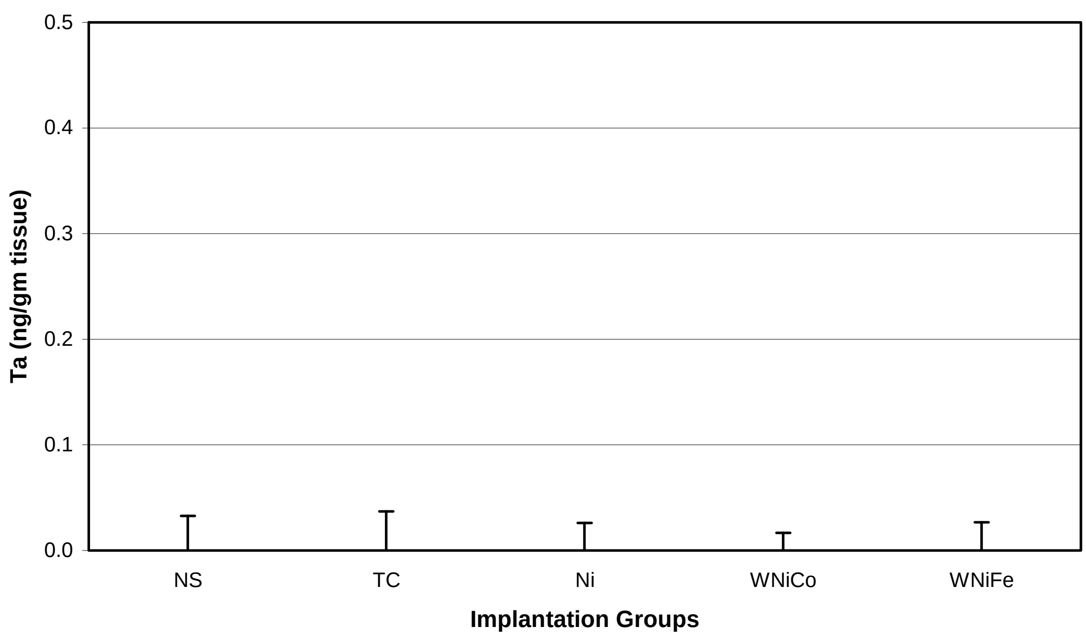

Figure 30: Femur Metal Levels in 12-Month Implantation Groups

A. Femur Tungsten Levels

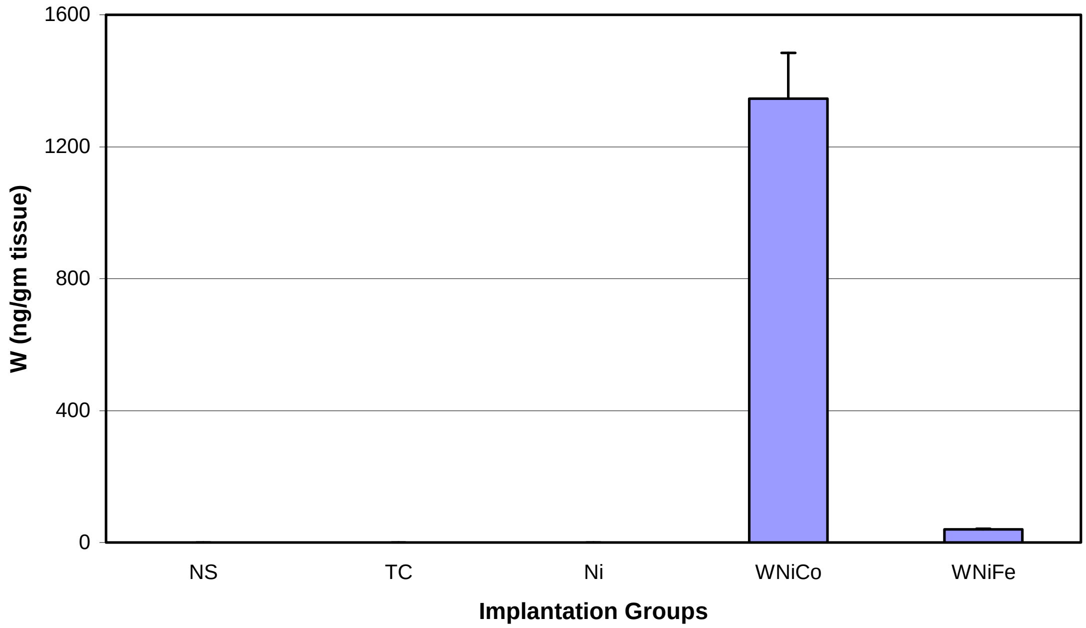

B. Femur Nickel Levels

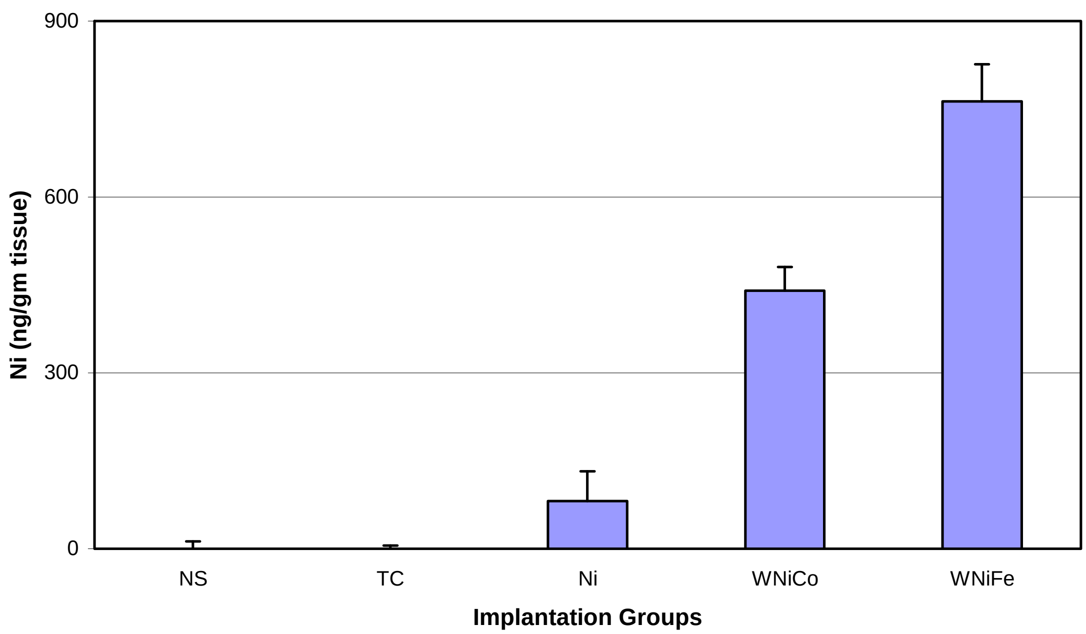

Figure 30 (continued): Femur Metal Levels in 12-Month Implantation Groups

C. Femur Cobalt Levels

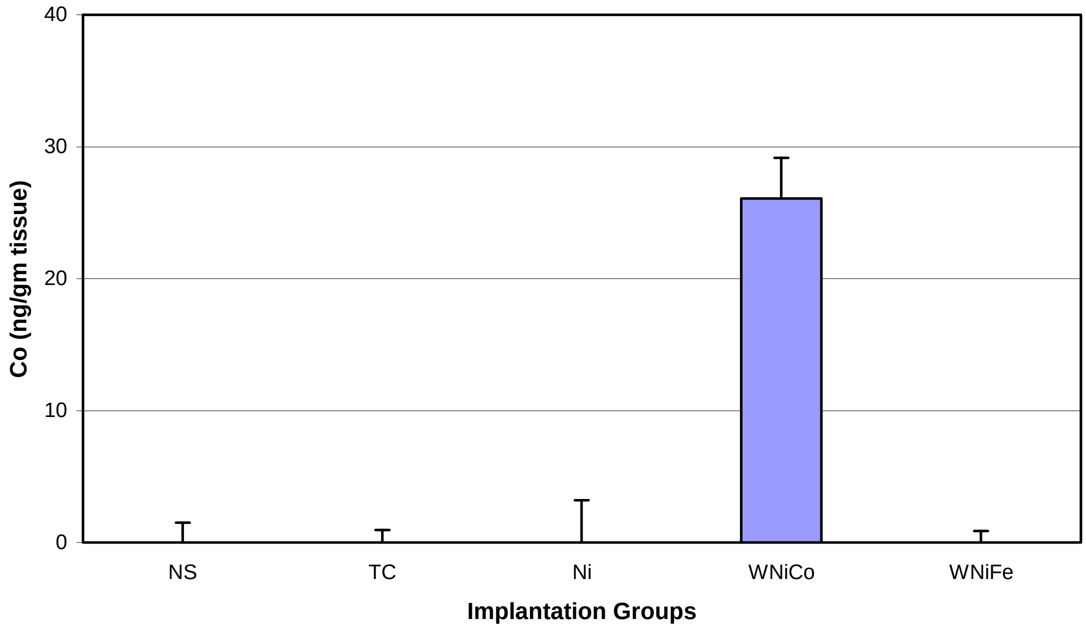

D. Femur Tantalum Levels

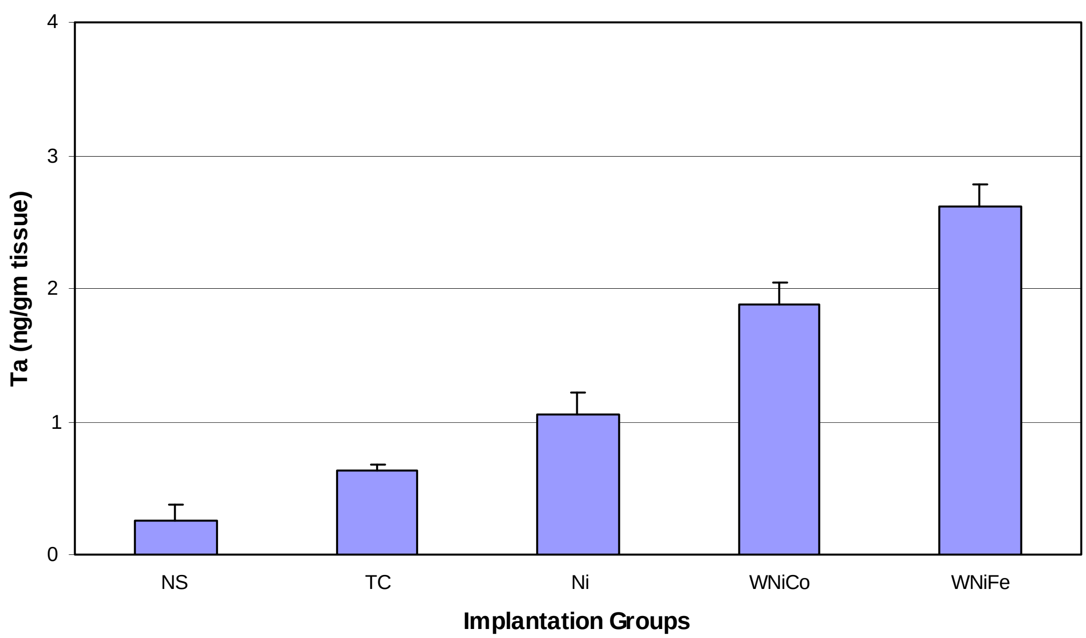

Figure 31: Kidney Metal Levels in 12-Month Implantation Groups

A. Kidney Tungsten Levels

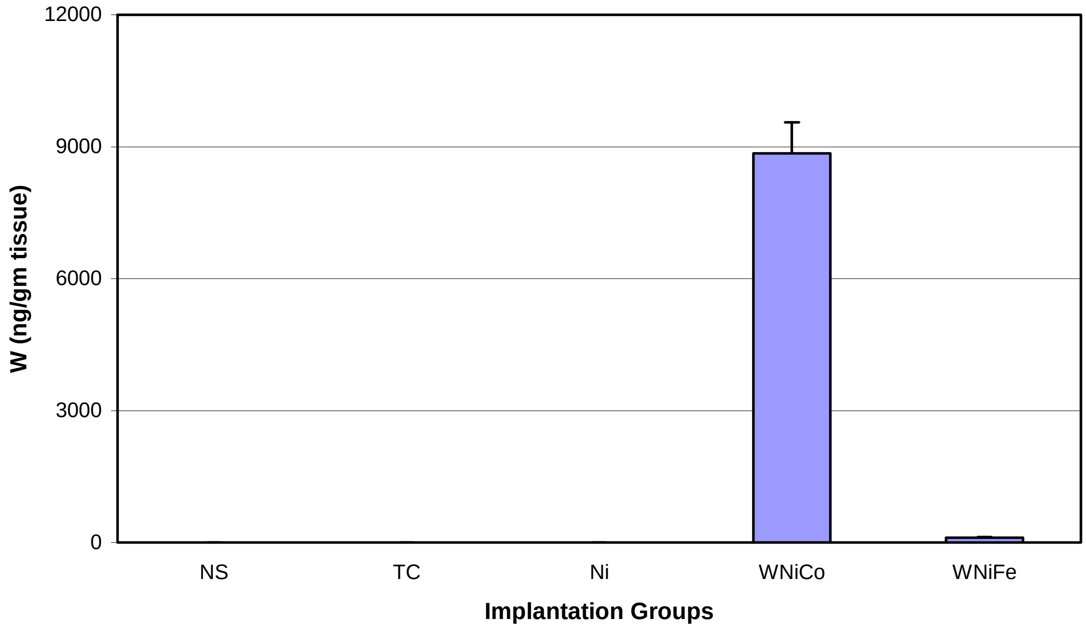

B. Kidney Nickel Levels

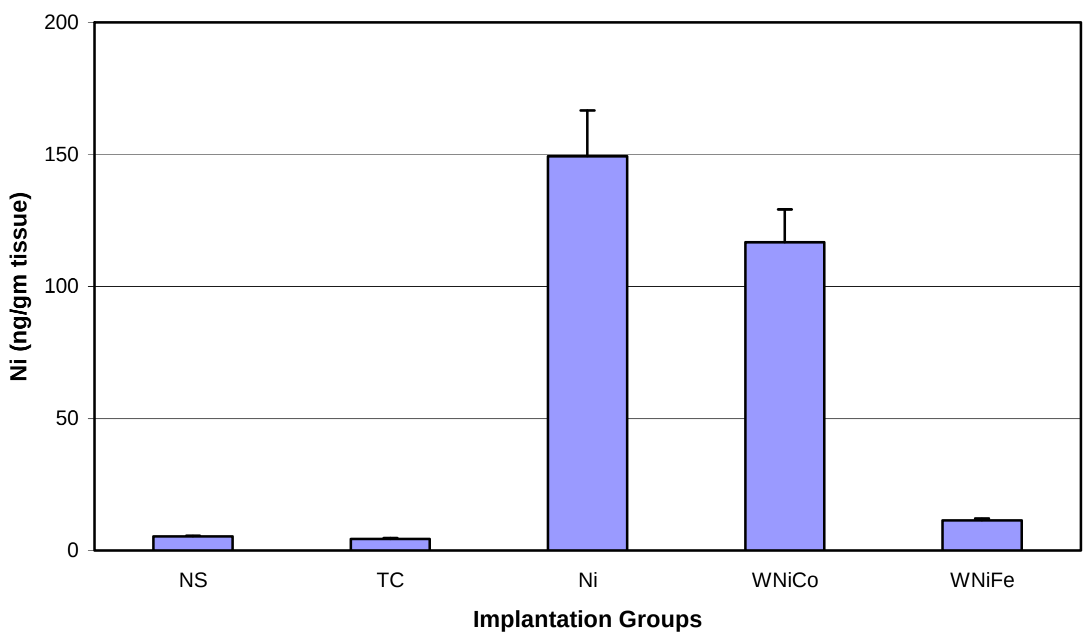

Figure 31 (continued): Kidney Metal Levels in 12-Month Implantation Groups

C. Kidney Cobalt Levels

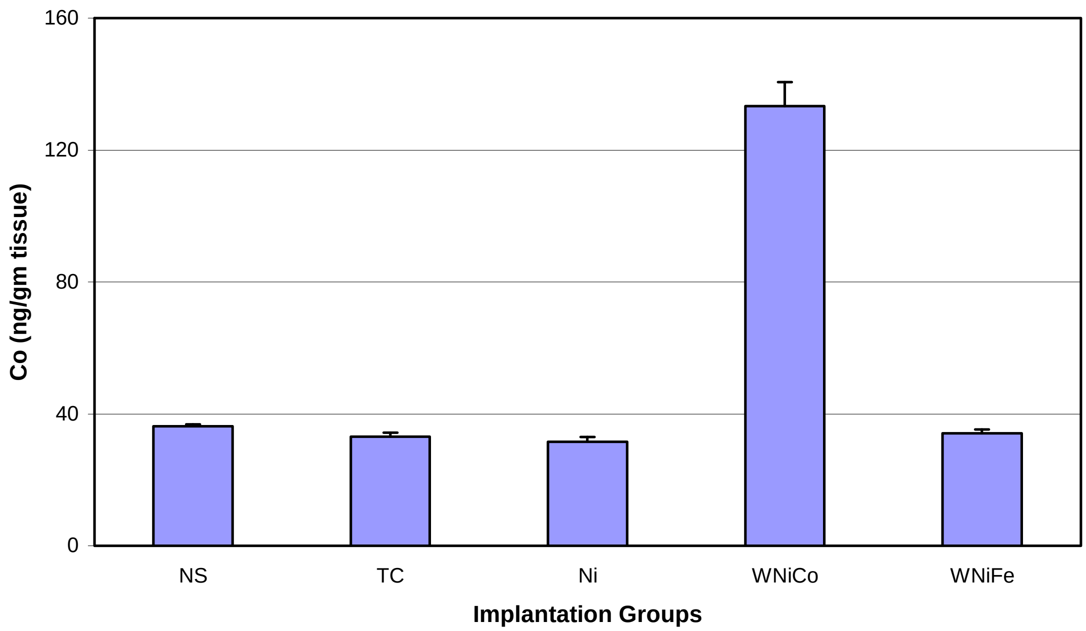

D. Kidney Tantalum Levels

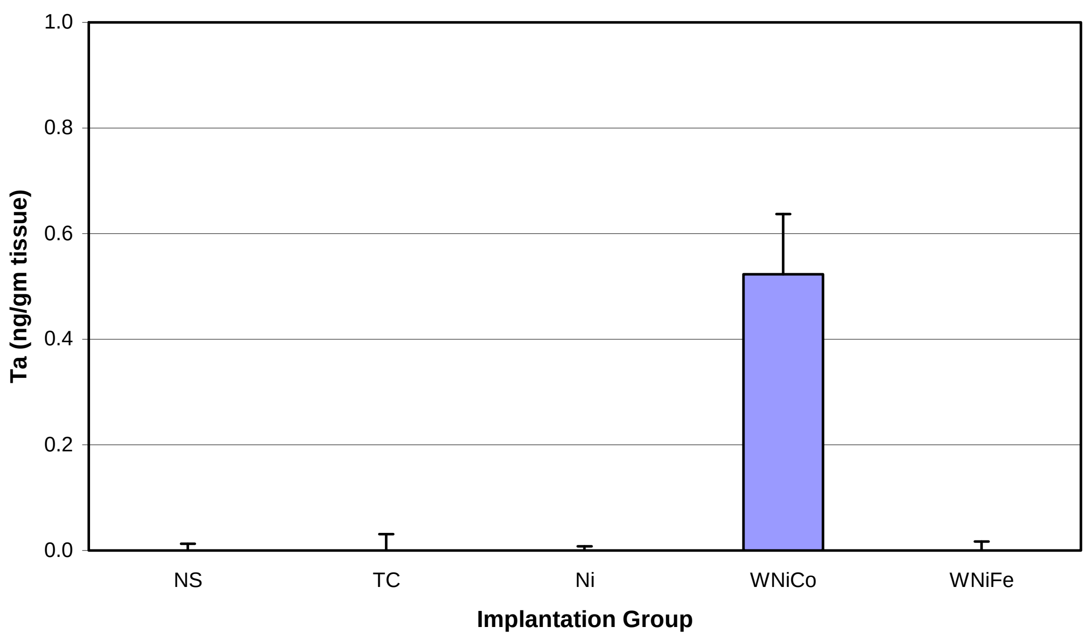

Figure 32: Liver Metal Levels in 12-Month Implantation Groups

A. Liver Tungsten Levels

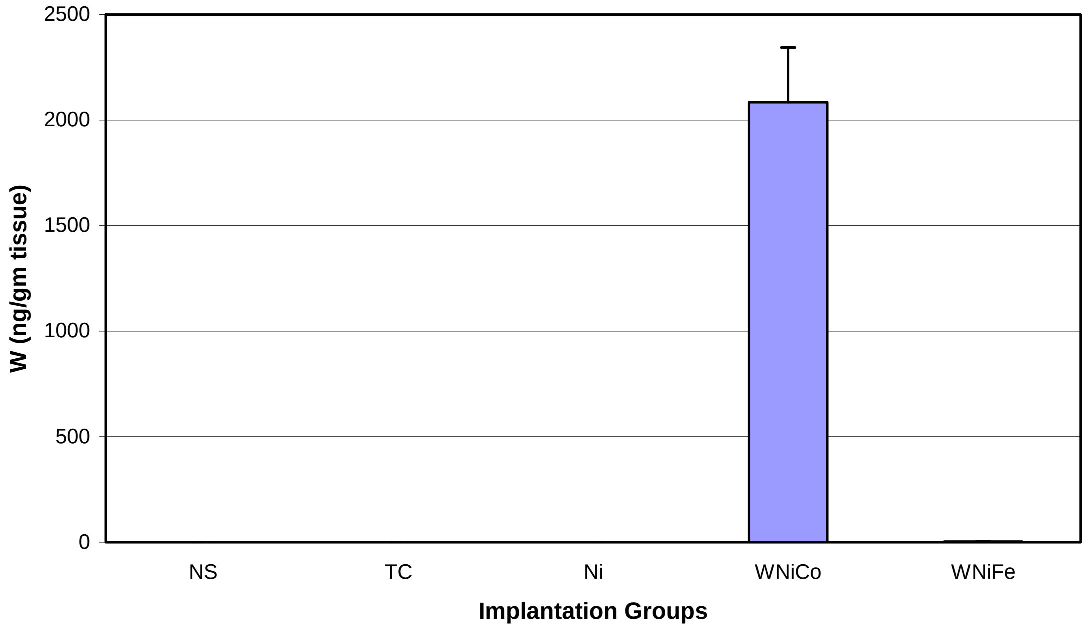

B. Liver Nickel Levels

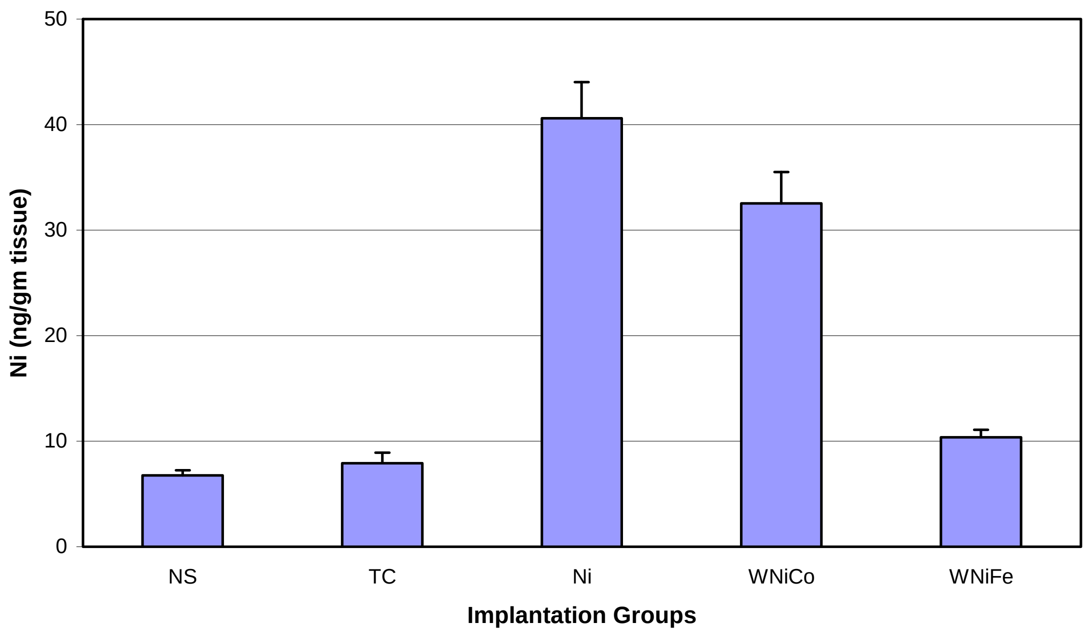

Figure 32 (continued) : Liver Metal Levels in 12-Month Implantation Groups

C. Liver Cobalt Levels

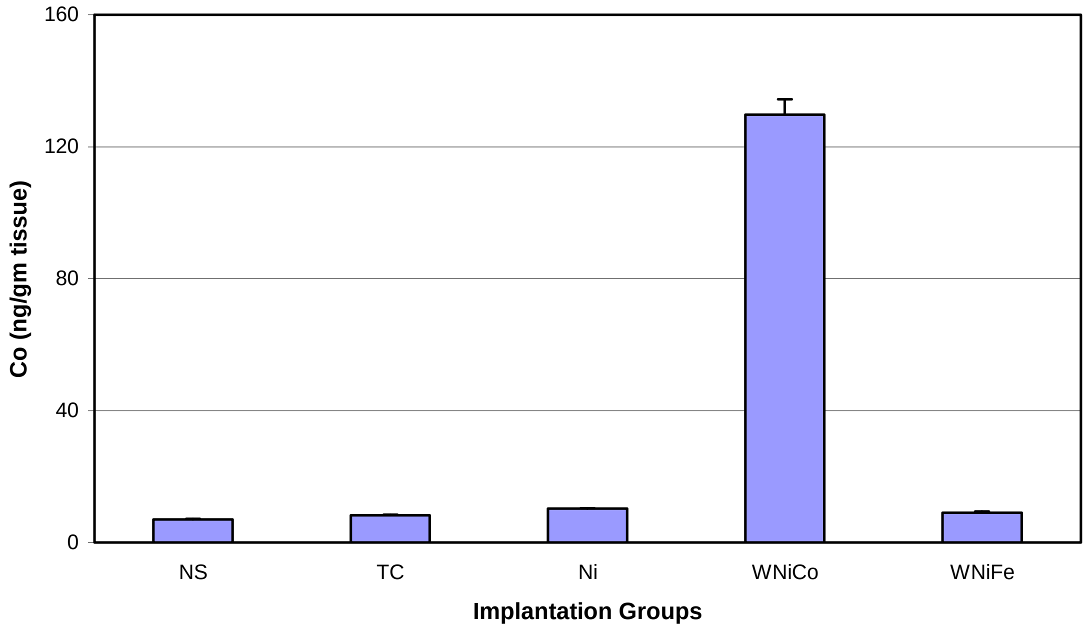

D. Liver Tantalum Levels

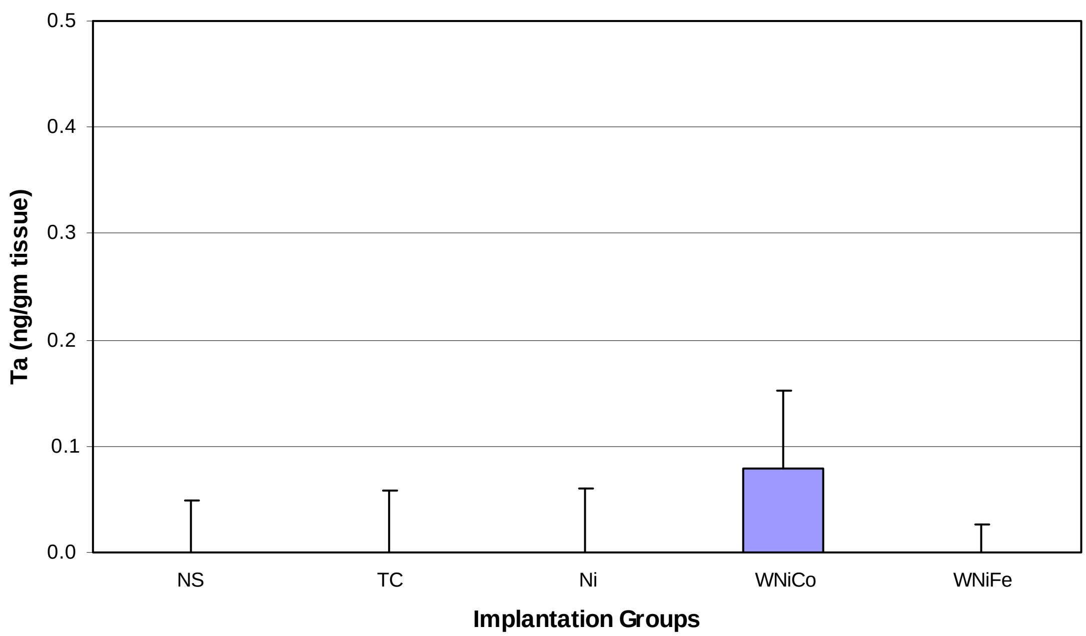

Figure 33: Serum Metals Levels in 12-Month Implantation Groups

A. Serum Tungsten Levels

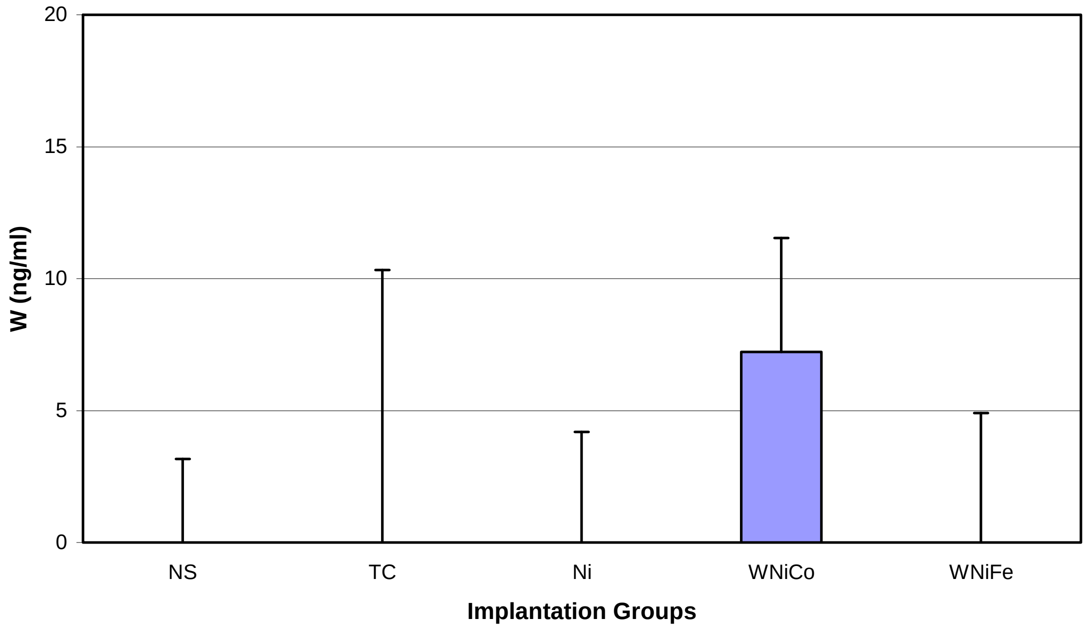

B. Serum Nickel Levels

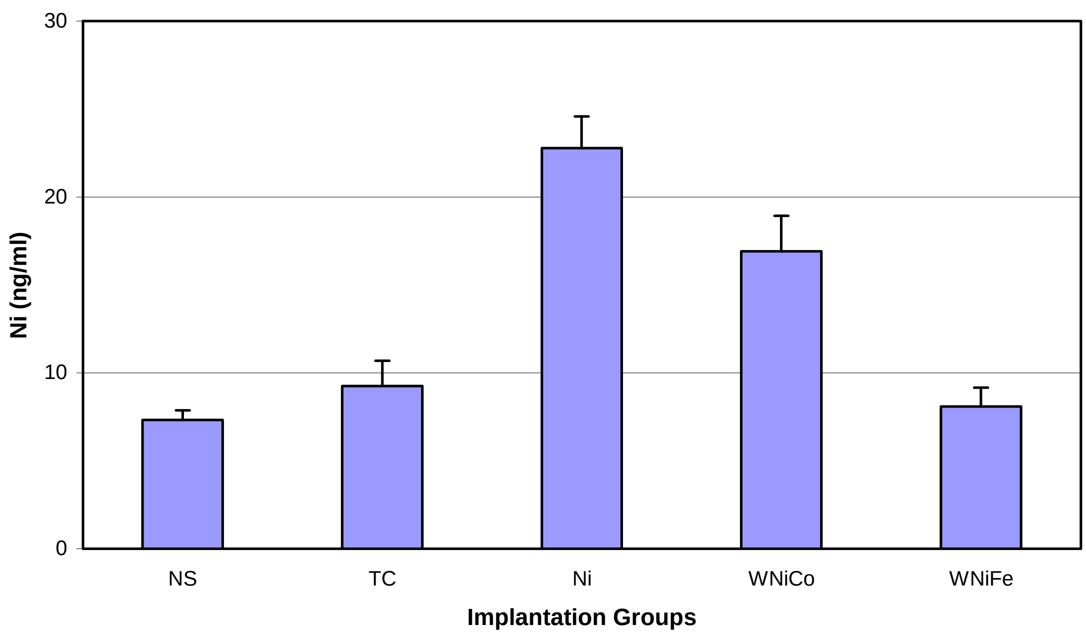

Figure 33 (continued): Serum Metals Levels in 12-Month Implantation Groups

C. Serum Cobalt Levels

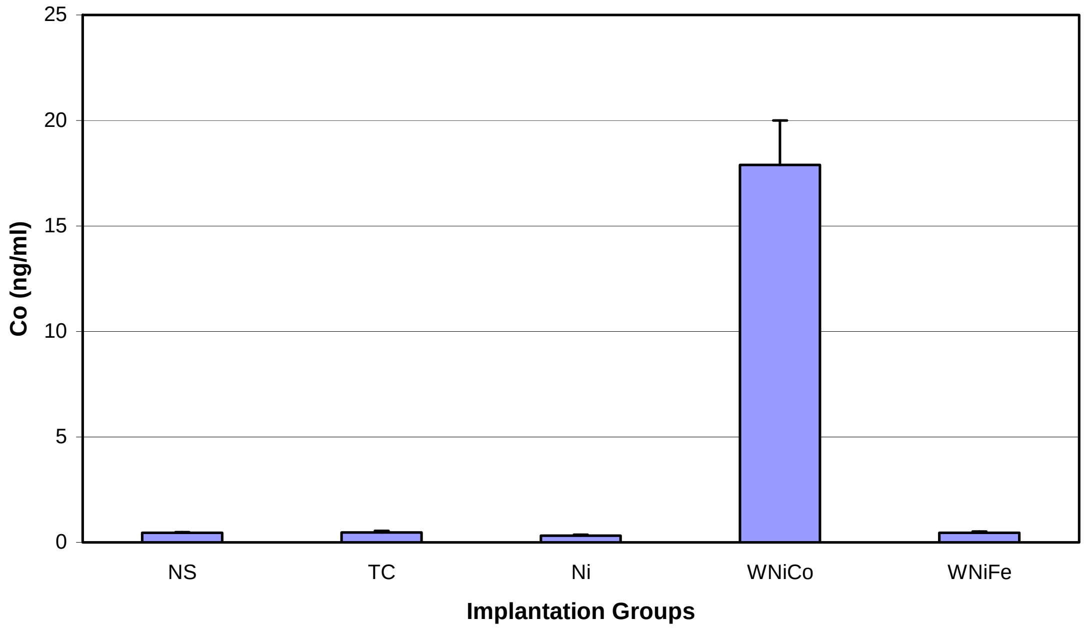

D. Serum Tantalum Levels

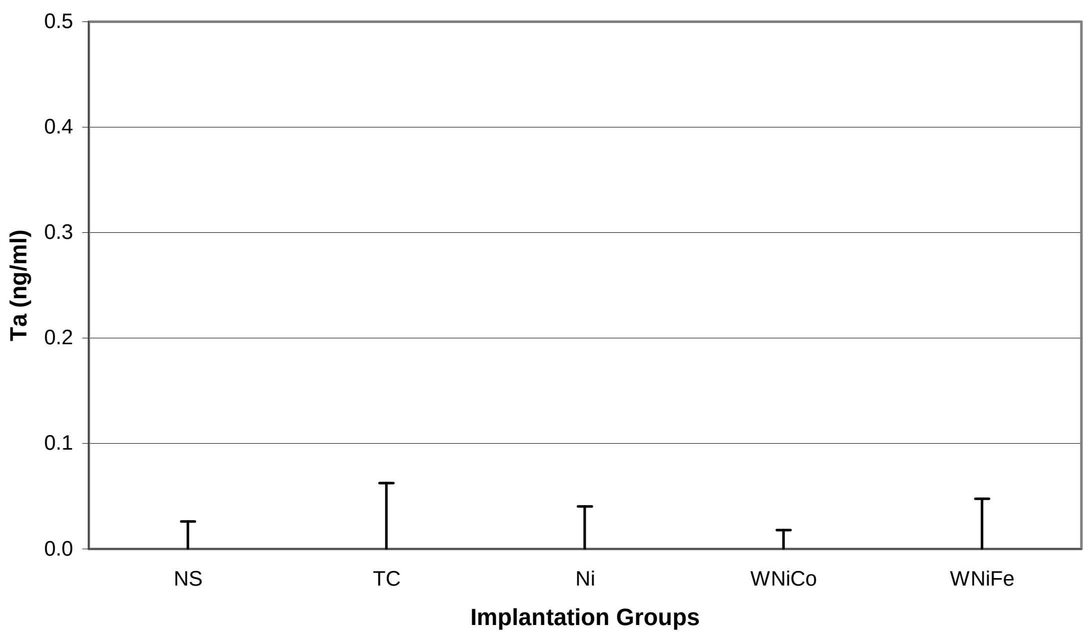

Figure 34: Spleen Metal Levels in 12-Month Implantation Groups

A. Spleen Tungsten Levels

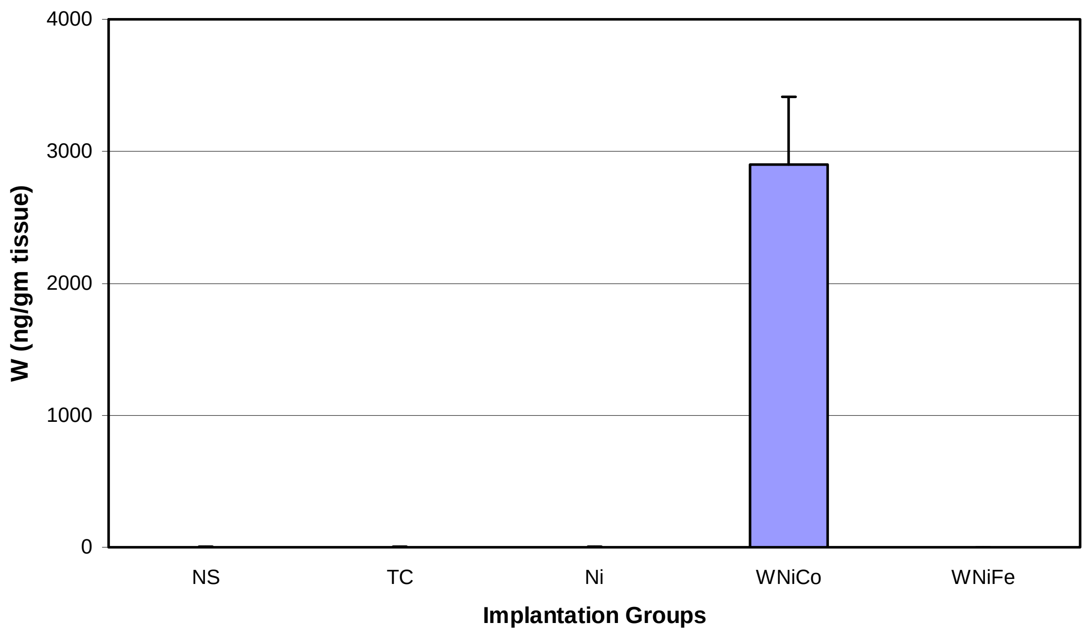

B. Spleen Nickel Levels

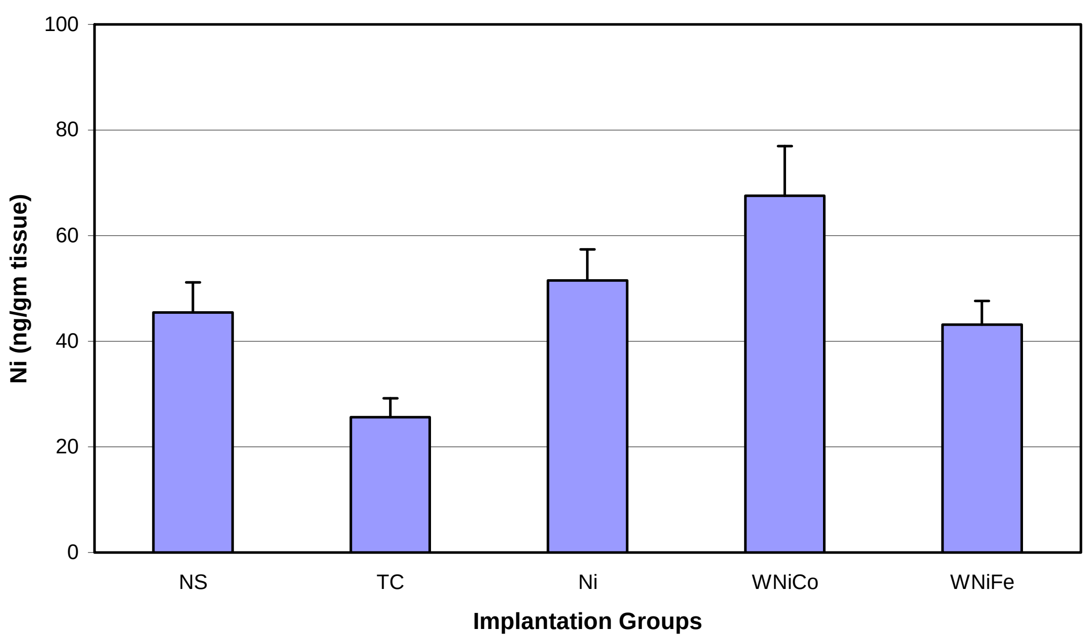

Figure 34 (continued): Spleen Metal Levels in 12-Month Implantation Groups

C. Spleen Cobalt Levels

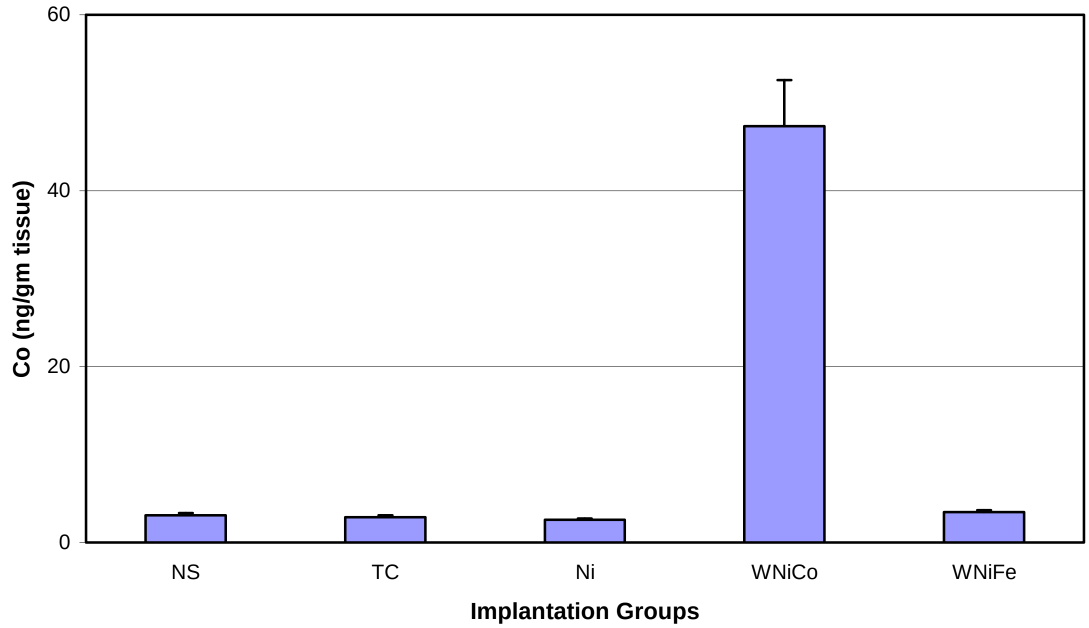

D. Spleen Tantalum Levels

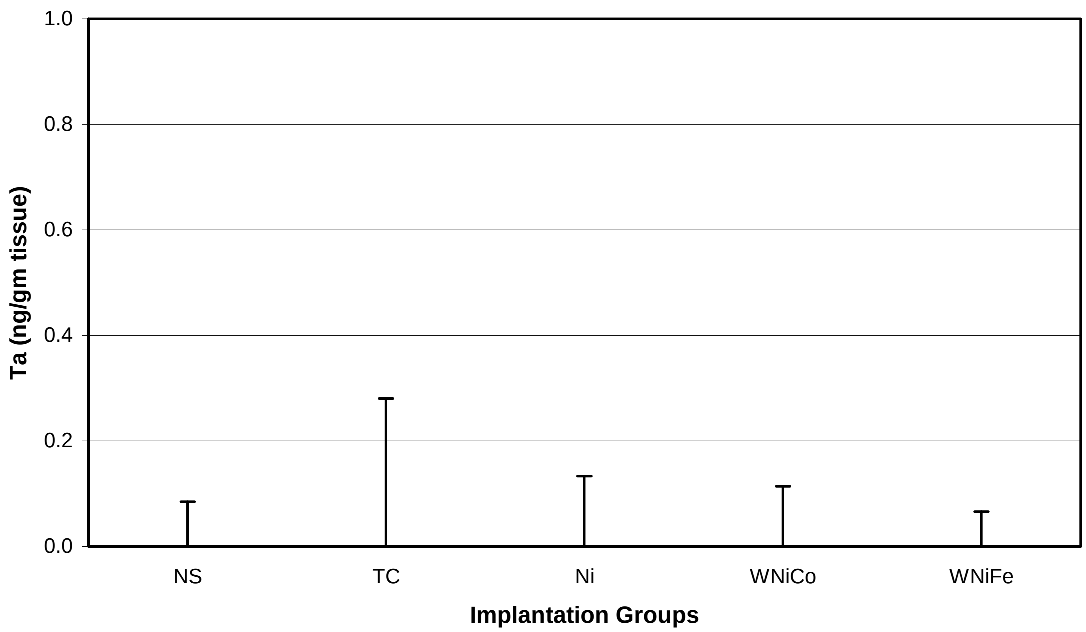

Figure 35: Testes Metal Levels in 12-Month Implantation Groups

A. Testes Tungsten Levels

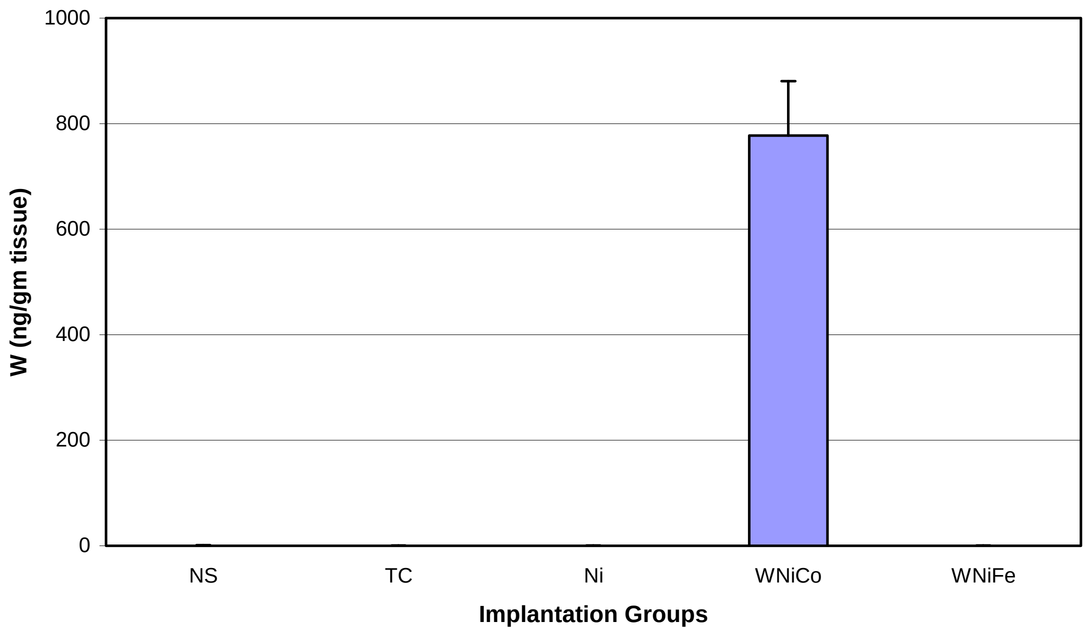

B. Testes Nickel Levels

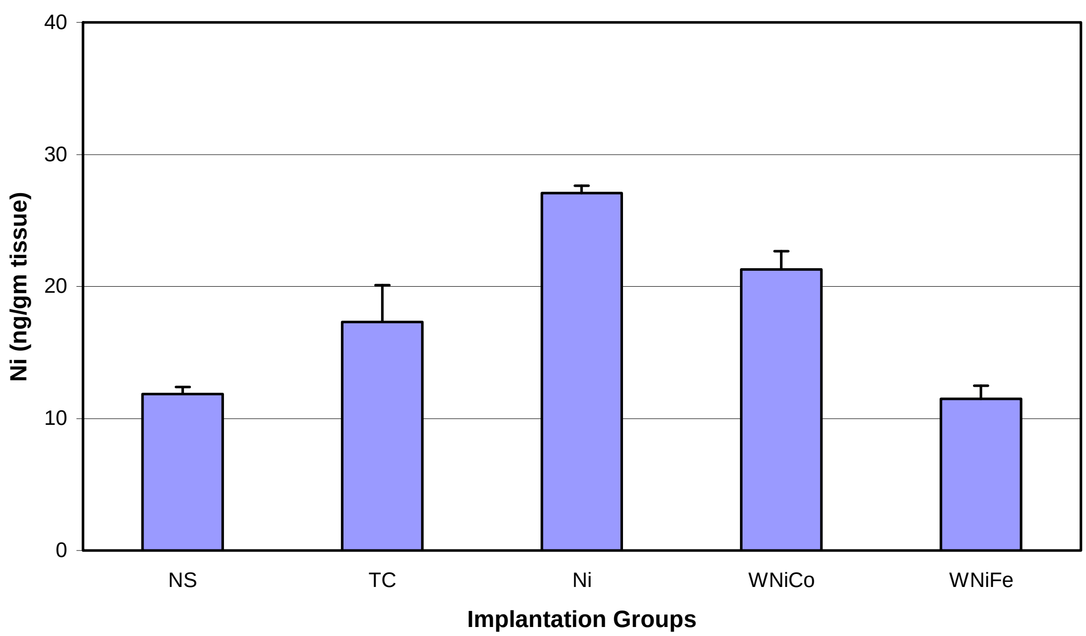

Figure 35 (continued): Testes Metal Levels in 12-Month Implantation Groups

C. Testes Cobalt Levels

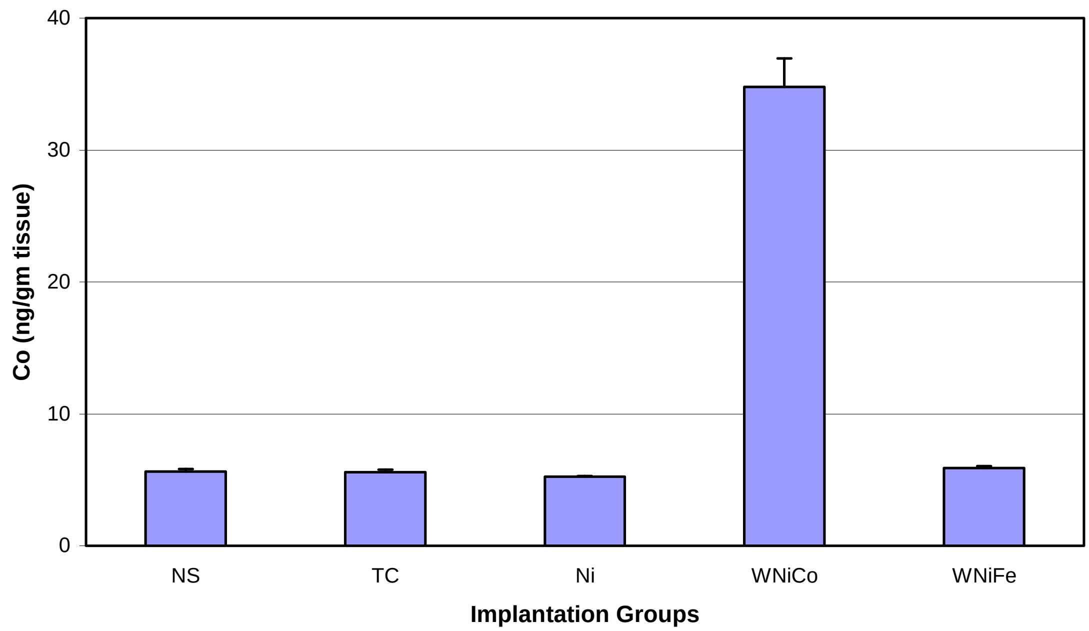

D. Testes Tantalum Levels

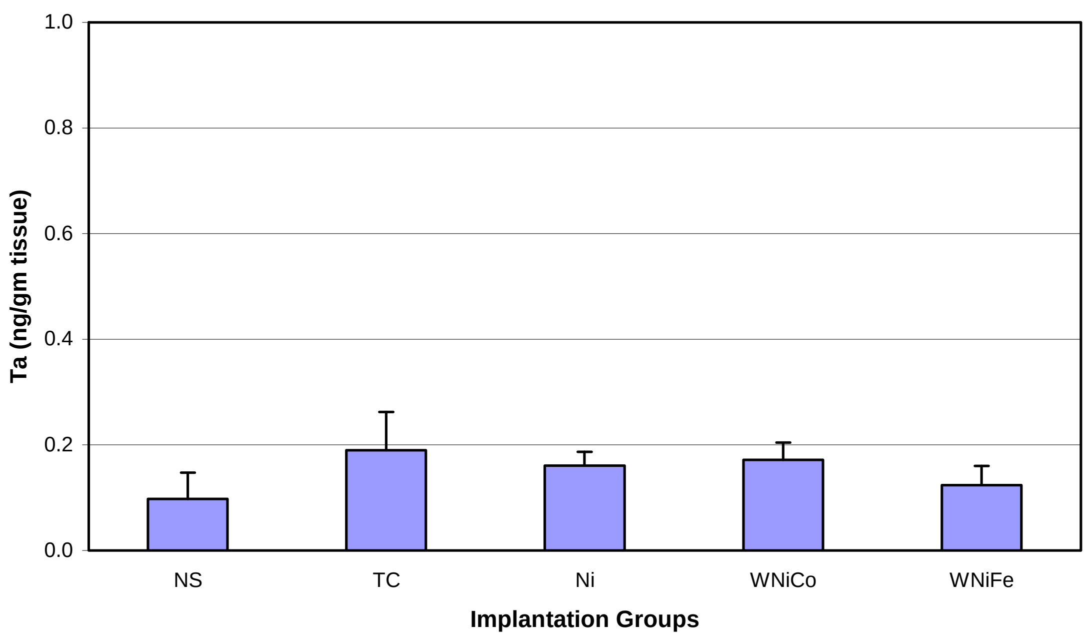

Figure 36: Urinary Metal Levels in 12-Month Implantation Groups

A. Urinary Tungsten Levels

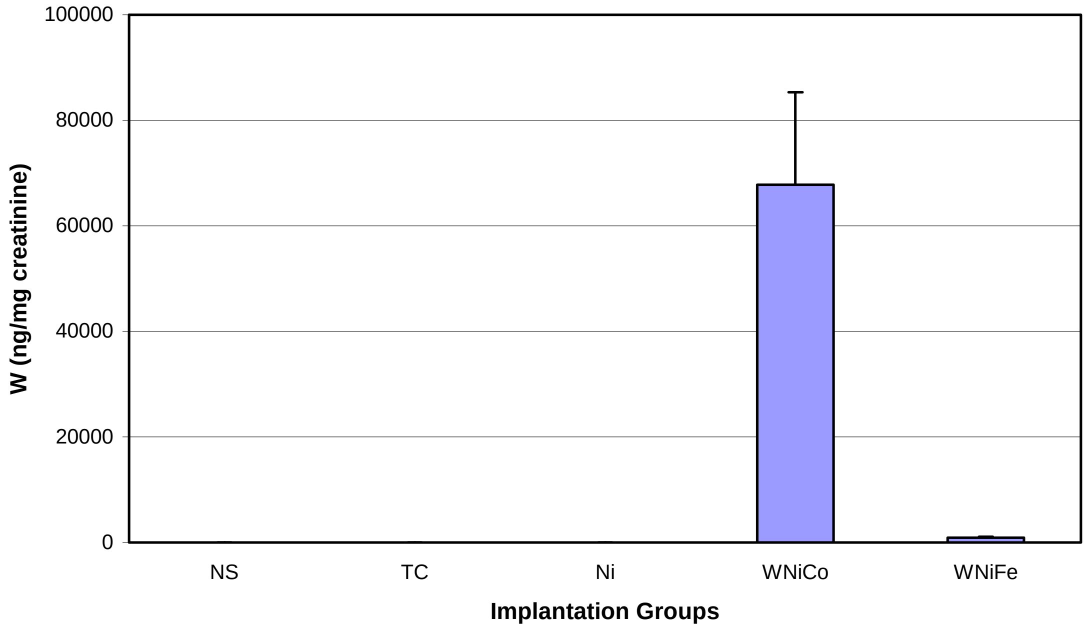

B. Urinary Nickel Levels

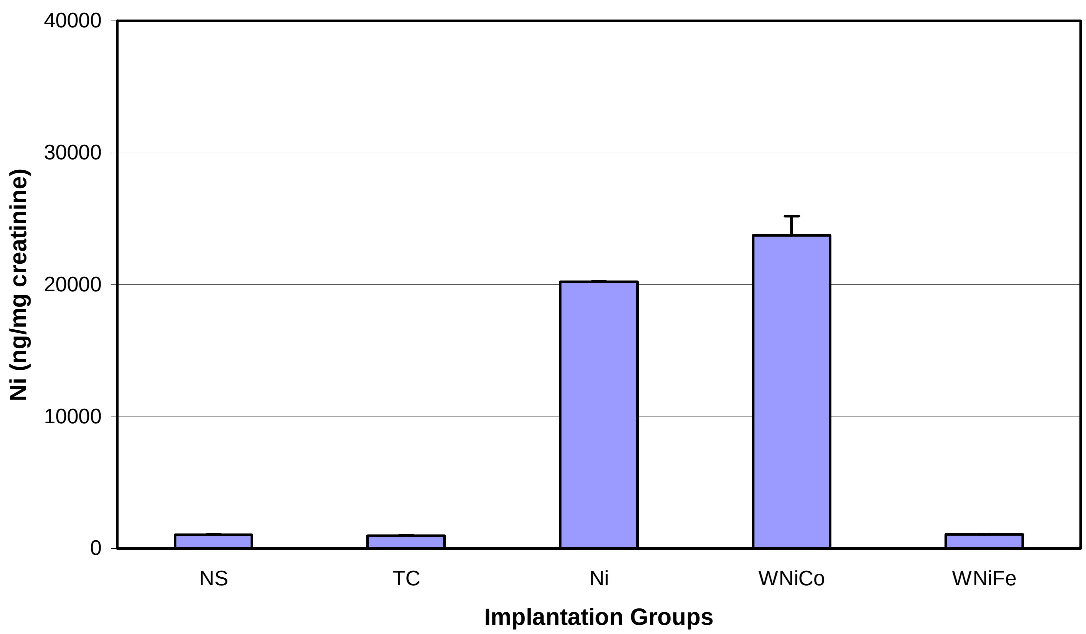

Figure 36 (continued): Urinary Metal Levels in 12-Month Implantation Groups

C. Urinary Cobalt Levels

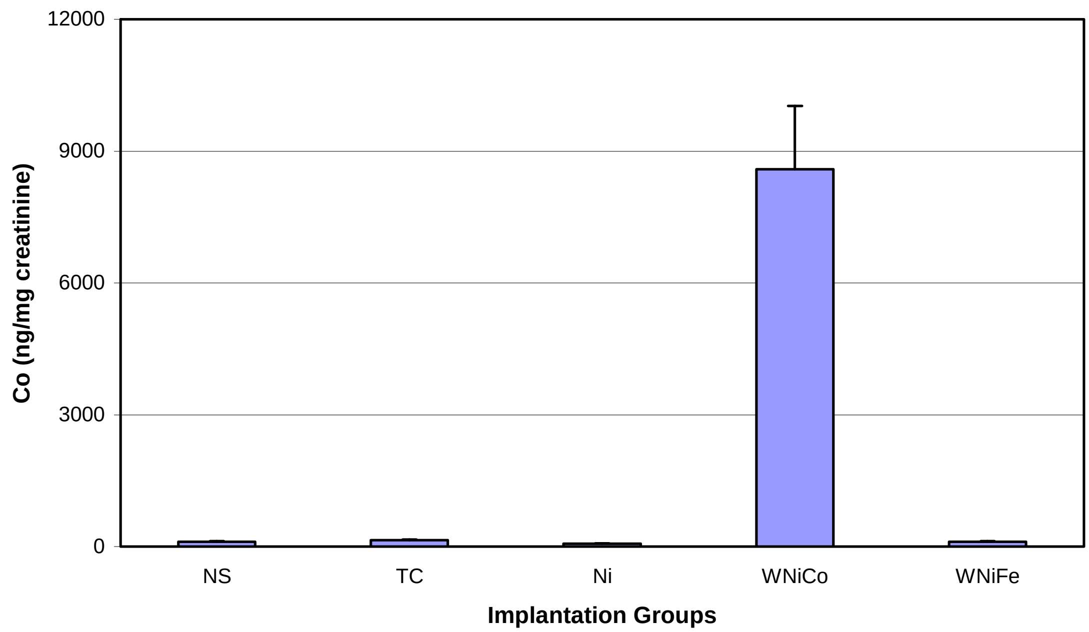

D. Urinary Tantalum Levels

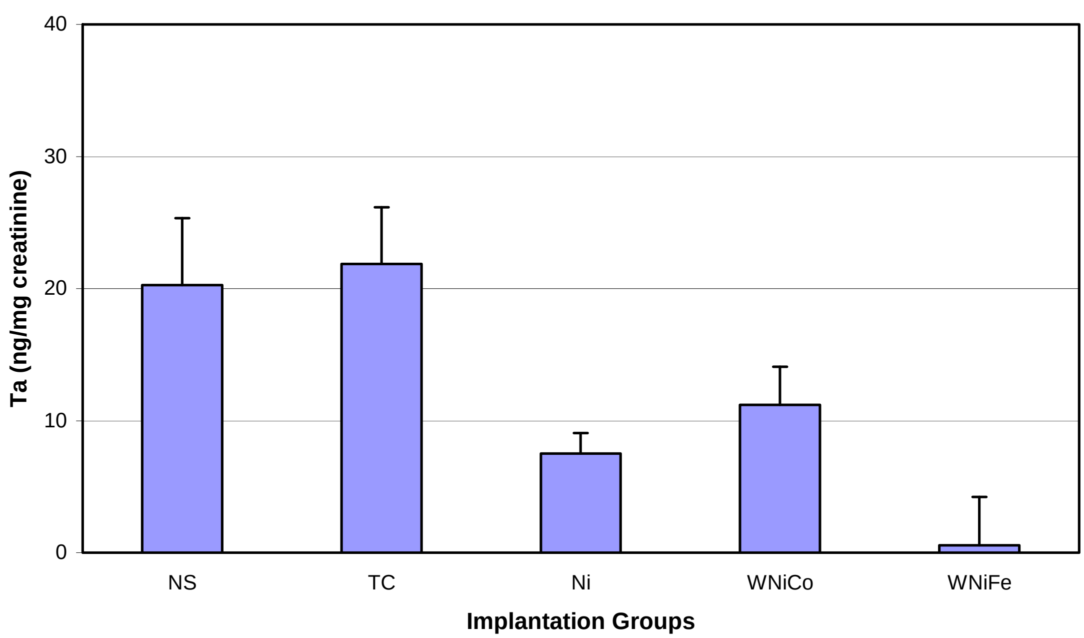

Figure 37: Brain Metal Levels in 24-Month Implantation Groups

A. Brain Tungsten Levels

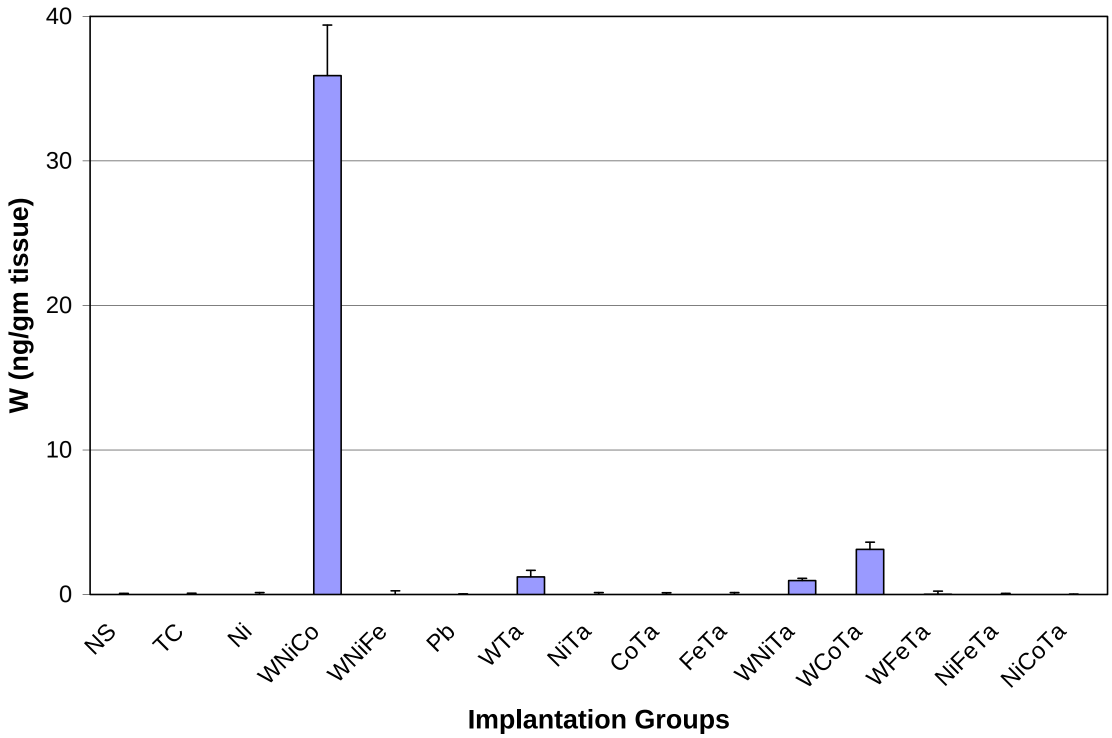

B. Brain Nickel Levels

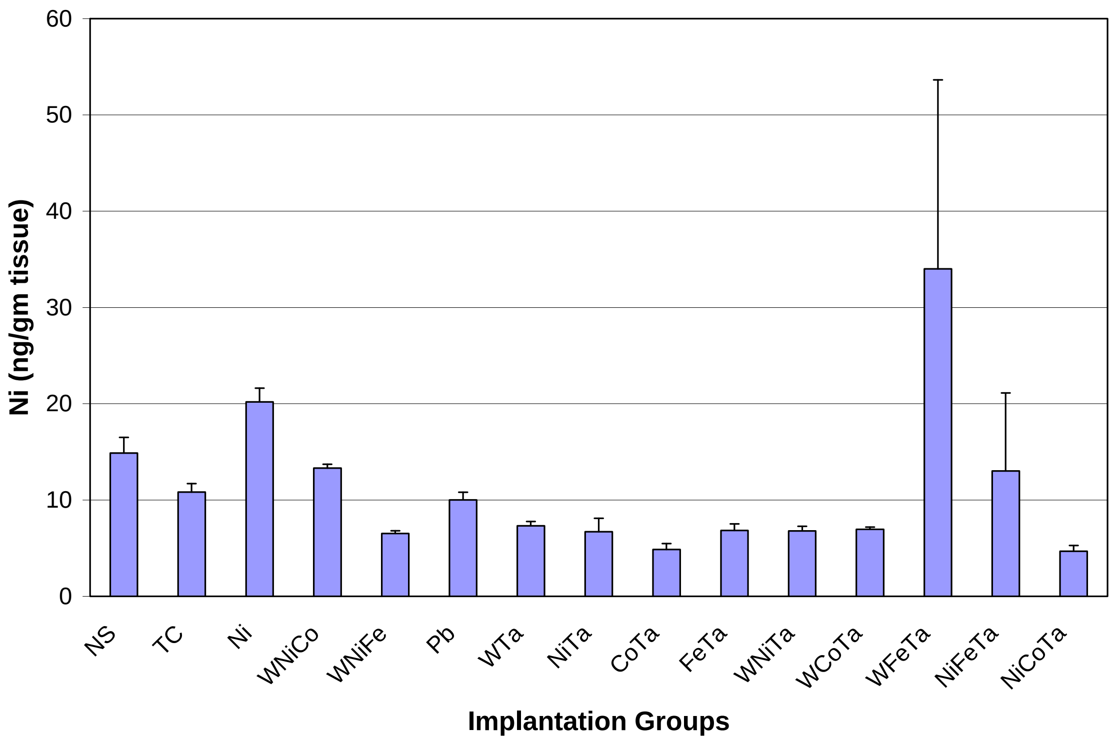

Figure 37 (continued): Brain Metal Levels in 24-Month Implantation Groups

C. Brain Cobalt Levels

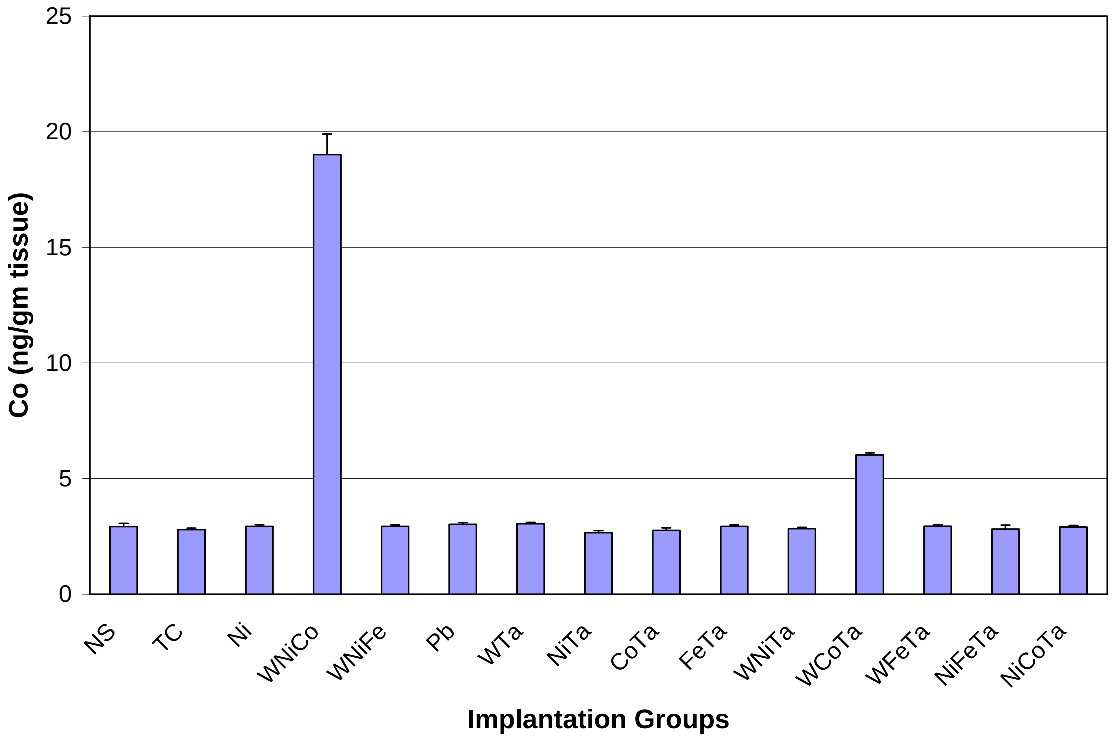

D. Brain Tantalum Levels

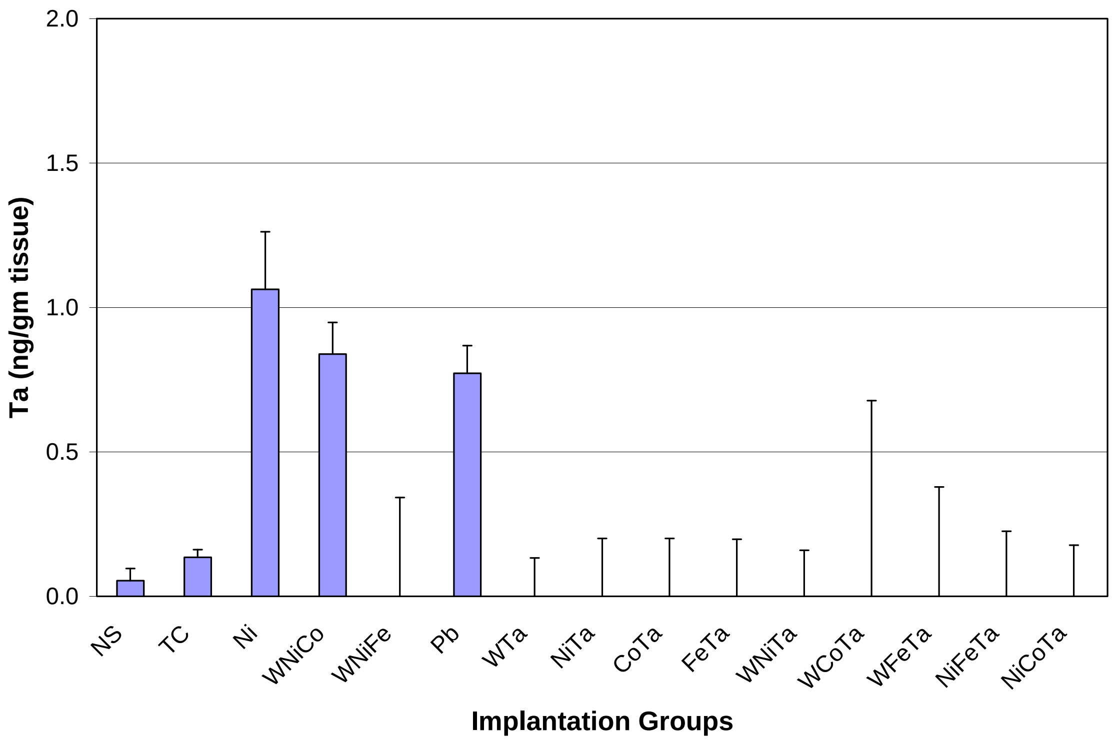

Figure 38: Femur Metal Levels in 24-Month Implantation Groups

A. Femur Tungsten Levels

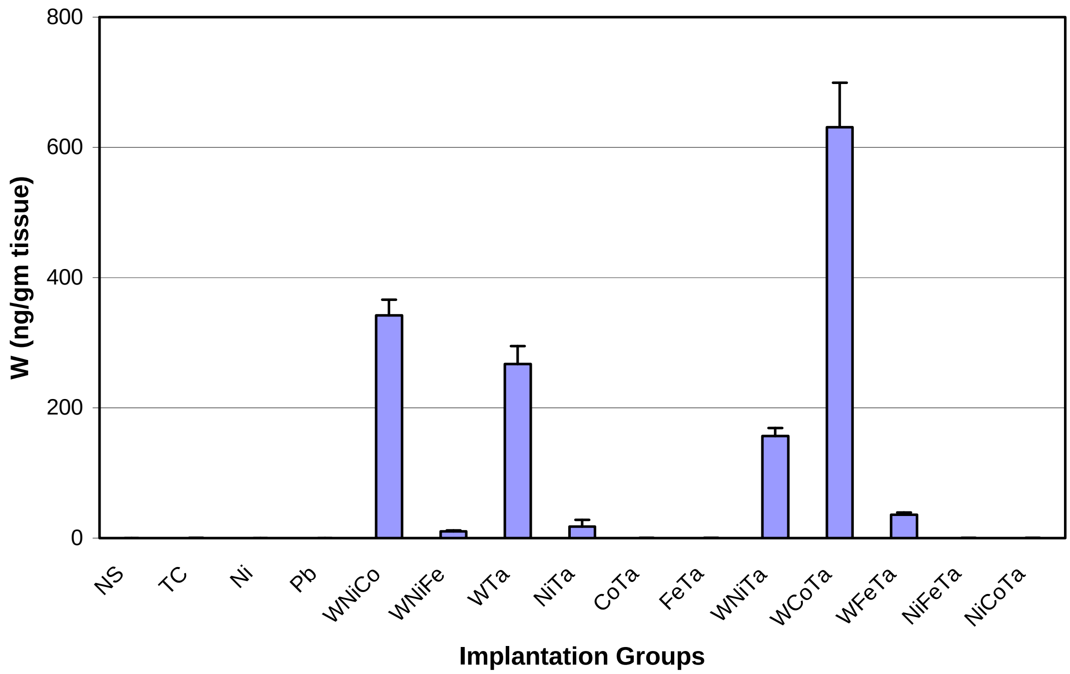

B. Femur Nickel Levels

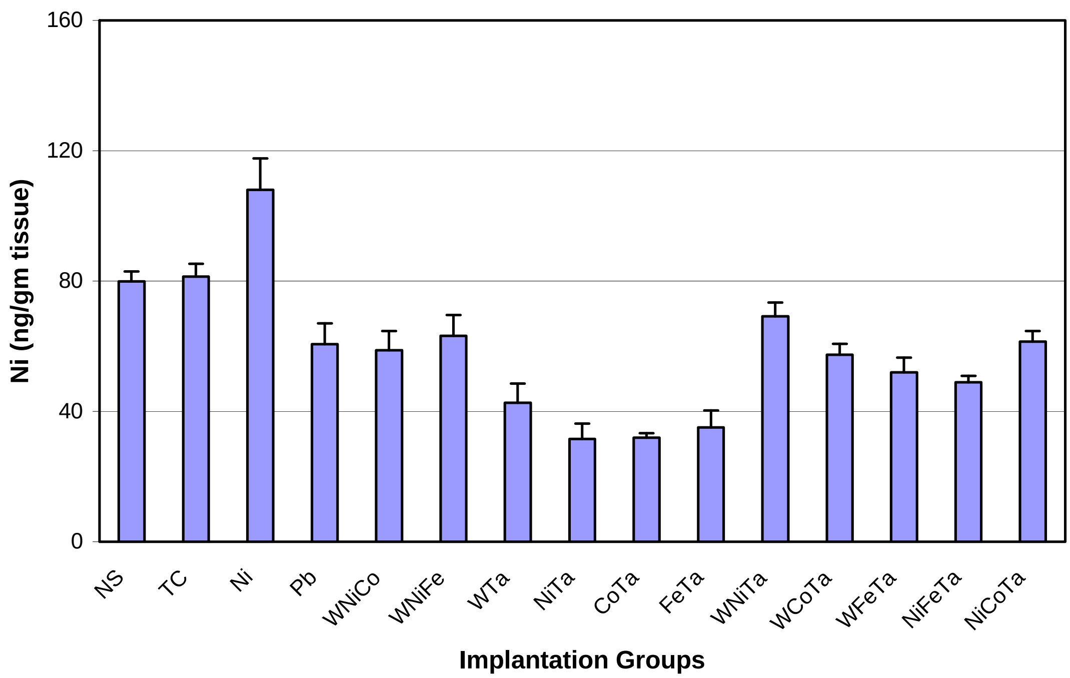

Figure 38 (continued): Femur Metal Levels in 24-Month Implantation Groups

C. Femur Cobalt Levels

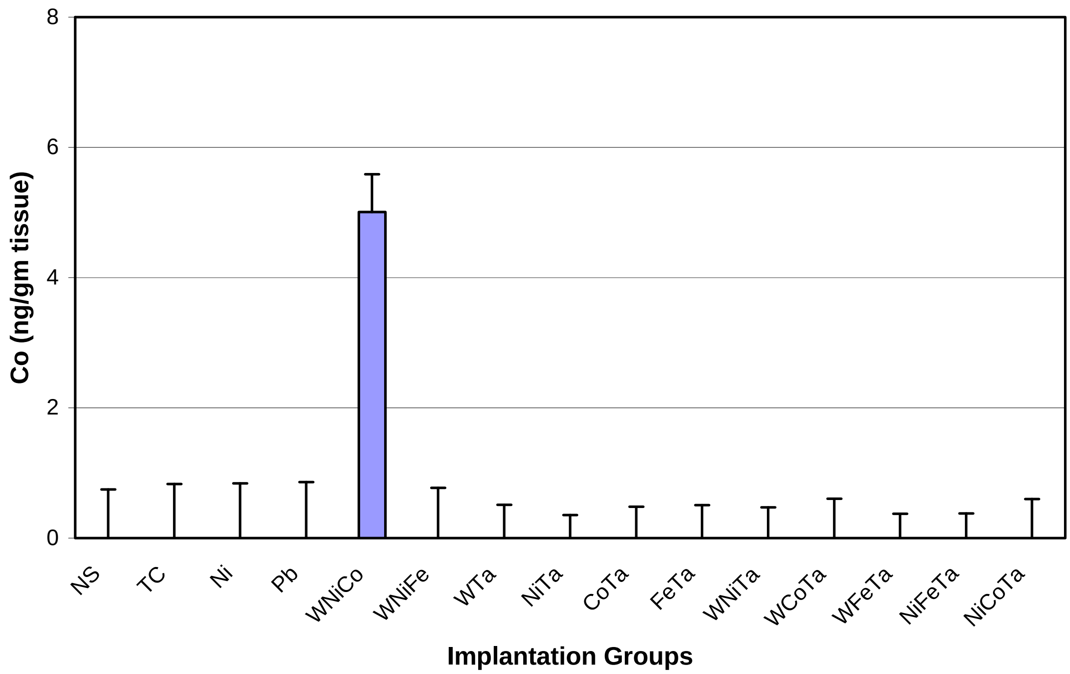

D. Femur Tantalum Levels

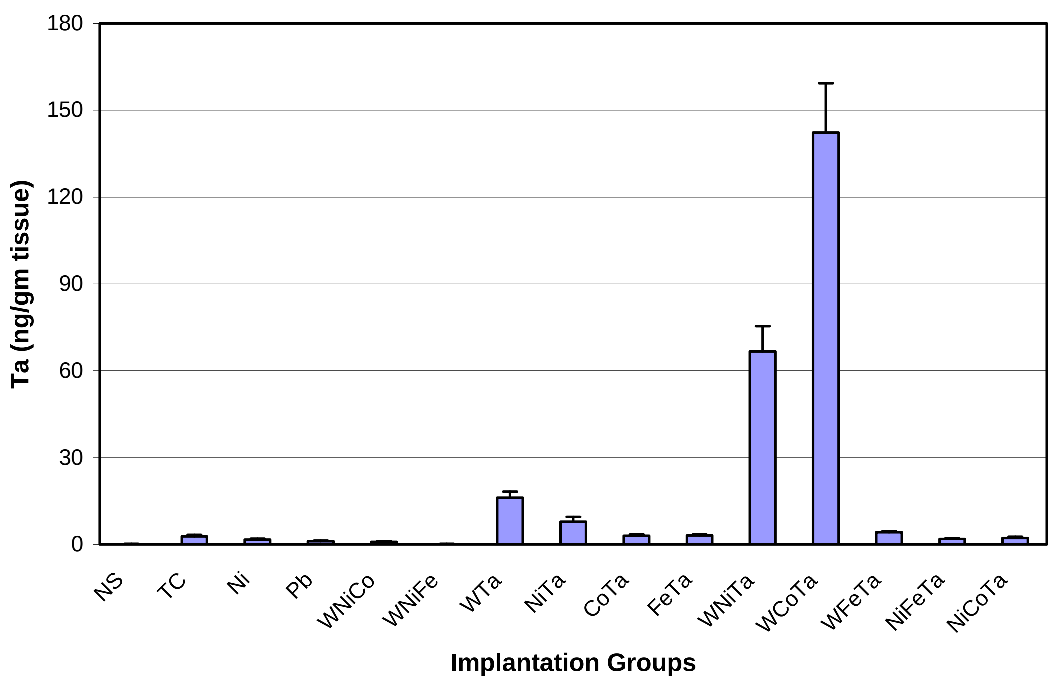

Figure 39: Kidney Metal Levels in 24-Month Implantation Groups

A. Kidney Tungsten Levels

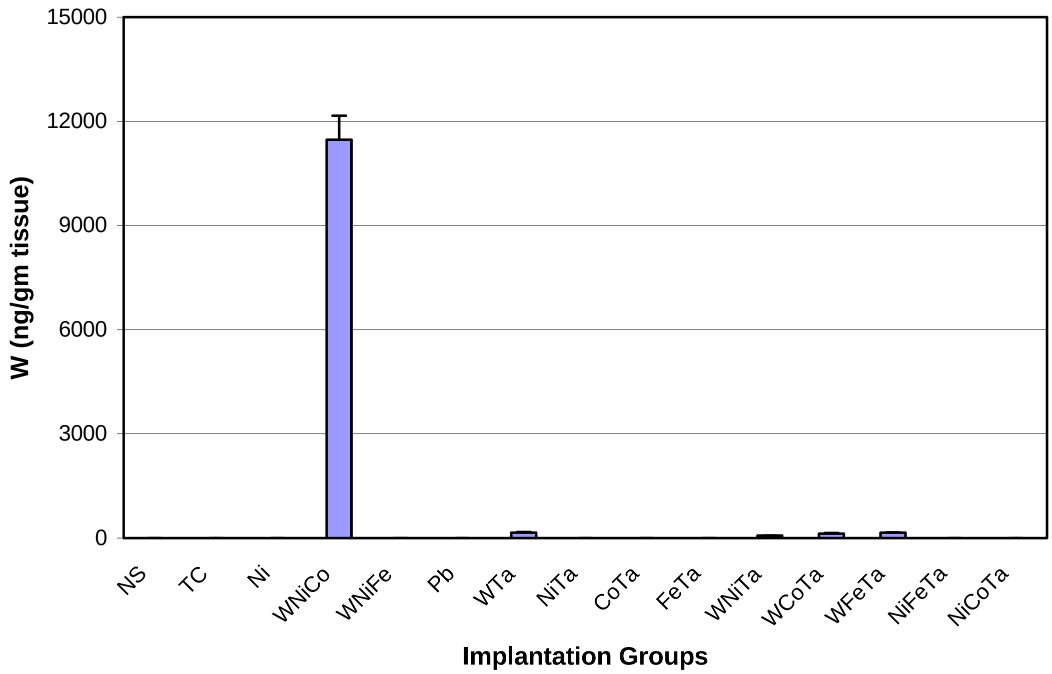

B. Kidney Nickel Levels

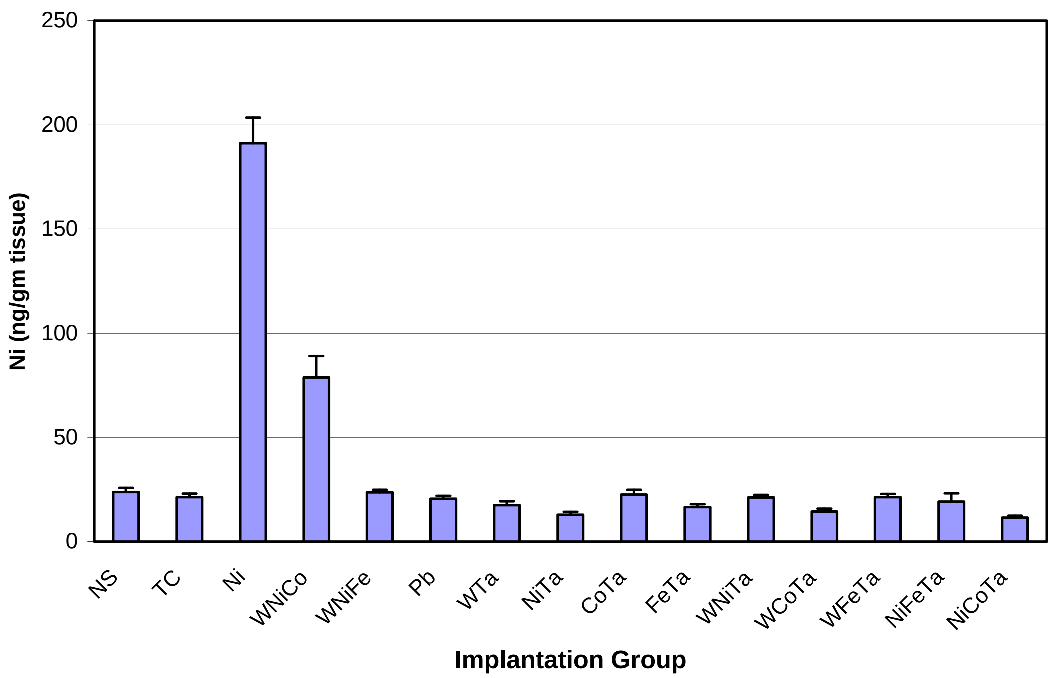

Figure 39 (continued): Kidney Metal Levels in 24-Month Implantation Groups

C. Kidney Cobalt Levels

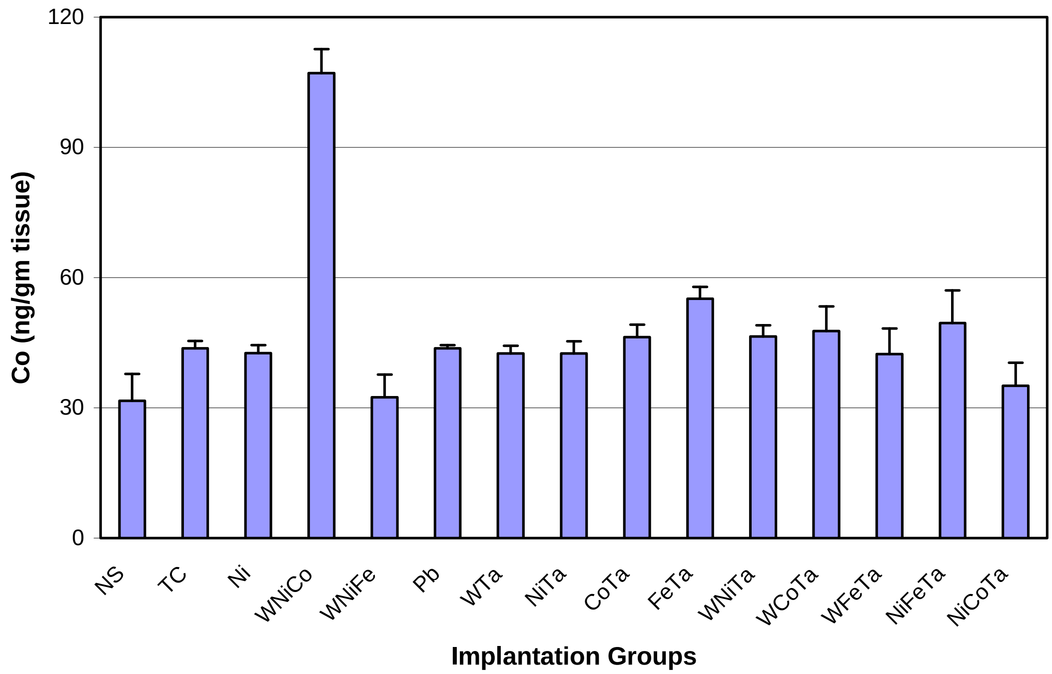

D. Kidney Tantalum Levels

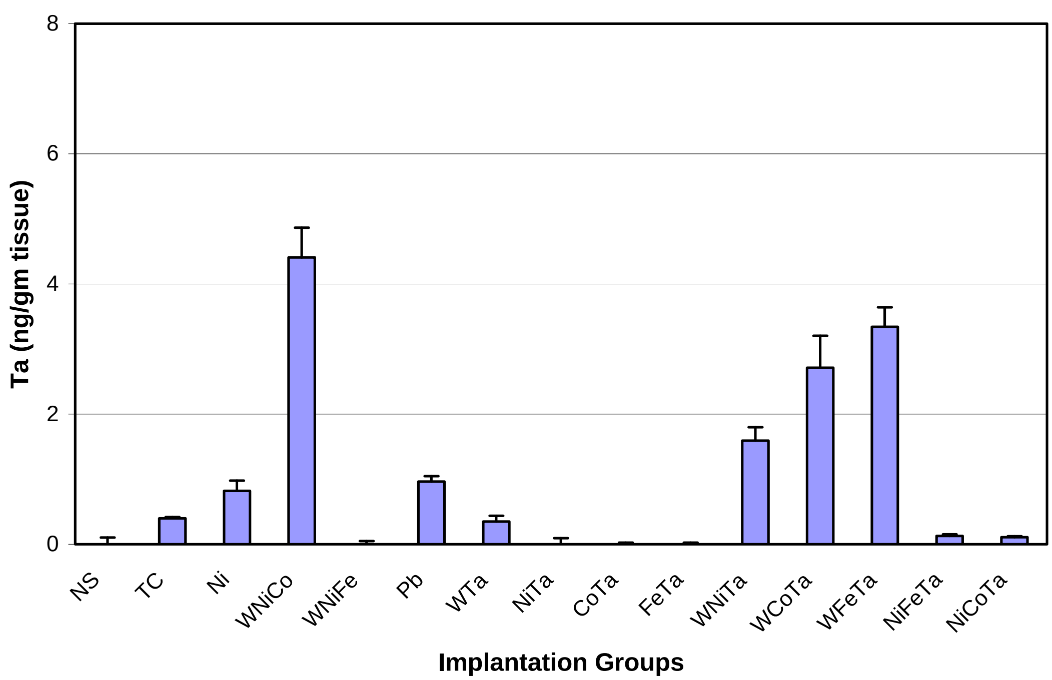

Figure 40: Liver Metal Levels in 24-Month Implantation Groups

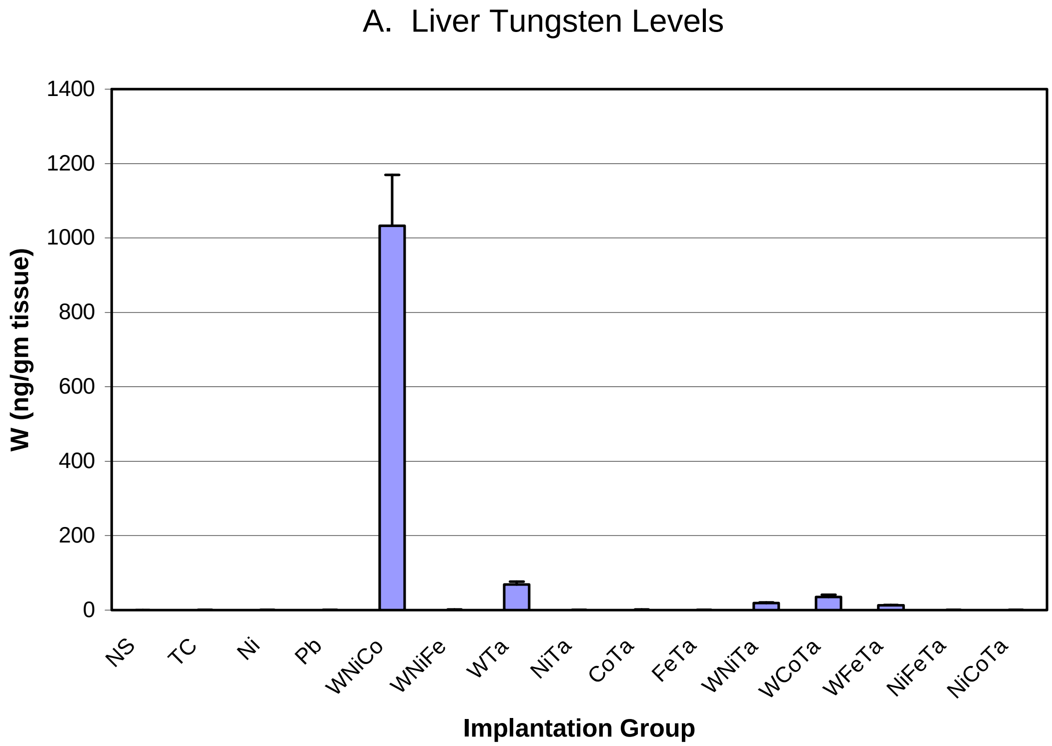

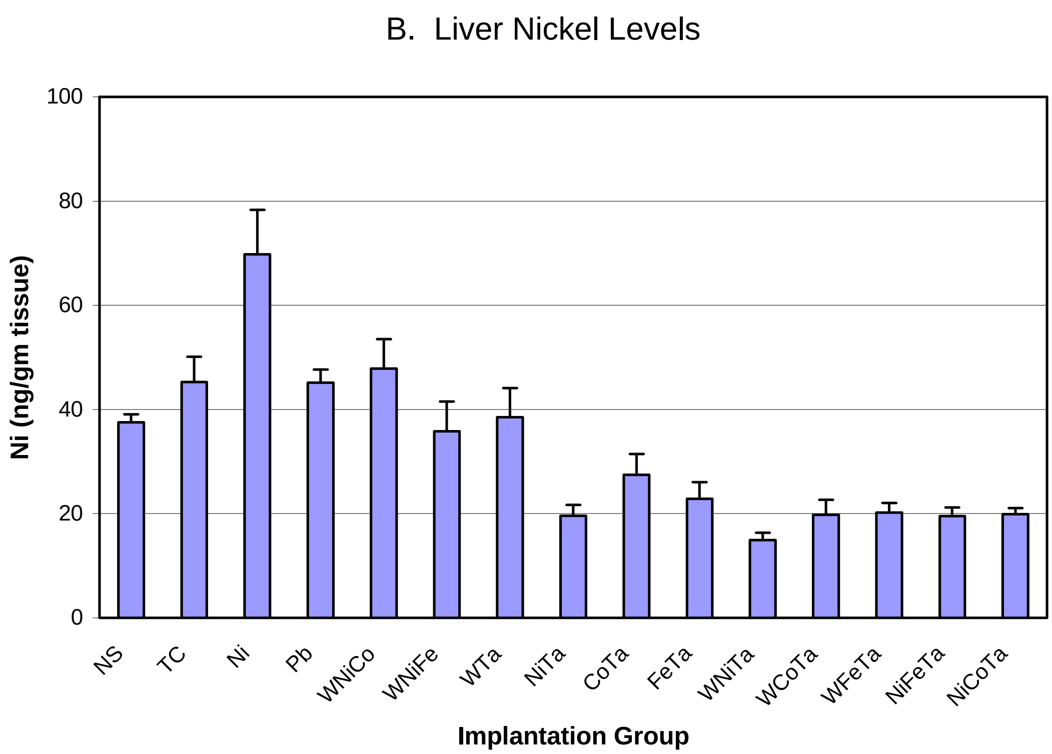

Figure 40 (continued): Liver Metal Levels in 24-Month Implantation Groups

C. Liver Cobalt Levels

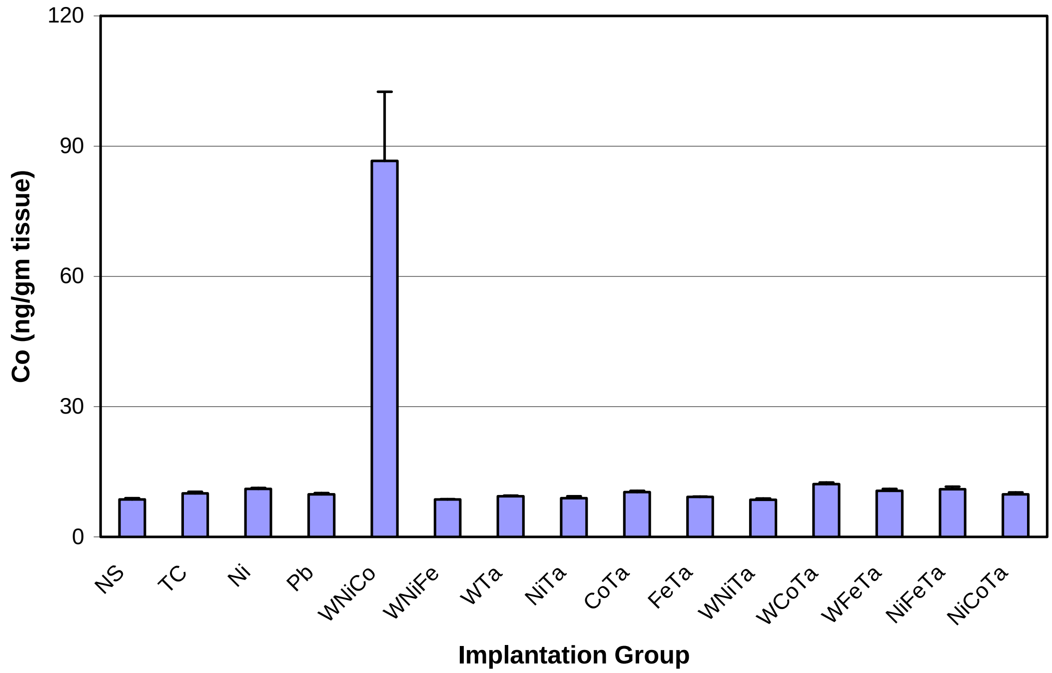

D. Liver Tantalum Levels

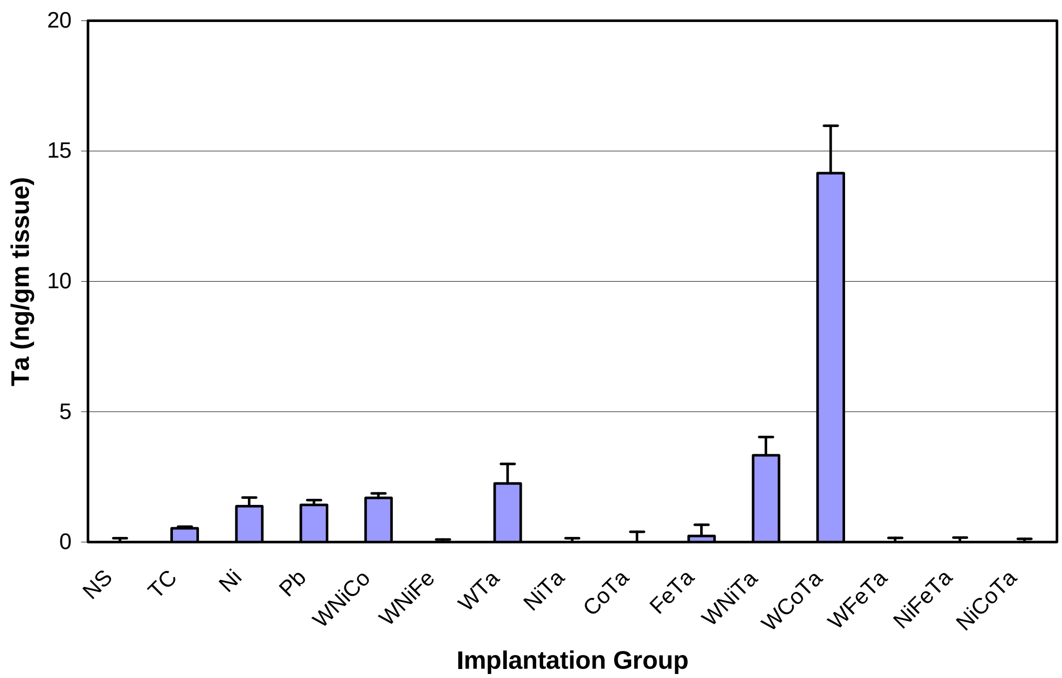

Figure 41: Serum Metals Levels in 24-Month Implantation Groups

A. Serum Tungsten Levels

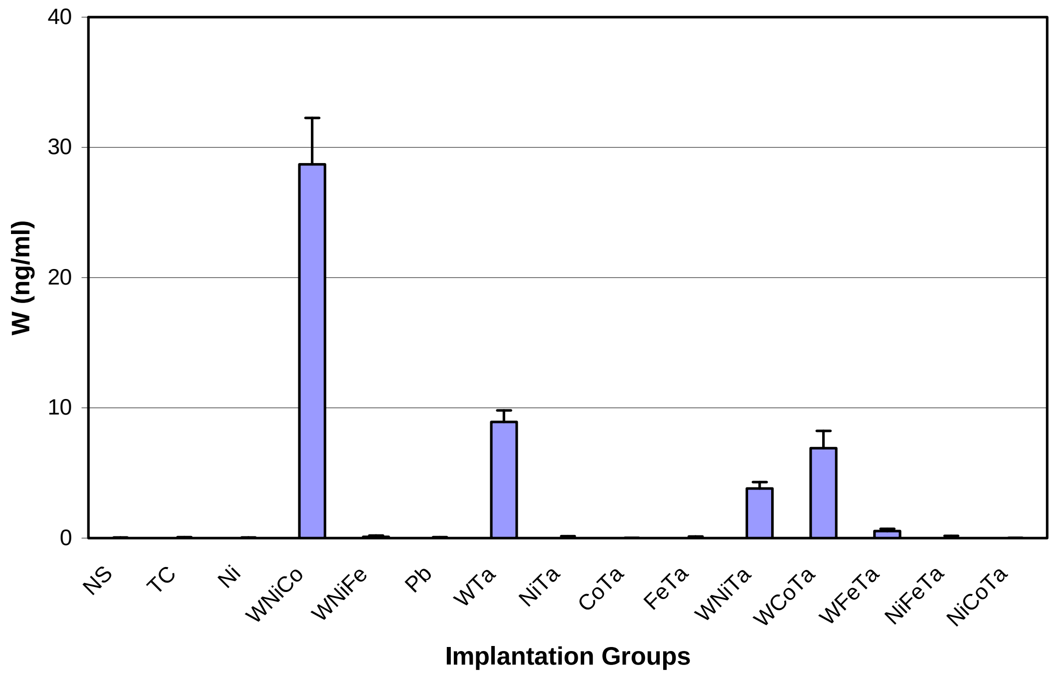

B. Serum Nickel Levels

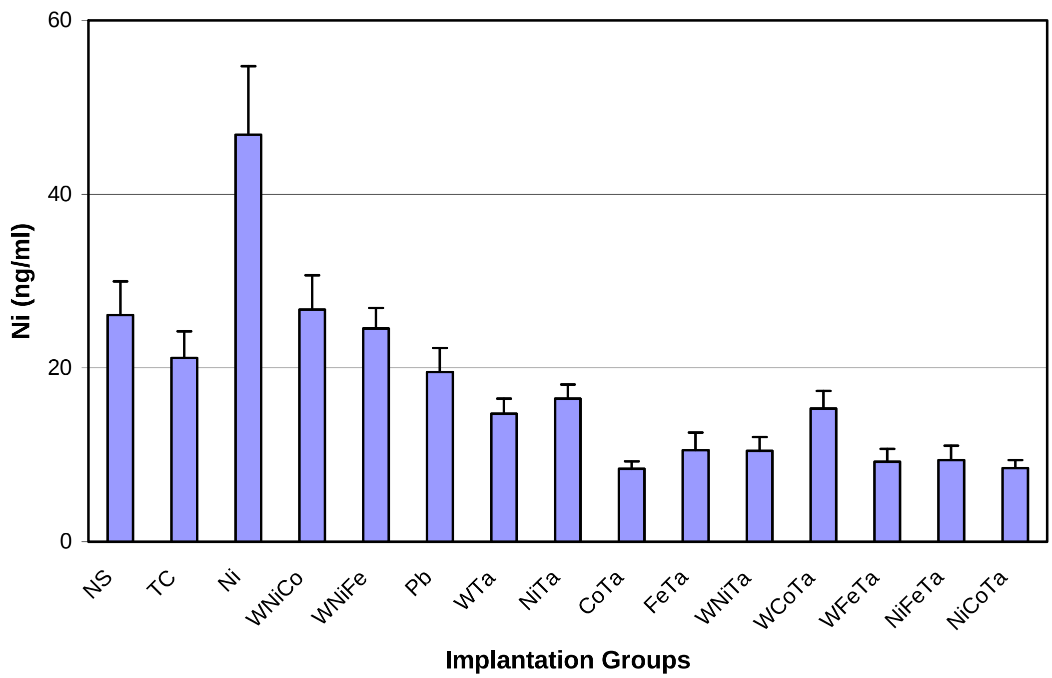

Figure 41 (continued): Serum Metals Levels in 24-Month Implantation Groups

C. Serum Cobalt Levels

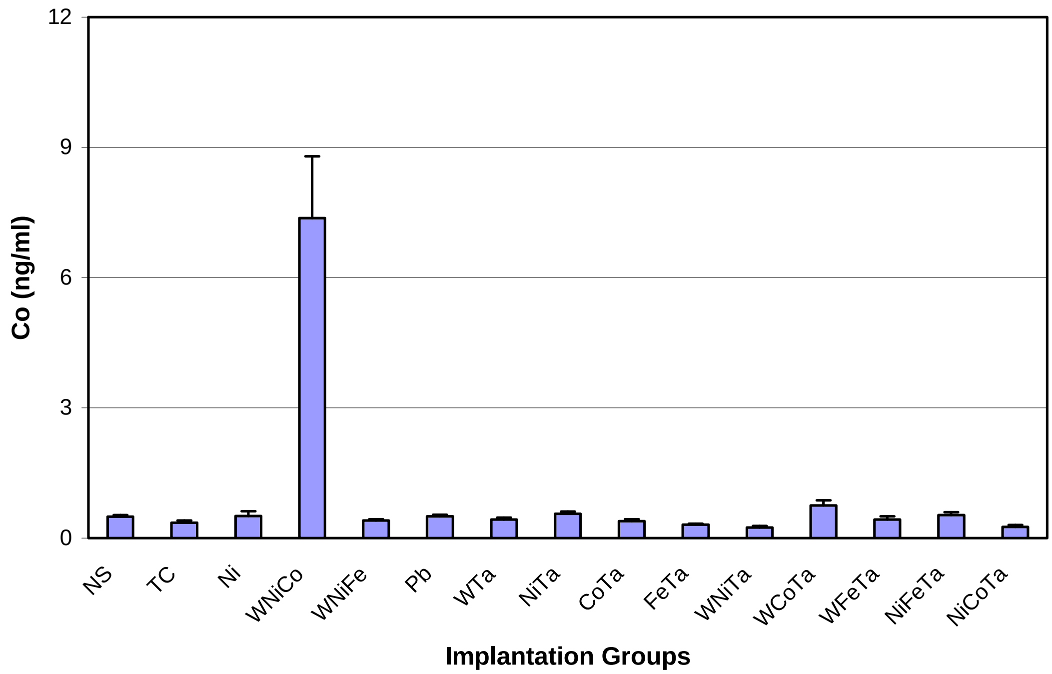

D. Serum Tantalum Levels

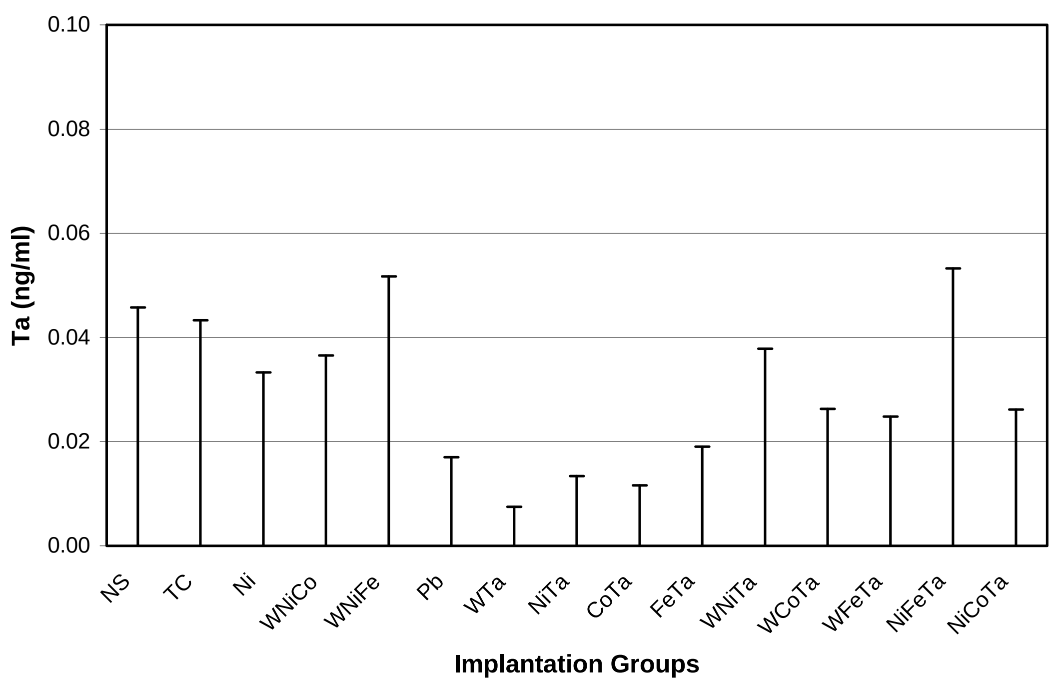

Figure 42: Spleen Metal Levels in 24-Month Implantation Groups

A. Spleen Tungsten Levels

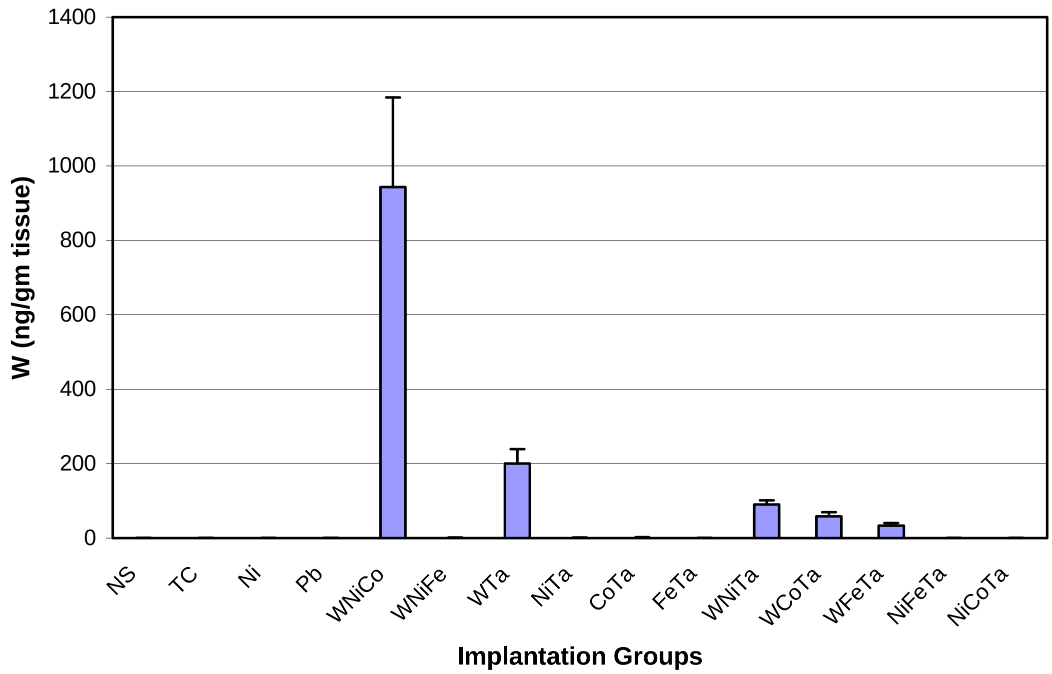

B. Spleen Nickel Levels

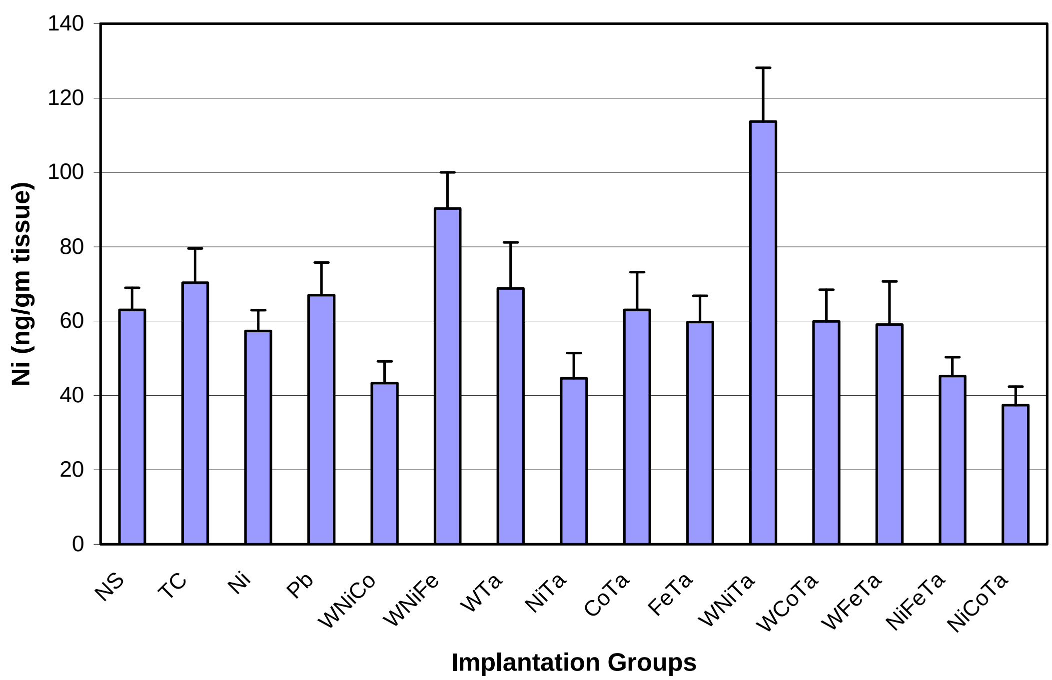

Figure 42 (continued): Spleen Metal Levels in 24-Month Implantation Groups

C. Spleen Cobalt Levels

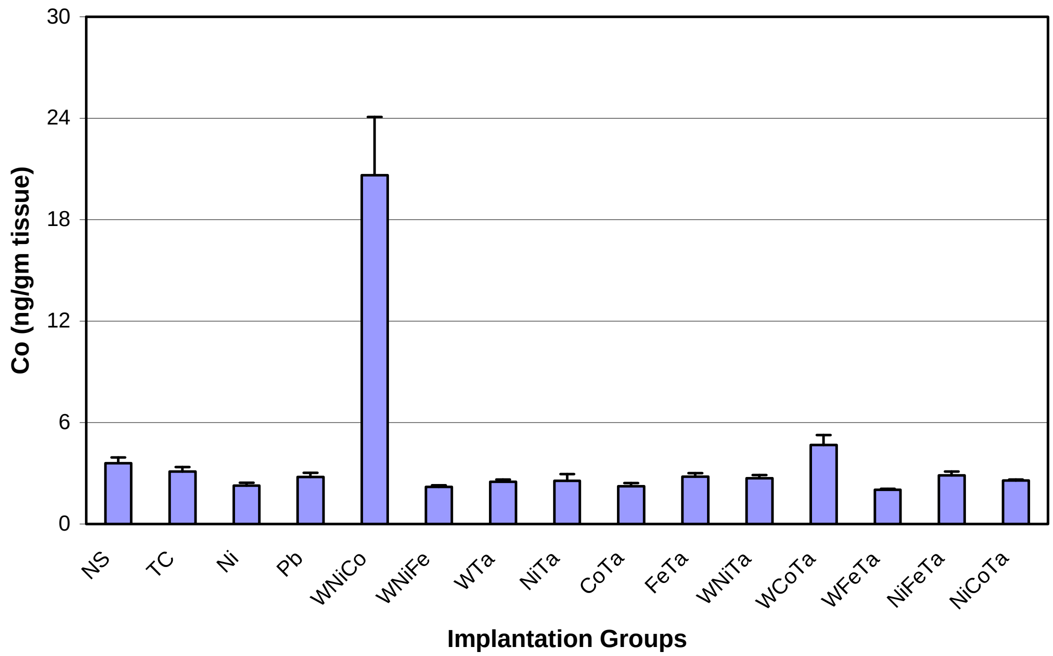

D. Spleen Tantalum Levels

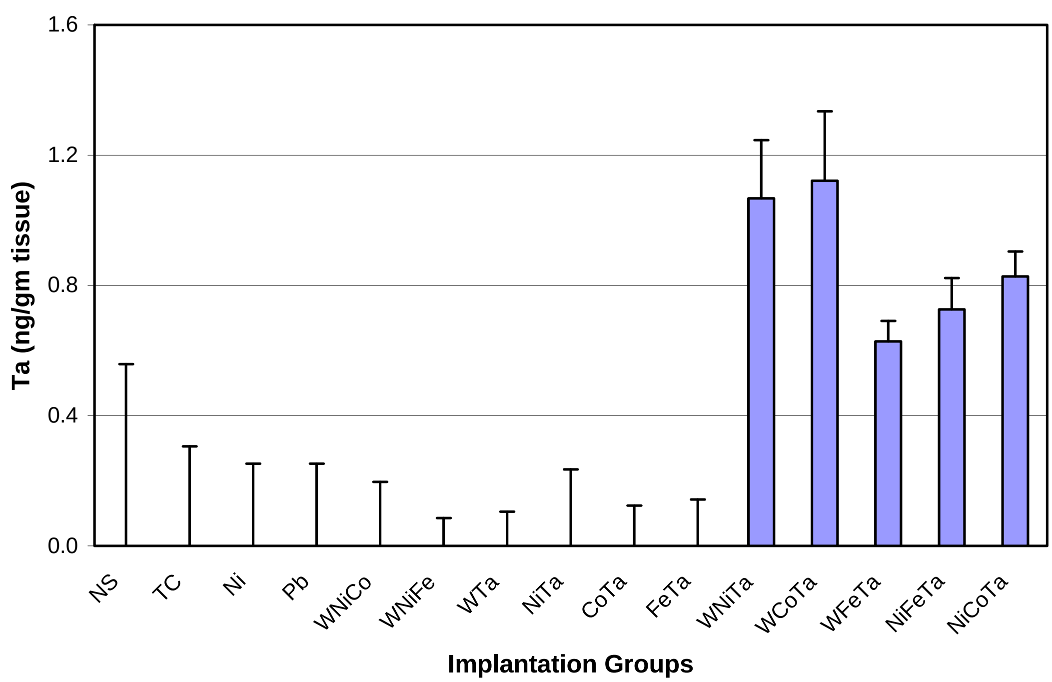

Figure 43: Testes Metal Levels in 24-Month Implantation Groups

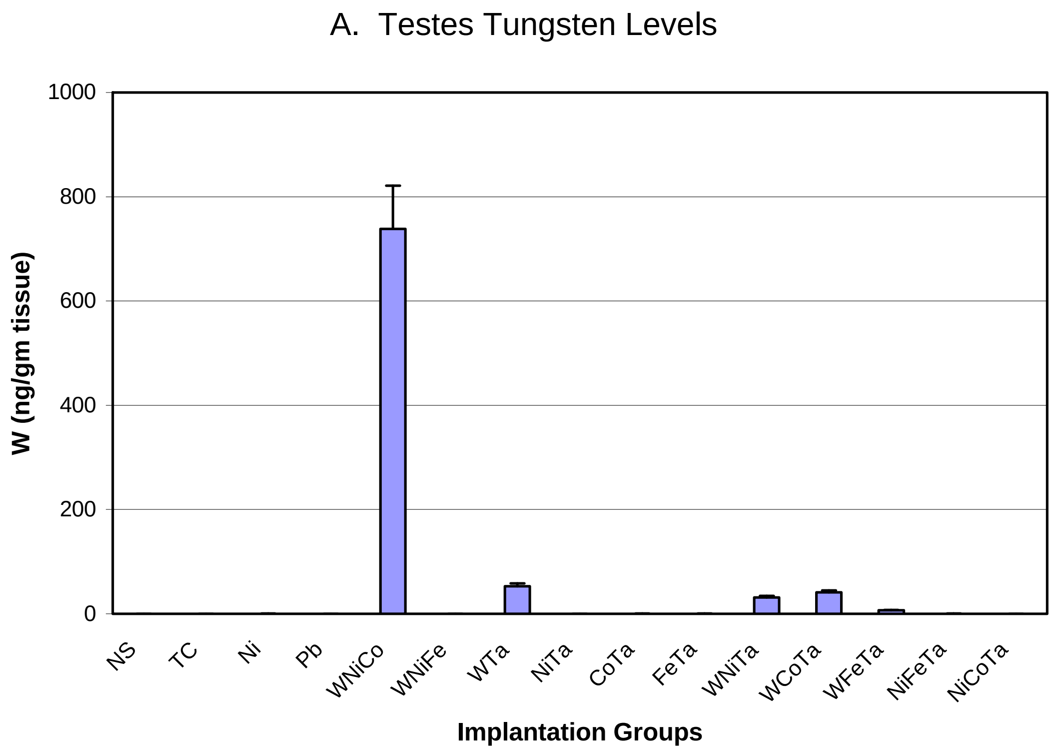

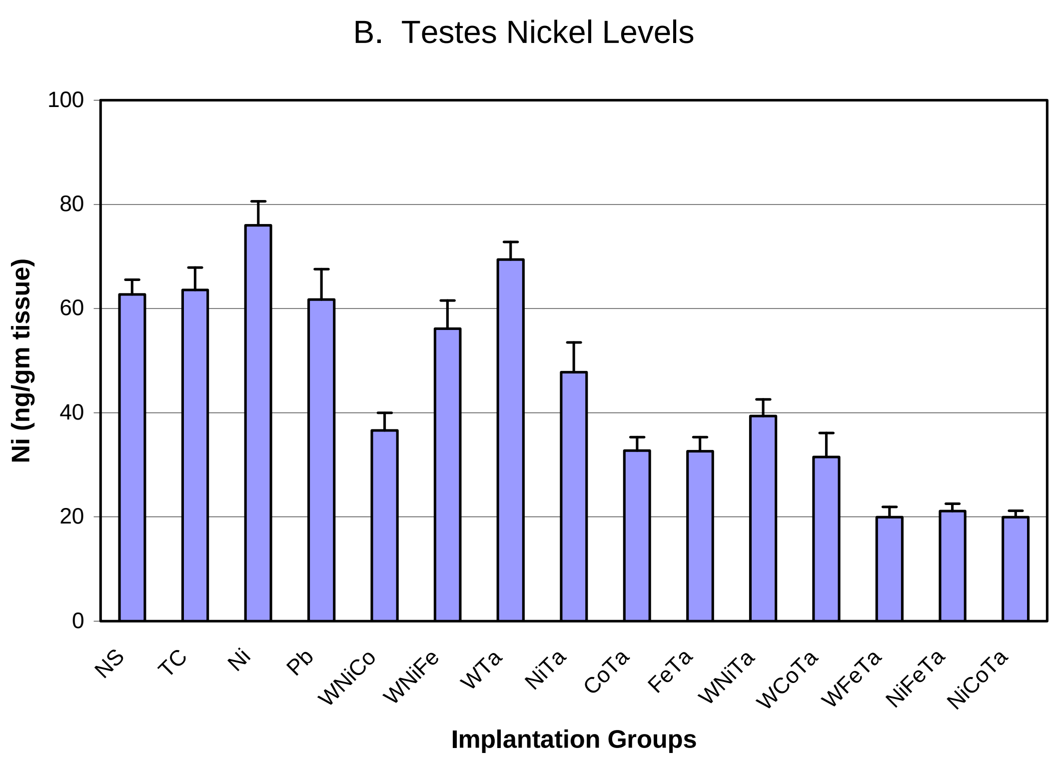

Figure 43 (continued): Testes Metal Levels in 24-Month Implantation Groups

B. Testes Cobalt Levels

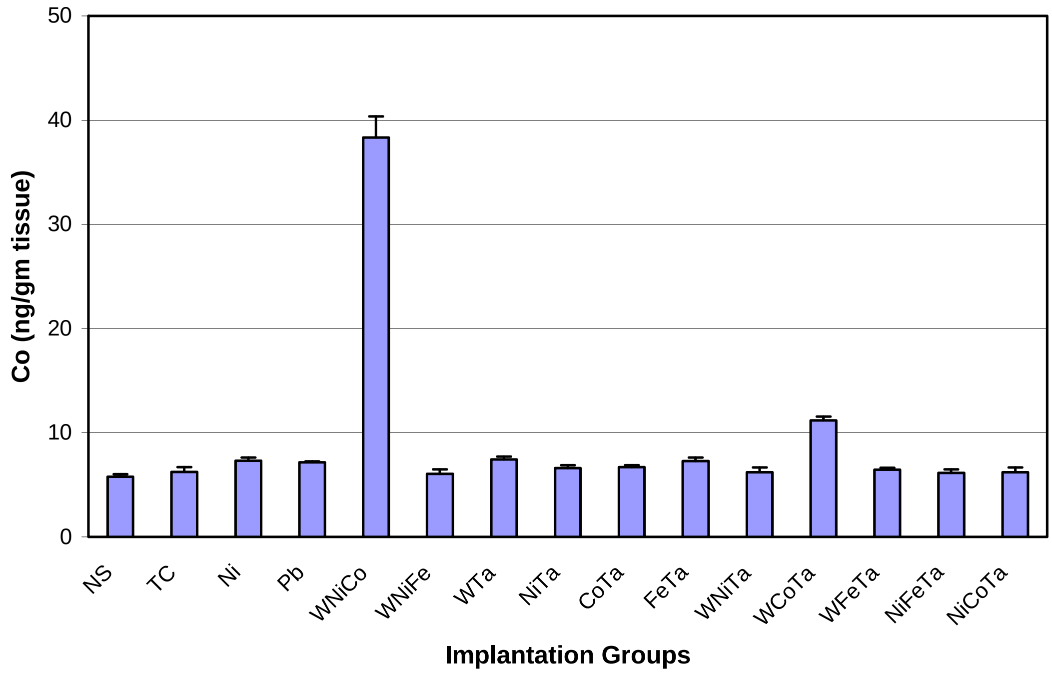

D. Testes Tantalum Levels

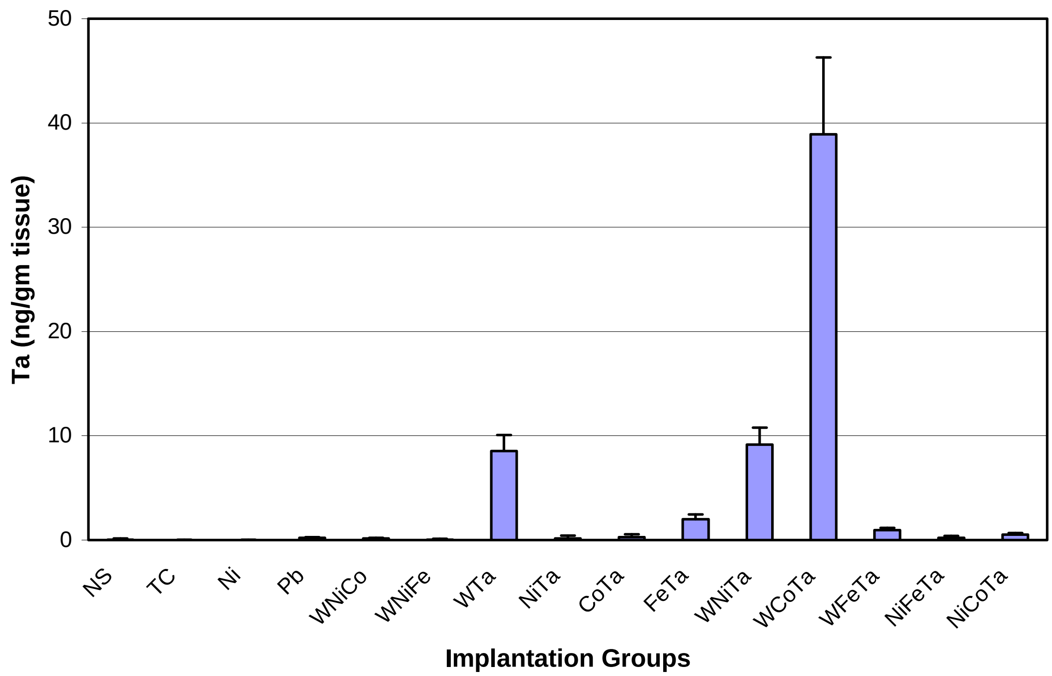

Figure 44: Urinary Metal Levels in 24-Month Implantation Groups

A. Urinary Tungsten Levels

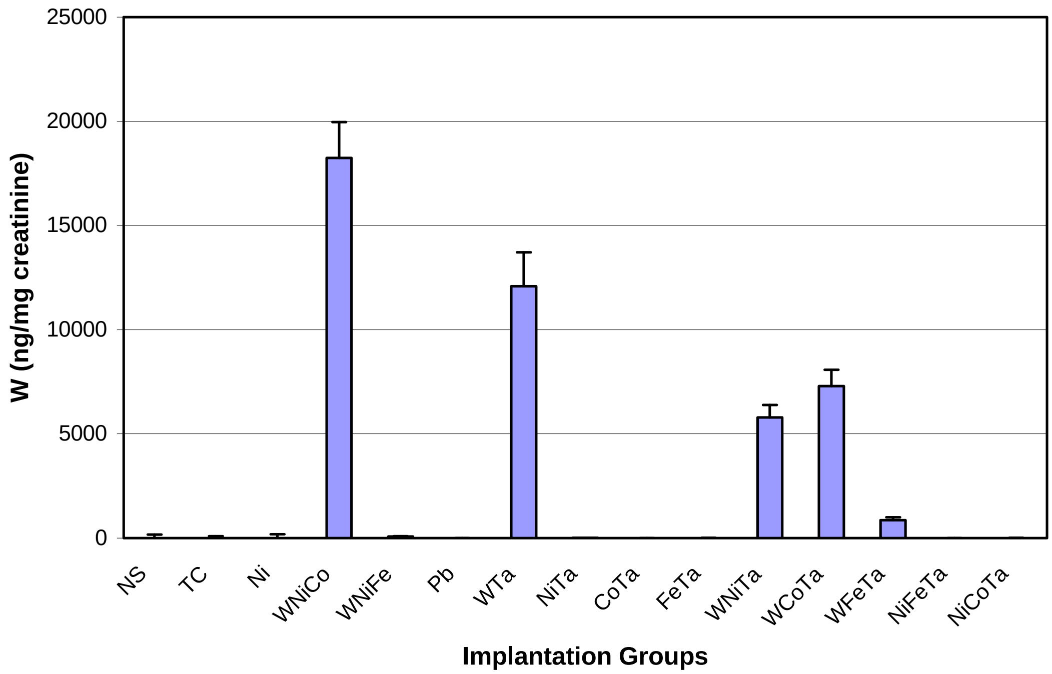

B. Urinary Nickel Levels

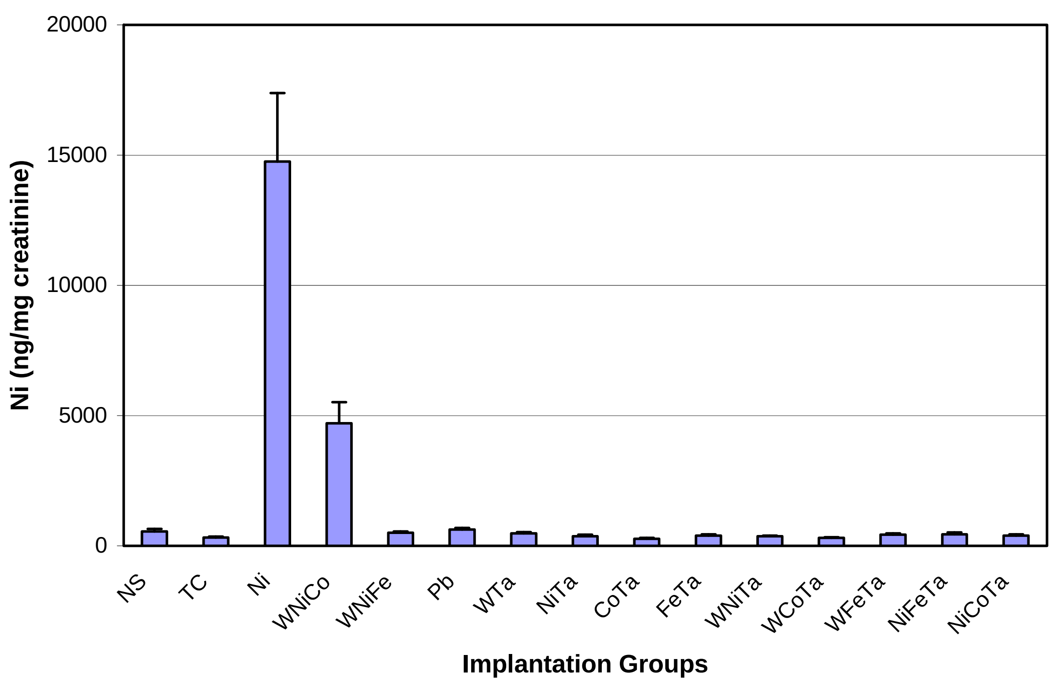

Figure 44 (continued): Urinary Metal Levels in 24-Month Implantation Groups

C. Urinary Cobalt Levels

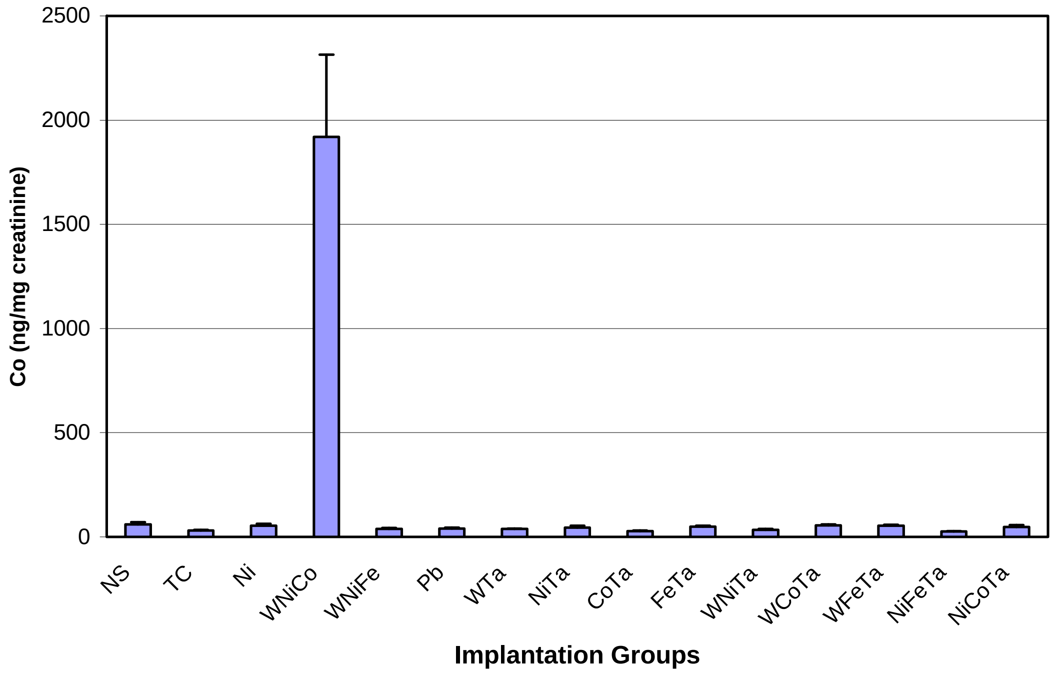

D. Urinary Tantalum Levels

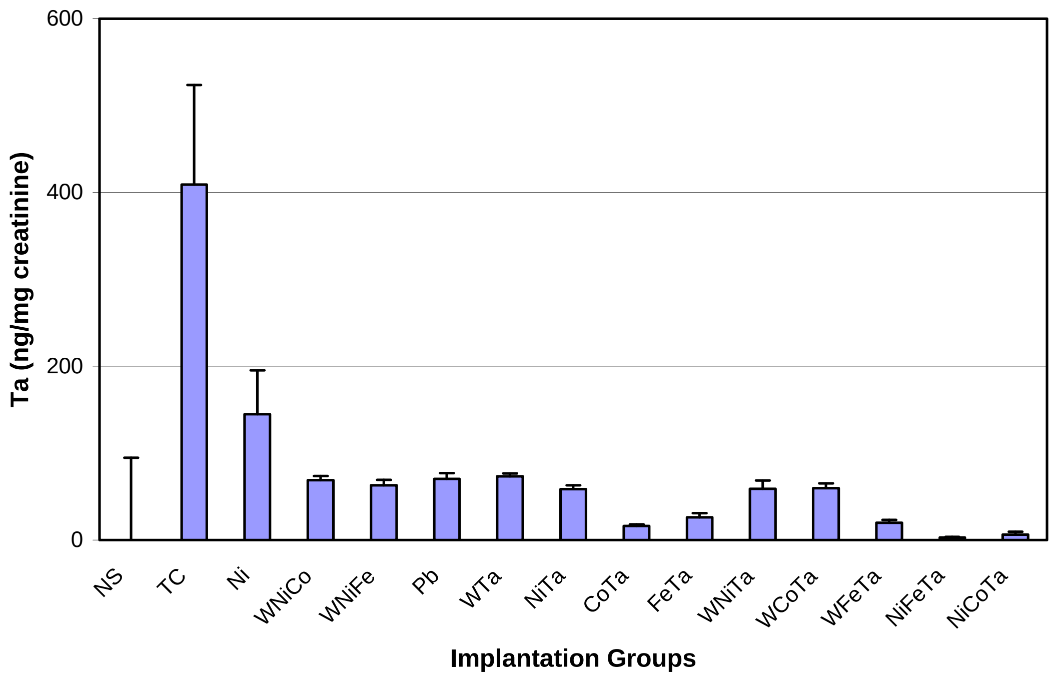

Figure 45: Metal Levels in Nickel- and WNiCo-Associated Muscle Tumors

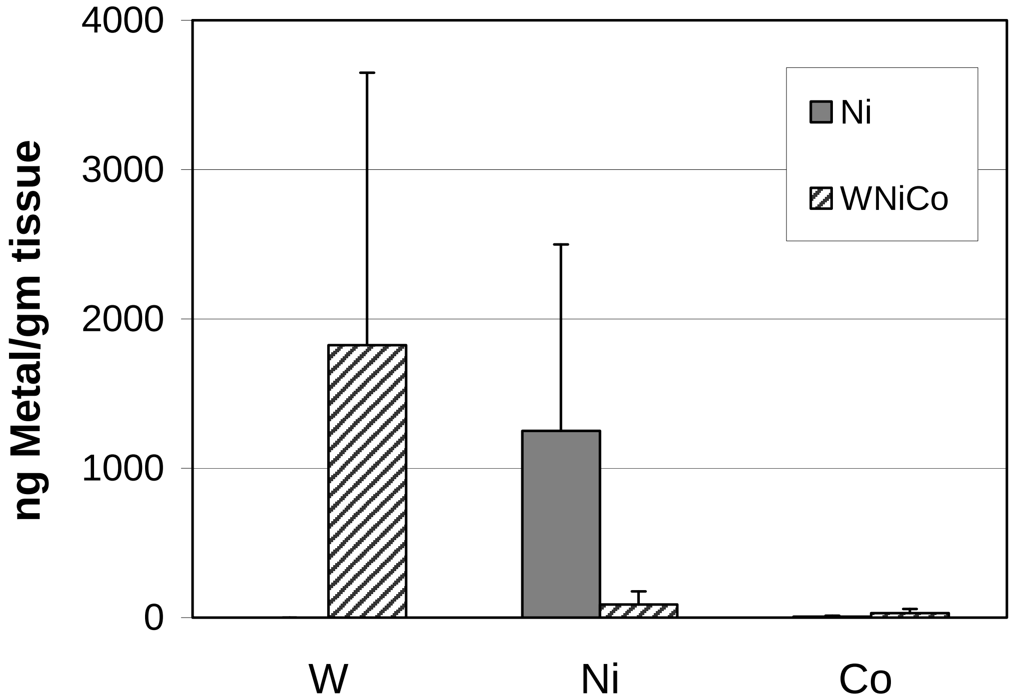

Figure 46: Hematoxylin and Eosin-Stained Quadriceps Muscle Sections from Nickel-Implanted (Panels A and B) and Tungsten/Nickel/Cobalt-Implanted (Panels C and D) Mice

A B

C D

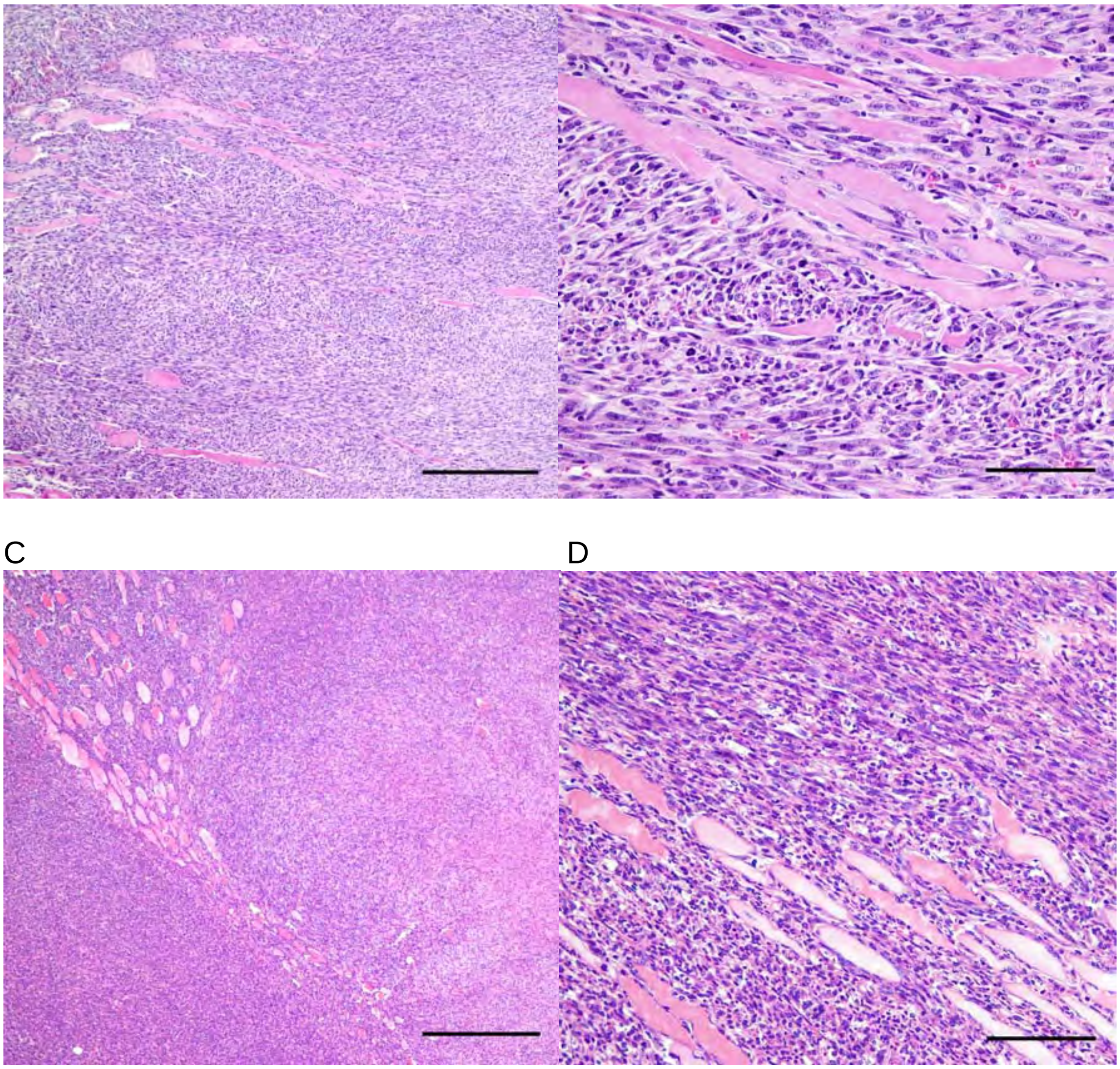

Panel A: H&E-stained quadriceps muscle section from nickel-implanted B6C3F1 mouse (68 weeks), 100X magnification.
Panel B: H&E-stained quadriceps muscle section from nickel-implanted B6C3F1 mouse (68 weeks), 400X magnification.
Panel C: H&E-stained quadriceps muscle section from tungsten/nickel/cobalt-implanted B6C3F1 mouse (66 weeks), 100X magnification.
Panel D: H&E-stained quadriceps muscle section from tungsten/nickel/cobalt-implanted B6C3F1 mouse (66 weeks), 400X magnification.

Chapter 10
Heavy Metal-Induced Carcinogenicity: Depleted Uranium and Heavy-Metal Tungsten Alloy

John F. Kalinich

Introduction

Advances in weapon design and the expanding terroristic use of Improvised Explosive Devices have opened the possibility of human exposure to metals or metal mixtures whose toxicological properties and physiological effects are not known. In this chapter, two of the more recent additions to the weapons arena, depleted uranium and heavy-metal tungsten alloy, will be discussed. The known toxicological properties of uranium and tungsten will be addressed with respect to a variety of human exposure scenarios, including inhalation, ingestion, and embedded fragments. The influence of depleted uranium and heavy-metal tungsten alloy on gene expression and signal transduction pathways leading to carcinogenicity will be considered and finally, areas requiring further research will be detailed.

Depleted Uranium (DU)

Uranium was first identified by Klaproth in 1789 and named after the planet Uranus. However, it wasn't until over 100 years later that the radioactive properties of uranium were described by Becquerel. Uranium is a naturally occurring element widely spread in the environment. It is normally found at low levels (parts per million) in soil, water, plants, and animals, including humans (ATSDR 1999). Average daily uranium intake in humans is approximately 3 µg, primarily through food and drinking water. Uranium, as found in nature, is slightly radioactive and consists predominantly of three isotopes, ^{234}U, ^{235}U, and ^{238}U (Table 10.1). Although all three isotopes are radioactive, ^{234}U and ^{235}U have a much higher specific activity than

J. F. Kalinich (✉)
Armed Forces Radiobiology Research Institute, 8901 Wisconsin Avenue, Bethesda MD 20889-5603, USA
Tel.: +1-301-295-9242
Fax: +1-301-295-1731
e-mail: kalinich@afrri.usuhs.mil

G. Bánfalvi (ed.), *Cellular Effects of Heavy Metals,*
DOI 10.1007/978-94-007-0428-2_10, © Springer Science+Business Media B.V. 2011

Table 10.1 Uranium characteristics

Chemical symbol	U
Atomic number	92
Atomic weight	238.029
Category	Actinide
Group/series/block	n.a./7/f
Melting point	1135°C
Common oxidation states	$^{+}4$, $^{+}5$, $^{+}6$
Density	18.95 gm/cm^3

^{238}U. Natural uranium consists largely of ^{238}U (99.274%) with smaller amounts of ^{234}U (0.006%) and ^{235}U (0.72%). The processing of uranium for use in nuclear reactors and nuclear weapons involves increasing the percentages of the high specific activity isotopes with respect to ^{238}U. This process is known as "enrichment" and results in the production of two different uranium fractions. The "enriched" fraction consists of approximately 97.010% ^{238}U, 0.03% ^{234}U, and 2.96% ^{235}U. The "depleted" fraction consists of approximately 99.745% ^{238}U, 0.005% ^{234}U, and 0.25% ^{235}U. Although radiologically different, both fractions remain identical chemically.

Depleted uranium has several commercial applications including shielding for radioactive material and as counterweights in aircraft and ships. However, it is because of its military applications that depleted uranium has received much of its attention. Because it is extremely dense, with a density second only to tungsten, depleted uranium is used for shielding for tanks and vehicles and as kinetic-energy armor-penetrating munitions. The use of DU munitions presents the greatest chance of human exposure. Although the toxicological hazards of uranium have been recognized for over a 100 years, many of these adverse effects were ascribed to radioactivity. Depleted uranium is approximately 40% less radioactive than natural uranium; thus, although radiation may play a role in the induction of cellular damage, the chemical properties of DU are also of paramount concern. In addition, metals such as titanium or molybdenum are often added during production of DU-containing munitions to provide specific metallurgic properties. The original uranium source from which DU was processed can also add minor contaminants to the final product. For example, DU obtained from reprocessed nuclear fuel can have small amounts of fission products and transuranics present, including strontium, cesium, plutonium, and americium. Also, the normal radioactive decay pathways of uranium can introduce additional contaminants (e.g., thorium) in the final product. Therefore, when evaluating the cellular effects of DU exposure, the presence of contaminants introduced as a result of processing, as well as those resulting from normal radioactive decay, cannot be discounted. As noted above, one of the main military uses of DU is in the production of kinetic-energy armor-penetrating munitions. The first widespread use of these munitions was in the 1991 Persian Gulf War. DU munitions were also used by NATO forces in the recent conflicts in Bosnia and Kosovo. Because of concern over the health and environmental effects of the use of DU munitions there has been a movement toward the use of alternative materials and the heavy-metal tungsten alloys are one of these.

Heavy-Metal Tungsten Alloy

Tungsten was first identified in 1758 by the Swedish chemist Cronstedt. The word tungsten is Swedish for "heavy stone" and is a tribute to its density; the highest of any naturally occurring element (Table 10.2). Tungsten is found in varying concentrations in air, water, and soil. In soil, tungsten is found as a mineral mixture, primarily as wolframite or scheelite (van der Voet et al. 2007). Weathering and dissolution of rocks and soil result in tungsten being released into the air or entering the groundwater. Environmental tungsten levels are generally very low, except in areas of tungsten mines or natural deposits (ATSDR 2005). As such, uptake levels are usually insignificant, with occupational exposure being the most likely route of tungsten internalization in humans.

Because of its density and high melting point, tungsten is used in a variety of commercial applications including light bulb filaments, counterweights, radiation shields, and thermocouples. It is also found, as tungsten carbide, in cutting blades and drill bits. Tungsten has also been used as replacement for lead in small-caliber ammunition. In 1991, the U.S. Fish and Wildlife Service banned the use of lead shot for the hunting of waterfowl and advocated the use of ammunition formulations that were not toxic when ingested by wildlife. Many of the subsequently approved ammunitions contain varying amounts of tungsten in combination with other metals such as nickel, tin, iron, copper, and bismuth. In addition, a formulation of tungsten with a polymer matrix has also been approved for use. Toxicity testing has shown no adverse health effects of these materials (Kraabel et al. 1996; Kelly et al. 1998; Mitchell et al. 2001a, b, c; Brewer et al. 2003).

Military applications of tungsten also include the use of tungsten-based composites, primarily tungsten/tin and tungsten/Nylon, as replacements for lead in small-caliber ammunition. As noted earlier, widespread public concern over the health and environmental impact of the continued use of depleted uranium has led many countries to replace depleted uranium with various tungsten alloys in their arsenals of armor-penetrating munitions. In many of these formulations, tungsten is combined with two or more of the following transition metals: nickel, cobalt, iron, and copper. Although these materials are referred to as "tungsten alloys", they are in fact two-phase composites, due to the extremely high melting point of tungsten. During manufacturing, powders of the appropriate metals are mixed and heated. Heating

Table 10.2 Tungsten characteristics

Chemical symbol	W
Atomic number	74
Atomic weight	183.85
Category	Transition Metal
Group/series/block	6/6/d
Melting point	3422°C
Common oxidation states	$^{+}6$
Density	19.25 gm/cm^3

occurs at temperatures below the melting point of tungsten, but above the melting points of the transition metals. The melted transition metals dissolve a small amount of tungsten; however, most of the tungsten powder remains intact. The result is a material consisting of pure tungsten grains surrounded by a "binder matrix" composed of tungsten and the added transition metals. In contrast, additional material added during the processing of depleted uranium results in a true alloy because of the similar melting points of the components.

Routes of Exposure

Depleted uranium and tungsten alloys can be internalized by three primary routes: inhalation, ingestion, or wound contamination via embedded fragments. Regardless of the route of exposure, several factors govern the eventual health effects induced by the internalized metals. Clearly, the amount of material internalized plays a major role in the end-result of any exposure. Equally important however are the chemical and physical properties of the metal. These properties include solubility characteristics (particularly in biological fluids), particle size, speciation, and chemical reactivity (Yokel et al. 2006). For inhalation exposures, the size of the inhaled particle as well as its solubility will determine its ultimate fate. Approximately 25% of inhaled particles are immediately exhaled (International Commission on Radiological Protection 1966). Of the remaining 75%, particles less than 5 μm in diameter can reach the alveolar space while particles greater than 10 μm tend to remain in upper areas of the lung (Morrow et al. 1967). Once deposited in the lung, the solubility of the particle is of importance. Soluble metals are rapidly dissolved and enter the circulatory system. Less soluble metals will eventually be removed through the process of phagocytosis by the alveolar macrophages. Larger inhaled particles, unable to access the alveolar space, ~~while~~ be removed from the lung via mucocilliary clearance. However, many of the particles, once cleared, will be swallowed and thus enter the gastrointestinal tract. In addition to swallowing after mucocilliary clearance, metals can be ingested through contaminated food or liquids. Once ingested, absorption of the metals will depend upon the chemical form and solubility. Both uranium and tungsten are usually poorly absorbed by the gastrointestinal tract (Leggett 1997; Leggett and Pellmar 2003). Wound contamination can occur as a result of metals entering open wounds (e.g., as dust or liquid) or as embedded fragments. As with other routes of exposure, the physicochemical properties of the metal are of prime importance when determining its fate *in vivo*. Research with intramuscularly injected metallic radionuclides has shown that even those considered insoluble can be solubilized *in vivo* (Bistline et al. 1972; Lloyd et al. 1974; Dagle et al. 1985). This fact was dramatically shown in studies investigating the health effects of embedded fragments of depleted uranium where solubilization and urinary excretion of the uranium was found within 48 h after implantation of the solid metal into the leg muscles of laboratory rodents (Pellmar et al. 1999).

Book ID: 215017_1_En Chapter ID: 10 Dispatch Date:02/12/2010 ProofNo: 1

~~Cellular Effects of Depleted Uranium~~

Regardless of the route of internalization, several different cell types could potentially be affected by exposure to metals. The epithelial cells of the gastrointestinal tract and the mesenteric lymph nodes have been shown to accumulate depleted uranium after chronic ingestion (Dublineau et al. 2006). Inhalation results in the exposure of epithelial cells and alveolar macrophages (Schins and Borm 1999; Monleau et al. 2006). As noted earlier, the alveolar macrophages play a key role in both particle clearance and retention in the lung (Tasat and De Ray 1987). Wound contamination and embedded fragments present a far more complex situation because of the wide variety of cell types and mediators involved in wound healing. Briefly, the process of wound healing can loosely be divided into three phases: inflammation, proliferation, and remodeling (Broughton and Janis 2006; Tsirogianni et al. 2006; Li et al. 2007). Immediately after a wound is suffered, platelets arrive to begin the process of clot formation to maintain hemostasis. Neutrophils and macrophages are the next cell types to arrive at the wound site and are responsible for eliminating foreign organisms and debris, including nonviable tissue. Macrophages are also capable of phagocytizing small metal particulates and can concentrate these metals in the phagolysosomal vesicles before exiting through the lymphatic system (Berry et al. 1997; Lizon and Fritsch 1999). However, the most important role of the macrophage is the secretion of numerous cell mediators that lead to the proliferation phase of wound healing. In the proliferation phase, fibroblasts migrate to the wound site to produce the extracellular matrix and granulation tissue required for proper wound healing. Maturation of the extracellular matrix occurs during the remodeling phase and, depending upon the type of wound, can take up to a year to complete. In many cases, the specific response of the macrophages to the internalized metals will determine the ultimate outcome of the exposure, including the induction of cancer (Sica et al. 2008).

In Vitro Studies

Depleted Uranium

Cell culture systems have been used for many years to model potential adverse health effects from exposure to metals. Macrophage, kidney, lung, and neuronal cell lines have all been utilized to assess metal toxicity, as well as genomic and proteomic changes occurring as a result of exposure. Treatment of Chinese hamster ovary cells with depleted uranium resulted in decreased cell viability and increased chromosomal aberrations (Lin et al. 1993). Cellular damage, evidenced by an increase in the release of lactate dehydrogenase, was observed in LLC-PK1 kidney cells after uranium treatment (Furuya et al. 1997; Mirto et al. 1999). Several studies have also shown that the mouse macrophage cell line, J774, is capable of internaliz-

ing extracellular depleted uranium (Kalinich and McClain 2001). Once internalized, the DU can induce cell death, via apoptosis, in a concentration-dependent manner (Kalinich et al. 2002). Not all cultured cell lines appear capable of internalizing DU. When assessed colorimetrically using the method of Kalinich and McClain (2001), Molt-4, a human T-cell leukemia line, and ~~REH~~, a human B-cell lymphoma line, did not appear to internalize DU added to the extracellular medium. In addition, these cell lines were far less susceptible to the cytotoxic effects of DU exposure, showing no significant change in viability compared to untreated cells (Fig. 10.1).

Peritoneal macrophages and splenic T-cells isolated from mice then exposed to varying concentrations of DU also demonstrated that macrophages are much more sensitive to the cytotoxic effects DU than other immune system cells (Wan et al. 2006). Treatment of cultured human osteoblast cells with either soluble or insoluble forms of DU transformed the cells to neoplastic phenotype. These transformed cells also formed tumors when injected into immunocompromised mice (Miller et al. 1998; McClain and Miller 2007). As noted earlier, although DU is 40% less radioactive than natural uranium, it is still radioactive and that characteristic also has the potential to induce significant cellular damage. The question of whether the chemical or radiological property is primarily responsible for the cellular damage inflicted by DU is still open to debate. At present, it appears that the chemical characteristics

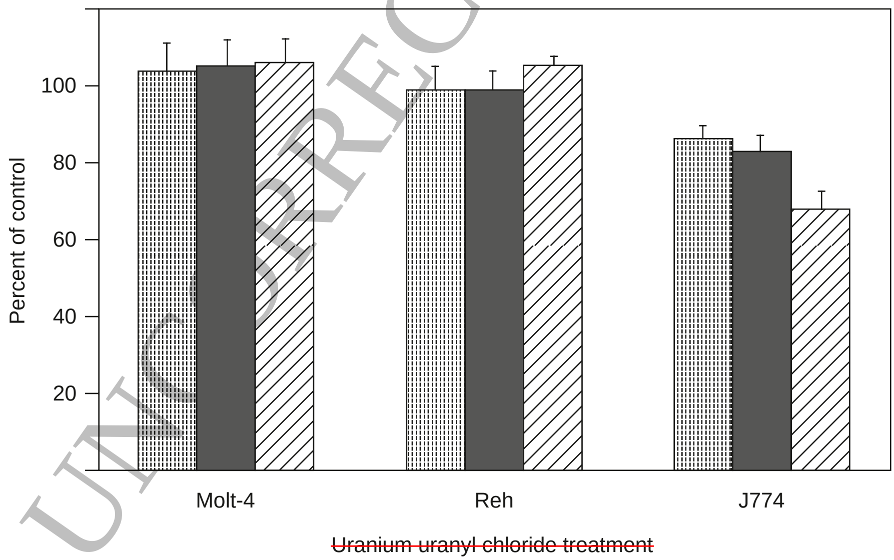

Fig. 10.1 Cell viability assessment of Molt-4, Reh, and J774 cells treated with depleted uranium-uranyl chloride for 24 h at 37°C. Viability was determined using the MTT assay and data normalized to values from untreated cells and ~~is~~ the mean of 6 independent experiments. *Error bars* represent standard error of the mean. The *stippled bars* represent a uranium concentration of 1 µg/ml, the *gray bars* represent a uranium concentration of 10 µg/ml, and the *slanted-line bars* represent a uranium concentration of 100 µg/ml

Book ID: 215017_1_En Chapter ID: 10 Dispatch Date:02/12/2010 ProofNo: 1

of DU are predominantly responsible for the observed cellular damage, with the radiological component playing a smaller role (Miller et al. 2002a, b, 2003).

Along with inducing genotoxic effects *in vitro*, low-level DU exposure can also alter gene expression patterns in many cell types. In NR8383 cells, a rat alveolar macrophage cell line, DU has been shown to induce secretion of tumor necrosis factor α (TNF-α), as well as activate the c-Jun N-terminal kinase (JNK) and p38 mitogen-activated protein kinase (p38 MAPK) pathways (Gazin et al. 2004). This work suggests that macrophages exposed to uranium, either through inhalation or wound contamination, can secrete elevated amounts of TNFα, a major proinflammatory cytokine. Because of the central role TNFα plays in regulating the release of secondary inflammation mediators (Cromwell et al. 1992), any perturbation can have far reaching consequences for the organism. DU can also induce a number of stress-related genes in HepG2 cells, a human liver carcinoma cell line. In this assay, HepG2 cells, stably transfected with chloramphenicol acetyltransferase under the transcriptional control of a variety of stress-gene regulatory sequences, were treated with insoluble DU (Miller et al. 2004). Several categories of promoters were affected in a dose-dependent manner including transcription factor binding sites (FOS, NFκBRE, CRE, p53RE, and RARE), cell cycle regulation sites (GADD45, GADD153), transport proteins (GRP78, HSP70), and the promoter for metallothionein IIA (HMTIIA). These data indicate that DU can activate gene expression through a variety of signal transduction pathways, including many that are involved in the carcinogenic process. Using microarray technology, Prat and colleagues (Prat et al. 2005), demonstrated that exposure of cultured HEK292 cells, a human embryonic kidney cell line, to DU resulted in both up- and down-regulation of numerous genes including many involved in signal transduction and trafficking pathways. Microarray technology was also used to assess the effect of DU exposure on gene expression patterns in mouse peritoneal macrophages and $CD4^+$ T cells (Wan et al. 2006). Again, DU was shown to alter gene expression profiles with genes responsible for signal transduction pathways, chemokines, and interleukins affected the greatest. As a result of these findings, Wan et al. (2006) postulated the potential for cancer development as a consequence of DU exposure.

Heavy-Metal Tungsten Alloy

There have been far fewer studies on the toxicological and genotoxic properties of the heavy-metal tungsten alloys. There are several reports investigating the toxicity of tungsten alone. The cytotoxicity of degrading tungsten coils used medically for vascular occlusions was assessed in cultured human smooth muscle, endothelial, vascular, and fibroblast cells. Cytotoxicity was observed only at tungsten concentrations above 50 µg/ml (Peuster et al. 2003). *In vitro* studies with J774, Molt-4, and Reh cells have shown that, unlike DU, exposure to a heavy-metal tungsten alloy composed of tungsten (92%), nickel (5%), and cobalt (3%) resulted in decreased viability of all three cell lines in a concentration-dependent manner (Fig. 10.2). The

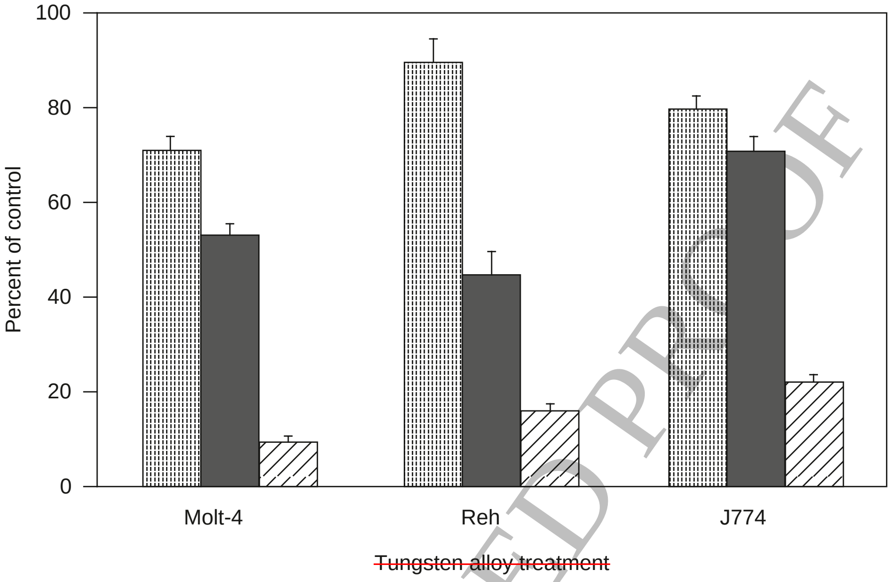

Fig. 10.2 Cell viability assessment of Molt-4, Reh, and J774 cells treated with heavy-metal tungsten alloy (91% tungsten, 6% nickel, 3% cobalt) for 24 h at 37°C. Viability was determined using the MTT assay and data normalized to values from untreated cells and ~~is~~ the mean of 6 independent experiments. *Error bars* represent standard error of the mean. The *stippled bars* represent an alloy concentration of 1 µg/ml, the *gray bars* represent an alloy concentration of 10 µg/ml, and the *slanted-line bars* represent an alloy concentration of 100 µg/ml

same tungsten alloy mixture, as well as one composed of tungsten (92%), nickel (5%), and iron (3%), was found to transform cultured human osteoblast (HOS) cells to a neoplastic phenotype (Miller et al. 2001). The individual metals comprising the alloys were also able to transform the HOS cells, but at a frequency far lower than the mixtures. In fact, when the transformation frequency data from the individual metals are compared with those of the alloys, it appears that there is synergistic effect between two or more of the metals, leading to increased transformation (Miller et al. 2002c). While both tungsten alloys (WNiCo and WNiFe) and all individual component metals could transform HOS cells, only those cells transformed by the tungsten alloys developed tumors when injected into immunocompromised mice (Miller et al. 2001). The tungsten/nickel/cobalt alloy was also capable of inducing the expression of several genes when assayed using chloramphenicol acetyltransferase-transfected HepG2 cells (Miller et al. 2004). As with DU, tungsten alloy had the ability to induce gene promoters in several categories including transcription factor binding sites (FOS, NFκBRE, CRE, and p53RE), transport proteins (HSP70), and the promoter for metallothionein IIA (HMTIIA). Surprisingly, tungsten alloy exposure had no effect on either of the cell cycle regulation promoters tested (GADD45, GADD153) in contrast to DU. When tested individually, the metals comprising the alloy were also able to induce the promoters affected by the alloy, but did so at a much lower level. Again, a synergistic effect of the metals in the alloy on gene induction was observed (Miller et al. 2004).

In Vivo Studies

Depleted Uranium

During the Persian Gulf War of 1991, several individuals suffered wounds containing embedded DU fragments. Concern, both chemical and radiological, over the long-term health effects of this unique material led to several studies investigating the toxicological and carcinogenic properties of embedded DU fragments. Development and validation of a rodent model system to study the biological effects of embedded fragments was undertaken at the Armed Forces Radiobiology Research Institute (Castro et al. 1996). This model system involves surgically implanting small pellets of test material into the leg muscles to mimic shrapnel wounds. An x-ray of the location of several 1×2 mm cylindrical pellets is shown in Fig. 10.3. Sprague Dawley rats, implanted with up to 20 DU pellets (1×2 mm cylinders) for periods up to 2 years, exhibited no overt adverse health effects. No tumors were observed at the pellet implantation sites for either DU or tantalum, an inert negative control metal (Pellmar et al. 1999).

The DU pellets degrade rapidly *in vivo*, with significant uranium levels measured in the urine as early as 2 days post-implantation. Some of the DU pellet material is not immediately solubilized and can be found at the pellet implantation site upon histopathological examination (Fig. 10.4). Over time, as more of the pellet degrades, DU can be found in a variety of tissues including kidney, liver, brain, testes, and lymph nodes (Pellmar et al. 1999). Similar results were reported by Hahn and colleagues using Wistar rats (Hahn et al. 2002). When DU was implanted as 1×2 mm cylindrical pellets, no tumors were observed. However, when embedded as squares (2.5×2.5×1.5 mm or 5×5×1.5 mm), DU induced soft-tissue sarcomas at the implantation sites. Rats implanted with tantalum did not develop tumors indi-

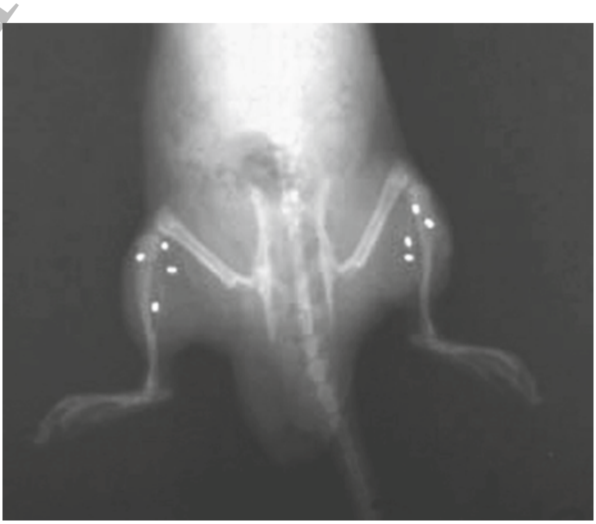

Fig. 10.3 Radiograph of rat showing location of depleted uranium pellets (1×2 mm cylinders) surgically implanted in the gastrocnemius muscles of the rear legs

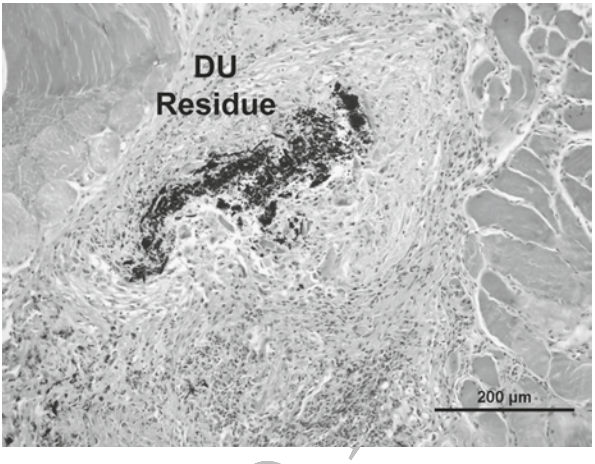

Fig. 10.4 Histopathological examination of a hematoxylin-and-eosin-stained section of leg muscle from a F344 rat implanted with depleted uranium pellets for 3 months. DU residue is visible at pellet implantation site. Scale bar = 200 µm

cating that the observed DU effects were not the result of foreign-body carcinogenesis (Brand et al. 1975, 1976). As with the Pellmar study, the DU material began to degrade shortly after implantation. Taken together these studies indicate that once a certain mass is reached, DU fragments are capable of inducing neoplastic changes resulting in soft-tissue sarcomas in laboratory rats.

Embedded DU fragments also induced gene changes in the muscle tissue surrounding the metal. Using Northern blot analysis, Miller et al. (2000) demonstrated elevated mRNA levels of p53, k-ras, and bcl-2 in muscle tissue adjacent to embedded DU pellets. Utilizing immunohistochemical techniques, Hahn (2007) showed increased p53 protein levels in tissue surrounding the implanted DU. However, MDM2, c-myc, and p21 levels were found to be no different than control.

Heavy-Metal Tungsten Alloy

Thus far only one study has been published in the peer-reviewed literature describing the health effects of embedded tungsten alloy. F344 rats implanted with a tungsten alloy comprised of tungsten (91.1%), nickel (6.0%), and cobalt (2.9%) developed highly aggressive rhabdomyosarcomas at the pellet implantation sites (Kalinich et al. 2005). The tumors grew rapidly and metastasized to the lungs requiring euthanasia of the animals. Tumor incidence was 100%. Rats implanted with nickel, a known carcinogen, also developed tumors, but did so at a slower rate than those rats treated with the tungsten alloy. Rats implanted with tantalum did not develop tumors. As with DU, the metals comprising the tungsten alloy rapidly solubilized and were found in the urine at an order of magnitude higher than control values (Kalinich et al. 2008). However, in contrast to DU, no particulate material was observed at the pellet implantation site upon histopathological examination (Fig. 10.5). Significant hematological changes were observed as early as 1 month after implantation; well before any neoplastic changes had occurred. Whether these

Fig. 10.5 Histopathological examination of a Gomori trichrome-stained section of leg muscle and tumor from a F344 rat implanted with heavy-metal tungsten alloy pellets (91.1% tungsten, 6% nickel, 2.9% cobalt) for 6 months. "P" indicates site of pellet implantation. "T" denotes the tungsten alloy-induced tumor (rhabdomyosarcoma). "MF" shows area of normal muscle fibers. Scale bar = 1.0 mm

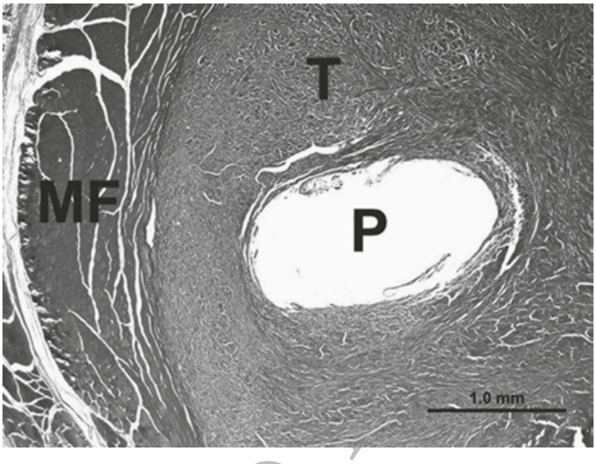

changes are attributable to an individual metal in the alloy or a synergistic effect between two or more components is not yet known.

Human Exposures

Depleted Uranium

As noted above, the first widespread use of DU was in the 1991 Persian Gulf War. During this conflict several individuals were wounded with DU fragments. United States military personnel with retained DU fragments have been followed clinically by the Veterans Affairs Medical Center in Baltimore, Maryland. After 16 years of follow-up surveillance, there has been no indication of any clinically significant DU-related health effects (McDiarmid et al. 2000, 2001, 2004, 2006, 2007a, b, 2009; Dorsey et al. 2009). However, there is some indication of a weak genotoxic effect as a result of the embedded DU fragments. This was determined by fluorescent in-situ hybridization (FISH) analysis of the hypoxanthine-guanine phosphoribosyl transferase (HPRT) locus in peripheral blood lymphocytes (McDiarmid et al. 2007a, b). As a result of these findings, the authors have recommended continued surveillance of these individuals.

Heavy-Metal Tungsten Alloy

A variety of tungsten-based munitions have been proposed as replacements for DU in armor-penetrating shells and for lead in small-caliber ammunition. As yet, there have been no reports on whether there are individuals with retained fragments of these materials and, further, that these fragments are resulting in adverse health ef-

fects. There are several reports in the literature describing adverse health effects due to exposure to tungsten and tungsten-based materials. As part of an initiation rite, a French artillery soldier drank 250 ml of a beer and wine mixture that had been used to rinse a gun barrel. Shortly after, he suffered seizures and was comatose for 24 h (Marquet et al. 1996). Extremely high levels of tungsten were found in his blood and urine and persisted for 2 weeks (Marquet et al. 1997). Although his malady was blamed on tungsten intoxication, there are some who believe the organic residue left in the gun barrel as a result of the explosive charge of the shell was actually to blame for his condition (Lison et al. 1997). There have also been two reports in the literature of granuloma formation as a result of embedded metal from a lawn mower blade (Saruwatari et al. 2009) and a chain saw blade (Osawa et al. 2006), respectively. In both cases, metal analysis of the excised fragment showed that it was composed primarily of tungsten with smaller amounts of other metals.

Conclusions

Little is known about metal-induced gene expression changes and carcinogenicity especially with respect to militarily-relevant metals. Improvement in weapons design and the terroristic use of Improvised Explosive Devices will continue to increase the possibility of embedded fragment injuries with metals or metal mixtures whose toxicological properties are not fully understood. The metals discussed in this chapter, depleted uranium and heavy-metal tungsten alloy, are only two such examples. In this final section, areas requiring additional research in order to enhance our understanding of heavy metal carcinogenicity will be discussed.

Although *in vivo* exposure scenarios may differ, the common factor in most is the presence of the macrophage. Macrophages are not only capable of phagocytizing small metal particulates (Berry et al. 1997; Lizon and Fritsch 1999), but have also been shown to interact with and modify the surface composition of metal alloys through the production of reactive chemical species (Thomsen and Gretzer 2001; Lin and Bumgardner 2004). The critical role the macrophage plays in wound repair, as well as its postulated regulatory link between inflammation and cancer induction (Sica et al. 2008), makes this cell type key in understanding heavy metal-induced carcinogenicity.

In vitro studies have demonstrated that macrophage viability is affected by both DU and heavy-metal tungsten alloy. In addition, gene expression patterns are perturbed by both treatments. No consensus has been reached on an exact list of specific up- and down-regulated genes by metal exposure primarily due to experimental design differences between the published studies. However, there is a pattern of upregulation of those genes involved in transcription regulation and signal transduction, as well as those coding for the interleukins and transport proteins. Areas that require further research include an investigation of gene induction by insoluble as well as soluble metals and alloys. As seen with DU, even though a fragment begins to rapidly degrade once implanted (as determined by urine uranium levels), sub-

stantial particulate material is still found at the implantation site. As yet unknown is whether exposure to the insoluble DU will result in a similar pattern of gene induction as for the soluble material. Exposure to heavy-metal tungsten alloy raises similar concerns and may be more difficult to decipher because of the number of metals comprising the alloy and their proposed synergism with respect to biological effects (Miller et al. 2004). Again, a detailed investigation of the alloy, as well as the individual metal components, in both soluble and insoluble forms will greatly enhance our knowledge of metal-induced gene expression.

Although *in vitro* studies will provide a foundation for our understanding of heavy metal-induced carcinogenicity, *in vivo* models will be necessary to definitively determine if embedded fragments of these materials have the potential to cause cancer. In addition, recent advances in laser microdissection and microarray techniques will be crucial in elucidating metal-induced gene-expression changes in the tissue immediately adjacent to the embedded fragment. Not only will this information allow correlation of *in vitro* and *in vivo* findings, but it will be critical if changes in treatment strategies, either surgically or pharmacologically, are required in order to maintain the health and well-being of wounded individuals.

Acknowledgements The views expressed here are strictly those of the author and not those of the Armed Forces Radiobiology Research Institute, the Uniformed Services University, or the United States Department of Defense. Mention of any commercial reagents or devices does not constitute endorsement by the United States Government. Dr. Kalinich has been supported in part by grants from the U.S. Army Medical Research and Materiel Command (Award #: DAMD17–01-1–0821) and the U.S. Army Peer-Reviewed Medical Research Program (Award #: W81XWH-06–2-0025). The author would like to thank Dr Steven Mog, DVM for obtaining histopathological images.

References

ATSDR (Agency for Toxic Substances and Disease Registry), Public Health Service, U.S. Department of Health and Human Services (1999) Toxicological profile for uranium

ATSDR (Agency for Toxic Substances and Disease Registry), Public Health Service, U.S. Department of Health and Human Services (2005) Toxicological profile for tungsten~~.~~

Berry JP, Zhang L, Galle P, Ansoborlo E, Henge-Napoli MH, Donnadieu-Claraz M (1997) Role of the alveolar macrophage lysosomes in metal detoxification. Microsc Res Tech 36:313–323

Bistline RW, Watters RL, Lebel JL (1972) A study of translocation dynamics of plutonium and americium from simulated puncture wounds in beagle dogs. Health Phys 22:829–831

Brand KG, Buoen LC, Johnson KH, Brand T (1975) Etiological factors, stages, and the role of the foreign body in foreign-body tumorigenesis: a review. Cancer Res 35:279–286

Brand KG, Johnson KH, Buoen LC (1976) Foreign body tumorigenesis CRC Crit Rev Toxicol 4:353–394

Brewer L, Fairbrother A, Clark J, Amick D (2003) Acute toxicity of lead, steel, and an iron-tungsten-nickel shot to mallard ducks (Anas platyrhynchos). J Wild Dis 39:638–648

Broughton G, Janis JE (2006) The basic science of wound healing. Plast Reconstr Surg 117 (Suppl):12S–34S

Castro CA, Benson KA, Bogo V, Daxon EG, Hogan JB, Jacocks HM, Landauer MR, McBride SA, Shehata CW (1996) Establishment of an animal model to evaluate the biological effects of intramuscularly embedded depleted uranium fragments Armed Forces Radiobiology Research Institute. Bethesda, MD, Technical Report 96-3

Cromwell O, Hamid Q, Corrigan CJ, Barkans J, Meng Q, Collins PD, Kay AB (1992) Expression and generation of interleukin-8, IL-6 and granulocyte-macrophage colony-stimulating factor by bronchial epithelial cells and enhancement by IL-1 beta and tumor necrosis factor. Immunology 77:330–337

Dagle GE, Lebel JL, Phemister RD, Watters RL, Gomez LS (1985) Translocation kinetics of plutonium oxide from the popliteal lymph nodes of beagles. Health Phys 28:395–398

Dorsey CD, Engelhardt SM, Squibb KS, McDiarmid MA (2009) Biological monitoring for depleted uranium exposure in US veterans. Environ Health Perspect 117:953–956

Dublineau I, Grison S, Grandcolas L, Baudelin C, Tessier C, Suhard D, Frelon S, Cossonnet C, Claraz M, Ritt J, Paquet P, Voisin P, Gourmelon P (2006) Absorption, accumulation and biological effects of depleted uranium in Peyer's patches of rats. Toxicology 227:227–239

Furuya R, Kumagai H, Hishida A (1997) Acquired resistence to rechallenge injury with uranyl acetate in LLC-PK1 cells. J Lab Clin Med 129:347–355

Gazin V, Kerdine S, Grillon G, Pallardy M, Raoul H (2004) Uranium induces TNFα secretion and MAPK activation in a rat alveolar macrophage cell line. Toxicol Appl Pharmacol 194:49–59

Hahn FF (2007) Carcinogenesis of depleted uranium: studies in animals. In: Miller AC (ed) Depleted uranium: properties, uses, and health consequences. CRC Press, Boca Raton, FL

Hahn FF, Guilmette RA, Hoover MD (2002) Implanted depleted uranium fragments cause soft tissue sarcomas in the muscles of rats. Environ Health Perspect 110:51–59

International Commission on Radiological Protection (1966) Deposition and retention models for internal dosimetry of the human respiratory tract. Task group on lung dynamics. Health Phys 12:173–207

Kalinich JF, McClain DE (2001) Staining of intracellular deposits of uranium in cultured murine macrophages Biotech Histochem 76:247–252

Kalinich JF, Ramakrishnan N, Villa V, McClain DE (2002) Depleted uranium-uranyl chloride induces apoptosis in mouse J774 macrophages. Toxicology 179:105–114

Kalinich JF, Emond CA, Dalton TK, Mog SR, Coleman GD, Kordell JE, Miller AC, McClain DE (2005) Embedded weapons-grade tungsten alloy shrapnel rapidly induces metastatic high-grade rhabdomyosarcomas in F344 rats. Environ Health Perspect 113:729–734

Kalinich JF, Vergara VB, Emond CA (2008) Urinary and serum metal levels as indicators of embedded tungsten alloy fragments. Mil Med 173:754–758

Kelly ME, Fitzgerald SD, Aulerich RJ, Balander RJ, Powell DC, Stickle RL, Stevens W, Cray C, Tempelman RJ, Bursian SJ (1998) Acute effects of lead, steel, tungsten-iron, and tungsten-polymer shot administered to game-farm mallards J Wild Dis 34:673–687

Kraabel BJ, Miller MW, Getzy DM, Ringelman JK (1996) Effects of embedded tungsten-bismuth-tin shot and steel shot on mallards (Anas platyrhynchos). J Wild Dis 32:1–8

Leggett RW (1997) A model of the distribution and retention of tungsten in the human body. Sci Total Environ 206:147–165

Leggett RW, Pellmar TC (2003) The biokinetics of uranium migrating from embedded DU fragments. J Environ Radioact 64:205–225

Li J, Chen J, Kirsner R (2007) Pathophysiology of acute wound healing. Clin Dermatol 25:9–18

Lin H-Y, Bumgardner JD (2004) Changes in the surface oxide composition of Co-Cr-Mo implant alloy by macrophage cells and their released reactive chemical species Biomaterials 25:1233–1238

Lin RH, Wu LJ, Lee CH, Lin-Shiau SY (1993) Cytogenetic toxicity of uranyl nitrate in Chinese hamster ovary cells. Mut Res 319:197–203

Lison D, Buchet JP, Hoet P (1997) Toxicity of tungsten. Lancet 349:58–59

Lizon C, Fritsch P (1999) Chemical toxicity of some actinides and lanthanides toward alveolar macrophages: an *in vitro* study. Int J Radiat Biol 75:1459–1471

Lloyd RD, Atherton DR, Mays CW, McFarland SS, Williams JL (1974) The early excretion, retention and distribution of injected curium citrate in beagles. Health Phys 27:61–67

Marquet P, Francois B, Vignon P, Lachatre G (1996) A soldier who had seizures after drinking quarter of a litre of wine. Lancet 348:1070

Marquet P, Francois B, Lotfi H, Turcant A, Debord J, Nedelec G, Lachatre G (1997) Tungsten determination in biological fluids, hair and nails by plama emission spectrometry in a case of severe acute toxication in man. J Forensic Sci 42:527–530

McClain DE, Miller AC (2007) Depleted uranium biological effects: introduction and early *in vitro* and *in vivo* studies. In: Miller AC (ed) Depleted uranium: properties, uses, and health consequences. CRC Press, Boca Raton

McDiarmid MA, Keogh JP, Hooper FJ, McPhaul K, Squibb K, Kane R, DiPino R, Kabat M, Kaup B, Anderson L, Hoover D, Brown L, Hamilton M, Jacobson-Kram D, Burrows B, Walsh M (2000) Health effects of depleted uranium on exposed Gulf War veterans. Environ Res 82:168–180

McDiarmid MA, Squibb K, Engelhardt S, Oliver M, Gucer P, Wilson PD, Kane R, Kabat M, Kaup B, Anderson L, Hoover D, Brown L, Jacobson-Kram D (2001) Surveillance of depleted uranium exposed Gulf War veterans: health effects observed in an enlarged "friendly fire" cohort. J Occup Environ Med 43:991–1000

McDiarmid MA, Engelhardt S, Oliver M, Gucer P, Wilson PD, Kane R, Kabat M, Kaup B, Anderson L, Hoover D, Brown L, Handwerger B, Albertini R, Jacobson-Kram D, Thorne CD, Squibb KS (2004) Health effects of depleted uranium on exposed Gulf War veterans: a ten-year follow-up. J Toxicol Environ Health—Part A—Curr Issues 67:277–296

McDiarmid MA, Engelhardt SM, Oliver M, Gucer P, Wilson PD, Kane R, Kabat M, Kaup B, Anderson L, Hoover D, Brown L, Albertini RJ, Gudi R, Jacobson-Kram D, Thorne CD, Squibb KS (2006) Biological monitoring and surveillance results of Gulf War I veterans exposed to depleted uranium. Int Arch Occup Environ Health 79:11–21

McDiarmid MA, Engelhardt SM, Oliver M, Gucer P, Wilson PD, Kane R, Cernich A, Kaup B, Anderson L, Hoover D, Brown L, Albertini R, Gudi R, Jacobson-Kram D, Squibb KS (2007a) Health surveillance of Gulf War I veterans exposed to depleted uranium: updating the cohort. Health Phys 93:60–73

McDiarmid MA, Squibb K, Engelhardt S, Gucer P, Oliver M (2007b) Surveillance of Gulf War I veterans exposed to depleted uranium: 15 years of follow-up. Euro J Oncol 12:235–242

McDiarmid MA, Engelhardt SM, Dorsey CD, Oliver M, Gucer P, Wilson PD, Kane R, Cernich A, Kaup B, Anderson L, Hoover D, Brown L, Albertini R, Gudi R, Squibb KS (2009) Surveillance results of depleted uranium-exposed Gulf War I veterans: sixteen years of follow-up. J Toxicol Environ Health—Part A—Curr Issues 72:14–29

Miller AC, Blakely WF, Livengood D, Whittaker T, Xu J, Ejnik JW, Hamilton MM, Parlette E, St John T, Gerstenberg HM, Hsu H (1998) Transformation of human osteoblast cells to the tumorigenic phenotype by depleted uranium-uranyl chloride. Environ Health Perspect 106:465–471

Miller AC, Xu J, Stewart M, Emond E, Hodge S, Matthews C, Kalinich J, McClain DE (2000) Potential health effects of the heavy metals, depleted uranium and tungsten, used in armor-piercing munitions: comparison of neoplastic transformation, mutagenicity, genomic instability, and oncogenesis. In: Centeno JA, Collery PH, Vernet G, Finkelman RB, Gibb H, Etienne JC (eds) Metals in biology and medicine, vol 6. John Libbey Eurotext, Paris

Miller AC, Mog S, McKinney L-A, Luo L, Allen J, Xu J, Page N (2001) Neoplastic transformation of human osteoblast cells to the tumorigenic phenotype by heavy metal-tungsten alloy particles: induction of genotoxic effects. Carcinogenesis 22:115–125

Miller AC, Stewart M, Brooks K, Shi L, Page N (2002a) Depleted uranium-catalyzed oxidative DNA damage: absence of significant alpha particle decay. J Inorg Biochem 91:246–252

Miller AC, Xu J, Stewart M, Brooks K, Hodge S, Shi L, Page N, McClain D (2002b) Observation of radiation-specific damage in human cells exposed to depleted uranium: dicentric frequency and neoplastic transformation as endpoints. Radiat Protec Dosim 99:275–278

Miller AC, Xu J, Stewart M, Prasanna PGS, Page N (2002c) Potential late health effects of depleted uranium and tungsten used in armor-piercing munitions: comparison of neoplastic transformation and genotoxicity with the known carcinogen nickel. Mil Med 167(Suppl 1):120–122

Miller AC, Brooks K, Stewart M, Anderson B, Shi L, McClain D, Page N (2003) Genomic instability in human osteoblast cells after exposure to depleted uranium: delayed lethality and micronuclei formation. J Environ Radioact 64:247–259

Miller AC, Brooks K, Smith J, Page N (2004) Effect of the militarily-relevant heavy metals, depleted uranium and heavy metal tungsten-alloy on gene expression in human liver carcinoma cells (HepG2). Mol Cell Biochem 255:247–256

Mirto H, Henge-Napoli MH, Gibert R, Ansoborlo E, Fournier M, Cambar J (1999) Intracellular behavior of uranium (VI) on renal epithelial cell in culture (LLC-PK1): influence of uranium speciation. Toxicol Lett 104:249–256

Mitchell RR, Fitzgerald SD, Aulerich RJ, Balander RJ, Powell DC, Tempelman RJ, Cray C, Stevens W, Bursian SJ (2001a) Hematological effects and metal residue concentrations following chronic dosing with tungsten-iron and tungsten-polymer shot in adult game-farm mallards. J Wild Dis 37:459–467

Mitchell RR, Fitzgerald SD, Aulerich RJ, Balander RJ, Powell DC, Tempelman RJ, Stevens W, Bursian SJ (2001b) Reproductive effects and duckling survivability following chronic dosing with tungsten-iron and tungsten-polymer shot in adult game-farm mallards. J Wild Dis 37:468–474

Mitchell RR, Fitzgerald SD, Aulerich RJ, Balander RJ, Powell DC, Tempelman RJ, Stickle RL, Stevens W, Bursian SJ (2001c) Health effects following chronic dosing with tungsten-iron and tungsten-polymer shot in adult game-farm mallards. J Wild Dis 37:451–458

Monleau M, De Meo M, Paquet F, Chazel V, Dumenil G, Donnadieu-Clarz M (2006) Genotoxic and inflammatory effects of depleted uranium particles inhaled by rats. Toxicol Sci 89:287–295

Morrow PE, Gibb FR, Gazioglu KM (1967) A study of particulate clearance from the human lungs. Am Rev Respirat Dis 96:1209–1221

Osawa R, Abe R, Inokuma D, Yokota K, Ito H, Nabeshima M, Shimizu H (2006) Chain saw blade granuloma: reaction to a deeply embedded metal fragment. Arch Dermatol 142:1079–1080

Pellmar TC, Fuciarelli AF, Ejnik JW, Hamilton M, Hogan J, Strocko S, Emond C, Mottaz HM, Landauer MR (1999) Distribution of uranium in rats implanted with depleted uranium pellets. Toxicol Sci 49:29

Peuster M, Fink C, von Schnakenburg C (2003) Biocompatibility of corroding tungsten coils: *in vitro* assessment of degradation kinetics and cytotoxicity on human cells. Biomaterials 24:4057–4061

Prat O, Berenguer F, Malard V, Tavan E, Sage N, Steinmetz G, Quemeneur E (2005) Transcriptomic and proteomic responses of human renal HEK293 cells to uranium toxicity. Proteomics 5:297–306

Saruwatari H, Kamiwada R, Matsushita S, Hashiguchi T, Kawai K, Kanekura T (2009) Tungsten granuloma attributable to a piece of lawn-mower blade. Clin Exp Dermatol 34:e268–e269

Schins RP, Borm PJ (1999) Mechanisms and mediators in coal dust induced toxicity: a review. Ann Occup Hygiene 43:7–33

Sica A, Allavena P, Mantovani A (2008) Cancer related inflammation: the macrophage connection. Cancer Lett 264:204–215

Tasat DR, De Ray BM (1987) Cytotoxic effect of uranium dioxide on rat alveolar macrophages. Environ Res 112:1628–1635

Thomsen P, Gretzer C (2001) Macrophage interactions with modified material surfaces. Curr Opin Solid State Mater Sci 5:163–176

Tsirogianni AK, Moutsopoulos NM, Moutsopoulos HM (2006) Wound healing: immunological aspects. Injury 375:S5–S12

van der Voet GB, Todorov TI, Centeno JA, Jonas W, Ives J, Mullick FG (2007) Metals and health: a clinical toxicological perspective on tungsten and review of the literature. Mil Med 172:1002–1005

Wan B, Fleming JT, Schultz TW, Sayler GS (2006) *In vitro* immune toxicity of depleted uranium: effects on murine macrophages, CD^{+} T cells, and gene expression profiles. Environ Health Perspect 114:85–91

Yokel RA, Lasley SM, Dorman DC (2006) The speciation of metals in mammals influences their toxicokinetics and toxicodynamics and therefore human health risk assessment. J Toxicol Environ Health Part B 9:63–85